ISTANBUL TECHNICAL UNIVERSITY ★ GRADUATE SCHOOL OF SCIENCE ENGINEERING AND TECHNOLOGY

INHIBITORY IMPACT OF SELECTED ANTIBIOTICS ON BIODEGRADATION CHARACTERISTIC AND MICROBIAL POPULATION UNDER AEROBIC CONDITIONS

Ph.D. THESIS

İlke PALA ÖZKÖK

Department of Environmental Engineering

Environmental Biotechnology Program

MAY 2012

ISTANBUL TECHNICAL UNIVERSITY ★ GRADUATE SCHOOL OF SCIENCE ENGINEERING AND TECHNOLOGY

INHIBITORY IMPACT OF SELECTED ANTIBIOTICS ON BIODEGRADATION CHARACTERISTIC AND MICROBIAL POPULATION UNDER AEROBIC CONDITIONS

Ph.D. THESIS

İlke PALA ÖZKÖK
(501052803)

Department of Environmental Engineering

Environmental Biotechnology Program

Thesis Advisor: Prof. Dr. Derin ORHON

MAY 2012

İSTANBUL TEKNİK ÜNİVERSİTESİ ★ FEN BİLİMLERİ ENSTİTÜSÜ

SEÇİLMİŞ ANTİBİYOTİKLERİN AEROBİK KOŞULLAR ALTINDA BİYOLOJİK AYRIŞABİLİRLİK VE MİKROBİYAL POPÜLASYON ÜZERİNE ETKİLERİNİN BELİRLENMESİ

DOKTORA TEZİ

İlke PALA ÖZKÖK
(501052803)

Çevre Mühendisliği Anabilim Dalı

Çevre Biyoteknolojisi Programı

Tez Danışmanı: Prof. Dr. Derin ORHON

MAYIS 2012

İlke Pala Özkök, **a Ph.D.** student of ITU **Graduate School of Science Engineering and Technology** student ID **501052803,** successfully defended the **dissertation** entitled "**INHIBITORY IMPACT OF SELECTED ANTIBIOTICS ON BIODEGRADATION CHARACTERISTIC AND MICROBIAL POPULATION UNDER AEROBIC CONDITIONS**", which she prepared after fulfilling the requirements specified in the associated legislations, before the jury whose signatures are below.

Thesis Advisor :	**Prof. Dr. Derin ORHON** İstanbul Technical University	.....
Jury Members :	**Prof. Dr. Emine UBAY ÇOKGÖR** İstanbul Technical University	.....
	Prof. Dr. Zeynep Petek ÇAKAR İstanbul Technical University	.....
	Assoc. Prof. Dr. Didem AKÇA GÜVEN Fatih University	.....
	Assist. Prof. Dr. Bilge ALPASLAN KOCAMEMİ Marmara University	.....

Date of Submission : 20 March 2012
Date of Defense : 24 May 2012

To loving memory of my grandmother Nazmiye ERGİNTAN,

This thesis was supported by the Turkish Academy of Sciences as part of Fellowship Program for Integrated Doctoral Studies.

Bu tez Türkiye Bilimler Akademisi Bütünleştirilmiş Doktora Programı kapsamında desteklenmiştir.

FOREWORD

I would like to express my deepest gratitude to my thesis supervisor and mentor Prof. Dr. Derin ORHON, who has showed me the way since the beginning of my professional life as an environmental engineer. I am also deeply thankful to Prof. Dr. Med. Daniel JONAS for the opportunities he has provided me. Moreover I would like to thank Prof. Dr. Emine UBAY ÇOKGÖR for her support and understanding that she showed in the last ten years that I have known her. I would also like to thank Associated Prof. Dr. Zeynep Petek ÇAKAR and Associated Prof. Dr. H. Güçlü İNSEL for their contributions in my studies.

As a National PhD Scholarship holder, I would like to thank The Scientific and Technological Research Council of Turkey for their contributions in my thesis.

This thesis is a product of the Fellowship Program for Integrated Doctoral Studies of the Turkish Academy of Sciences and I would like to express my gratitude for the opportunities they have provided me with.

Moreover I would like to thank Associated Professors Dr. Tuğba ÖLMEZ HANCI, Dr. Özlem KARAHAN, Assistant Professors Dr. Nevin YAĞCI, Dr. Mahmut ALTINBAŞ and Dr. Gülsüm Emel ZENGİN BALCI. Supports of Dr. Aslı Seyhan ÇIĞGIN, Aslıhan URAL (M.Sc.) and Gökçe KOR (M.Sc.) during my studies are sincerely appreciated.

My friends Elke SCHMIDT-EISENLOHR, Inge ENGELS, Christa HAUSER and Melanie BROSZAT helped and supported me during my year at the Institute of Hospital Hygiene and Environmental Health of University Klinik in Freiburg Germany, I would like to extend my gratitude to them. Moreover, I would like to thank Sabine KAISER and Dr. Ateequr REHMAN for all the things they taught me and also for their friendship and support.

My dear friends and colleagues, Dr. Asude HANEDAR, Dr. Banu GENÇSOY, Dr. Burçak KAYNAK and Research Assistants Egemen AYDIN, Ayşe Dudu ALLAR, Edip AVŞAR, Emel TOPUZ and Burçin COŞKUN, thank you for the encouragement and support during my studies. During our studies we supported each other, shared memorable times and built the foundations of unforgettable friendships. I would like to express my gratitude to all of you.

I can’t begin to express the depth of gratitude I have for my very good friend and colleague Research Assistant Tuğçe KATİPOĞLU YAZAN. I would like to thank her for her friendship, all support she has given me in every stage of my study.

My dear friends Duygu EROLGİL and Müge ŞENGÖNÜL always supported me, for that I would like to express my deep gratitude.

I would like to thank and express my deepest appreciation to my dearest family, who has been there for me whenever I needed support and never stopped believing in me. Especially my parents Prof. Dr. Sumru PALA and Tayfun PALA were and are always there for me, for that I will always be grateful.

My dear sister Dr. Özge PALA WUYTS always supported me; knowing that she would always be there for me has meant the world to me. Also my brother Dr. Stefan WUYTS and nephew Arda WUYTS, never withhold their love and support. Moreover I would like to thank the ÖZKÖK family for supporting and believing in me. I am grateful to all my loving family and for all they have done for me.

I would like to extend my gratitude to Prof. Dr. Esin İNAN, Prof. Dr. Köksal BALOŞ and Prof. Dr. Füsun BALOŞ TÖRÜNER for their support throughout my studies.

Last but not the least I would like to thank my beloved husband Tuncay ÖZKÖK, who endured through all the difficulties during my studies and cherish the beauties together beside me.

Finally, I would like to dedicate this thesis, hoping that it would fulfill their dreams for me, to my dear grandfather Hüseyin PALA and my beloved late grandmother Nazmiye ERGİNTAN, who made it all possible for many people she helped and taught. She has given dreams and opportunities to many people, including her own family, just by planting the seed of love to learn in our hearts.

July, 2012

İlke PALA ÖZKÖK
Environmental Engineer and
Molecular Biologist

TABLE OF CONTENTS

ABBREVIATIONS

ASM	**:** Activated Sludge Model
COD	**:** Chemical Oxygen Demand
EC_{50}	**:** Effective Concentration 50%
ERY	**:** Erythromycin
IC	**:** Ion Chromatography
OTU	**:** Operational Taxonomic Unit
OUR	**:** Oxygen Uptake Rate
PCR	**:** Polymerase Chain Reaction
PHA	**:** Ploy Hydroxy Alkanoates
PHB	**:** Poly Hydroxy Butyric Acid
SMX	**:** Sulfamethoxazole
SRT	**:** Sludge Retention Time
SS	**:** Suspended Solids
TET	**:** Tetracycline
TOC	**:** Total Organic Carbon
UV	**:** Ultra Violet
VSS	**:** Volatile Suspended Solids

LIST OF SYMBOLS

Endogenous decay rate for X_H	: $\boldsymbol{b_H}$
Fraction of biomass converted to S_P	: $\boldsymbol{f_{ES}}$
Fraction of biomass converted to X_P	: $\boldsymbol{f_{EX}}$
Half saturation constant for growth of X_H	: $\boldsymbol{K_S}$
Half saturation constant for storage of PHA by X_H	: $\boldsymbol{K_{STO}}$
Heterotrophic half saturation coefficient for oxygen	: $\boldsymbol{K_{OH}}$
Hydrolysis half saturation constant for S_{H1}	: $\boldsymbol{K_X}$
Hydrolysis half saturation constant for X_{S1}	: $\boldsymbol{K_{XX}}$
Initial active biomass	: $\boldsymbol{X_{H1}}$
Initial amount of biodegradable COD	: $\boldsymbol{C_{S1}}$
Initial amount of hydrolysable COD	: $\boldsymbol{X_{S1}}$
Initial amount of PHA	: $\boldsymbol{X_{STO1}}$
Initial amount of readily biodegradable COD	: $\boldsymbol{S_{S1}}$
Initial amount of readily hydrolysable COD	: $\boldsymbol{S_{H1}}$
Maximum growth rate for X_H	: $\boldsymbol{\mu_H}$
Maximum growth rate on PHA for X_H	: $\boldsymbol{\mu_{STO}}$
Maximum hydrolysis rate for S_{H1}	: $\boldsymbol{k_h}$
Maximum hydrolysis rate for X_{S1}	: $\boldsymbol{k_{hx}}$
Maximum storage rate of PHA by X_H	: $\boldsymbol{k_{STO}}$
Nitrogen fraction in biomass	: $\boldsymbol{i_{XB}}$
Particulate microbial products	: $\boldsymbol{X_P}$
Soluble microbial products	: $\boldsymbol{S_P}$
Yield coefficient of PHA	: $\boldsymbol{Y_{STO}}$
Yield coefficient of S_P	: $\boldsymbol{Y_{SP}}$
Yield coefficient of X_H	: $\boldsymbol{Y_H}$

LIST OF TABLES

Page

LIST OF FIGURES

Page

INHIBITORY IMPACT OF SELECTED ANTIBIOTICS ON BIODEGRADATION CHARACTERISTICS AND MICROBIAL POPULATION UNDER AEROBIC CONDITIONS

SUMMARY

The study evaluated the inhibitory impact of antibiotics on the biodegradation of peptone mixture by an acclimated microbial culture under aerobic conditions, together with their effects on the microbial population and the resistance profile of the biomass. Two fill and draw reactors fed with the peptone mixture defined in the ISO 8192 procedure and sustained at steady state at a sludge age of 10 days and 2 days were used as the biomass pool with a well-defined culture history.

Acute inhibition experiments involved running a total of six and five parallel batch reactors, for each sludge age of 10 and 2 days, respectively, seeded with biomass from control reactors (SRT 10d and 2 d) and the same peptone mixture together with pulse feeding of 50 mg/L and 200 mg/L of *Sulfamethoxazole, Tetracycline* and *Erythromycin.*

Moreover, the effects of chronic exposure of the antibiotics were evaluated, for which a total number of six chronic reactors were set and investigated on different days throughout the study. Substrate utilization was evaluated by observing the respective oxygen uptake rate profiles and compared with both control reactors, which were started without antibiotic addition.

All the data obtained were simulated using Activated Sludge Model No.3. Results showed that while all available external substrate was removed from solution, addition of antibiotics induced a significant decrease in the amount of oxygen consumed, indicating that a varying fraction of peptone mixture was blocked by the antibiotic and did not participate to the on-going microbial growth mechanism. This observation was also compatible with the concept of the *uncompetitive inhibition* mechanism, which defines a similar substrate blockage through formation of an enzyme-inhibitor complex.

Additionally, resistance genes profiles and the microbial population characteristics of chronically inhibited systems were investigated. Moreover, microbial population dynamics studies by pyrosequencing revealed that the microbial population structure alters significantly under constant exposure to antibiotic substances. Results of both investigations revealed that organisms harboring resistance genes against antibiotics were able to survive under constant exposure to the inhibitory substances at both sludge ages.

SEÇİLMİŞ ANTİBİYOTİKLERİN AEROBİK KOŞULLAR ALTINDA BİYOLOJİK AYRIŞABİLİRLİK VE MİKROBİYAL POPÜLASYON ÜZERİNE ETKİLERİNİN BELİRLENMESİ

ÖZET

Teknoloji, endüstri ve tarımsal aktivitelerdeki gelişmeler neticesinde sentetik ve genellikle toksik organik maddeler atıksulara girmeye başlamıştır. Çeşitli endüstriyel proseslerde ortaya çıkan kalıcı organik maddelerin ve mikrokirleticilerin varlığı, bu maddelerin gideriminin ve arıtma sistemlerine etkilerinin belirlenmesinin önemini arttırmıştır. Bu kalıcı organik maddelerden olan ve son yıllarda çevre için büyük tehlike arz etmeye başlayan zenobiyotikler, genellikle sentetik olarak üretilen ve organizmaya yabancı olan maddeler olarak tanımlanmaktadır.

Antibiyotikler de doğada ayrışmadan kalabilen ve besin zincirinde biyoakümüle olan zenobiyotiklerden biridir. Günümüzde başta tıp alanında olmak üzere veterinerlik ve tarımda yaygın olarak uygulanan antibiyotiklerin, bilinçsiz kullanımı ile sularda ve toprakta miktarları her geçen gün artmaktadır. Günümüzde bu kontrolsüz kullanım sonucu birçok bakteri türünün, özellikle patojen türlerin, antibiyotik direnci kazanması söz konusudur. Antibiyotik direnci kazanan mikroorganizmaların doğal ekosistemlerde yaygın olarak bulunması, başta insanlar olmak üzere hayvanlar ve bitkiler açısından büyük bir risk oluşturmaktadır.

Literatürde antibiyotiklerin atıksu arıtma tesislerinin giriş ve çıkışlarındaki konsantrasyon değerleri ve alıcı ortamlardaki konsantrasyonları ile ilgili birçok çalışma bulunmaktadır. Buna karşın bu maddelerin arıtma tesislerindeki ayrışma mekanizmaları ve sistemdeki mikrobiyal popülasyon üzerine olan etkilerin ayrıntılı olarak araştırılmadığı görülmüştür. Yapılan araştırmalarda ise sistemde ya sadece kollektif parametrelerin ölçüldüğü ya da sadece antibiyotik konsantrasyonlarının izlendiği görülmektedir. Mikrobiyal popülasyonun antibiyotiklere verdikleri tepkiler ve popülasyon dinamiği de incelenmemiştir. Ayrıca, literatürde antibiyotiklerin biyolojik ayrışmaları ile ilgili yapılan çalışmalarda birbirinden çok farklı sonuçlara ulaşılmış olduğu da görülmektedir.

Sulfonamidler insanlarda toplam antibiyotik kullanımının % 16-21 kadarını kapsamaktadır, kullanım sonrasında genellikle metabolitleri ve bir kısmı da orijinal aktif madde olmak üzere idrar ile dışarı atılmaktadır. Bu grubu temsilen seçilen sulfametoksazol en yaygın görülen sulfonamid grubu antibiyotiktir. Literatürde yapılan çalışmalarda sulfametoksazolün giderimi ile ilgili olarak kesin bir bilgi bulunmamaktadır.

Seçilen ikinci antibiyotik olan tetrasiklin ve türevi antibiyotikler, hayvancılık ve tarımda en yaygın kullanılan antibiyotiklerdendir. Tetrasiklin grubu antibiyotiklerinin %80'i fotokatalitik reaksiyonlar ile ayrışma özelliğine sahiptir. Tetrasiklin antibiyotiğinin, aktif çamur sistemlerinde çamura tutunma yolu ile

giderildiği ve bunun tetrasiklinin kalsiyum ve benzeri iyonlar ile, çözünürlüğü çok düşük bileşikler oluşturma eğiliminin bir sonucu olabileceği belirtilmiştir.

Makrolidler ise insanlarda toplam antibiyotik kullanımının % 9-12 kadarını kapsayan en önemli antibiyotik gruplarından biridir ve penisilinlere alternatif olarak kullanılmaktadırlar. Makrolidler genellikle metabolize edilememekte ve değişmeden dışkı ile atılmaktadır.

Gerçekleştirilmiş olan çalışma, antibiyotik maddelerin pepton karışımına aklime edilmiş bir aerobik mikrobiyal kültürün substrat ayrıştırması üzerine olan etkilerini, mikrobiyal popülasyon üzerine olan etkilerini ve aynı zamanda sistemin direnç profilini incelemiştir. İki adet doldur-boşalt tipi reaktör ISO8192 prosedüründe belirlenmiş olan pepton karışımı ile beslenmiş ve iki farklı çamur yaşında (çamur yaşı 10 gün ve 2 gün) kararlı halde devam ettirilerek, çalışma boyunca biyokütle kaynağı olarak kullanılmıştır.

Akut inhibisyon çalışmaları için, kontrol reaktörlerinden alınan kaynak çamur kullanılarak kurulan paralel kesikli reaktörlerde, toplamda her iki çamur yaşı için onbir set deneysel çalışma gerçekleştirilmiştir. 50 mg/L ve 200 mg/L olmak üzere ani *Sulfamethoksazol, Tetrasiklin* ve *Eritromisin* ilavesi yapılmıştır.

Ayrıca, aktif çamur sistemlerinin antibiyotiklere kronik maruz kalmalarının etkilerinin incelenmesi amacıyla toplamda altı adet reaktör işletilmiş ve farklı günlerde deneysel çalışmalar gerçekleştirilmiştir. Substrat tüketimi, ilgili oksijen tüketim profillerinin gözlemlenmesi ile incelenmiş ve antibiyotik etkisi altında olmayan ilgili kontrol reaktörünün oksijen tüketim profili ile karşılaştırılmıştır.

Serbest substratın temel stokiyometrisi ve kütle dengesi, inhibitörlerin etkisinin açıklanması açısından çok önemlidir, bunun nedeni ise substratın bloke edilmesinin göz ardı edilmesi ile elde edilen kinetik değerlendirmenin yanlış yönlerdici özelliğe sahip olmasıdır. Literatürdeki birçok çalışma substrat bağlanmasını göz ardı etmiştir ve sadece substrat profillerine dayalı incelemelerde bulunmuşlardır. Bu çalışmalarda biyokimyasal reaksiyonlara katılmayan bağlı substrat ayrıdedilmemiştir. Oksijen tüketim hızı (OTH) profillerinin inhibisyon etkisi incelemelerinde kullanılmaları bu çalışmanın orijinalliğini oluşturmaktadır. Bu kapsamda seçilmiş olan antibiyotiklerin substrat bağlayıcı özellikleri unkompetitif inhibisyon yaklaşımı ile belirlenebilmiştir.

Seçilmiş olan antibiyotik maddelerin pepton karışımının biyolojik olarak ayrışması üzerindeki akut ve kronik inhibisyon etkilerinin belirlenmesi amacıyla, bütün OTH profilleri temin eden respirometrik testler çalışmanın temelini oluşturmuşlardır. İnhibisyon etkisi, antibiyotik ilavesinin olmadığı kontrol testinde elde edilen orijinal OTH profilinin şeklindeki değişiklikler ile ortaya konmuştur.

Antibiyotiklerin, peptonun piyolojik ayrışmasına en önemli etkisi, OTH testlerinde tüketilen oksijen miktarının azalmasıdır. Bu etki, maksimum büyüme hızını (μ_H) azaltarak ve/veya yarı doygunluk sabitini (K_S) arttırarak biyolojik ayrışmayı etkileyen geleneksel inhibisyon kavramı ile açıklanamamaktadır. Bu iki etki de kinetik olarak substrat kullanımını yavaşlatma özelliğine sahiptir. Bu tür bir inhibisyon OTH eğrilerinin endojen solunum aşamasına ulaşma süresini uzatacak ancak OTH eğrisi altındaki alana tekbül eden oksijen tüketim miktarının sabit kalmasına neden olacaktır.

Ancak, bu çalışmada elde edilen OTH profilleri farklı özelliklere sahiptir. Antibiyotik ilavesi ardından, biyolojik ayrışma süresi sabit kalmakta, buna karşın tüketilen oksijen miktarı kullanılan antibiyotik türü ve dozajına bağlı olarak

azalmaktadır. Bu kapsamda, farklı oranlarda pepton karışımının antibiyotik tarafından bloke edildiği ve devam eden mikrobiyal büyüme reaksiyonlarına katılamadığı sonucu ortaya çıkmaktadır. Bu gözlem sadece *unkompetitif inhibisyon* mekanizması ile açıklanabilmektedir. Bu kapsamda, bütün gözlemler unkompetitif inhibisyon kavramı ile açıklanmıştır ancak inhibisyon etkisinin antibiyotik dozu ve türüne bağlı olarak değiştiği gözlemlenmiştir.

Elde edilen deneysel data Aktif Çamur Model No.3 kullanılarak simüle edilmiştir. Sonuçlar, bütün dışsal substrat giderilirken, antibiyotik ilavesi ile oksijen tüketiminde önemli bir düşüş yaşandığını ortaya koymuştur. Bu durum, pepton karışımının değişken fraksiyonlarının antibiyotik madde tarafından bloke edildiğini ve biyolojik ayrışmaya girmediğini göstemiştir. Bu gözlem, enzim-inhibitör kompleksi oluşumu ile benzer bir substrat blokajına neden olan unkompetitif inhibisyon mekanizması ile örtüşmektedir.

Ayrıca, kronik reaktörlerinde görülen direnç profili ve pirosekanslama yöntemi kullanılarak kronik sistemlerin mikrobiyal popülasyon dinamikleri incelenmiştir. Bu çalışmalardan elde edilen sonuçlar sistemlerin dominant türlerinde kayma gerçekleştiğini ve sistemlerde antibiyotik etkisi altında canlılığını sürdürebilen organizmaların antibiyotik maddelere dirençli olma özelliklerini ortaya koymuştur.

Çalışmalardan elde edilen sonuçlar çamur yaşının mikrobiyal popülasyona olan etkilerini de açığa çıkarmıştır. Elde edilen sonuçlara gore, yavaş büyüme özelliği olan *Actinobacteria* türlerinin hızlı büyüyen SRT2d sistemini domine etme özelliklerinin olmadığını göstermiştir. Buna karşın SRT2d sistemini *Proteobacteria* türlerinin domine ettiği görülmüştür. Ancak, çamur yaşı 10 gün sisteminde *Actinobacteria* yıkanmamış ve sistemi domine edebilmişlerdir. ERY etkisi altında ise SRT 10gün sisteminde popülasyonda bir kayma geçeklemiş ve dominantlik *Actinobacteria*'dan *Proteobacteria*'ya geçmiştir. Bunun nedeni dirençli *Proteobacteria*'nın sistemde yaşamını sürdürebilmesidir. Sistemde *Comamonas* sp OTU#293 en baskın canlılardan olmuştur. SRT2gün sisteminde ise ERY etkisi yok iken *Proteobacteria* baskın olmasına ragmen ERY etkisi altında kültüre alınamamış aday phylum olan *TM7* türü (OTU#83) baskın hale gelmiştir. Ancak TET ve SMX'in etkilerinin popülasyonda bir kaymaya neden olmadığı görülmüştür. Buna karşın, TET SRT2d sisteminde *Deinococcus-Thermus* phylumu yok olurken, SMX SRT2d sisteminde OTU#1, *Deinococcus-Thermus* phylumu türünün en baskın organizmalardan biri haline geldiği görülmektedir. SMX SRT2d sisteminde *Proteobacteria* önemli derecede azalmiş ve *Deinococcus-Thermus* phylumu artmıştır. Ancak SRT0d sisteminde *Bacteroidetes* önemli derece azalmıştır. Bütün SMX ve TET sistemlerinde *Arthrobacter* türlerinin baskın oldukları belirlenmiştir (OTU#2, OTU#55 ve OTU#4).

Antibiyotik çalışmalarının devam ettirilmesi halinde, bu maddelerin giderilmesi ile ilgili çalışmaların gerçekleştirilmesi ve antibiyotikleri ayrıştırabilen organizmaların belirlenmesi üzerinde çalışılmasının faydalı olacağı düşünülmüştür. Ayrıca bu tür çalışmalarda da mutlaka modelleme simülasyon çalışmalarının devam ettirilmesi gerekmektedir. Böylece sistemin verdiği tepkinin doğru şekilde belirlenmesi mümkün olacaktır.

1. INTRODUCTION

Due to developments in technology, industry and agriculture, synthetic and generally toxic organic substances started to occur in wastewaters. The occurrence of persistent organic substances and micropollutants produced in various industrial processes increased the need to determine effects of such substances on wastewater treatment systems. Xenobiotics, among these persistent organic substances, are defined as substances foreign the organisms that are generally produced synthetically (Van der Meer et al., 1992).

Antibiotics are among the xenobiotic compounds that are persistent to biodegradation and have the tendency to accumulate in the environment (Chrencik et al., 2005). They are extensively used in human and veterinary medicine. Possible irresponsible usage of these substances leads to resistant pathogenic microorganisms living in the surface waters and soil, which causes a large threat to human and environmental health (Boxall et al., 2003, Martinez et al., 2008, Li and Zhang, 2010).

Antibiotics enter the sewerage with wastewater and reach the wastewater treatment plants. In wastewater treatment plants activated sludge systems are one of the most applied treatment technologies, and they date back to the beginning of the 20^{th} century (Orhon and Artan, 1994). Due to their biological nature, activated sludge systems are one of the most susceptible parts of the treatment pipeline to antibiotics.

In the literature there are many studies that have measured the concentrations in the influent and the effluent of the wastewater treatment plants and also in the receiving water media (Giger et al., 2003; Hirsch et al., 1999; Alexy et al., 2006). On the other hand, there is not enough information on their effects on treatment plant microbial population. Moreover, in the conducted studies it can be seen that either only collective parameters or antibiotic concentrations were measured, but the responses of the microbial population to the antibiotics and population dynamics were not analyzed thoroughly. Additionally in the studies conducted on the biodegradability

characteristics of the chosen antibiotics it can be seen that each study has given different results.

2. AIM OF THE STUDY

The scope of the current study was to conduct a detailed analysis of the effect of antibiotics on the activated sludge systems. For this purpose it aimed to determine the acute and chronic inhibition effects of three model antibiotics on non-acclimated and acclimated aerobic activated sludge cultures and their effects on the degradation mechanisms of the substrate using activated sludge modeling tools. Moreover it is aimed to determine the microbial species and antibiotic resistance genes in the system to enlighten the chronic effects of antibiotics on microbial diversity.

Three model antibiotics, sulfamethoxazole, tetracycline and erythromycin, were chosen to determine their effects on the aerobic activated sludge systems and the removal mechanism of the substrate, peptone-meat extract mixture. In the current study, different concentrations of these three antibiotics were applied individually to determine their acute and chronic effects on the activated sludge systems. Respirometric methods and activated sludge modeling tools were implemented for the characterization of the response of the biomass to the antibiotic considered as an inhibitor substance. Moreover the antibiotic resistance genes were monitored qualitatively, showing the response of the biomass to chronic exposure to the model antibiotics, and this data was supported with microbial population analysis using ultrafast 454-pyrosequencing technology.

3. LITERATURE REVIEW

3.1 Xenobiotics

Nowadays, concentrations of synthetic and generally toxic compounds in wastewaters increase drastically due to developments in technology, industry and agricultural activities (Dogruel et al., 2004; Oktem et al., 2006). Occurrence of persistent organic substances and micropollutants in various industrial processes increased the importance of determining the effects of these substances on the treatment systems.

These compounds are generally synthetically produced and cover many groups of chemicals including persistent compounds (van der Meer et al., 1992). Pharmaceuticals (antibiotics, antidepressants, and many other chemicals) are examples of such xenobiotic compounds which have the potential to accumulate in the food chain and threaten human health (van der Meer et al., 1992). In spite of the fact that in the literature there are studies on bio-reclamation of natural ecosystems polluted with these compounds (O'Neill et al, 2000; Dou et al, 2008), there is not enough knowledge about the treatability of xenobiotic rich wastewaters and their effects on active species in the treatment systems.

3.2 Antibiotics

According to Kümmerer (2009), the classical definition of antibiotics is "a compound produced by a microorganism (such as *Streptomyces* spp.) which inhibits the growth of another microorganism". However the meaning of antibiotic has changed over the years, leading to the current meaning of "substances with antibacterial, anti-fungal, or anti-parasitical activity", which include synthetic and semi-synthetic products that have killing or inhibiting effect on bacteria, fungi or viruses (Kümmerer, 2009). Antibiotics are among the xenobiotic compounds (Alonso et al., 2001) that are persistent to biodegradation and have the tendency to

accumulate in the environment (Chrencik et al., 2005), and are widely used in human and veterinary medicine, aquaculture for preventing or treating microbial infections. Several hundred different antibiotic and antimycotic substances are used in human and veterinary medicine (Kümmerer and Henninger, 2003). Possible irresponsible usage of these substances leads to resistant pathogenic microorganisms living in the surface waters and soil, which causes a large threat to human and environmental health.

There are different classes of antibiotics; an overview of main classes of antibiotics is given in Table 3.1. However in order to investigate the elimination mechanism of antibiotic substances in activated sludge systems and their effects on these systems three model substances were chosen. These substances were chosen to represent major groups of antibiotics and are among the abundantly used antibiotic substances in the world and in Turkey. Sulfamethoxazole was chosen to represent sulfonamides group, tetracycline to represent tetracyclines and erythromycin for macrolide group of antibiotics.

Table 3.1: Major classes of antibiotics (taken from Kümmerer, 2009).

Class	Group	Subgroup	Example
ß-lactams	Penicillins	Benzyl-penicillins	Phenoxypenicillin
		Isoxazolylpenicillins	Oxacillin
		Aminopenicillins	Amoxicillin
		Carboxypenicillins	Carbenicillin
		Acylaminopenicillins	Piperacillin
	Cephalosporins	Cefazolin group	Cefazolin
		Cefuroxim group	Cefuroxim
		Cefotaxim group	Cefotaxim
		Cefalexin group	Cefprozil
	Carbpenems	–	Meropenem
Tetracyclines	–	–	Doxycycline
Aminoglycosides	–	–	Gentamicin 1c
Macrolides			Erythromycin A
Glycopeptides			Vancomycin
Sulfonamides			Sulfamethoxazole
Quinolones			Ciprofloxacin

3.2.1 Sulfamethoxazole

Sulfamethoxazole is a member of the sulfonamide family and 16-21% of the antibiotic drugs used for human needs are from the sulfonamide group (Göbel et al., 2005). The mode of action of the bacteriostatic agent Sulfamethoxazole is preventing

the dihydrofolic acid formation in bacteria (Drilla et al., 2005; Masters et al., 2003, Sköld, 2001), which is essential in the pathway of producing purines and pyrimidines. Due to development of bacterial resistance against Sulfamethoxazole, it is nowadays being used in combination with Trimethoprim (Drilla et al., 2005).

3.2.2 Tetracycline

Tetracyclines, discovered in the 1940's, are broad-spectrum antibiotics that work against a large number of gram-negative and –positive bacteria, chlamydiae, mycoplasmas, rickettsiae and protozoa (Chopra and Roberts, 2001), and are one of the majorly used antimicrobials. Tetracycline as Sulfamethoxazole is a bacteriostatic agent (Le-Minh et al., 2010). Tetracycline group of antibiotics are strong chelating agents, which supports their antimicrobial properties (Blackwood, 1985, Chopra et al., 1992, Chopra and Roberts, 2001). They inhibit the protein synthesis by hindering the binding of amiacyl-tRNA with the ribosome (Chopra et al.,1992; Schnappinger and Hillen, 1996; Chopra and Roberts, 2001).

3.2.3 Erythromycin

Macrolides are among most widely used antibiotics for treatment of human diseases by 9-12% of the total use of antibiotics and they are used as an alternative to penicillin. They bind to the large subunit of the ribosome. Eryhromycin, especially, blocks the entrance to the tunnel of the large ribosomal subunit, hindering the exit of the peptide chains. This blockage causes creations of short uncompleted polypeptide chains (Tenson et al., 2003). Even though Erythromycin is a bacteriostatic agent (Louvet et al., 2010), in larger concentrations it can be cidial.

3.3 Treatment of Antibiotics

3.3.1 Antibiotics in the environment

Residences, hospitals, poultry farms and pharmaceutical industries can be given as main sources of antibiotics that are among specific pollutants. Antibiotics used for animal breeding can pass into soil and receiving waters by animal manure. It has been reported that only 60-80% of used antibiotics is by prescription and that the main source of antibiotics in the receiving media is human usage (Göbel et al., 2005). Antibiotics are adsorbed in tissues and undergo metabolic changes in the receiving

body; however the unmetabolized parent product is also excreted together with the biotransformation products (Boxall et al., 2004; Perez et al., 2005).

The hydrophilic structure of antibiotics enables their travel through water and makes it easier to reach the water reservoirs. Studies showed that elimination of antibiotics in wastewater treatment systems is not complete (Göbel et al., 2005; Xu et al., 2007, Golet et al., 2002; Li and Zhang, 2010). In this case, they are discharged into the surface waters and therefore able to reach the drinking water reservoirs.

Antibiotic concentrations detected in wastewaters can be classified as high and low concentrations. Wastewaters contaminated with antibiotics during the production level are classified high concentration antibiotic containing wastewaters, whereas wastewaters contaminated with antibiotics after usage are classified as low concentration antibiotic containing wastewaters.

In the literature there are studies that measured concentrations of antibiotics in the influent and the effluent of treatment plants and reported that the values are at ng/L to µg/L level (Drilla et al., 2005; Watkinson et al., 2007; Li and Zhang, 2010), µg/kg to mg/kg level in soil and sludge (Hamscher et al., 2002; Golet et al., 2003; Li and Zhang, 2010). Antibiotics that enter the wastewater treatment plants have the potential to affect the biomass in sewage systems. The inhibition of wastewater bacteria may seriously affect organic matter degradation; therefore, effects of antibiotics on the microbial population are of great interest (Kümmerer, 2009).

Other than the usage of antibiotics, pharmaceutical industries are also important sources of antibiotics in the environment. Pharmaceutical wastewaters contain high suspended solids concentrations and inert soluble organic matter. Moreover, pharmaceutical wastewaters having high chemical oxygen demand (COD) are either very alkaline or very acidic depending on the production at the industry and it is known that the substances in the wastewater have toxic effects on the biological community in the receiving media (Raj and Anjaneyulu, 2005).

Typical pharmaceutical wastewater has the COD, sulfate and total suspended solids (TSS) concentrations of 12.500 mg/L, 9.000 mg/L and 36.000 mg/L, respectively. Moreover the antibiotic concentrations in some point sources like hospital wastewaters and pharmaceutical wastewaters have been reported to be as high as 10 to 600 mg/L (Sponza and Celebi, 2012). Coagulation, chemical precipitation and

biological treatment by activated sludge systems can be given among the classical treatment methods of pharmaceutical wastewaters. Two stage chemical and biochemical treatment can be counted among the treatment strategies for the pharmaceutical wastewater (Raj and Anjaneyulu, 2005).

Bernard and Gray (2000) reported that compared to domestic wastewater treatment plant sludge, with a dense and strong flocculation characteristic; the floc structure in activated sludge systems treating pharmaceutical wastewater was weak and dispersed.

Elimination of pharmaceuticals in wastewater treatment plants is depended on many parameters like the sludge age, hydraulic retention time, temperature, pH, biomass concentration, polarity and biodegradability of the substance. It has been reported that there are different removal mechanisms of antibiotics in activated sludge systems. Among these abiotic and biotic processes can be given. Antibiotics bound to the activated sludge can be removed by adsorption (attachment to the surface) and absorption (diffusion into the solid phase) (Press-Kristensen, 2007).

3.3.2 Sulfamethoxazole

15% of Sulfamethoxazole is reported to be excreted from the body unmetabolized (Hirsch et al.,1999; Perez et al., 2005). Sulfamethoxazole concentration in German surface waters was measured between 30 and 85 ng/L (Hartig et al., 1999). It is one of the most commonly detected sulfonamides in wastewater (Göbel et al., 2007; Choi et al., 2008; Le-Minh et al., 2010). Sulfamethoxazole has the property to bind to soil organic matter by different mechanisms like cation bridging and cation exchange (Xu et al., 2011). In the literature there is no definitive information on the elimination of Sulfamethoxazole (Baran et al., 2011).

In biodegradability tests it has been determined that sulfamethoxazole was stable during the test period of 28 days (Gartiser et al., 2007; Alexy et al., 2004) and seen to be resistant to biodegradation (Garcia-Galan et al., 2008). On the other hand when sulfamethoxazole was fed to an activated sludge system operated as a sequencing batch reactor, the acclimated microbial culture was able to use the substance as the carbon and/or nitrogen source (Drillia et al., 2005). Drillia et al. (2005) investigated the removal of sulfamethoxazole simulating a common situation in wastewater treatment plants, i.e. presence of excess ammonium and readily biodegradable carbon

source. It has been found out that under these conditions the enzymes responsible for the removal of the antibiotic were inactive, and that if enough time was given for the synthesis of these enzymes, degradation of sulfamethoxazole was also possible under ammonium poor conditions. According to the results obtained from the study, it has been concluded that sulfamethoxazole can be removed in systems like extended aeration systems, where there is an absence of a readily biodegradable substrate. Moreover, according to Xu et al (2011), higher temperatures and higher humic acid content induced Sulfamethoxazole biodegradation, and they have also confirmed abiotic removal of the substance. Additionally, the study suggested that Sulfamethoxazole resistant bacteria *Bacillus firmus* and *Bacillus cereus* have the capacity to degrade Sulfamethoxazole in natural waters by high rates.

3.3.3 Tetracycline

Tetracycline antibiotics are known to be susceptible against light, therefore have the property to be degraded by photocatalytic reactions (Kümmerer, 2009). They were proved to be more stable in sediments. Moreover, the knowledge suggests that they remain in sediments for longer time periods, given that are is no known degradation mechanism of tetracyclines (Oka et al., 1989; Lunestad and Goksøyr, 1990, Kümmerer 2009). According to the study by Smith (2002), the tetracycline concentration in the Lee River near London was reported as 9.5 µg/L and 1 µg/L.

It has been determined that in activated sludge systems tetracycline is removed by sorption onto sludge (Gartiser et al., 2007, Kim et al., 2005) and that this removal mechanism may be the result of tetracycline's tendency to form very low solubility complexes by binding with divalent cations like calcium, magnesium, cadmium, cobalt and magnesium (Yamaguchi et al., 1990a; Alexy et al., 2004) and of their strong chelating capability (Chopra and Roberts, 2001). Alexy et al (2004) studied the biodegradability characteristics of antibiotics by Closed Bottle Biodegradability Test (OECD 301D). The obtained results showed tetracycline removal up to 75%.

Shi et al (2011) investigated removal of tetracycline in nitrifying granular systems by short term exposure to the substance and also for sorption and biodegradation of the substance. In order to determine short term effects the authors treated the biomass with 20 mg/L tetracycline and measured the specific oxygen utilization rates of heterotrophic, ammonia oxidizing bacteria and nitrite oxidizing bacteria using

glucose, sodium acetate and NH_4^+-N as carbon and nitrogen sources, respectively. They characterized the removal process by quick sorption and slow biodegradation of the compound. At initial tetracycline concentrations of 10, 20 and 30 mg/L, the system was shown to present high tetracycline removal rates. Additionally, they determined that presence COD and ammonia nitrogen (< 150 mg/L) enhanced the removal process. However, they determined that the short term effect of the substance is to inhibit the respirometric activities of the biomass.

3.3.4 Erythromycin

Erythromycin was reported to be resistant to biodegradation by Richardson and Bowron (1985) and to be excreted from the body unaltered (Göbel et al., 2005). On the other hand high removal efficiencies of erythromycin in activated sludge systems operated with high sludge ages were reported, which shows that different reactor configurations have effects on the removal of erythromycin. Studies on the biological removal of erythromycin showed that in membrane bioreactors erythromycin was removed with 67% of removal efficiency (Radjenovic et al., 2007), whereas in completely mixed reactors efficiencies this high were not obtainable (Radjenovic et al., 2007; Göbel et al., 2007).

Giger et al (2003), reported that in wastewater treatment plants complete removal of macrolide antibiotics was not possible and therefore residual antibiotics accumulate in the receiving water bodies. In order to minimize the antibiotic concentrations in the receiving media, the wastewater treatment plant effluent antibiotic concentrations have to be minimized. According to Giger et al (2003) another method to lower the antibiotic concentrations in the receiving media was to minimize the amount of antibiotic containing wastewater at the source.

Louvet et al (2010) studied the effect of erythromycin on activated sludge biomass flock structure. They monitored the reactors for 24 hours and fed the system with 10 mg/L erythromycin. Obtained results showed that the substance was toxic to the biomass and that it destroyed the flock structure.

3.4 Enzyme Inhibition

Chemical reactions in biological systems are mediated by enzymes, catalysts that lower the activation energy of a reaction. Enzymes are highly specific for particular

reactions and they carry out different reactions like hydrolysis, polymerization, oxidation-reduction, isomerization etc. However substances, called inhibitors, have the ability to bind with the enzyme influencing the binding of the substrate to the enzyme and reduce the enzymes activity, and there are different mechanisms that inhibitor substances can act (Voet and Voet, 1990).

3.4.1 Competitive inhibition

In this type of inhibition, the inhibitor substance acts as the substrate and competes with the substrate for the enzymatic-binding site. These types of inhibitors are called competitive inhibitors and they resemble the substrate. When bound to the enzyme active site the enzyme becomes unreactive. The model for competitive inhibition is given in the following reaction scheme:

$$E + S \overset{k_1}{\leftrightarrow} ES \overset{k_2}{\rightarrow} P + E \quad \textbf{(3.1)}$$

$$E + I \overset{K_I}{\leftrightarrow} EI \quad \textbf{(3.2)}$$

$$EI + S \rightarrow no\ reaction \quad \textbf{(3.3)}$$

By competitive inhibition it is assumed that the competitive inhibitor reversibly binds to the enzyme active site and the enzyme-inhibitor complex is catalytically inactive (Voet and Voet, 1990). The competitive inhibitor reduces the active enzyme concentration available for substrate binding, leading to increased half saturation constants in the system. The dissociation constant (K_I) is defined by:

$$K_I = \frac{[E][I]}{[EI]} \quad \textbf{(3.4)}$$

The competitive inhibition can however be overcome by increasing the substrate concentration, therefore lowering the chances of the inhibitor to compete with the substrate for the enzyme active site. The effect of competitive inhibition on enzyme reaction is given in Figure 3.1.

3.4.2 Non-competitive inhibition

In contrary to competitive inhibition, by non-competitive inhibition the effects of inhibition cannot be reversed by increasing the substrate concentration (Orhon and Artan, 1994).

Figure 3.1 gives the effect of non-competitive inhibition on the enzyme reaction. In non-competitive inhibition a portion of the enzyme concentration is blocked by the inhibitor that binds to a site other than the active site of the enzyme. It results in a decreased maximum growth rate of the system, where the dissociation constant (K_I) is defined by:

$$\boldsymbol{K_I = \frac{[E_0'][I]}{[EI]}} \qquad \textbf{(3.5)}$$

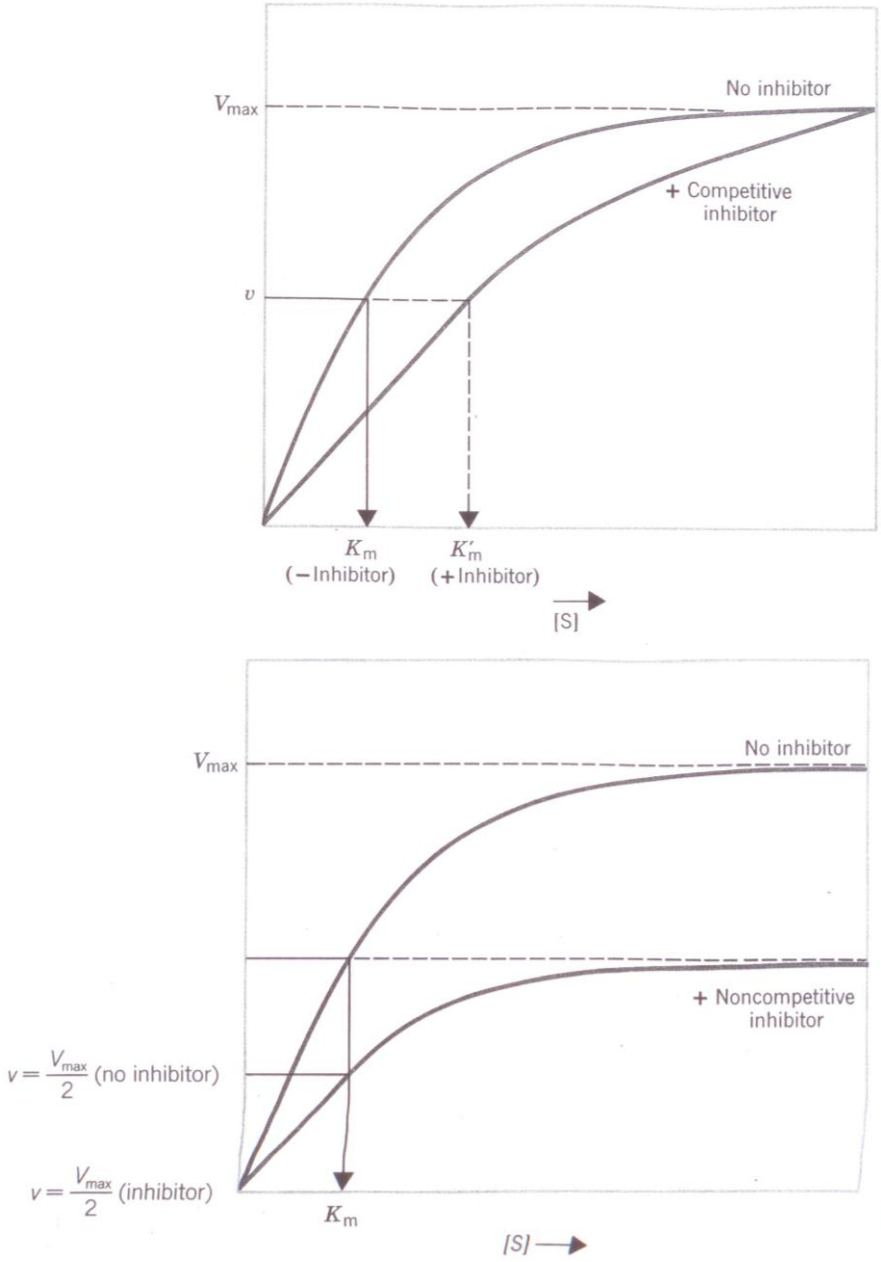

Figure 3.1: Effect of competitive and non-competitive inhibitors on the enzyme kinetics (Conn et al., 1987).

3.4.3 Un-competitive inhibition

In un-competitive inhibition the inhibitor substance binds to the enzyme-substrate complex, and not to the free enzyme. Moreover the uncompetitive inhibitor like the noncompetitive inhibitor binds to a separate site than the active site. The kinetic scheme for uncompetitive inhibition is given in the following reaction scheme:

$$\boldsymbol{E + S \overset{k_1}{\leftrightarrow} ES \overset{k_2}{\rightarrow} P + E} \quad \textbf{(3.6)}$$

$$\boldsymbol{ES + I \overset{K_I}{\leftrightarrow} ESI} \quad \textbf{(3.7)}$$

$$\boldsymbol{ESI \rightarrow no\ reaction} \quad \textbf{(3.8)}$$

, where the dissociation constant (K_I) is defined by:

$$\boldsymbol{K_I = \frac{[ES][I]}{[ESI]}} \quad \textbf{(3.9)}$$

Since the uncompetitive inhibitor does not need to resemble the substrate while binding with the enzyme, it causes structural damage to the enzyme active site and increases the apparent affinity of the enzyme to the substrate, therefore lowering the K_S (Boyer, 2006). Moreover the maximum growth rate of the system decreases, since it takes longer time for the product to leave the enzyme active site.

Uncompetitive inhibition affects the enzymes catalytic function; however it does not have an effect on its substrate binding properties. This type of inhibition is especially important for multi-substrate enzymes (Voet and Voet, 1990).

The effects of un-competitive inhibition cannot be reversed by increasing the substrate concentration, however at low substrate concentrations, where $[S] \ll K_M$, the effect of uncompetitive inhibition becomes negligible (Voet and Voet, 1990). Figure 3.2 gives the effect of un-competitive inhibition on the enzyme reaction.

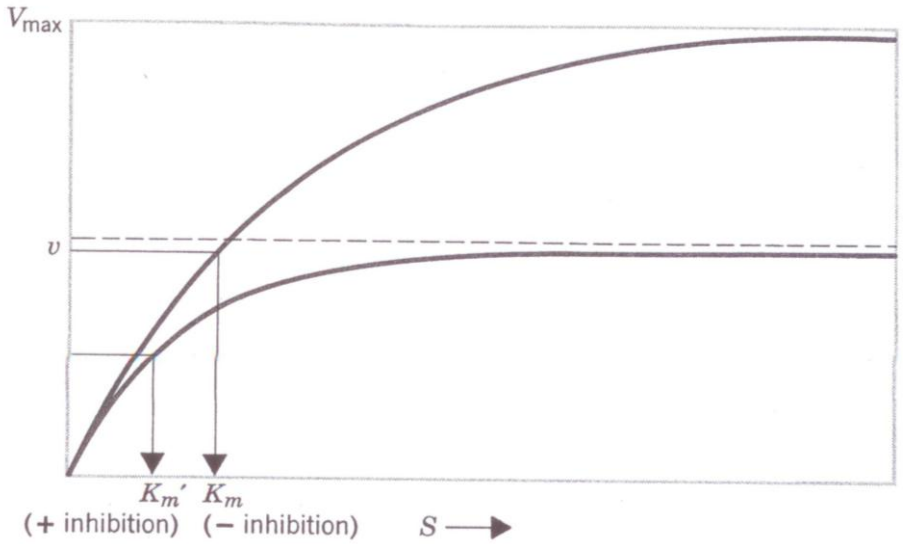

Figure 3.2: Effect of un-competitive inhibitors on the enzyme kinetics (Conn et al., 1987).

3.4.4 Mixed inhibition

Mixed inhibition is a type of inhibition where the inhibitor binds to both free enzyme and the enzyme-substrate complex. It is a combination of competitive and un-competitive inhibition. The model for mixed inhibition is given in the following reaction scheme:

$$\boldsymbol{E + S \overset{k_1}{\leftrightarrow} ES \overset{k_2}{\rightarrow} P + E} \quad \textbf{(3.10)}$$

$$\boldsymbol{E + I \overset{K_I}{\leftrightarrow} ESI} \quad \textbf{(3.11)}$$

$$\boldsymbol{EI \rightarrow no\ reaction} \quad \textbf{(3.12)}$$

$$\boldsymbol{ES + I \overset{K_I'}{\leftrightarrow} ESI} \quad \textbf{(3.13)}$$

$$\boldsymbol{ESI \rightarrow no\ reaction} \quad \textbf{(3.14)}$$

The effect of mixed inhibition on the system is that both maximum growth rate and the half saturation constants are affected, so that whereas the maximum growth rate decreases, the half saturation constant increases (Storrey, 2004).

3.5 Respirometry

Two main research points in toxicity/inhibition works can be found in the literature. One of which is the determination of specific pollutant concentrations and the other one is the determination of the concentrations and their biodegradability in biological

treatment systems. In these studies, either only the substance or collective parameters were measured. Especially in biological treatment systems, this approach leads to characterization of the response of the biomass only on substrate removal.

Nowadays, in the studies on activated sludge systems respirometric methods are preferred instead of characterizing the system over substrate removal. The reason for this is that the change in the oxygen utilization rates (OUR) gives a better insight to the response of the biomass than substrate removal efficiency, because oxygen consumption is directly related to both substrate utilization and biomass production (Vanrolleghem, 2002).

Wastewaters flowing into activated sludge systems are complex substrates that are combinations of various compounds and different metabolic processes are required for their breakdown. However, evaluating all the kinetic processes in the system is made possible with respirometry. Respirometry is measuring and interpreting biological oxygen consumption under defined conditions (Vanrolleghem, 2002). The results obtained from respirometry are being compared with substrate removal efficiencies and the all the data is evaluated with a multicomponent point of view. Finally, obtained oxygen utilization rate (OUR) profiles are evaluated with mathematical models. By comparing the change in model parameters it is also possible to determine the level of inhibition.

Respirometry may be specifically designed for the differentiation of different chemical oxygen demand (COD) fractions in the substrate (Ekama et al., 1986; Orhon et al., 2002) or for the assessment of specific kinetic and stoichiometric coefficients such as the maximum heterotrophic specific growth rate (Kappeler and Gujer, 1992), the endogenous decay rate (Avcioglu et al., 1998) or the storage yield (Karahan-Gul et al., 2002). The OUR profile may also be conveniently calibrated using a suitable activated sludge model to yield the most appropriate values for the kinetic and stoichiometric coefficients associated with different biochemical processes defined in the selected model.

Ekama et al. (1986) pioneered the usage of OUR profiles for the determination of biodegradable COD fractions and model parameters. Later OUR profiles were started to be used in many areas and especially for the experimental determination of process kinetics (Sollfrank and Gujer, 1991; Kappeler and Gujer, 1992; Spanjers and

Vanrolleghem, 1995; Avcıoglu et al., 1998; Cokgor et al., 1998; Sozen et al., 1998; Karahan-Gul et al., 2002; Insel et al., 2003). Nowadays, respirometric techniques are used commonly for the determination of activated sludge behavior. The response of the biomass to any inhibitory substance is observed by the change in substrate utilization and/or in maximum growth conditions. This observation is obtained by OUR profiles from batch experiments (Ellis et al., 1996; Guissesola et al., 2003). OUR profile sets an appropriate basis for the evaluation of inhibition for activated sludge (Insel et al., 2006).

In this context, using OUR profiles obtained by adding antibiotics on the biomass at high concentrations, characterizing pharmaceutical wastewater, the acute and chronic effects of antibiotics on the activated sludge culture were investigated.

In order to determine the applicable concentrations a concentration screening test has been applied. ISO8192 Respiration inhibition has been implemented for this purpose. However inhibition tests like ISO 8192 were shown to be misleading since the comparison of inhibited and control OUR's are reported at certain specific time points during the test (Insel et al., 2006), and these tests do not provide detailed information like complete OUR profiles. For this reason ISO 8192 has not been used for the characterization of the response of the activated sludge culture. Antibiotic concentrations obtained from ISO8192 experiments have only been used as an indicator.

3.6 Activated Sludge Modeling

The purpose of using dynamic models is to design treatment plants, to optimize and control plant operation. Generally the models in use today are deterministic, which give a realistic approach to the treatment process (Henze, 2005). The elements of a model contain biological and chemical processes, like growth and decay of heterotrophic biomass, together with hydraulics, components, like the biomass (X_H) or soluble readily biodegradable COD (S_S) and transport processes, which is only about the transportation of water inside the plant. (Henze, 2005).

Model evaluation of activated sludge systems enables to (i) identify all the microbial processes involved for the biodegradation of the selected substrate; (ii) visualize the impact of inhibition on each process; and (iii) quantify numerical terms the impact of

inhibition by assessing the change in the values of relevant model coefficients after addition of the selected inhibitor. It also helps to visualize the overall impact of the inhibitory compound on every stage of substrate biodegradation, through inspection and evaluation of the entire OUR profile (Insel et al., 2002).

In 1987, The International Association on Water Quality task group released the IAWQ Activated Sludge Model No.1, which ended up being the base of all the subsequent models (Henze, 2005). ASM1 is a very simple model, which can be expanded according to the systems requirements. Therefore in order to solve a system, complex kinetic equations and different components can be added to the ASM1 in order to increase the degree of complexity (Henze, 2005).

3.6.1 Wastewater characterization in activated sludge modeling

The wastewater carbon content characterization is done according to the biodegradability characteristics of the carbon fragments in the wastewater. The total influent COD (C_T) having two major components represents the total substrate for the activated sludge biomass. A schematic distribution is given in Figure 3.3.

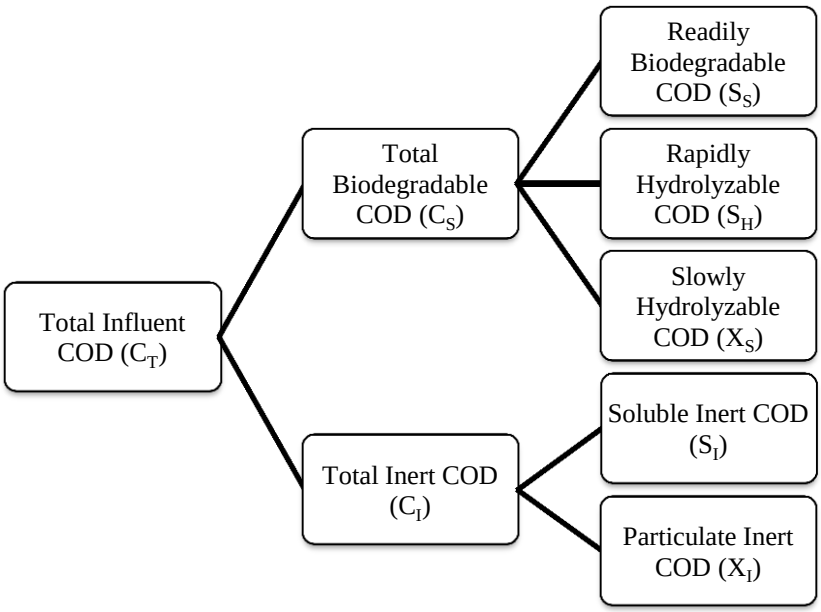

Figure 3.3: Distribution of COD fractions in wastewater (Orhon and Artan, 1994).

The two components of C_T are the total biodegradable COD (C_S) and the total non-biodegradable COD (C_I) fractions. One of which, the non-biodegradable COD fraction leaves the system without being processes in any biochemical reaction. However whereas the soluble part of the inert COD fraction (S_I) stays in the soluble fragment and py-passes the system, the particulate inert COD fraction (X_I) leaves the

system via waste sludge accumulating in the activated sludge biomass (Orhon and Artan, 1994).

The biodegradable fraction of the total COD (C_S), is further divided into three major fractions, readily biodegradable COD (S_S), rapidly hydrolysable COD (S_H) and slowly biodegradable COD (X_S) (Orhon and Artan, 1994).

The readily biodegradable COD (S_S) is assumed to be soluble and consistent of simple compounds that can be directly used by the organism for synthesis reactions. However both the rapidly hydrolysable COD (S_H) and the slowly biodegradable COD (X_S) consist of larger and more complex organic particles that need to be hydrolyzed prior to absorption by the bacteria (Orhon and Artan, 1994).

3.6.2 Activated sludge model no. 1

ASM1 includes both nitrification and denitrification and is basically designed for domestic and municipal wastewater. However it is used for industrial wastewaters by careful calibration of the model parameters (Henze, 2005). Schematic view of the biological processes taking place in an activated sludge system according to ASM1 is can be seen in Figure 3.4.

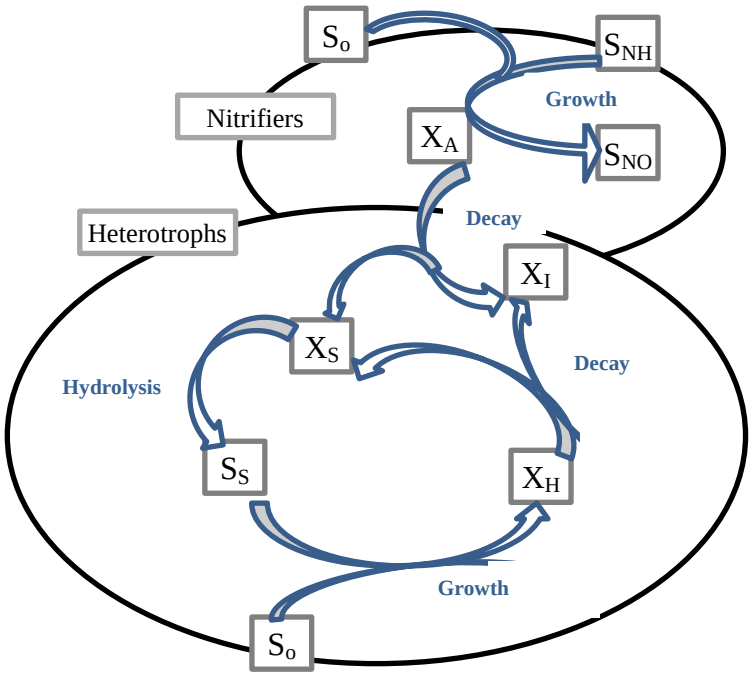

Figure 3.4: Process for heterotrophic and nitrifying bacteria in ASM1 **(**Gujer et al., 1999).

3.6.2.1 Process kinetics for carbon removal

IWAQ ASM1 has different processes to explain the behavior of an activated sludge system. Since the model includes nitrification and denitrification along with carbon removal the processes include microbial growth and decay of autotrophic and denitrifying organisms, as well as aerobic metabolic activities of heterotrophic bacteria.

In the model there are two processes associated with carbon removing heterotrophic bacteria; aerobic growth and decay of heterotrophic bacteria. For the aerobic growth process the bacteria can only utilize the readily biodegradable substrate (S_S) as the carbon source for growth, during which the bacteria utilize oxygen (S_O) as the final electron acceptor. The reaction is modeled according to the Monod Kinetics, where K_S and K_{OH} are the half saturation constants of S_S and S_O, respectively:

$$\frac{dX_H}{dt} = \mu'_H \left(\frac{S_S}{K_S+S_S}\right)\left(\frac{S_O}{K_{OH}+S_O}\right) X_H \qquad \textbf{(3.15)}$$

Only the readily biodegradable substrate (S_S) is utilized by the bacteria for growth, which decreases its concentration. However rapidly hydrolysable (S_H) and slowly biodegradable substrates (X_S), contained in the wastewater, need to be hydrolyzed in order for them to be utilized by the bacteria in the growth process. Hydrolysis of these COD fractions increases the concentration of S_S. Therefore the transformation of S_H and X_S into S_S takes place as the hydrolysis of rapidly hydrolysable and slowly biodegradable substrates (Orhon and Artan, 1994). Equations 3.16, 3.17 and 3.18 represent the removal of S_H, X_S and S_S, respectively:

$$\frac{dS_H}{dt} = \left[-k_h \left(\frac{S_H/X_H}{K_X+\left(S_H/X_H\right)}\right)\left(\frac{S_O}{K_{OH}+S_O}\right)\right] X_H \qquad \textbf{(3.16)}$$

$$\frac{dX_S}{dt} = \left[-k_{hX} \left(\frac{X_S/X_H}{K_{XX}+\left(X_S/X_H\right)}\right)\left(\frac{S_O}{K_{OH}+S_O}\right)\right] X_H \qquad \textbf{(3.17)}$$

$$\frac{dS_S}{dt} = \left(\left[-\frac{\mu'_H}{Y_H}\left(\frac{S_S}{K_S+S_S}\right)\left(\frac{S_O}{K_{OH}+S_O}\right)\right] + \left[k_{hX}\left(\frac{X_S/X_H}{K_{XX}+\left(X_S/X_H\right)}\right)\left(\frac{S_O}{K_{OH}+S_O}\right)\right] + \left[k_h\left(\frac{S_H/X_H}{K_X+\left(S_H/X_H\right)}\right)\left(\frac{S_O}{K_{OH}+S_O}\right)\right]\right) X_H \qquad \textbf{(3.18)}$$

, where Y_H is the yield coefficient, which represent the amount of COD used for biosynthesis.

Decay of heterotrophic bacteria can be defined as the loss of microbial biomass, which mathematically can be explained in a first order differential equation (Orhon and Artan, 1994):

$$\frac{dX_H}{dt} = b_H X_H \quad \textbf{(3.19)}$$

Therefore the general equation for the net amount of aerobic growth of heterotrophic bacteria is:

$$\frac{dX_H}{dt} = \left[\mu'_H \left(\frac{S_S}{K_S+S_S}\right)\left(\frac{S_O}{K_{OH}+S_O}\right) - b_H\right] X_H \quad \textbf{(3.20)}$$

During endogenous decay a fraction of the decayed biomass cannot be degraded completely and accumulates in the sludge, which forms the particulate inert organic products (X_P) (Orhon and Artan, 1994):

$$\frac{dX_P}{dt} = -f_{EX}\frac{dX_H}{dt} = f_{EX} b_H X_H \quad \textbf{(3.21)}$$

Moreover the endogenous decay of microorganisms also results in formation of soluble inert products (S_P) that cannot be further oxidized (Orhon and Artan, 1994):

$$\frac{dS_P}{dt} = -f_{ES}\frac{dX_H}{dt} = f_{ES} b_H X_H \quad \textbf{(3.22)}$$

$$f_E = f_{EX} + f_{ES} \quad \textbf{(3.23)}$$

The final electron acceptor, oxygen (S_O), in activated sludge systems, is utilized throughout the whole process. Oxygen is used for growth and decay processes.

$$\frac{dS_O}{dt} = \left[-\frac{1-Y_H}{Y_H}\mu'_H\left(\frac{S_S}{K_S+S_S}\right)\right] - (1-f_E) b_H X_H \quad \textbf{(3.24)}$$

Finally the ammonia nitrogen (S_{NH}) is incorporated into the biomass by i_{XB} during growth, which can be considered as the potential nitrogen removal of carbon removal (Orhon and Artan, 1994). Moreover the nitrogen in the biomass is being released into the wastewater as the biomass is being decayed. Utilization of S_{NH} is also in expense of some alkalinity.

$$\frac{dS_{NH}}{dt} = \left[-i_{XB}\mu'_H\left(\frac{S_S}{K_S+S_S}\right)\left(\frac{S_O}{K_{OH}+S_O}\right)\right] + i_{XB}(1-f_E)b_H X_H \quad \textbf{(3.25)}$$

The matrix representation of ASM No.1can be found in Table 3.2.

3.6.3 Activated sludge model no. 3

10 years after the release of ASM1 the IWAQ Task Group on Mathematical Modeling for Design and Operation of Biological Wastewater Treatment Processes introduced a new model, which overcame the weaknesses of ASM1. The ASM3, included a storage process, which has been seen in some aerobic and anoxic conditions in activated sludge plants (Gujer et al., 1999).

Internal storage compounds like polyhydroxyalkanoates (PHA) and glycogen (GLY) were present in aerobic and anoxic processes. Therefore the in ASM1 absent storage process it was added to ASM3 (Gujer et al., 1999). Schematic view of the biological processes taking place in an activated sludge system according to ASM3 is can be seen in Figure 3.5.

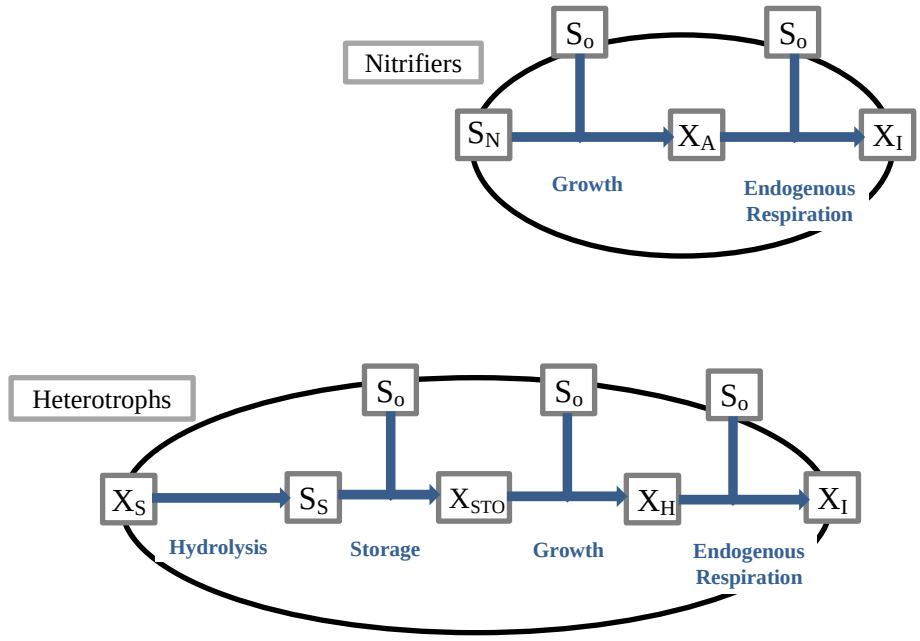

Figure 3.5: Process for heterotrophic and nitrifying bacteria in ASM3 (Gujer et al., 1999).

Table 3.2: Matrix representation of activated sludge model no.1.

Components→ Processes↓	S_O	S_S	S_H	X_S	X_H	X_P	S_P	S_{NH}	S_{Alk}	Rate Equations
Growth of X_H	$-\frac{1-Y_H}{Y_H}$	$-\frac{1}{Y_H}$			1			$-i_{XB}$	$-\frac{i_{XB}}{14}$	$\mu'_H\left(\frac{S_S}{K_S+S_S}\right)\left(\frac{S_O}{K_{OH}+S_O}\right)X_H$
Hyrolysis of S_H		1	-1							$k_h\left(\frac{S_H/X_H}{K_X+\left(S_H/X_H\right)}\right)\left(\frac{S_O}{K_{OH}+S_O}\right)X_H$
Hydrolysis of X_S		1		-1						$k_{hX}\left(\frac{X_S/X_H}{K_{XX}+\left(X_S/X_H\right)}\right)\left(\frac{S_O}{K_{OH}+S_O}\right)X_H$
Decay of X_H	$-(1-f_E)$				-1	f_{EX}	f_{ES}	$i_{XB}(1-f_{EX})$		$b_H X_H\left(\frac{S_O}{K_{OH}+S_O}\right)$
Parameters	O_2	COD	COD	COD	cell COD	COD	COD	NH_3-N		

The metabolism of storage suggests that it occurs under two different conditions, one of which includes cases where electron donors and acceptors are separately available, like in polyphosphate accumulating organisms (PAOs) and glycogen accumulating organisms (GAOs). The other is when the microorganisms are not subjected to a continuous substrate flow, which is a more general reason of internal storage concerning non-steady state conditions (Reis et al., 2003).

Dawes (1990), states that ceasing of protein synthesis results in high concentrations of NADH, which inhibits the enzyme citrate synthase. The enzyme citrate synthase is a key enzyme in the tricarboxylic acid (TCA) cycle. According to Doi (1990), acetyl-CoA cannot enter the TCA cycle under unbalanced conditions. Therefore the inhibition of the enzyme citrate synthase causes acetyl-CoA's inability to enter the TCA cycle. Finally the excess acetyl-CoA in the cell is used as substrate for PHA synthesis, a substance, which serves as a carbon or energy source during starvation periods (Punrattanasin, 2001).

Another storage product glycogen is a branched polymer consisting of glucose monomers and its granules are smaller than of PHA, straight-chain polymer (Prescott et al., 1990). It is formed if the primary substrate is glucose or a compound that can be converted to pyruvate are present in the wastewater, where glucose is taken into the cell and converted into glycogen (van Loosdrecht et al., 1997). Glycogen storage mechanism is used to balance the growth process under dynamic conditions (Dircks et al., 2001). The stored glycogen then serves as an energy source in the famine conditions.

3.6.3.1 Process kinetics for carbon removal

ASM3 incorporated the internal storage of heterotrophic bacteria into the model, in which the internal storage product (PHA or GLY) are associated with X_H, however they are not included into the mass of X_H. They are considered separately as X_{STO} (mgCOD/L).

The assumption of ASM3 is that the readily biodegradable substrate (S_S) is first stored as internal storage product and then utilized as substrate for biosynthesis. The storage process describes the storage of S_S as X_{STO}, and the energy required for this process is gained from aerobic respiration, utilizing oxygen (S_O) (Gujer et al., 1999). Moreover the internal storage products are assumed to be decayed together with the

biomass during endogenous respiration phase. Finally, the storage yield coefficient (Y_{STO}) gives the amount of substrate converted into storage products under aerobic conditions.

As described in ASM3, the readily biodegradable substrate is directly being stored by the microorganisms as X_{STO} (Gujer et al., 1999), with a maximum storage rate of k_{STO} and storage yield of Y_{STO},

$$\frac{dS_S}{dt} = -k_{STO}\left(\frac{S_S}{K_S+S_S}\right)\left(\frac{S_O}{K_{OH}+S_O}\right)X_H \quad \textbf{(3.26)}$$

$$\frac{dX_{STO}}{dt} = Y_{STO}k_{STO}\left(\frac{S_S}{K_S+S_S}\right)\left(\frac{S_O}{K_{OH}+S_O}\right)X_H \quad \textbf{(3.27)}$$

Growth of heterotrophic biomass under aerobic conditions is depended on the X_{STO} concentration since the biomass will use the stored polymers as substrate for biosynthesis (Gujer et al., 1999).

$$\frac{dX_H}{dt} = \mu_H\left(\frac{X_{STO}/X_H}{K_{STO}+X_{STO}/X_H}\right)\left(\frac{S_O}{K_{OH}+S_O}\right)X_H \quad \textbf{(3.28)}$$

Finally, degradation of the storage compounds is depended on the heterotrophic yield coefficient (Y_H):

$$\frac{dX_{STO}}{dt} = \frac{\mu_H}{Y_H}\left(\frac{X_{STO}/X_H}{K_{STO}+X_{STO}/X_H}\right)\left(\frac{S_O}{K_{OH}+S_O}\right)X_H \quad \textbf{(3.29)}$$

The matrix representation of ASM No.3 can be found in Table 3.3.

Table 3.3: Matrix representation of activated sludge model no.3.

Components→ Processes↓	S_O	S_S	S_H	X_S	X_H	X_P	S_P	X_{STO}	S_{NH}	S_{Alk}	Rate Equations
Growth of X_H	$-\frac{1-Y_H}{Y_H}$				1			$-\frac{1}{Y_H}$	$-i_{XB}$	$-\frac{i_{XB}}{14}$	$\mu'_H\left(\frac{S_S}{K_S+S_S}\right)\left(\frac{S_O}{K_{OH}+S_O}\right)X_H$
Hyrolysis of S_H		1	-1								$k_h\left(\frac{S_H/X_H}{K_X+\left(S_H/X_H\right)}\right)\left(\frac{S_O}{K_{OH}+S_O}\right)X_H$
Hydrolysis of X_S		1		-1							$k_{hX}\left(\frac{X_S/X_H}{K_{XX}+\left(X_S/X_H\right)}\right)\left(\frac{S_O}{K_{OH}+S_O}\right)X_H$
Storage of X_{STO}	$-(1-Y_{STO})$	-1						Y_{STO}			$k_{STO}\left(\frac{S_S}{K_S+S_S}\right)\left(\frac{S_O}{K_{OH}+S_O}\right)X_H$
Degradation of X_{STO}	-1							-1			$b_{STO}X_{STO}\left(\frac{S_O}{K_{OH}+S_O}\right)$
Decay of X_H	$-(1-f_E)$				-1	f_{EX}	f_{ES}		$i_{XB}(1-f_{EX})$		$b_H X_H\left(\frac{S_O}{K_{OH}+S_O}\right)$
Parameters	O_2	COD	COD	COD	cell COD	COD	COD		NH_3-N		

3.7 Effect of Inhibition Types on Respirometric Profiles

3.7.1 Competitive inhibition

In the situation, where competitive inhibition is present the mass balance for enzyme components is given as, where the amount of ES complex is the amount left from unbound enzyme and the EI complex (Orhon and Artan, 1994):

$$\boldsymbol{ES = E_0 - E - EI} \tag{3.30}$$

Using both equations the ES complex can be defines as (Orhon and Artan, 1994):

$$\boldsymbol{ES = \frac{E_0 S}{K_S\left(1+\frac{I}{K_I}\right)+S}} \tag{3.31}$$

, which changes the basic rate equation for substrate utilization to (Orhon and Artan, 1994):

$$\boldsymbol{\frac{dS}{dt} = -\frac{\hat{\mu}}{Y}\frac{S \,.\, X}{K_S\left(1+\frac{I}{K_I}\right)+S}} \tag{3.32}$$

, which means that the maximum growth rate of the system is left unchanged. However competitive inhibition effects the half saturation constant of the system and increases it by $\left(1 + \frac{I}{K_I}\right)$. This leads to the concept of apparent K_S (K_S') (Orhon and Artan, 1994):

$$\boldsymbol{K_S' = K_S\left(1 + \frac{I}{K_I}\right)} \tag{3.33}$$

The effect of competitive inhibition on the OUR curve is given in Figure 3.6. It can be seen that the system reaches endogenous decay level after the uninhibited system, however in this case the area under the curve stays however unchanged. In recent biochemical models incorporating dissolved oxygen (S_O) as the main model parameter, the corresponding oxygen uptake rate (OUR) expression becomes:

$$\boldsymbol{OUR_{CI} = -\left(\frac{1-Y_H}{Y_H}\right)\hat{\mu}\frac{S}{K_S\left(\frac{K_I+I}{K_I}\right)+S}X_H} \tag{3.34}$$

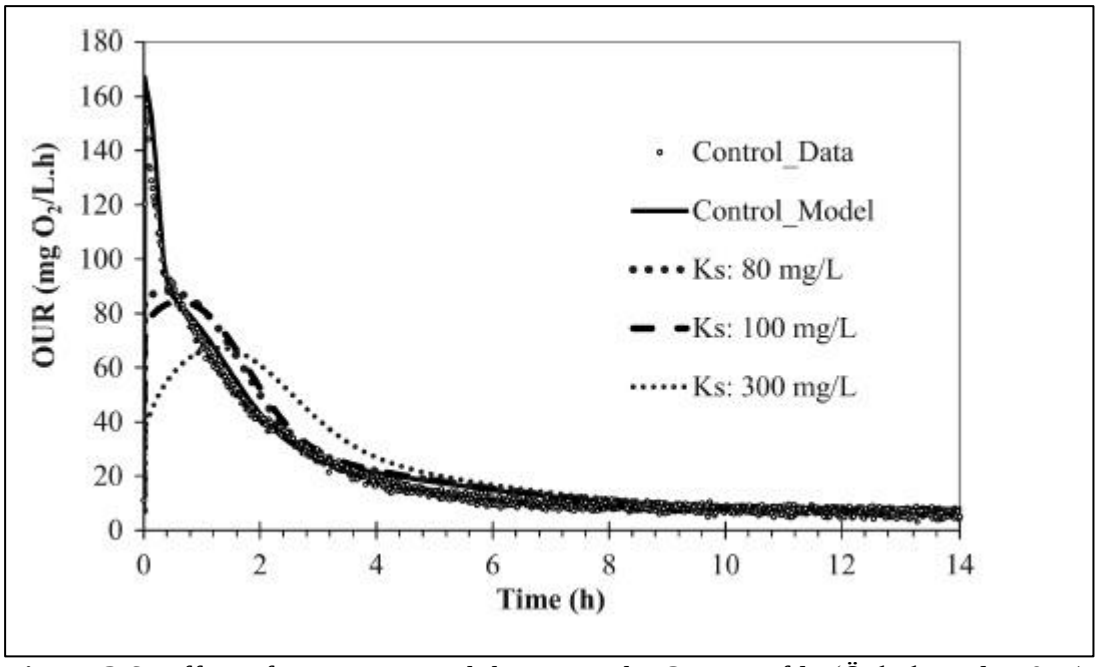

Figure 3.6: Effect of competitive inhibition on the OUR profile (Özkök et al., 2011).

3.7.2 Non-competitive inhibition

A portion of the initial enzyme concentration is blocked by the inhibitor substance:

$$E_0' = E_0 - EI = E + ES \tag{3.35}$$

, which leads to the definition of the dissociation constant K_I (Orhon and Artan, 1994):

$$K_I = \frac{[E_0'][I]}{[EI]} \tag{3.36}$$

In non-competitive inhibition the half saturation constant stays unchanged; however the maximum growth rate decreases.

Using both equations the ES complex can be defined as (Orhon and Artan, 1994):

$$ES = \frac{E_0\left(\frac{K_I}{1+K_I}\right)S}{K_S+S} \tag{3.37}$$

, which changes the basic rate equation for substrate utilization to (Orhon and Artan, 1994):

$$\frac{dS}{dt} = -\frac{\hat{\mu}}{Y}\left(\frac{K_I}{1+K_I}\right)\frac{S\,.\,X}{K_S+S} \tag{3.38}$$

, which means that in non-competitive inhibition the half saturation constant is left unaltered. However the maximum growth rate of the system decreases by $\left(\frac{K_I}{1+K_I}\right)$ ($\widehat{\mu'}$):

$$\widehat{\boldsymbol{\mu}'} = \widehat{\boldsymbol{\mu}}\left(\frac{\boldsymbol{K_I}}{\boldsymbol{1+K_I}}\right) \quad \textbf{(3.39)}$$

The effect of non-competitive inhibition on the OUR curve is given in Figure 3.7. Like in competitive inhibition it can be seen that under the effect of non-competitive inhibition the system reaches endogenous decay level later than that of the uninhibited system, in which case the area under the curve stays unchanged. The following rate expression defines the resulting OUR:

$$\boldsymbol{OUR_{NCI}} = -\left(\frac{\boldsymbol{1-Y_H}}{\boldsymbol{Y_H}}\right)\widehat{\boldsymbol{\mu}}\left(\frac{\boldsymbol{K_I}}{\boldsymbol{I+K_I}}\right)\frac{\boldsymbol{S}}{\boldsymbol{K_S+S}}\boldsymbol{X_H} \quad \textbf{(3.40)}$$

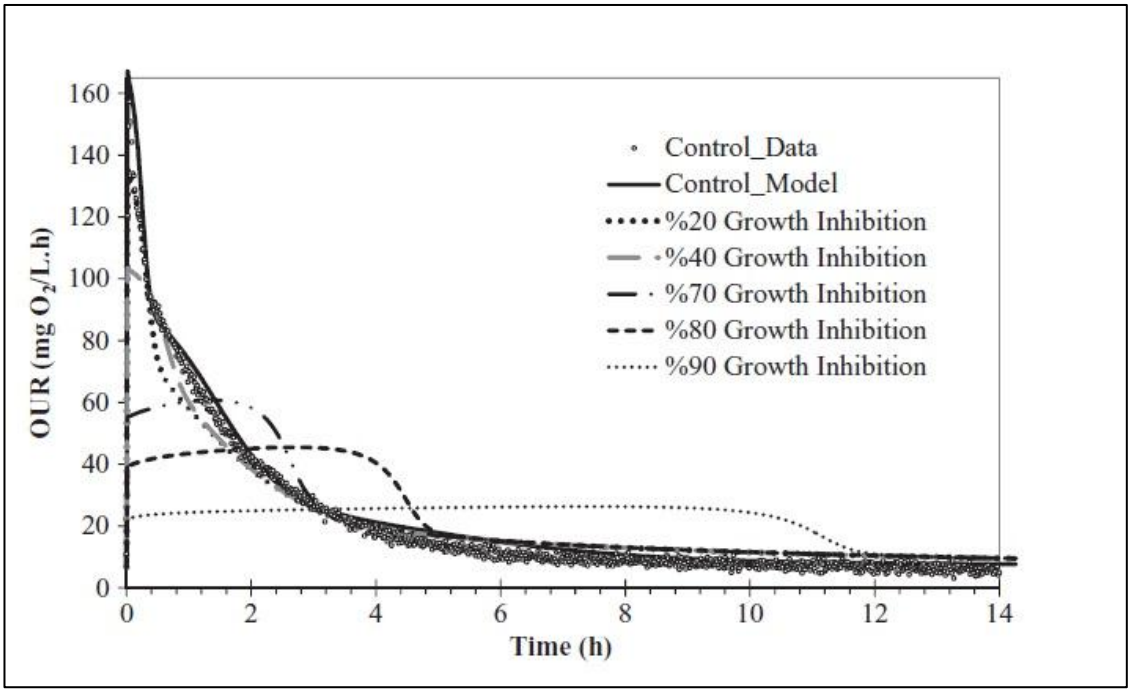

Figure 3.7: Effect of non-competitive inhibition (growth inhibition) on the OUR profile (Özkök et al., 2011).

3.7.3 Un-competitive inhibition

Figure 3.8 shows the effect of uncompetitive inhibition on the OUR profile. It can be seen that the inhibited profile clearly shows that with increasing inhibition the area under the curve is getting smaller; meaning amount of oxygen is consumed in each

degree of uncompetitive inhibition. Additionally, all the curves reach the endogenous decay level same time as the control system. Moreover,

Figure 3.8 also shows the effect of lower substrate additions on the OUR profile. Since in uncompetitive inhibition, the inhibitor (I) attacks the enzyme substrate sites, [ES], and forms an [ESI] complex, which does not undergo further biochemical reactions and this way, it blocks a part of the available substrate for biodegradation, as indicated by the following kinetic expression:

$$OUR_{UCI} = -\left(\frac{1-Y_H}{Y_H}\right)\hat{\mu}\left(\frac{K_I}{I+K_I}\right)\frac{S}{K_S\left(\frac{K_I}{I+K_I}\right)+S}X_H \qquad \textbf{(3.41)}$$

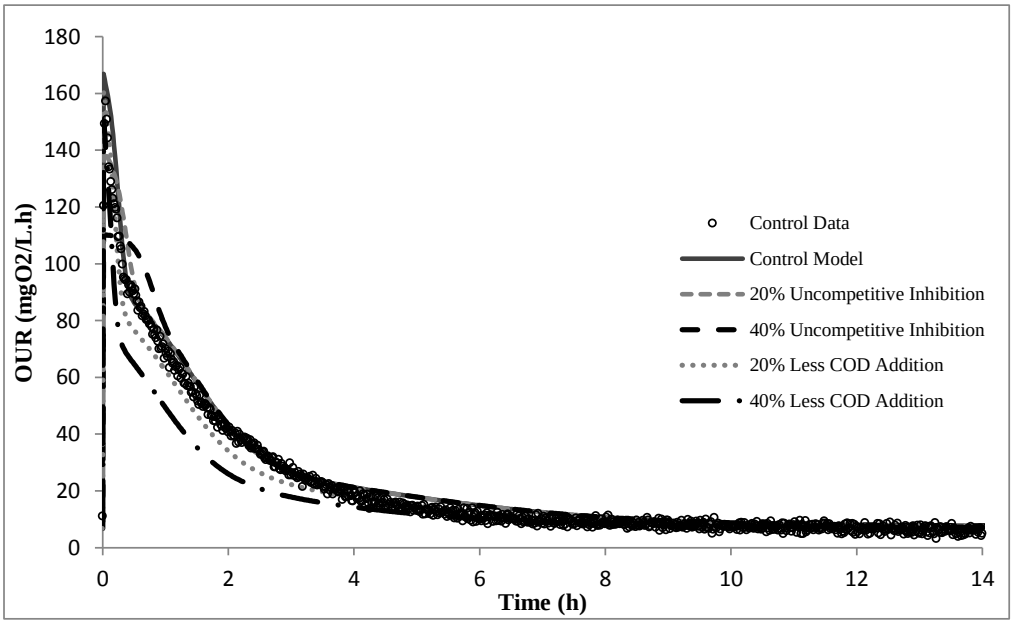

Figure 3.8: Effect of un-competitive inhibition on the OUR profile.

3.7.4 Mixed inhibition

The effect of mixed inhibition on the OUR curve is given in

Figure **3.9**. It can be seen that the system reaches the endogenous decay level later than that of the non-inhibited system, however the area under the OUR curve is kept unchanged. The kinetic effect of mixed inhibition on the OUR expression is as in the following equation:

$$OUR_{MI} = -\left(\frac{1-Y_H}{Y_H}\right)\hat{\mu}\frac{S}{K_S\left(\frac{K_I+I}{K_I}\right)+S\left(\frac{K_I+I}{K_I}\right)}X_H \qquad \textbf{(3.42)}$$

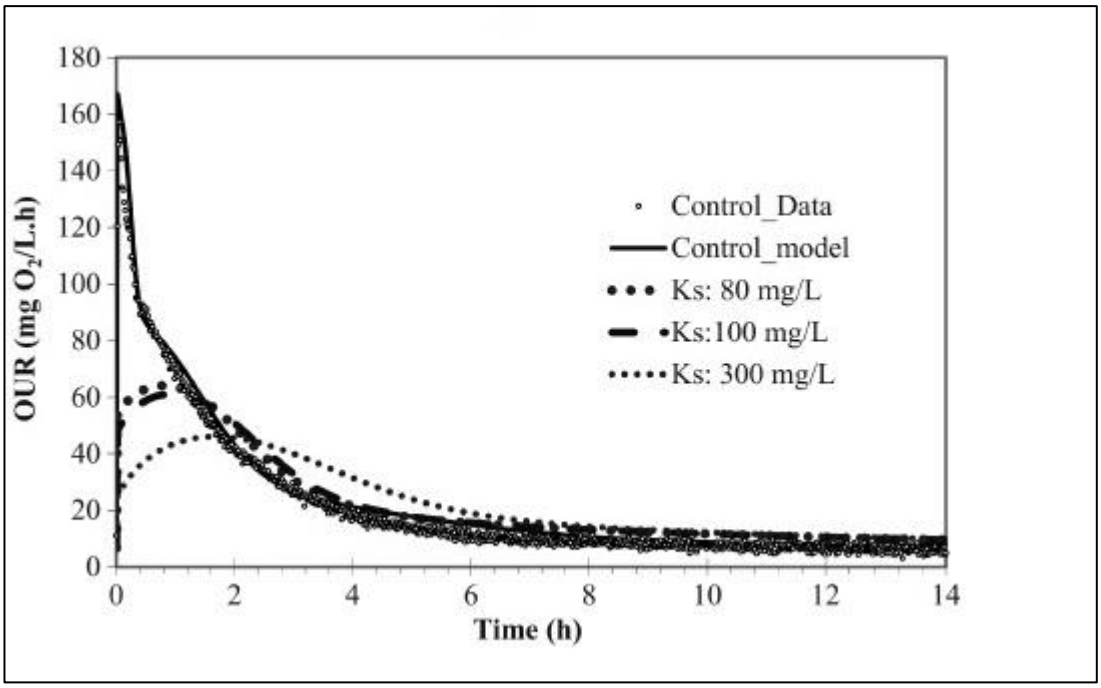

Figure 3.9: Effect of mixed inhibition on the OUR curve (Özkök et al., 2011).

3.8 Microbial Community Analysis

3.8.1 Antibiotic resistance gene analysis

3.8.1.1 Resistance to antibiotics

Prescription of high doses of antibiotics by doctors and unperscribed usage of these substances increases the inflow of antibiotics to natural habitats. Antibiotic substances, causing pollution in receiving waters are resistant to biodegradation and therefore they tend to persist in the environment, which increases the probability of environmental organisms to become resistant to these substances. Finally, today in most of the tested water bodies and soil samples antibiotic resistance genes are being detected (Zhang et al., 2009; Kemper, 2008), proving the effect of antibiotics in natural habitats.

Besides the environmental concerns, increasing clinical resistance leads to inability of treating illnesses by taking antibiotics. In addition resistant bacteria in subterranean water bodies may reach surface waters, which are used as drinking water supplies, and cause illnesses (Feuerpfeil et al., 1999). Therefore, antibiotic resistance constitutes a major problem for human and animal and therefore for World health (Kemper, 2008).

According to Kemper (2008), veterinary antibiotics cause selection of resistant bacteria, which leads to being exposed to resistant bacteria via food chain in addition to direct contact. Keeping in mind that the bacteria isolated from humans are proved to be environmentally originated, the author also states that even though antibiotics are not directly used, presence of antibiotic resistance shows the importance of the problem. Since genetic molecules are coded on mobile elements in the bacteria, they can easily be transmitted from one to another, which causes the resistance to be spread even from non-pathogenic organisms to pathogenic organisms (Ma et al., 2011).

Wastewater treatment plants are like reservoirs of human and animal bacteria, and antibiotic resistance genes are leaving these reservoirs through effluent reaching the receiving waters (Zhang et al., 2009; Tennstedt et al., 2003; Ma et al., 2011). Activated sludge systems, one of the biological treatment systems, are diverse and dynamic ecosystems and have large potential for exchange of genetic information (Parsley et al., 2010). This has been proved by different studies on activated sludge systems, showing that activated sludge systems contains high amounts and wide diversities of antibiotic resistance genes (Auerbach et al., 2007; Tennstedt et al., 2003; Ma et al., 2011).

In most of the studies, culture dependent methods have been applied to environmental samples prior to detection of antibiotic resistance genes for screening purposes. These studies depend on the capability of bacteria to grow on media containing antibiotic substances. These have also showed the increasing trends of resistance genes (Harwood et al., 2000; Reinthaler et al., 2003; McKeon et al., 1995; Auerbach et al., 2007). However, due to the fact that most of the environmental bacteria are not cultivable, it is not an appropriate method to determine the resistance of complicated biological systems (like activated sludge) depending on cultivable bacteria, which only reflects 1% of total community (Auerbach et al., 2007). Therefore methods based on polymerase chain reaction (PCR) give more reliable results, which in this study were used to determine the resistance genes in complex activated sludge samples.

3.8.1.2 Antibiotic resistance mechanisms

There are four different resistance mechanisms against antibiotic substances (Zhang et al., 2009):

1. Efflux Pumps: Due to structural changes in the cell membrane intracellular antibiotic concentration is kept low, causing the ribosomes to function normally.
2. Target Modification: The target cellular component is modified by different mechanisms, so that the antibiotic cannot affect the component.
3. Target By-Pass: Due to mutations on the target enzyme or deletion mutations on the gene sequence coding the enzyme, it is prevented for the enzyme to be affected by the antibiotic.
4. Inactivation of Antibiotic Substance: This mechanism directly inactivates the antibiotic substance.

3.8.1.3 Resistance to sulfonamides

The effect mechanism of sulfonamide antibiotics is to inhibit the formation of dihydrofolic acid, which catalyzes the condensation reaction of p-aminobenzoic acid (PABA) and 7,8-dihydro-6-hydroximethylptesin-pyrophosphate (DHPPP) that results in formation of dihydropteroic acid. For this to happen the antibiotic inhibits the dihydropteroate syntase (DHPS) enzyme (Sköld, 2000).

Sulfonamide resistance gene is generally coded by the mutations in the highly conserved regions of DHPS gene (*sul*) (Sköld, 2000). Different sulfonamide resistant mechanisms have been detected, which occur due to mutations on the *sul* gene and spread through mobile genetic elements (Antunes et al., 2007; Houvinen, 2001).

In environment bacteria four different sulfonamide resistance genes have been defined (*sul*I, II, III, ve A). *sul*I and *sul*II were detected in stool samples taken from cattle farms (Srinivasan et al. 2005), in sediments of wetlands (Akinbowale et al. 2007; Agersø and Petersen 2007), and also in polluted river and sea waters (Lin and Biyela 2005; Hu et al. 2008; Mohapatra et al. 2008). *sul*I is a part of class 1 integrone and it can be transferred from one to another bacterial specie in water media like river and sea (Tennstedt et al. 2003, Mukherjee and Chakraborty 2006, Taviani et al. 2008). *sul*A is the chromosomal gene in *S.Pneumoniae*, which codes DHPS and it has been mutated by 3-6bp insertion leading to sulfonamide resistance (Maskell et

al., 1997). Sulfonamide resistance genes, their biological and environmental sources are given in Table 3.4. In this study activated sludge samples chronically inhibited with Sulfamethoxazole were examined for the presence of *sul*I *sul*II and *sul*III genes.

Table 3.4: Sulfonamide resistance genes in water environments (Zhang et al., 2009).

Gene	Biological Source	Environmental Source [1]
*sul*I	Aeromonas, Escherichia, Listeria; pB2, pB3, pB8, pB10 Plasmids; Microbial Community	AS, DW, NW, SD, SW
*sul*II	Acinetobacter, Escherichies, Salmonella, Vibrio; Microbial Community	DW, NW, SD, SW
*sul*III	Escherichia; Microbial Community	NW, SD
*sul*A	Microbial Community	SD

1) SW: Special wastewaters like hospital, animal farms and agricultural areas, AS: Activated sludge from treatment plants, NW: Natural waters, SD: Sediments, DW: Drinking waters

3.8.1.4 Resistance to tetracyclines

Resistance to tetracyclines can be explained by different mechanisms, such as efflux pumps, ribosomal protection proteins and enzymatic mechanisms. In the literature, 43 *tet* and *otr* genes have been defined coding resistance against tetracyclines, among which 27 are coding efflux pumps, while 12 are coding ribosomal protection proteins. In addition to these, there are 3 genes for enzymatic resistance and 1 gene for an unknown mechanism (http://faculty.washington.edu/marilynr/). The number of *tet* genes that can be found in water environments is less. However the *tet* genes found in activated sludge systems are even more limited. Moreover *tet* genes that can be detected in gram-positive and gram-negative bacteria are also different (http://www.antibioresistance.be/).

Table 3.5 and Table 3.6 show the tetracycline resistance genes found in activated sludge and the distinction between genes found in gram-positive and –negative bacteria, respectively.

Table 3.5: Tetracycline resistance genes detected in activated sludge systems (taken from Zhang et al. 2009).

Function	Gene	Reference
Efflux Proteins	*tet*A, *tet*B, *tet*C, *tet*D, *tet*E, *tet*G *otr*B	Szczepanowski et al., 2004; Tennstedt et al., 2005; Agersø and Sandvang, 2005; Auerbach et al., 2007; Schmidt et al., 2001; Nikolakopoulou et al., 2005
Ribosomal Protection Proteins	*tet*M, *tet*O, *tet*Q, *tet*S *otr*A	Auerbach et al., 2007; Nikolakopoulou et al., 2005

Table 3.6: Tetracycline resistance genes detected in gram-positive and -negative bacteria (http://www.antibioresistance.be/).

Function	Gram-Positive	Gram-Negative
Efflux Proteins	*tet*K, *tet*L, *tet*P, *tet*V, *tet*Z, *otr*B	*tet*A, *tet*B, *tet*C, *tet*D, *tet*E, *tet*G, *tet*H
Ribosomal Protection Proteins	*tet*M, *tet*O, *tet*Q, *tet*S	*tet*M, *tet*O, *tet*Q

Sludge samples taken from an activated sludge system chronically fed with tetracycline were qualitatively analyzed for the presence of *tet* A, B, C, D, E, G, K, L, *otr*B and *tet* M, O genes, covering both efflux protein and ribosomal protection genes, respectively.

3.8.1.5 Resistance to macrolides

Over time bacteria developed different resistance mechanisms against erythromycin as well, one of macrolide antibiotics that was chosen as the model antibiotic to represent macrolides. (Figure 3.10)

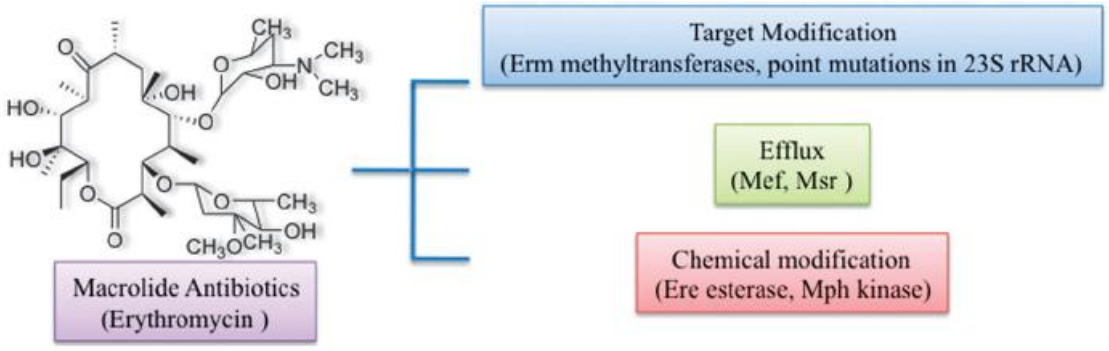

Figure 3.10: Different macrolide resistance mechanisms (Wright, 2011).

The first mechanism is the rRNA methylase (*erm*) group, which change the binding point of macrolides on the 23S rRNA *(*Leclercq and Courvalin, *1991;* Martineau et al., 2000; Sutcliffe et al., 1996; Weisblum, 1995). Among them *erm*(A), (B), (C), (E), (F), (T), (V), (X) have been detected in farm and poultry wastes, lagoon and treatment systems (Hayes et al., 2005; Chen et al., 2007; Patterson et al., 2007; Zhang et al., 2009). Since *erm* genes are found on mobile genetic elements like plasmids and transposons they are easily transferred to another microorganism (Roberts, 2003; Liu et al., 2007; Okitsu et al., 2005; Zhang et al., 2009).

Another resistance mechanism is the enzymatic inactivation of the antibiotic substance. Esterases, lyases, transferses and phosphorylases are the enzymes responsible for this action. Among macrolide resistance genes, only *mph*(A), macrolide-2'-phosphotransferase, has been detected in activated sludge biomass (Szczepanowski et al., 2004; Zhang et al., 2009). Moreover, efflux mechanism could not be defined in activated sludge systems, but it has been detected in *Staphylococcus spp.* (Martineau et al., 2000). Resistance mechanisms and genes against macrolide antibiotics are given in Table 3.7.

Table 3.7: Macrolide resistance mechanisms and genes (Roberts, 2008).

rRNA-methylases	Efflux Proteins	Inactivation Enzymes			
		Esterases	Lyases	Transferases	Phosphorylases
erm(A), (B), (C), (D), (E), (F), (G), (I), (H), (N), (O), (R), (S), (T), (U), (V), (W), (X), (Y), (Z), (30), (31), (32), (33), (34), (35), (36), (37), (38), (39), (40), (41)	*nef*(A), *mef*(B), *msr*(A), (C), (D) *car*(A), *lmr*(A), *ole*(B), (C) *srm*(B), *tlc*(C) *lsa*(A), (B), (C), *vga*(A), (B), (C)	*ere*(A), (B)	*vgb*(A), (B)	*lnu*(A), (B), (C), (D), (F) *vat*(A), (B), (C), (D), (E), (F)	*mph*(A), (B), (C), (D)

In the current study, presence of *erm*(A), (B) and (C) from *erm* class genes were examined, which were frequently determined in microbial communities, treatment plant effluents and in hospital wastewaters, even though they have not yet been detected in activated sludge biomass. In the literature it has been stated that the amounts and distribution of *erm* genes in total microbial communities, of which the most important source is the animal wastes, should be determined (Chen et al.,

2007). Moreover, the presence of *mph*(A) that has been detected in activated sludge systems (Szczepanowski et al, 2004) and *msr*(A) were examined. *msr*(A) was not previously found in activated sludge biomass but this gene codes ATP dependent efflux mechanism and causes resistance against the antibiotic erythromycin both in gram-positive and –negative bacteria (Martineau et al., 2000; Roberts 2008).

According to Roberts (2008) the *erm*(B) gene can frequently be found in gram-positive and –negative bacteria and aerobic and anaerobic bacteria and in many different ecosystems. Moreover it has the widest host range with 33 genera due to its association with mobile genetic elements (Roberts, 2008). *erm*(F), the second most detected macrolide resistance gene (24 genera) has been eliminated due to its appearance mostly in anaerobic genera, which are in aerobic activated sludge systems not to be seen. Whereas *erm*(A) gene can be found in 7 genera and *erm*(C) in 16. Moreover, it has been repoted that in *S.pyrogenes*, *S. Aureus* and *S. Epidermidis* bacteria *erm*(B) and *erm*(A) are frequently present (Roberts, 2008). In addition in different studies it has been stated, that *erm*(A) and *erm*(C) are responsible genes for macrolide resistance in *Staphylococcus* species (Weisblum, 1995; Leclercq, 2002; Fiebelkorn et al., 2003; Aktaş et al., 2007).

3.8.2 454-pyrosequencing

Classification of organisms started with traditional methods like culture depended techniques, which depends on organism's ability to survive on different growth media, and phenotypic differences and similarities with one and other. These methods included gram staining and biochemical tests, which take growth characteristics and culture requirements into account. However it has been stated that objective taxonomic classification would not be sufficient with traditional methods due to variations in phenotypic characteristics (Woo et al., 2008). Moreover traditional methods cannot be used for uncultivable bacteria, a group in which the environmental bacteria are also a part of, since most of the environmental bacteria are not cultivable.

By the use of 16S rDNA genes of bacteria for analyzing organisms draw backs caused by cultivation based techniques have been overcome. Moreover invention and use of polymerase chain reaction (PCR), together with sequencing has started a new

era, in which uncultivable bacteria were classified and phylogenic relationships were determined. Moreover new bacteria were discovered (Woo et al., 2008).

PCR based techniques have widely been used for determining the community structure of activated sludge systems. Microbial community structures of laboratory and full scale engineered activated sludge systems and natural systems have been analyzed by the use of different methods, including PCR-DGGE (polymerase chain reaction-denaturing gradient gel electrophoresis), t-RFLP (terminal restriction fragment length polymorphism), FISH (fluorescence *in situ* hybridization), RISA (ribosomal spacer analysis), and analysis of 16S rRNA clone libraries (Ye et al., 2011). However due to the exceptionally rich microbial diversity of activated sludge biomass these methods fail to characterize the total community. According to Ye et al (2011) the diversity of the activated sludge exceeds the sensitivity range of aforementioned methods. Moreover Xia et al (2010) states that the knowledge on microbial communities in activated sludge systems is incomplete due to limitation of traditional methods, as they cannot capture the whole complexity of these communities.

The aforementioned methods although effective determining the microbial community their effectiveness tends to decrease with increasing complexity of the community. For example, 16S rRNA clone libraries with even more than 1000 clones still have moderate sensitivity, which result in missing rare taxa (Xia et al, 2010; DeSantis et al, 2007; Fuhrman, 2009). Muyzer et al (1998) states that DGGE and TGGE detect groups that are larger than 1% of the bacterial population, however single bands do not coincide with single bacterial species (Xia et al, 2010). Lastly t-RFLP is also inadequate to determine the microbial characteristics of a very complex community, since its sensitivity is limited to only approximately fifty most abundant organisms in the community (Sakano and Kerkhof, 1998; Dunbar et al., 2000; Xia et al., 2010).

On the other hand the development of methods like 454-pyrosequencing and microarrays have been used for characterizing complex ecosystems and, have shown to have significantly higher throughput then the traditional methods. The next-generation sequencing methods, even though more expensive, produce large amounts of DNA reads, giving more accurate results. There are commercially available Genome sequencers operated on pyrosequencing based chemistries: GS-FLX

Genome sequencer from Roche/454 Life Sciences, 1G Analyzer from Illumina/Solexa and SOLID System from Applied Biosystems (Desai *at al.*, 2010).

The Roche (454) Genome Sequencer technology depends on detection of pyrophosphate release upon nucleotide incorporation, and it generates massive amounts of parallel DNA sequence reads from amplified PCR products with a sequencing-by-synthesis approach (Margulies et al., 2005, Ye et al., 2011) . It provides 300,000 sequences at once (Desai et al., 2010). With the 454-pyrosequencing method 400-600 bp can be sequenced in one reaction, which cannot be obtained by any other technology. The platform operates as a high-throughput sequencing tool (Roh et al., 2010). Moreover, prior cloning steps for DNA sequencing are not required for performing this very fast method, 454-pyrosequencing, and therefore it has been accepted as one of the ideal tools to analyze complex microbial communities (Edwards et al., 2006, Krause et al., 2006, Szczepanowski et al., 2008).

High-throughput pyrosequencing technology is being used in the different microbial ecology branches, such as microbial diversity and functional genes diversity (Roh *et al.*, 2010). It has also been used for analyzing environmental samples including soil, marine water and wastewater treatment plant influent (Roesch et al., 2007, Qian *et al.*, 2011, McLellan et al., 2010, Ye et al., 2011). However, in the literature only few studies can be found conducted on activated sludge applying this technology. Zhang et al (2011) and Ye et al (2011) applied 454-pyrosequencing in their full-scale and laboratory-scale wastewater treatment plants, respectively to determine the diversity and abundance of nitrifying bacteria in their systems. Park et al (2011) investigated the microbial community structure of a laboratory-scale Bardenpho Process using pyrosequencing. Microbial diversity of a full scale fixed-film activated sludge systems has been investigated by the use of 454-pyrosequencing by Kwon et al. (2010). Sanapareddy et al (2009) successfully determined the microbial community structure of a domestic wastewater treatment plant in North Carolina, USA.

Moreover the plasmid metagenome of a wastewater treatment plant showing reduced susceptibility to antimicrobials has been analyzed by the same technique. Activated sludge samples grown on antibiotic supplemented growth media and their plasmids were extracted. The sequencing results revealed that the wastewater bacteria were important reservoirs for clinically important resistance determinants and they may

contribute to rapid dissemination of antibiotic resistances (Szczepanowski et al., 2008). Moreover the authors stated that the ultrafast 454-pyrosequencing was proven to be a powerful tool for analyzing plasmid metagenome of wastewater bacteria (Szczepanowski et al., 2008). In another study Schlüter et al. (2008) investigated the genetic diversity of a plasmid metagenome of a wastewater treatment plant using the same methodology as Szczepanowski et al. (2008) and stated that wastewater treatment plants play an important role as hot-spots for circulation of antibiotic resistance determinants, as they serve as interfaces between different environmental compartments. Szczepanowski et al. (2011) also conducted a study on the IncP-1α plasmids. Three important antibiotic resistance plasmids of IncP-1α group originating from two different wastewater treatment plants were analyzed by 454-pyrosequencing and the obtained results revealed that these plasmids were effective tools for antibiotic and heavy metal resistance dissemination (Szczepanowski et al., 2011).

4. MATERIALS AND METHODS

4.1 Reactor Setup and Operation

4.1.1 Control reactors

A 14 L and an 8 L (V_T) fill and draw control reactors, with the sludge age of 10 and 2 days, respectively, were set using the seed sludge taken from the aeration tank of a domestic wastewater treatment plant. The sludge age 10 days control reactor was fed with 600 mgCOD/L concentration of peptone-meat extract mixture and the sludge age 2 days control reactor was fed with peptone-meat extract mixture of 720 mg COD/L concentration. 1 L of the peptone-meat extract mixture (ISO 8192) consisted of 16 g of peptone, 11 g of meat extract, 3 g of urea, 0.7 g of NaCl, 0.4 g of $CaCl_2.2H_2O$, 0.2 g of $MgSO_4.7H_2O$ and 2.8 g of K_2HPO_4. Besides carbon source (peptone-meat extract mixture), macro (K_2HPO_4: 320 g/L, and KH_2PO_4: 160 g/L) and micro ($MgSO_4.7H_2O$: 15 g/L, $FeSO_4.7H_2O$: 0.5 g/L, $ZnSO_4.7H_2O$: 0.5 g/L, $MnSO_4.H_2O$: 0.41 g/L, $CaCl_2.2H_2O$: 2.65 g/L) nutrients were added to the reactors. pH in the reactor was kept at neutral levels. Reactors were fed once a day (HRT: 1 d). During each feeding period, reactors were settled for 1 h (t_s) and decanted until 2 L (V_0). Reactors were aerated continuously and the oxygen concentration in the reactor was kept above 3 mg/L to maintain aerobic conditions. pH of the reactor was kept around 7 to maintain neutral pH levels. After the reactor reached steady state, the acclimated biomass was used for respirometric experiments.

4.1.2 Chronic reactors

Seed sludge of the chronic reactors was taken from both control reactors depending on the sludge age and operated until all systems reached steady state. The chronic reactors were fed with peptone – meat extract mixture (720 mgCOD/L) and the antibiotic substance together. In the case of SMX (SRT:2d) the antibiotic concentration was 100 mg/L for SMX (SRT:10d), and 50 mg/L for TET (SRT: 2 and 10d) and ERY (SRT: 2 and 10d).

4.2 Experimental Procedures

Chemical Oxygen Demand (COD) was measured using the procedure defined by ISO 6060. For soluble COD determination, samples were subjected to filtration by means of Millipore membrane filters with a pore size of 0.45 μm. The Millipore AP40 glass fiber filters were used for SS and VSS measurements that were performed as defined in Standard Methods (2005). During the experiments Orion 520 A pH meter was used for pH measurements and before each usage of the device the pH meter was calibrated. For TOC measurements a Shimatsu VPCN model Carbon Analyzer has been used. A PerkinElmer Lambda 25 model UV/VIS Spectrophotometer has been used for UV scan of antibiotics. Finally IC measurements were done on a Dionex ICS-1500 model Ion Chromatograph.

4.2.1 EC_{50} inhibition experiments (ISO 8192)

The inhibitory effects of antibiotics on activated sludge were determined with ISO 8192 method. ISO 8192 method determines EC_{50} value as the inhibitor concentration, which causes 50% decrease in the respiration rate of the bacterial culture.

During the test a Manotherm RA-1000 respirometry was used for measuring the oxygen concentrations at different times. Oxygen Uptake Rate (OUR) of activated sludge with and without the addition of inhibitors was calculated.

The method determines OUR of control system without inhibitors ($OUR_{control}$). Additionally, it defines effective concentration (EC_{50}) of inhibitor giving an OUR ($OUR_{inhibited}$) in the system. The obtained OUR corresponds to the 50 % of OUR of control system without inhibitors ($OUR_{control}$). EC_{50} is calculated as given below:

$$\boldsymbol{EC_{50} = \frac{OUR_{control} - OUR_{inhibited}}{OUR_{control}} x 100 = 50\%} \qquad \textbf{(4.1)}$$

4.2.2 Respirometry

Respirometric tests were conducted with relevant acclimated biomass seeding alone to obtain endogenous oxygen uptake rate (OUR) level of biomass. Samples with desired F/M ratios are added to the reactor and the OUR data was monitored. Control analysis without antibiotic addition was conducted before inhibition analysis for each study. OUR measurements were performed with an Applitek RA-Combo-1000

continuous respirometer with PC connection. During each test a nitrification inhibitor (Formula 2533, Hach Company) was added to the OUR reactors to prevent any possible interference induced by nitrification.

4.2.3 Polyhydroxy butyric acid (PHB) measurements

PHB samples were taken into 2x10 ml centrifuge tubes containing 2 drops formaldehyde to prevent the biological activity. The PHB content of the washed (K-P buffer solution) and freeze-dried biomass were subjected to extraction, hydrolization, and esterification in a mixture of hydrochloric acid, 1-propanol, and dichloroethane at 100°C (Beun et al., 2000). The resulting organic phase was extracted with water to remove free acids. The propylesters were analyzed by a gas chromatograph and benzoic acid was used as an internal standard throughout the procedure.

4.2.4 Sulfamethoxazole measurements

SMX was analyzed by high-performance liquid chromatography (Agilent) with a Novapac C18 column. A 30:70 v/v methanol-water mixture was used as a mobile phase at a constant flow rate of 0.6 ml/min (Beltran et al., 2008). The mobile phase was acidified at pH 2.5 with phosphoric acid (0.1 % concentration). Detection was made with a Diode Array Detector at 280 nm. Injection volume and flow were 40 µl and 1 ml/min, respectively. Figure 4.1 shows the SMX calibration curve. Moreover according to the results obtained from the measurements in the liquid phase the SMX measurements in the activated sludge have been cancelled.

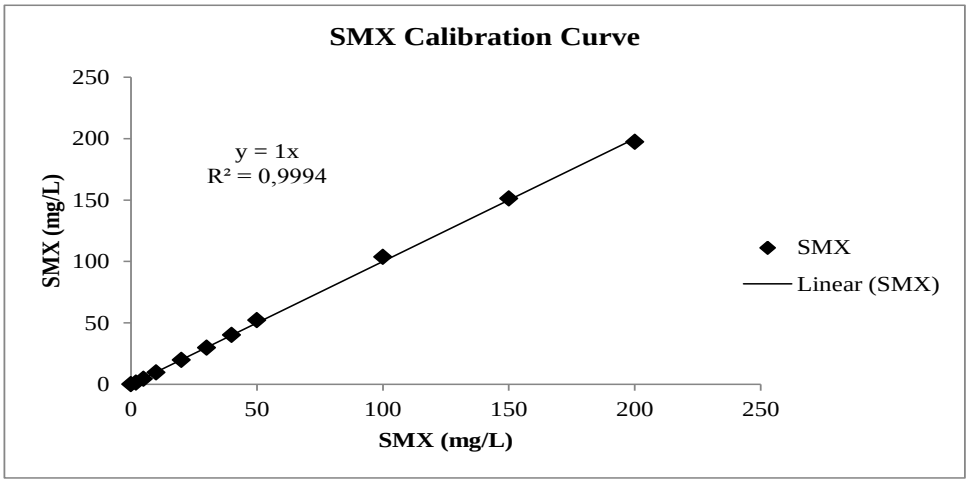

Figure 4.1: SMX calibration curve.

4.2.5 Microbial community analysis

4.2.5.1 Determination of antibiotic resistance genes

For the determination of resistance genes present in activated sludge samples the genomic DNA was extracted from each sample, and after determining the obtained DNA concentration, using appropriate primers designed to target the specific regions the regions coding the antibiotic resistance genes were amplified. The PCR products were visualized by gel electrophoresis and ethidium bromide staining.

DNA Extraction from Activated Sludge

Activated sludge biomasses are complex microbial communities. Therefore for extracting the entire DNA, effective methods have to be used to destroy the cellular membranes and isolate the DNAs from different members of the community. In addition to the complexity of the community, since these samples are environmental the sample may contain PCR inhibitors such as KCl, NaCl, urea and/or iron. Therefore these inhibitors have to be eliminated during DNA extraction procedure. In this context in order to determine the most effective DNA extraction procedure different methods were applied and the results were compared to each other. Among these methods, most effective and high yield method has been chosen and DNA from the activated sludge samples was extracted using the chosen method.

In order to determine the most efficient DNA extraction method 3 different methods were run with same amount of sludge, and the results were compared. The method was expected to yield the highest DNA concentration and lyse gram-positive bacteria. Among 3 different extraction methods Macherey-Nagel NucleoSpin Soil DNA extraction kit has been chosen, due to its performance depending on the previous criteria.

The Macherey-Nagel NucleoSpin Soil DNA extraction kit was executed according to the procedure of the manufacturer. 25 mg of precentrifuged activated sludge biomass from each sample has been used for DNA extraction. The DNA extraction procedure applied on the activated sludge samples is given in Table 4.1. In addition to the DNA extraction procedure, in order to eliminate the RNA in the sample, RNAse treatment was added to the procedure.

Determination of DNA Concentration

The amount of DNA obtained was measured by a NanoDrop DNA/RNA-Concentration Measurement Spectrometer (ND-1000). The device measures the highest absorbance emitted by nucleic acids at 260nm and calculates the DNA concentration in [ng/µl].

Table 4.1: Macherey-Nagel (MN) NucleoSpin Soil DNA extraction manual.

1. Sample Preparation	Load the sample into NucleoSpin Soil Bead Tubes Add 700 µl SL2
2. Adjusting the Lysis Conditions	Add 150 µl Enhancer SX (not applied)
3. Sample Lysis	Horizontally vortex for 5min at RT
4. Precipitation of Contaminants	Centrifuge at 11.000 x g for 2min Add 150 µl SL3 Vortex for 5sec Incubate at 0 – 4 ^{o}C for 5min Centrifuge at 11.000 x g for 1min
5. Inhibitor Removal	Load supernatant on NucleoSpin Inhibitor Removal Column Centrifuge at 11.000 x g for 1min
6. Adjusting Binding Conditions	Add 250 µl Binding Solution (SB) Vortex for 5sec
7. Binding the DNA	Load 550 µl sample on NucleoSpin Soil Column Centrifuge at 11.000 x g for 1min
8. Washing the Silica Membrane	1 – Add 500 µl SB – Centrifuge at 11.000 x g for 30sec 2 – Add 550 µl Washing Solution1 (SW1) – Centrifuge at 11.000 x g for 30sec 3 – Add 700 µl Washing Solution2 (SW2) – Vortex 2sec – Centrifuge at 11.000 x g for 30sec 4 – Add 700 µl SW2 – Vortex 2sec – Centrifuge at 11.000 x g for 30sec
9. Drying the Silica Membrane	Centrifuge at 11.000 x g for 2min
10. Eluting the DNA	Add 50 µl Elution Buffer (SE) Incubate 1 min at RT Centrifuge at 11.000 x g for 1min

Polymerase Chain Reaction (PCR)

Polymerase Chain Reaction (PCR) is an enzymatic method to amplify a region between two segments of known sequence on the DNA. There are three main steps of PCR, each having different temperature conditions: denaturation, annealing, and elongation, which constitute a cycle. A schematic representation of PCR is given in Figure 4.2.

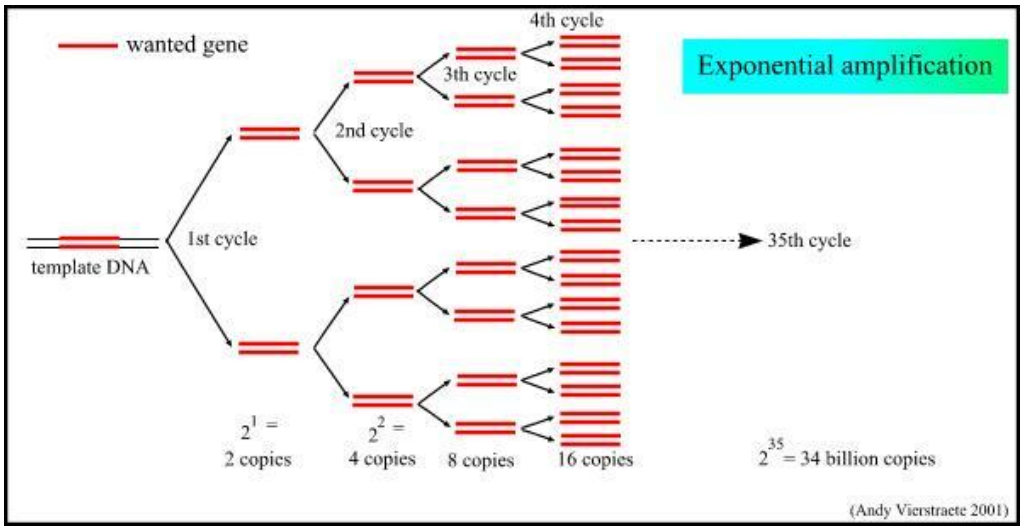

Figure 4.2: Schematic representation of polymerase chain reaction.

In the denaturation step the double stranded DNA is being denatured and the strands are separated from each other. In the annealing step the forward and reverse primers are being bound to continuous and noncontinuous strands of the DNA, respectively. The last step, elongation, is when the enzymatic reaction takes place, in which the Taq-polymerase makes a copy of the wanted DNA segment, in which it uses the dNTP's present in the reaction mixtures. In PCR the product of each cycle is being used as the template for the next cycle. With each cycle the amount of DNA increases exponentially. For an effective DNA amplification, 20-30 cycles have to be run. Using this method, the amount of DNA fragment of interest is being amplified and millions of copies are being obtained (Alberts et al., 2002).

PCR mixture consists of template DNA, forward and reverse primer pairs, DNA-polymerase, deoxynucleosid trifosfates (dNTPs), PCR buffer solution, and a divalent cation solution like $MgCl_2$. For controlling the accuracy of the PCR system, each set of experiments includes a positive and a negative control. Negative control is a sample that contains no DNA, therefore is not supposed to yield any DNA amplification products. It verifies that there is no contamination in the reaction mixture. However a positive control is a sample, which certainly contains the DNA to be amplified. Therefore it is expected to yield amplified DNA. Positive control verifies that the DNA fragments amplified are the correctly amplified.

Control of DNA Extraction Method

In activated sludge systems gram-positive and –negative bacteria exist together. Gram-positive bacteria, because of the thick peptidoglycan layer in their cell wall are

more resistant to outside effects. Therefore in order to ensure the destruction of cell walls of gram-positive bacteria the factors applied during DNA extraction should be made more drastic. DNA extraction procedures for gram-positive bacteria therefore include enzymatic extraction methods in addition to physical and chemical extraction methods.

During the study different methods were applied to activated sludge samples, and the method showing good extraction performance has been chosen for application. In order to determine the effectiveness of the methods on gram-positive bacteria, a special PCR method has been applied.

In the literature, it has been stated that a 100bp stable insertion to the DomainIII (helix 54a) of 23S ribosomal DNA has used to distinguish the high GC-Gram-positive bacteria (Roller et al., 1992; Yu et al., 2002). For this purpose 23InsV (5'-MADGCGTAGNCGAWGG-3') and 23InsR (5'-GTGWCGGTTTNBGGTA-3') primers have been used to determine the gram-positive bacteria. Each PCR tube contained 2.5µl of 10X PCR Buffer solution (Applied Biosystems, Roche), 1µl of 2.5mM dNTP mixture, 2µl of $MgCl_2$ (25mM) solution (Applied Biosystems, Roche), 1µl of each 100µm 23InsV and 23InsR primers and 0.2µl of 5U/µl Taq DNA Polymerase. 1µl genomic DNA was added to the PCR tubes and filled with H_2O until the final volume of 25 µl. The conditions of the Thermal Cycler were; 9min of pre-denaturation at 95^{o}C, followed by 33 cycles of 30sec denaturation at 94^{o}C, 45sec annealing at 63^{o}C and 1min elongation at 72^{o}C, and later 5min of final incubation at 72^{o}C. Obtained PCR products were visualized on a 1% agarose gel by gel electrophoresis. It has been stated that this PCR amplifies the 270 and/or 380 bp fragment of the III.Domain of the 23S rDNA. Therefore it is expected to visualize 270 and/or 380 bp bands on the agarose gel.

Agarose Gel Electrophoresis

Agarose gel electrophoresis is an analytical technique, which is generally used to separate the amplified DNA fragments according to their size and to control the PCR procedure. Following this procedure the bands forming on the gel can be cut off and after cleaning up the DNA can be used for quantification purposes.

In this procedure gel provides a viscous medium, where the nucleic acids can travel. When electricity is applied; DNA molecule, an acid, being negatively charged moves

though the gel from the anode to the cathode. The length of distance traveled by the amplified PCR product is reversely proportional to its size. Therefore shorter DNA fragments can move farther along the gel than the longer DNA fragments, since longer fragments encounter more resistance.

During gel electrophoresis, a marker is used to determine the size of the DNA fragments on the gel. Marker consists of a mixture of different DNA fragments of different sizes, and it also serves as a positive control, showing that the gel electrophoresis procedure has been run correctly.

Qualitative Determination of Antibiotic Resistance Genes

PCR based techniques have been applied for qualitative analysis of antibiotic resistance. Appropriate primers were chosen to amplify the gene sequence coding the resistance gene. Moreover strains that contain these genes have also been collected, which served as positive control during PCR experiments, showing that the correct fragment has been amplified. For resistance genes, for which no positive controls were available, the PCR product was sequenced and BLASTed to verify that the correct region was amplified. Due to changing annealing temperatures of chosen primers, different cycling conditions have been applied according to the information given for each specific primer in the literature.

4.2.5.2 Resistance to sulfonamides

Qualitative analysis of *sul* genes coding resistance to sulfamethoxazole has been completed using primers, of which the information is given in Table 4.2. Each PCR mixture consisted of 2.5µl 10X PCR Buffer solution (Applied Biosystems, Roche), 1µl of 2.5mM dNTP mixture, 2µl of $MgCl_2$ (25mM) solution (Applied Biosystems, Roche), 1µl of each 25µM *sul* forward and reverse primers, 0.2µl 5U/µl Taq DNA Polymerase (Applied Biosystems, Roche), and 1µl genomic DNA. Finally required amount of sterile water was added to reach the final volume of 25µl. Moreover, Thermal Cycler conditions were as follows: 9min pre-denaturation at 95^{o}C, 40 cycles of 15sec denaturation at 95^{o}C, 30sec annealing (annealing temperatures are given in Table 4.2) and 1min elongation at 72^{o}C, and then 5min final incubation at 72^{o}C.

Table 4.2: Primers used for the determination of sulfonamide resistance genes.

Gene	Primers	Sequence	Annealing Temperature	Amplicon Size	Reference
*sul*I	*sul*I-FW	cgcaccggaaacatcgctgcac	55.9	163	(Pei et al., 2006)
	*sul*I-RV	tgaagttccgccgcaaggctcg			
*sul*II	*sul*II-FW	tccggtggaggccggtatctgg	60.8	191	
	*sul*II-RV	cgggaatgccatctgccttgag			
*sul*III	*sul*III-FW	tccgttcagcgaattggtgcag	60.0	128	
	*sul*III-RV	ttcgttcacgccttacaccagc			

4.2.5.3 Resistance to tetracyclines

In order to determine the presence of tetracycline resistance genes and the tetracycline resistance profile in activated sludge samples several *tet* genes covering efflux (*tet* A, B, C, D, E, G, K, L and *otr*B) and ribosomal protection proteins (*tet* M, O) have been chosen, which have previously been detected in wastewater and activated sludge systems. Information on primers used in PCR experiments is given in Table 4.3.

Each PCR mixture consisted of 2.5µl 10X PCR Buffer solution (Applied Biosystems, Roche), 1µl of 2.5mM dNTP mixture, 2µl of $MgCl_2$ (25mM) solution (Applied Biosystems, Roche), 1µl of each 25µM *tet* forward and reverse primers, 0.2µl 5U/µl Taq DNA Polymerase (Applied Biosystems, Roche), and 1µl genomic DNA. However, for *tet*C and *tet*B different Taq polymerase and PCR buffer has been used. Therefore the PCR mixture for determination of these genes consisted of 2.5µl 10X PCR Buffer solution (Applied Biosystems, Roche), 1µl of 2.5mM dNTP mixture, 1µl of each 25µM *tet* forward and reverse primers, 0.2µl 5U/µl Taq DNA Polymerase (Applied Biosystems, Roche), and 1µl genomic DNA Finally required amount of sterile water was added to reach the final volume of 25µl. Moreover all the PCR mixtures contained 1µl Dimethyl sulfoxide (DMSO) to inhibit the secondary structures minimizing interfering reactions. The thermal cycler conditions for *tet* genes are given in Table 4.4.

Table 4.3: Primers used for the determination of tetracycline resistance genes.

Gene	Primers	Sequence	Amplicon Size	Reference
*tet*A	*tet*A-FW	gctacatcctgcttgccttc	210	(Ng et al., 2001)
	*tet*A-RV	catagatcgccgtgaagagg		
*tet*B	*tet*B-FW	ttggttaggggcaagttttg	659	
	*tet*B-RV	gtaatgggccaataacaccg		
*tet*C	*tet*C-FW	cttgagagccttcaacccag	418	
	*tet*C-RV	atggtcgtcatctacctgcc		
*tet*D	*tet*D-FW	aaaccattacggcattctgc	787	
	*tet*D-RV	gaccggatacaccatccatc		
*tet*E	*tet*E-FW	aaaccacatcctccatacgc	278	
	*tet*E-RV	aaataggccacaaccgtcag		
*tet*G	*tet*G-FW	gctcggtggtatctctgctc	468	
	*tet*G-RV	agcaacagaatcgggaacac		
*tet*K	*tet*K-FW	tcg ata gga aca gca gta	169	
	*tet*K-RV	cag cag atc cta ctc ctt		
*tet*L	*tet*L-FW	tcg tta gcg tgc tgt cat tc	267	
	*tet*L-RV	gta tcc cac caa tgt agc cg		
*tet*M	*tet*M-FW	gtggacaaaggtacaacgag	406	
	*tet*M-RV	cggtaaagttcgtcacacac		
*tet*O	*tet*O-FW	aacttaggcattctggctcac	515	
	*tet*O-RV	tcccactgttccatatcgtca		
*otr*B	*otr*B-FW	ccgacatctacgggcgcaagc	947	(Nikolakopoulou et al., 2005)
	*otr*B-RV	ggtgatgacggtctgggacag		

Table 4.4: Thermal cycler conditions for determination of tetracycline resistance genes.

Gene	Thermal Cycler Conditions
*tet*A	Pre-denaturation: 9min at 95°C, 40 cycles: 45sec at 95°C, 45sec at 55°C, 90sec at 72°C. Final incubation: 7min at 72 °C.
*tet*B	Pre-denaturation: 2min at 95°C, 30 cycles: 30sec at 95°C, 30sec at 57°C, 50sec at 72°C.
*tet*C	
*tet*D	Pre-denaturation: 9min at 95°C, 30 cycles: 45sec at 95°C, 45sec at 57°C, 90sec at 72°C. Final incubation: 7min at 72 °C.
*tet*E	Pre-denaturation: 9min at 95°C, 35 cycles: 30sec at 95°C, 30sec at 55°C, 50sec at 72°C. Final incubation: 7min at 72 °C.
*tet*G	Pre-denaturation: 9min at 95°C, 30 cycles: 30sec at 95°C, 30sec at 57°C, 50sec at 72°C.
*tet*K	
*tet*L	
*tet*M	
*tet*O	Pre-denaturation: 9min at 95°C, 35 cycles: 30sec at 95°C, 30sec at 55°C, 50sec at 72°C. Final incubation: 7min at 72 °C.
*otr*B	

4.2.5.4 Resistance to macrolides

For qualitative determination of resistance to erythromycin the method reported by Martineau et al (2000) has been applied. Presence of *erm*(A), *erm*(B), *erm*(C) and *msr*(A) genes were determined by multiplex PCR. These PCR's, besides primers to amplify the specific resistance gene, contained an internal control which amplifies the 16S rRNA gene (universal bacterial amplification) resulting in a 241bp PCR product, showing that the PCR system has worked properly. However, in order to determine the presence of *mph*(A) in activated sludge samples the method reported by Sutcliffe et al (1996) has been applied. Moreover, positive controls were used to ensure that the correct region has been amplified, and negative controls to ensure that there were no contaminations. Information on primers is given on Table 4.5.

Table 4.5: Primers used for the determination of macrolide resistance genes.

Gene	Primers	Sequence	Amplicon Size	Reference
erm(A)	*erm*A-FW	tatcttatcgttgagaagggatt	139	(Martineau et al., 2000)
	*erm*A-RV	ctacacttggcttaggatgaaa		
erm(B)	*erm*B-FW	ctatctgattgttgaagaaggatt	142	
	*erm*B-RV	gtttactcttggtttaggatgaaa		
erm(C)	*erm*C-FW	cttgttgatcacgataatttcc	190	
	*erm*C-RV	atcttttagcaaacccgtatt		
msr(A)	*msr*A-FW	tccaatcattgcacaaaatc	163	
	*msr*A-RV	aattccctctatttggtggt		
Internal control (16S rRNA)	FW	ggaggaaggtggggatgacg	241	
	RV	atggtgtgacgggcggtgtg		
mph(A)	*mph*A-FW	aactgtacgcacttgc	837	(Sutcliffe et al., 1996)
	*mph*A-RV	ggtactcttcgttacc		

For the determination of *erm* and *msr* genes, each PCR tube contained 2.5µl of 10X PCR Buffer solution (Applied Biosystems, Roche), 2µl of 2.5mM dNTP mixture, 2µl of $MgCl_2$ (25mM) solution (Applied Biosystems, Roche), 1µl of each 25µM genes specific forward and reverse primers, 0.4µl of 5U/µl Taq DNA Polymerase (Applied Biosystems, Roche), and 1µl genomic DNA. Finally appropriate amount of sterile water has been added to reach the final volume of 25 µl. Additionally each tube contained 16S rRNA universal primers with 1/10 concentration of gene specific primers to eliminate competition. Finally, the Thermal Cycler conditions for *erm* genes and *msr*(A) were: 9min at 95^{o}C pre-denaturation, 30 cycles of 30sec at 95^{o}C

denaturation, 30sec at 55^{o}C annealing and 30sec at 72^{o}C elongation. The thermal cycler conditions for *mph*(A) were: : 9min at 95^{o}C pre-denaturation, 35 cycles of 15sec at 95^{o}C denaturation, 30sec at 52^{o}C annealing and 60sec at 72^{o}C elongation, and 5min final incubation at 72 ^{o}C.

4.2.5.5 454-pyrosequencing

454 technology amplified using the "emulsion PCR" method. At the beginning small DNA fragments (400-600 bp) are ligated to adapters and separated into single strands. Later favorable conditions are created so that one fragment is bound to one DNA capture bead. These fragments are then amplified by "emulsion PCR" technique, in which each DNA capture bead is isolated within a oil emulsion, droplet of a PCR reaction mixture. The amplification results in beads each bead carries several million copies of a unique DNA fragment. In the next steps the emulsion is broken, the DNA is denatured and the beads are deposited in the PicoTiterPlate, of which the wells are designed to fit only one bead. (Delseny et al., 2010)

The PicoTiterPlate contains millions of wells, which serve as individual reactors for the sequencing reactions. In 454-pyrosequencing, the sequencing reactions are catalysed by the *Bacillus stearothermophilus* (Bst) DNA-polymerase. (Delseny et al., 2010)

PicoTiterPlate is placed in a flow cell, into which reagents are injected. During sequencing at the end of each addition of a nucleotide by the DNA-polymerase a pyrophosphate molecule is released, which is then converted into ATP by a sulfurylase. Finally, luciferase reaction produces a chemiluminescent signal using the produced ATP molecule. The chemiluminescent signal released by the ATP molecule is recorded by a camera, indicating in which well the nucleotide has been incorporated. The unincorporated nucleotides are washed away and replaced by other nucleotides. (Delseny et al., 2010)

The sequencing cycle, consisting of incorporation, recording and washing steps, is repeated with the all four nucleotides until sufficient length of the primer is achieved. The intensity of the signal recorded by the camera is proportional to the number of nucleotides that have been incorporated by the DNA-polymerase. (Delseny et al., 2010)

Prior to applying 454-pyrosequencing of activated sludge genomic DNA for community analysis the V1-V2 hypervariable regions of the 16S rRNA gene of the genomic DNA were amplified, during which a special Multiplex Identifier (MID) was attached to every sample (Hamady et al., 2008). Barcodes (MIDs) that allow sample multiplexing during pyrosequencing were incorporated between the 454 adapter and the reverse primer. MID's were attached to the reverse primer used for 16S rDNA amplification. The primers used for amplification were 27F (5'-GCCTTGCCAGCCCGCTCAGTC**AGAGTTTGATCCTGGCTCAG**-3') and 338R (5'GCCTCCCTCGCGCCATCAGNNNNNNNN**CATGCTGCCTCCCGTAGGAGT**-3'), where the bold sequences stand for the universal primers amplifying the V1-V2 hypervariable regions of the 16S rRNA gene (Baker et al., 2003). Moreover the underlined sequences represent the 454 Life Sciences FLX sequencing primers incorporated in universal primers, that are Adapter B and A in 27F and 338R, respectively. The 8Ns in 338R primer represent the MID within the primer. The PCR mixture consisted of 2.5µl of 10X PCR Buffer solution (Applied Biosystems, Roche), 2µl of 2.5mM dNTP mixture, 2µl of $MgCl_2$ (25mM) solution (Applied Biosystems, Roche), 0.5µl of each primers, 0.2µl of 5U/µl Taq DNA Polymerase (Applied Biosystems, Roche), 1µl of dimethylsulfoxid (DMSO) and 1µl genomic DNA. Finally appropriate amount of sterile water has been added to reach the final volume of 25 µl. Thermal cycler conditions were as follows: 9min at 95^{o}C pre-denaturation, 30 cycles of 10sec at 95^{o}C denaturation, 30sec at 55^{o}C annealing and 30sec at 72^{o}C elongation, and 10min final incubation at 72 ^{o}C. The PCR products were visualized by gel electrophoresis in a 2% agarose gel and staining by ethidium bromide.

Following gel electrophoresis, the bands on the gel were cut and purified by Qiagen MinElute Gel Extraction Kit Qiagen, CA, USA). The Gel extraction protocol is given in Table 4.6.

Pyrosequencing on purified amplicon mixtures was performed by Institute of Clinical Molecular Biology at University of Kiel (Kiel, Germany) using Roche Genome Sequencer 454 FLX (Roche, NJ, USA).

Table 4.6: Qiagen MinElute gel extraction protocol (MinElute Handbook 03/2006).

1. Excision of DNA Fragment	DNA Fragment was excised from the gel by a clean scalpel. Extra gel was removed and the size was minimized.
2. Solubilization of the Agarose Gel	3 volumes of Buffer QG was added to 1 volume of gel
	The mixture was incubated at 50^{o}C for 10 min. Tube was subjected to vortexing every 2-3 min to help dissolving.
3. Adjusting the pH	The mixture obtained after solubilization of the agarose gel should have a yellow color, indicating the pH value of ≤7.5.
	For orange of violet colors of the mixture, 10 µl of 3M sodium acetate was added to adjust the pH.
4. Adjusting Binding Conditions	1 volume of isopropanol was added to 1 volume of gel slice and the tube was inverted several times (no centrifugation). – Especially applied for DNA fragments <500bp and >4kb.
5. Binding the DNA	Mixture is applied to a MinElute column and centrifuged for 1 min. (flow-through was discarded) 500 µl Buffer QG was added to the spin column and centrifuged for 1 min to remove the traces of agarose left in the mixture.
6. Washing the Column	750 µl of Buffer PE was added to the MinElute Column and incubated for 2-5 min at room temperature. Tube was centrifuged for 1 min.
7. Drying the Column	Centrifuge at 13,000 x g for 1min
8. Eluting the DNA	10 µl of Buffer EB was added on the center of the membrane and incubated for 1 min at room temperature. Then centrifuged for 1 min. The eluted DNA was stored at -20^{o}C.

16S rRNA Gene Sequence Community Composition Analysis

DNA extracted from activated sludge samples collected at different days of antibiotic treatments were amplified using barcoded universal primers and a DNA pool has been prepared for pyrosequencing. Obtained sequencing products were cleaned up prior to analysis. After removing primer sequences, sequences with more than six homopolymers, ambiguous bases and chimera, each sample resulted with different amount of sequences. Following the primary clean-up of sequences groups were formed and the data has been compared amongst each other.

During the analysis all the sequences were used, and no subsampling has been done. However evaluation has been done by normalization against the total number of sequences of each sample and obtaining percentages. For clean-up PANGEA

program (Giongo et al., 2010) and for analysis of sequences MOTHUR software was utilized (Schloss et al., 2009). Taxonomic classification has been done using the RDP Classifier and alignment has been done using the SILVA bacterial reference files obtained from MOTHUR webpage (www.mothur.org). 80% confidence threshold has been used for classification. Moreover, for each group significant changes on phylum level were determined using RDP library comparison program.

To evaluate the change in richness in between samples in each group, rarefaction curves were established. Rarefaction curves were obtained by plotting the number of OTUs observed against the number of sequences sampled. The rarefaction curves for all samples gave a trend how the curve progresses as the number of samples increases, however most curves did not reach a plateau, and more number of sequences might have been needed. Theoretically, species richness was estimated by using Chao1 and ACE calculations.

To determine the estimated richness of the activated sludge samples non-parametric richness estimators, abundance-based coverage estimator (ACE) and Chao1 were calculated. All samples amongst each group were compared to each other at 3% (species) and 20% (phylum) levels.

Shannon's index was used to measure diversity of all three samples at both distances. Additionally, evenness has been calculated with E=H/lnS, where H is the Shannon's index and S is the total number of observed OTUs. Good's estimator of coverage has been calculated by the formula (1-(n/N)), where n is the number of singletons and N is the total number of observed OTUs. Shannon's index of diversity is commonly used to characterize the diversity of a community and it considers both abundance and evenness of species present. Shannon's equitability (Evenness) is a measure of the equality or distribution of individuals. It results in a number between 0 and 1, with 1 being complete even. A community in which each species present is equally abundant has high evenness; a community in which the species differ widely in abundance has low evenness (Smith and Wilson, 1996), meaning lower evenness shows increasing dominance in a population. Moreover Venn diagrams were established, using the MOTHUR program that shows the shared and unshared OTUs on species (3%) and phylum (20%) levels.

In order to determine the change in population the number of sequences of observed OTUs has been normalized to the total number of sequences in each sample, and occurrence percentages of OTUs have been obtained. Moreover to determine if the changes in the abundances are significant p-values have been calculated using MOTHUR's "metastats" command based on the Metastats program (White et al., 2009), which compares all samples to each other. In this study the significance threshold level has been selected as 0.05. Therefore for changes in OTUs, if the p-value that is the individual measure for false positive rate, is smaller than 0.05 the changes in the OTU abundances are accepted significant. For calculations of p-values the null distribution has been estimated using the permutation method (White et al., 2009). Moreover using the same method, q-values have been calculated using the "metastats" command of MOTHUR, which is an adjusted p-value using an optimized False Discovery Rate approach. Both p and q values were taken into consideration during evaluation. Statistical evaluations and classification of OTUs were done on the species level.

Due to the fact that minimum amount of unclassified operational taxonomic units (OTUs) occur on the phyla level, results were evaluated starting at the phylum level (20% difference). Significant changes observed at this level required deeper evaluation of activated sludge populations at the species level (3% difference).

5. RESULTS AND DICUSSIONS

5.1 Characterization of Antibiotics

In order to determine the basic characteristics of the antibiotic substances to be studies chemical oxygen demand (COD), total organic carbon (TOC) and ion chromatography (IC) measurements were conducted. Moreover in order to determine the wavelength in which the compounds give a peak a UV scan of the compounds has been done. Table 5.1 gives some basic information on the chosen antibiotics.

Table 5.1: Basic properties of the selected antibiotics.

Compound	Molecular Formula	CAS No	Structure
Sulfamethoxazole	$C_{10}H_{11}N_3O_3S$	723-46-6	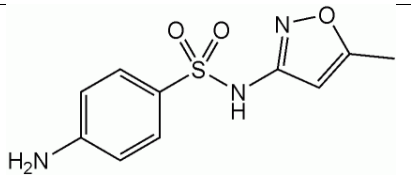
Tetracycline	$C_{22}H_{24}N_2O_8$. xH_2O	60-54-8	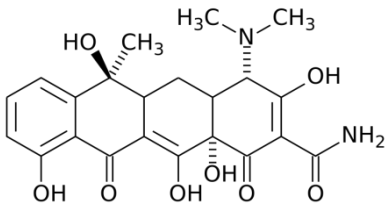
Erythromycin	$C_{37}H_{67}NO_{13}$	114-07-8	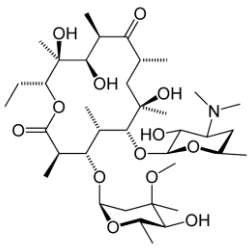

The results of characterization studies showed that TOC measurements were in accordance with the theoretical TOC (ThTOC). On the other hand, although the measured total COD concentrations were different than the theoretical COD (ThCOD) values, the soluble COD concentrations both filtered through 0.45 μm and 0.22 μm filters showed that the substances were solved in distilled water with high

efficiency. Table 5.2 and Figure 5.1 give the results for the TOC and COD measurements.

Table 5.2: COD and TOC characterization of antibiotics.

	Concentration (mg/L)	ThCOD (mg/L)	Total COD (mg/L)	ThTOC (mg/L)	TOC (mg/L)
Sulfamethoxazole	200	253	236	94.8	95.9
Tetracycline	200	318	232	119	109
Erythromycin	200	406	299	121.2	114.5

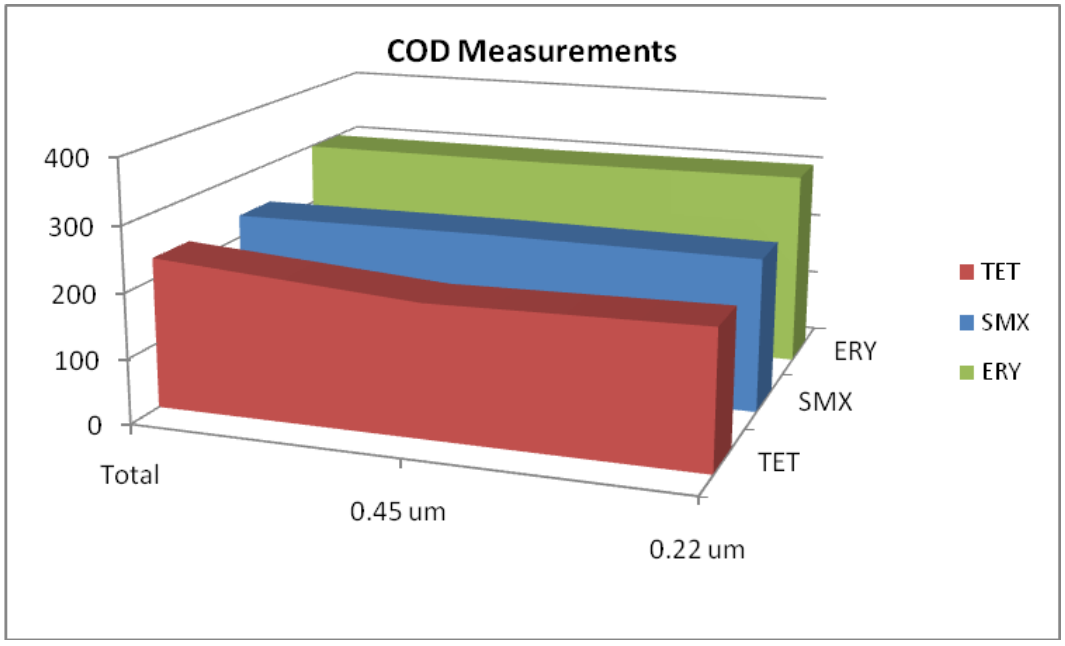

Figure 5.1: Total and soluble COD concentrations of antibiotics.

In order to determine at which wavelength these antibiotics are giving a peak, a UV scan was conducted. Results showed that erythromycin does not yield a peak between wavelengths of 400 and 700 nm. On the other hand sulfamethoxazole and tetracycline showed peaks at 262.75 nm and between 357-276 nm, respectively. For the purpose of characterization an anion scan of antibiotic solutions was conducted using an IC device. The analysis results are given in Table 5.3.

Table 5.3: UV and IC characterization of antibiotics.

	UV Absorbance (nm)	Anion Concentrations				
		Floride (mg/L)	Chloride (mg/L)	Nitrate (mg/L)	Phosphate (mg/L)	Sulphate (mg/L)
SMX	262.75	0.0206	3.16	7.0938	1.0337	4.5239
TET	357 - 276	-	2.0106	9.2641	1.1128	3.6442
ERY	-	-	2.3107	5.8882	0.814	2.0292

5.2 Reactor Operation

The control reactors were operated throughout the study period. The SS, VSS and effluent COD concentrations together with removal efficiencies and pH were monitored. The reactors were operated with a sludge age of 10d and 2 days. Influent COD concentrations were 720 mg/L. At steady state conditions the biomass concentrations for the reactors were 2000 mgVSS/L and 570 mgVSS/L, yielding the F/M ratios of 0.36 mgCOD/mgVSS and 1.26 mgCOD/mgVSS, for SRT 10d and SRT 2d reactors, respectively.

5.3 EC_{50} Inhibition Experiments (ISO 8192)

ISO8192 Respiration inhibition test was conducted in order to determine the EC50 values of the antibiotic substances. The results of the test did not show any accurate results; therefore it has been decided to choose high antibiotic concentrations, which would characterize wastewaters with high antibiotic contents. Using the selected concentrations OUR profiles were obtained by respirometry (Section 5.5.) and 30 min and 180 min OUR values were compared with 30 min and 180 min of the ISO8192 test.

The comparison showed that both tests yielded very different results. Table 5.4 and Figure 5.2 shows the differences of the measured OUR values. Moreover in the literature it has been stated that inhibition tests like ISO 8192 might be misleading since the comparison of OUR with inhibition and the control are reported at only specified times during the test and correct information about the inhibition cannot be obtained without additional information on the stoichiometry and kinetics applicable to the specific experimental conditions (Insel et al., 2006).

Table 5.4: The comparison of EC_{50} results with respirometric studies.

Inhibition Test	Control	SMX, 50 mg/L	TET, 50 mg/L	ERY, 50 mg/L
EC_{50}-30 min		57	80	75
OUR-30 min	98	83	52	40
EC_{50}-180 min		17	29	24
OUR-180 min	28	34	20	18

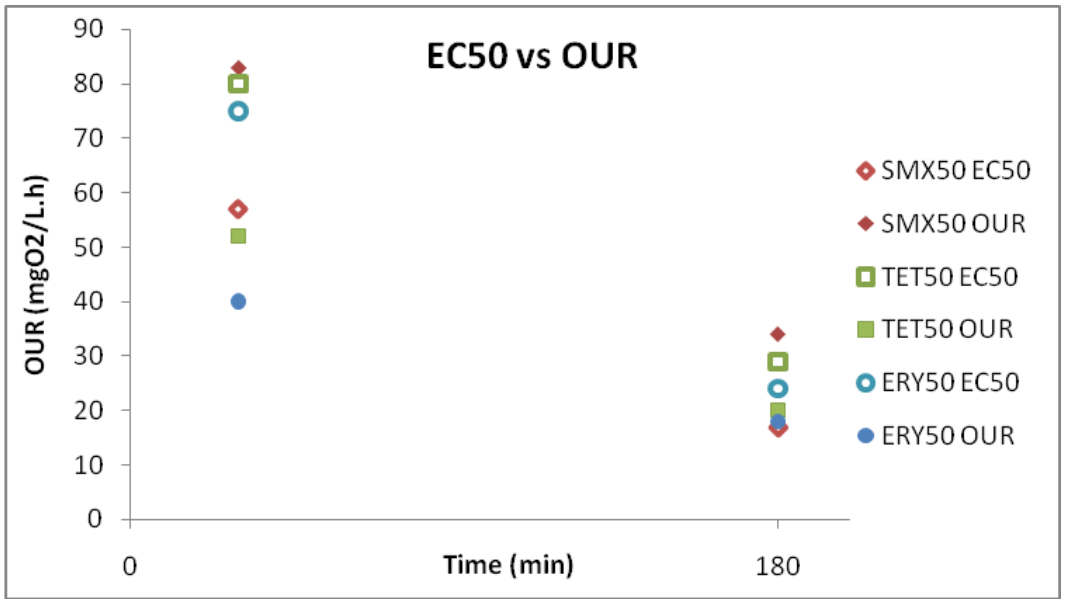

Figure 5.2: Differences between EC50 and OUR measurements.

5.4 Respirometric Studies

The study involves assessment of acute effects of antibiotics, to which the microbial system is exposed for the first time. The evaluation assumes that antibiotics remain non-biodegradable for the short term tests as indicated in the literature. On the other hand as a further study, chronic inhibition effects of antibiotics were also investigated involving continuous exposure of peptone-meat extract acclimated biomass. For the investigation of the acute effect of antibiotics 50 mg/L and 200 mg/L antibiotic concentrations were chosen. Moreover, 50 mg/L concentration was chosen for determination of chronic effects, except for SMX SRT 2d chronic reactor, to which 100 mg/L SMX was fed.

5.4.1 Acute inhibition studies SRT: 10 d

The reactors were operated with a sludge age of 10d and influent COD concentrations were 600 mg/L. At steady state conditions the biomass concentrations for the reactors were for the Peptone reactor 2000 mg/L, yielding the F/M ratios of 0.3 mgCOD/mgVSS. In order to avoid oxygen limitation during the experiments the F/M ratio of batch systems were selected as 0.42 mgCOD/mgVSS.

Using the acclimated biomass, batch reactors were set to investigate the inhibitory effects of selected antibiotics and operated under parallel conditions with the control

reactor. In this context, 7 runs of experiments were conducted; detailed information related to the batch experiments is given in Table 5.5.

Table 5.5: Characteristics of acute experiments.

Runs	Antibiotic Conc. (mg/L)	Peptone COD (mg/L)	F/M (mgCOD/ mgVSS)	Antibiotic COD (mg/L)	Total COD (mg/L)	Remaining Total COD (mg/L)
Control	-	600	0.42	0	600	36
SMX	50	600	0.45	70	670	182
	200	650	0.42	280	930	343
TET	50	600	0.43	66	666	52
	200	600	0.41	264	864	143
ERY	50	600	0.42	84	684	109
	200	600	0.42	336	939	329

During the acute inhibition experiments the biomass was exposed to the substances for the first time. The evaluation assumes that antibiotics remain non-biodegradable for the short term tests as indicated in the literature. In order to overcome oxygen limitation the F/M ratio of the batch tests was chosen as 0.42 mgCOD/mgVSS.

The OUR curve obtained from biodegradation of peptone-meat extract mixture is shown in

Figure **5.3**. The maximum oxygen uptake rate of the biomass gives the first peak around 160 mg/L.h, which is due to readily biodegradable COD components in the peptone-meat extract mixture. The profile continues to drop with different rates corresponding to degradation of different COD fractions present in the peptone-meat extract mixture. The area under the OUR curve gives the total oxygen consumption, which is calculated as 211 mg/L. The COD removal of the biomass was 94%.

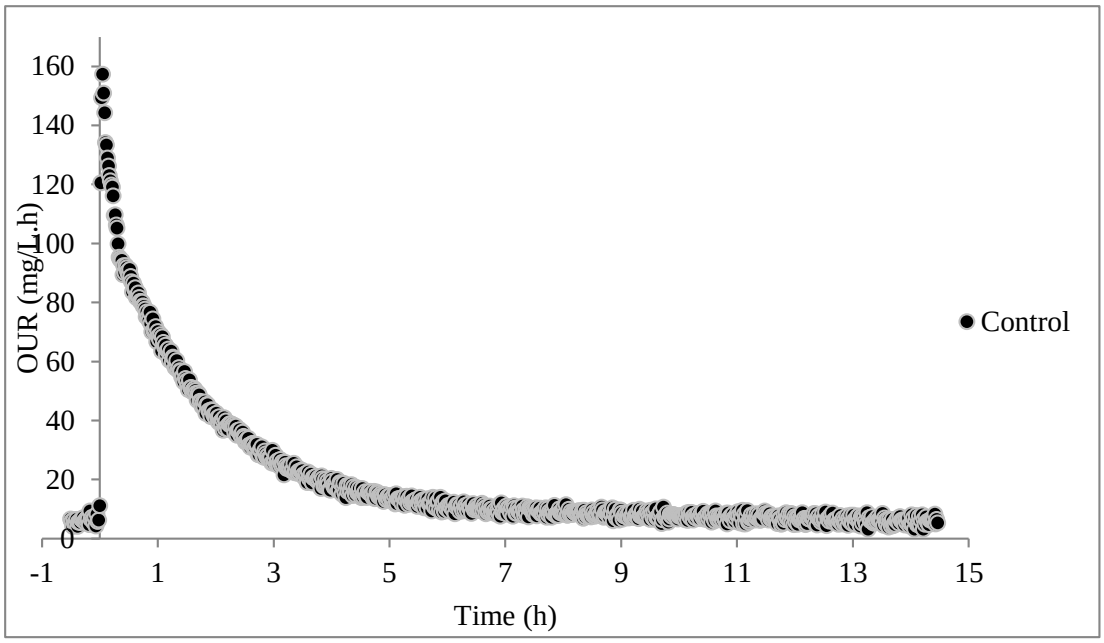

Figure 5.3: OUR curve of peptone-meat extract mixture degradation (SRT 10d).

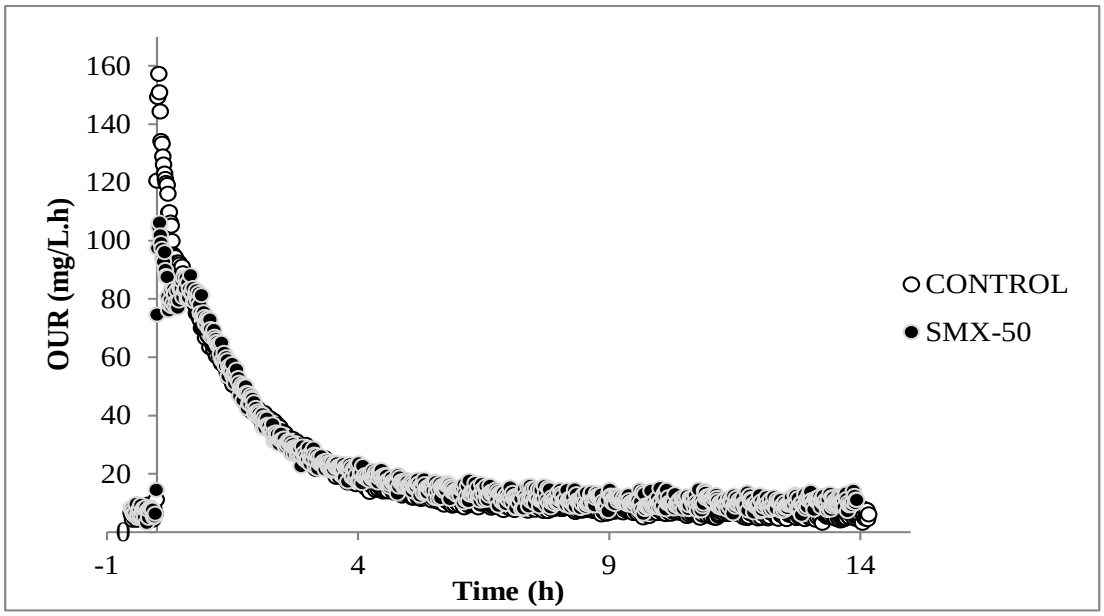

Figure 5.4: Effect of 50 mg/L SMX addition (SRT 10d).

Acute effects of 50 mg/L antibiotic addition on peptone-meat extract mixture acclimated biomass were investigated and each compound yielded different OUR profiles. SMX caused it to drop to around 106 mg/L.h (Figure 5.4). However, in the case of TET and ERY additions, the maximum oxygen uptake rate of the biomass has dropped from 160 mg/L.h to 120 mg/L.h, as shown in Figure 5.5 and Figure 5.6. The amount of oxygen consumed for the growth of microorganisms for additions of *SMX*, *TET* and *ERY* are calculated as 206, 171 and 112 mg/L, respectively.

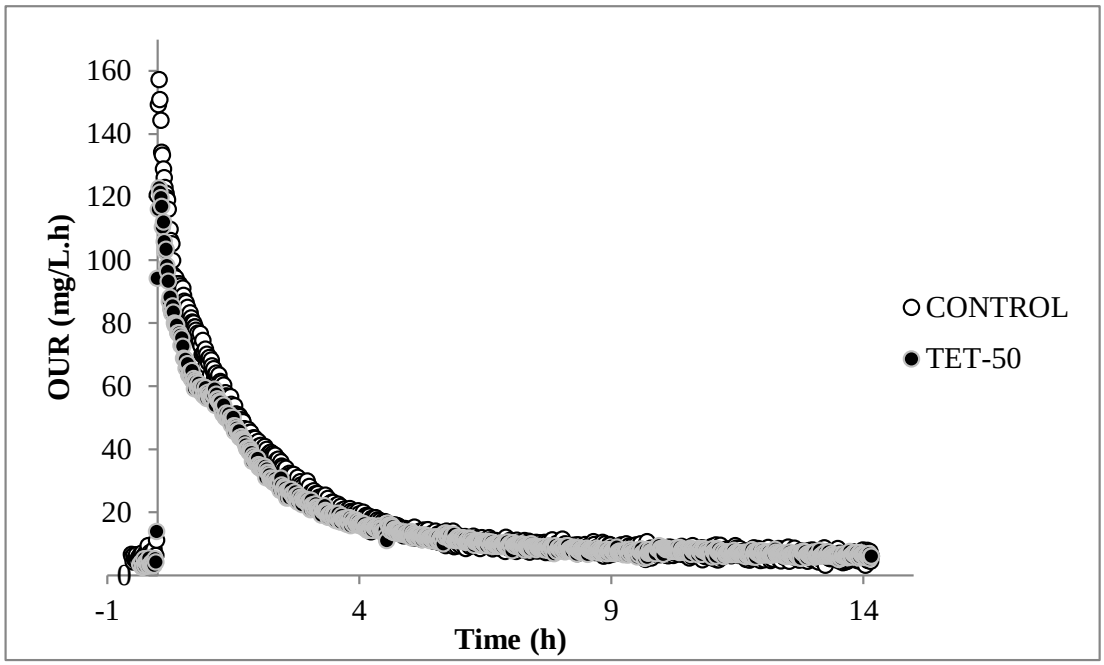

Figure 5.5: Effect of 50 mg/L TET addition (SRT 10d).

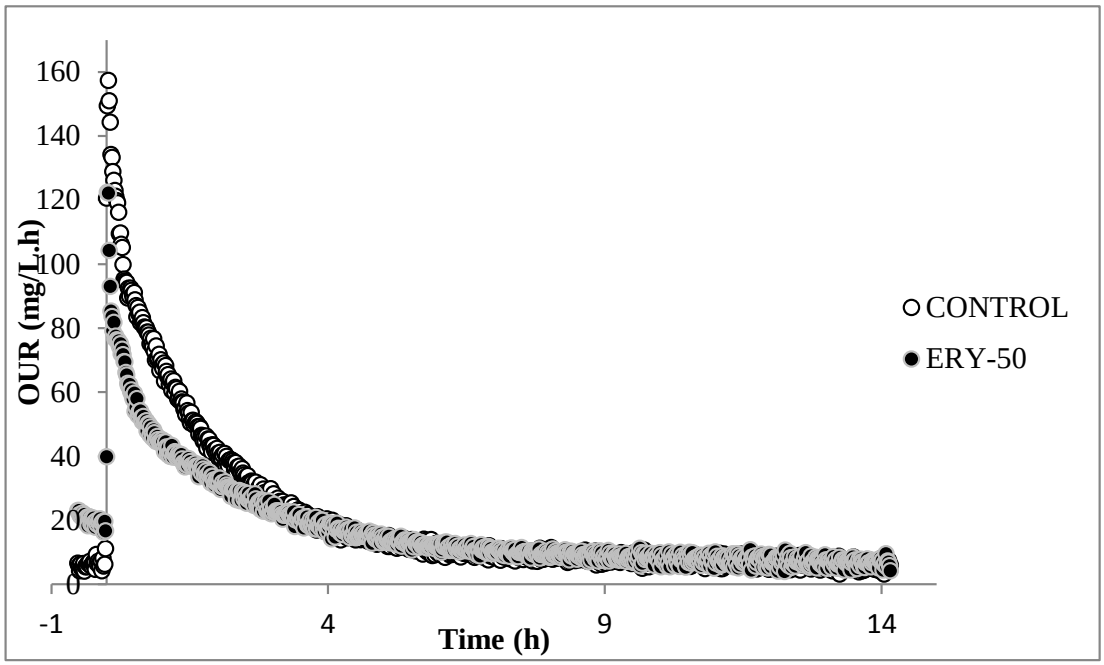

Figure 5.6: Effect of 50 mg/L ERY addition (SRT 10d).

The inhibition effects of increasing antibiotic concentrations on the biomass were investigated. In this context, antibiotic solutions of 200 mg/L concentrations were applied and the maximum oxygen uptake rate has dropped from 160 mg/L.h to 150 and 100 mg/L.h in the cases of *SMX* and *ERY* additions (Figure 5.7 and Figure 5.9). Addition of *TET* however did not cause a significant drop in the maximum oxygen uptake rate (Figure 5.8).

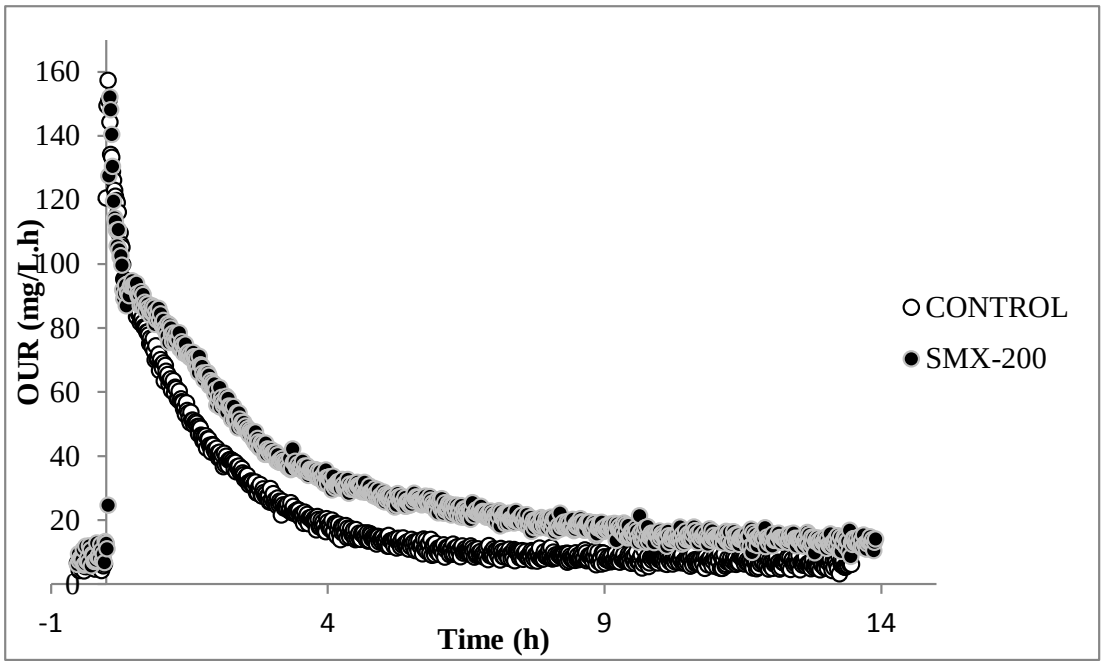

Figure 5.7: Effect of 200 mg/L of SMX addition (SRT 10d).

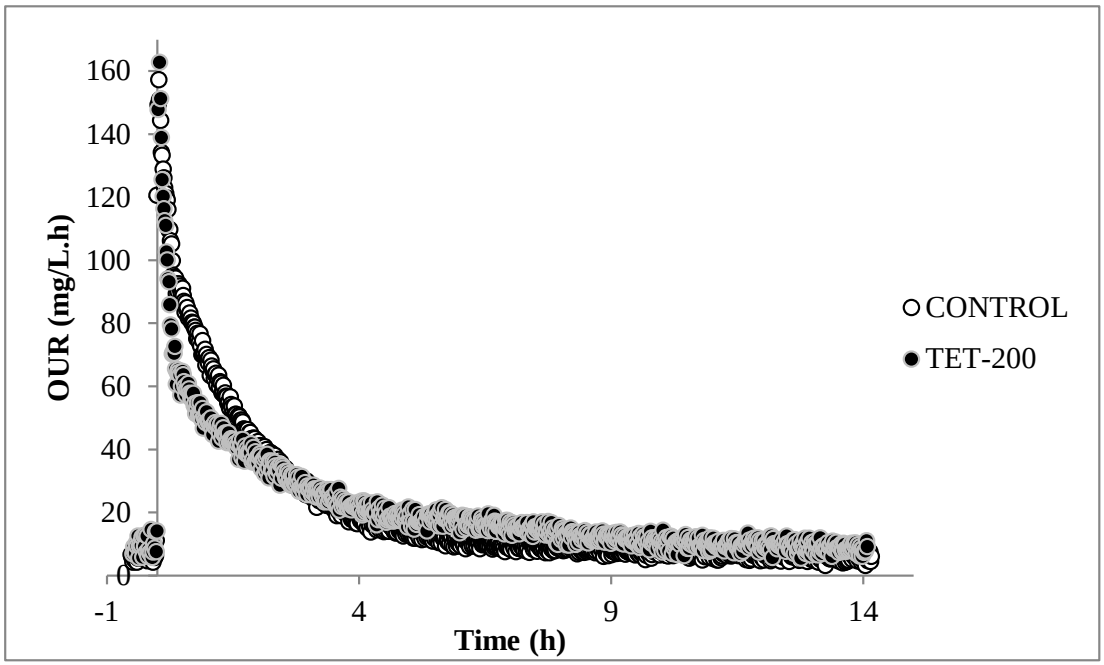

Figure 5.8: Effect of 200 mg/L of TET addition (SRT 10d).

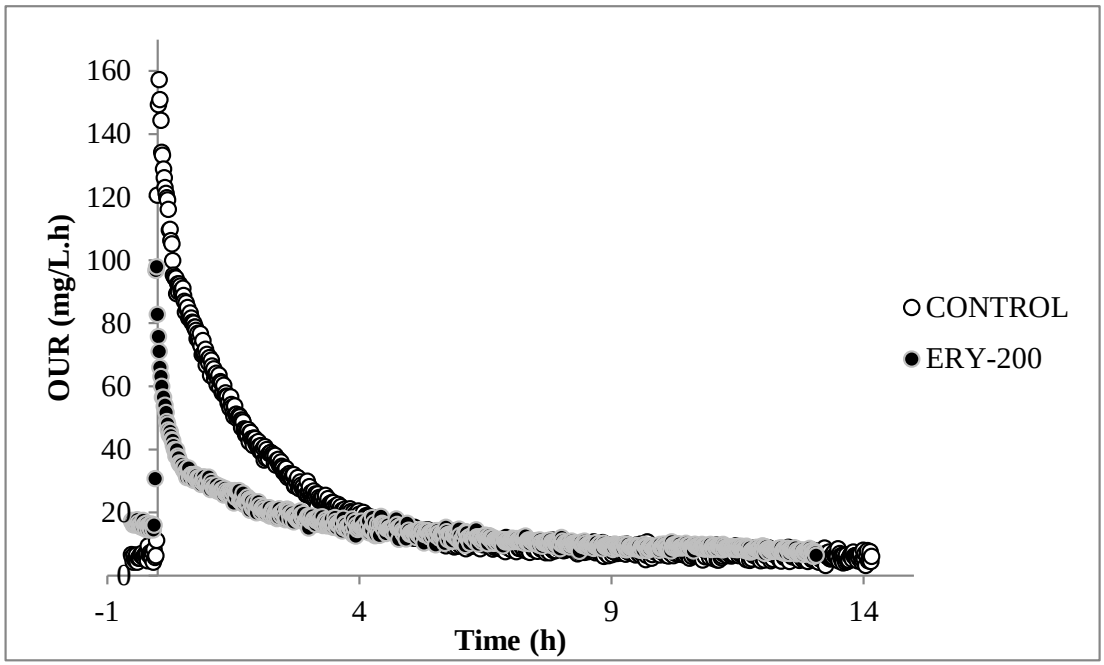

Figure 5.9: Effect of 200 mg/L of ERY additions (SRT 10d).

The system performance is better observed in terms of the total oxygen consumed during the OUR test, which were evaluated as 251 mg O_2 for *SMX* for 650 mg/L peptone-meat extract mixture addition, *174* mg O_2 for *TET* and 56 mg O_2 for *ERY* for 600 mg/L peptone-meat extract additions during 200 mg/L antibiotic acute inhibition experiments.

Addition of antibiotics has also affected the COD removal efficiency of the sludge. The peptone-meat extract mixture COD removal efficiency was calculated by assuming that in short amounts of time the antibiotic substance is not degraded. Therefore the effluent peptone-meat extract mixture COD concentration was obtained by subtracting the antibiotic COD equivalent from the total amount of effluent COD concentration, which can be called the "traditional method". However the traditional calculation is given for informational purposes, the COD removal properties of all systems will be evaluated differently in the following sections.

According to this calculation for SMX additions of 50 and 200 mg/L the peptone-meat extract removal efficiency dropped from 94% to 81% and 90%, respectively. 50 mg/L ERY addition however resulted in peptone- meat extract removal efficiencies of 96%. However the property of ERY to bind with the biomass, suggests that these values do not reflect the real response of the system. The peptone-meat extract mixture COD removal efficiencies of 50 and 200 mg/L TET added systems could not be calculated, since it is known that TET has the tendency to adsorb onto the sludge

and also bind and settle with the divalent ions in the system like calcium and magnesium that can also be found in the feeding solutions of the reactor. COD removal trend of all batch experiments can be seen in Figure 5.10.

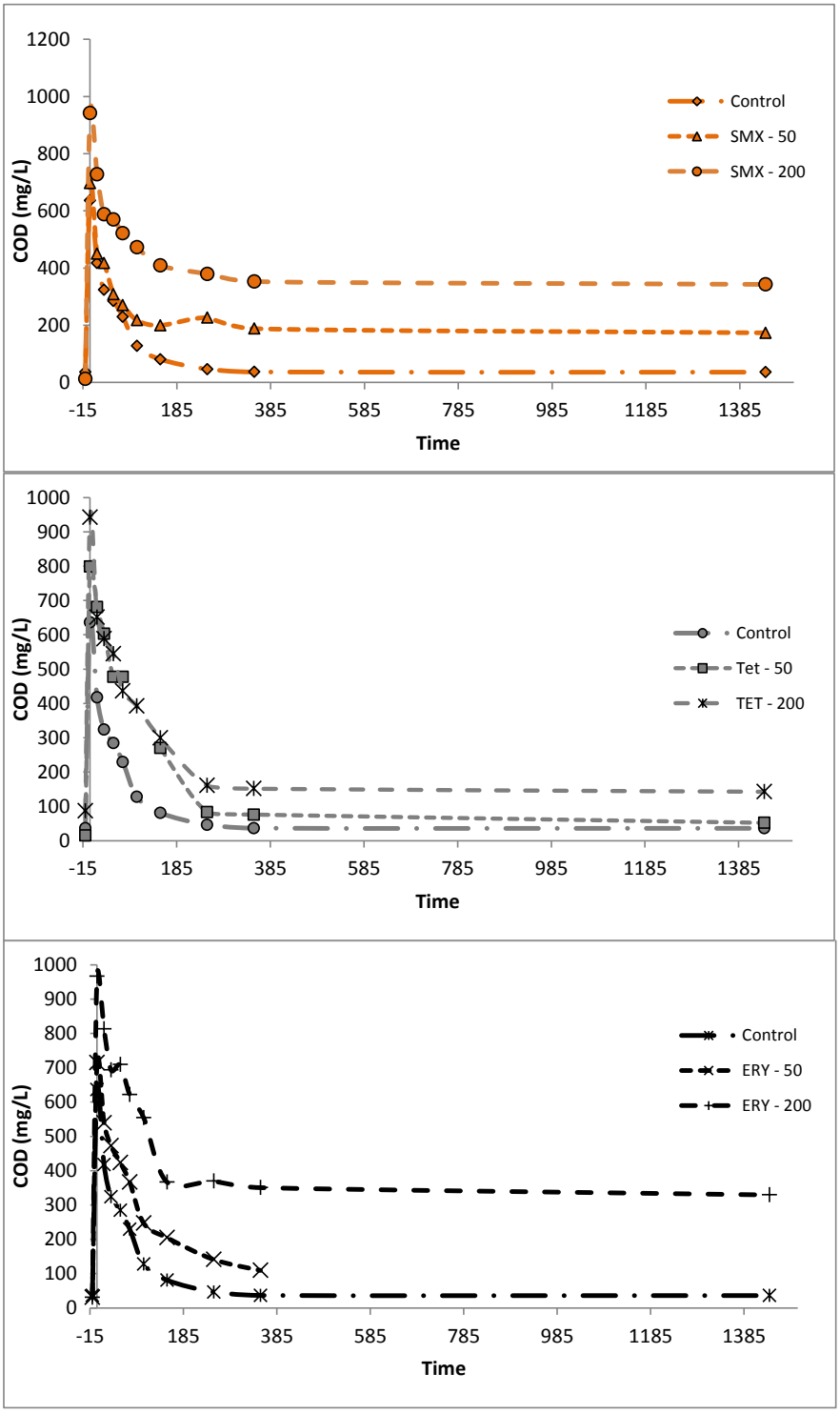

Figure 5.10: Effect of acute antibiotic addition on COD removal performance.

5.4.2 Acute inhibition studies SRT: 2 d

Using the acclimated biomass from the control reactor (SRT: 2d), batch reactors were set to investigate the inhibitory effects of selected pharmaceuticals and operated under parallel conditions with the control reactor. The sludge age 2d control reactor was fed with 720mgCOD/L. At steady state conditions the biomass concentrations for the reactors were for the Peptone reactor 570 mg/L, yielding the F/M ratios of 1.26 mgCOD/mgVSS. Sludge taken from the control reactor was used to determine the acute inhibition impact of antibiotics on the sludge age 2d biomass. In this context, 6 runs of experiments were conducted; detailed information related to the batch experiments is given in Table 5.6.

Table 5.6: Characteristics of batch experiments SRT: 2d.

Runs	Antibiotic Conc. (mg/L)	Peptone COD (mg/L)	F/M (mgCOD/ mgVSS)	Antibiotic COD (mg/L)	Total COD (mg/L)	Remaining Total COD (mg/L)
Control	-	760	1.33	0	760	71
SMX	50	720	1.14	70	770	189
	200	720	1.28	280	1000	326
TET	50	720	1.03	66	786	75
	200	720	1.14	264	984	267
ERY	50	720	1.27	84	804	379

The OUR curve obtained from peptone-meat extract mixture of the sludge age 2 d system gives the first peak around 80 mg/L.h, which is due to readily biodegradable COD components in the peptone-meat extract mixture, and coincides with the maximum oxygen uptake rate of the biomass. The area under the OUR curve giving the total oxygen consumption for the degradation of the substrate by a fast growing biomass consortia was calculated as 284 mg/L. The COD removal efficiency of the sludge age 2d control reactor was 91%.

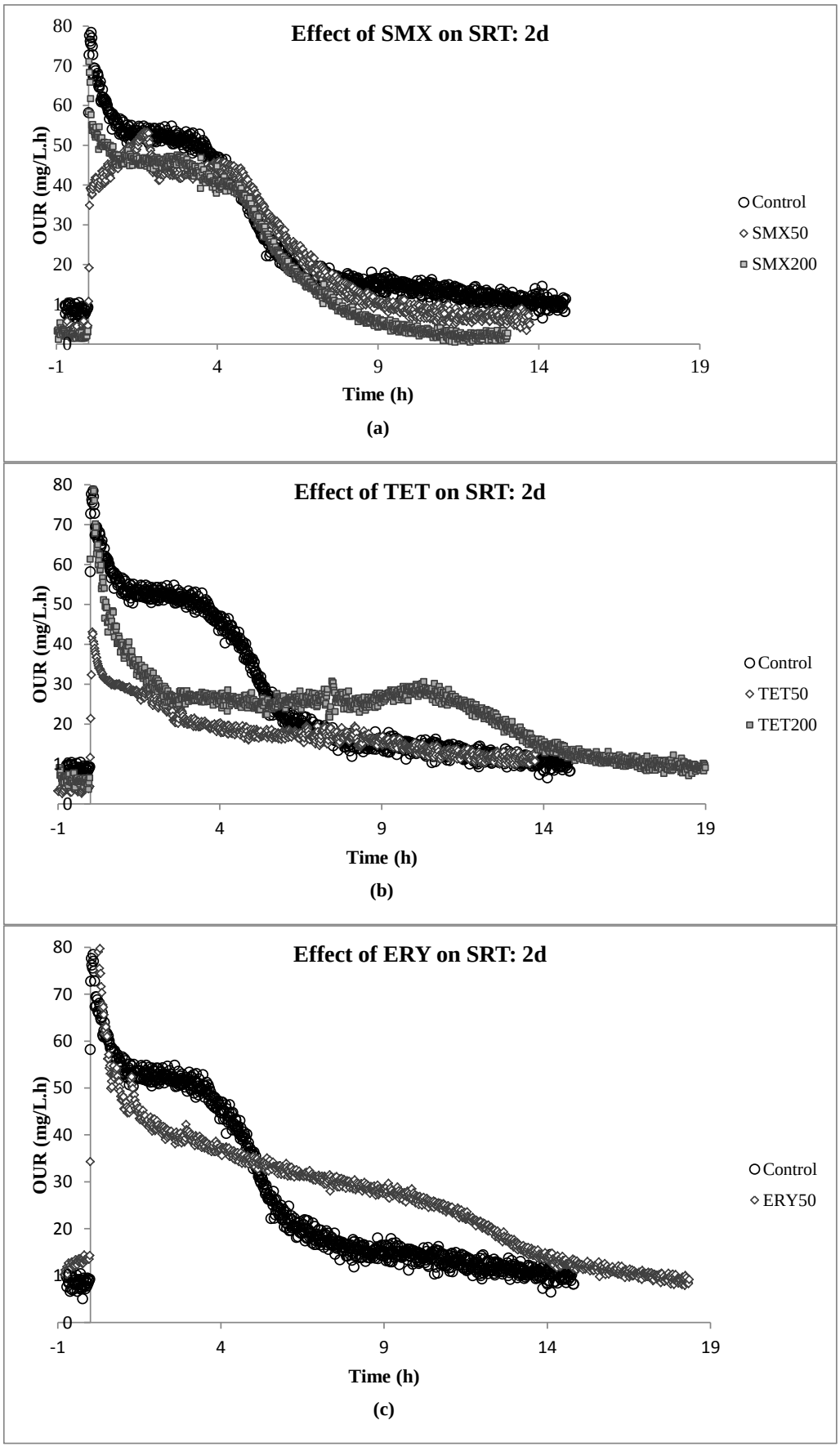

Figure 5.11: Acute inhibition effects of antibiotics on peptone-meat extract mixture degradation SRT: 2d.

Addition of 50 mg/L of SMX, TET and ERY had different effects on the substrate removal of the system. The maximum oxygen uptake rate of the control system dropped to 53 mg/L.h for SMX addition, whereas TET addition caused it to drop to 43 mg/L.h. The maximum oxygen uptake rate for ERY50 acute inhibition system was 67 mg/L.h (Figure 5.11). Moreover the total amount of oxygen consumptions of inhibited systems has also lowered, showing that the COD removal capacity of the system has been altered. The total area under the OUR curves are 266 mg/L, 229 mg/L and 124 mg/L for SMX, TET and ERY, respectively. Maximum oxygen uptake rates of SMX200 and TET200 acute systems were 71 mg/L.h and 95 m/L.h, respectively. Total amount of oxygen consumptions were 260 mg/L, 187 mg/L for SMX and TET, respectively. The degree of inhibition caused by the antibiotic substance can be seen by the amount of decrease of the oxygen consumption.

The experiments showed that antibiotic substances have different effects on the COD removal efficiencies of batch systems, which were calculated using the traditional method. The peptone-meat extract mixture COD removal efficiency was calculated for SRT 2d acute experiments as well. The peptone-meat extract mixture COD removal efficiency for 50 and 200 mg/L SMX additions were calculated as 84% and 94%, respectively. Addition of 50 mg/L ERY retarded the COD removal at most and made it to drop until 59%. On the other hand the tendency of TET to bind with ions and settle may have caused peptone to be unavailable for biodegradation and also in the effluent liquid phase, since the removal efficiencies were calculated as 99% for both 50 and 200 mg/L addition of TET. Figure 5.12 shows the COD removal trends of all SRT 2d acute inhibition experiments.

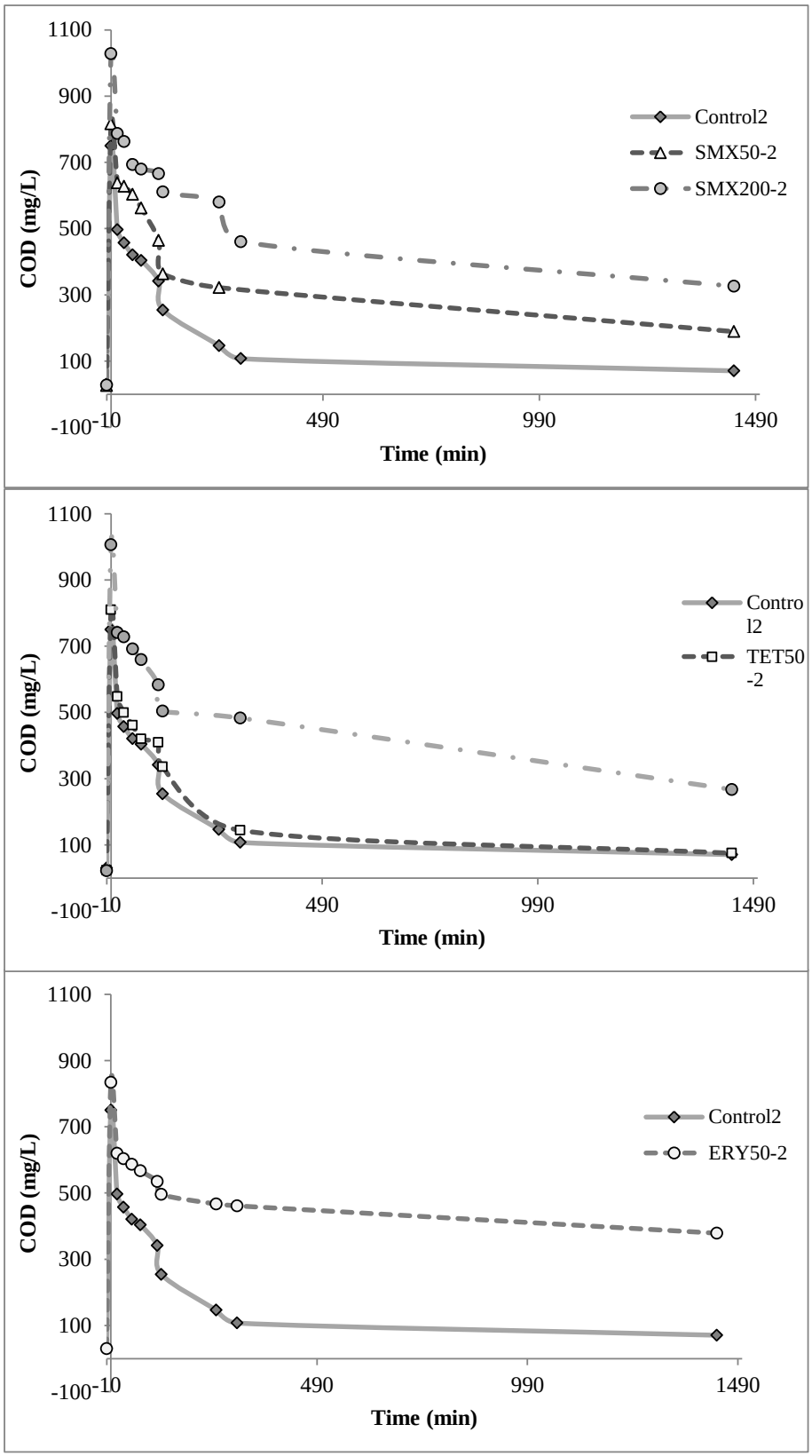

Figure 5.12: COD removal trends of batch experiments.

5.4.3 Chronic inhibition studies

Total number of six chronic inhibition tests has been run. During SRT 2d experiments, respirometric tests were conducted together with a parallel reactor on 0, 2nd, 4th, 6th and 7th days, of which for the last two days only antibiotic and only peptone-meat extract mixture were given as substrates. On the other hand during SRT 10 d experiments, respirometric tests were conducted on 0, 5th, 10th, 20th and 30th days. On the 30th day a parallel system was set to determine only the effect of the antibiotic substance on the system. Table 5.7 gives the characteristics of chronic experiments.

Table 5.7: Characteristics of chronic experiments.

Runs	Sludge Age (days)	Antibiotic Concentration (mg/L)	Peptone COD (mg/L)	Antibiotic COD (mg/L)	Total COD (mg/L)
Control	2	-	760	0	760
	10	-	600	0	600
SMX	2	100	720	140	860
	10	50	720	70	790
TET	2	50	720	66	786
	10	50	720	66	786
ERY	2	50	720	84	804
	10	50	720	84	804

Moreover in the last day of all chronic sets, degradation of each antibiotic compound was analyzed, which showed that the amount of oxygen consumed was not due to degradation of the antibiotic compounds. The areas under the OUR curves could not be calculated, due to the fact that the biomass did not consume oxygen. The only effect was that the addition of antibiotics increased the endogenous decay level of the biomass. In the case of SMX all the added SMX was measured in the effluent liquid phase, showing that it was not degraded by microorganisms.

S100 SRT 2d chronic reactor was fed with a combination of 720 mgCOD/L of peptone-meat extract mixture and 100mg/L of SMX, which in total resulted in 860 mgCOD/L. Each day the SMX concentration was measured and all the substance was found in the effluent liquid. Moreover SMX altered peptone removal of the system, as well, which can be seen looking at the amount of oxygen consumed on the 7th day, where only peptone was fed to the system. System was fed with only

peptone-meat extract mixture it only consumed 217 mg/L oxygen. Additionally, the change in the total amount of oxygen consumed and also the OUR curve profile during the course of 7 days also suggest that chronic exposure to SMX alters the behavior of the biomass. The amount of oxygen consumed decreased as well; 181 mg/L and 255 mg/L in 2nd and 4th days of exposure, respectively, whereas the control system utilized 284 mg/L oxygen without the interference of the antibiotic substance. The OUR profiles and COD removal trends of S100 SRT 2d chronic reactor can be seen in Figure 5.13 and Figure 5.16, respectively.

Table 5.8: Amount of oxygen consumed during chronic experiments.

Day/Run	S100 SRT:2d [mg/L]	T50 SRT:2d [mg/L]	E50 SRT:2d [mg/L]	S50 SRT:10d [mg/L]	T50 SRT:10d [mg/L]	E50 SRT:10d [mg/L]
0	284	284	284	211	211	211
2	181	278	-	-	-	-
4	255	-	218 (D3)	-	-	-
5	-	-	-	-	207	110
6	-	-	-	-	-	-
7	217	271	-	-	-	-
10	-	-	274	275	206	-
20	-	-	-	277 (D24)	-	-
30	-	-	-	278	243	238 (D31)
50	-	-	-	275	-	216

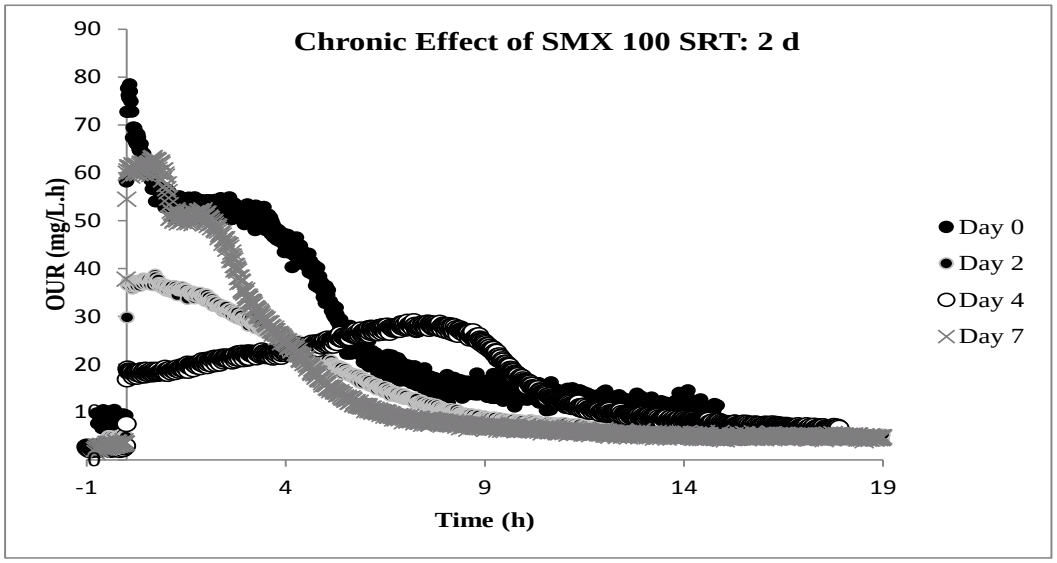

Figure 5.13: Chronic effect of SMX on activated sludge system (SRT: 2d, 100 mg/L).

T50 SRT 2d chronic reactor was fed with a combination of 720 mgCOD/L of peptone-meat extract mixture and 50mg/L of TET, which in total resulted in 786 mgCOD/L. In the 6th day, where only TET was fed, the obtained OUR curve suggests that TET was not degraded by the biomass. Moreover peptone-meat extract mixture removal efficiency of the biomass seems only slightly to be affected, since on the 7th day the amount of oxygen consumed for the degradation of peptone-meat extract addition was close to the control system, as well as the COD removal efficiency. However in the case of TET, as in the former COD efficiency calculations, the calculated removal efficiency may not reflect the truth due to the binding properties of the antibiotic substance with divalent ions. Moreover, even though the area under the OUR curves are the same, showing that the same amount of oxygen is utilized, it can be seen that the profile has altered. More insight in the change of degradation kinetics will be revealed in the activated sludge modeling section. The OUR profiles and COD removal trends of T50 SRT 2d chronic reactor can be seen in Figure 5.14 and Figure 5.16, respectively.

E50 SRT 2d chronic reactor was fed with a combination of 720 mgCOD/L of peptone-meat extract mixture and 50mg/L of ERY, which in total resulted in 804 mgCOD/L. The chronic test of ERY 50 mg/L of SRT 2d showed lower oxygen consumption of 218 mg/L in the 3rd day of exposure. The obtained OUR curve during only ERY feeding on the 7th day, suggests that ERY was not degraded by the biomass. Chronic exposure of ERY has changed the OUR profile and the oxygen consumption decreased slightly. On the 10th day, where only peptone was fed to the system, the biomass consumed 274 mg/L oxygen for growth, whereas the control reactor required 284 mg/L oxygen for growth. The OUR profiles and COD removal trends of E50 SRT 2d chronic reactor can be seen in Figure 5.15 and Figure 5.16, respectively.

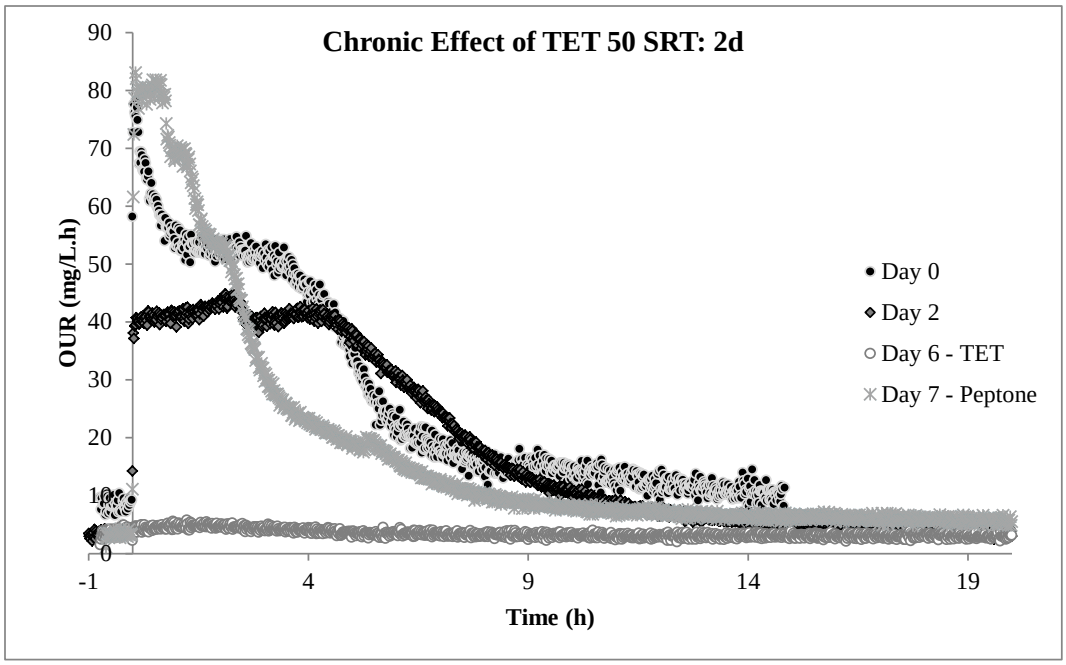

Figure 5.14: Chronic effect of TET on activated sludge system (SRT: 2d, 50 mg/L).

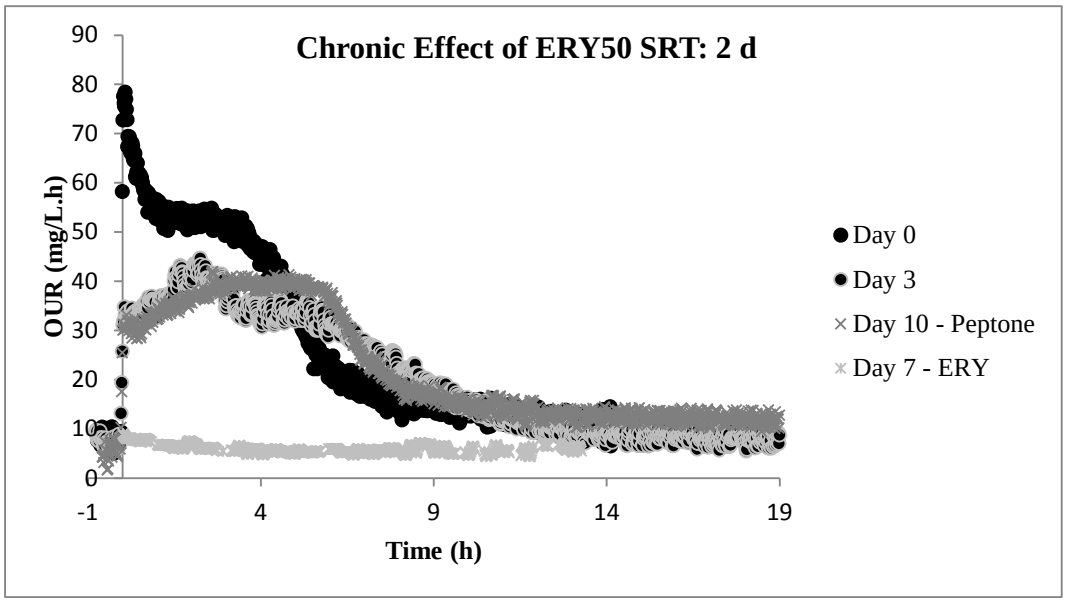

Figure 5.15: Chronic effect of ERY on activated sludge system (SRT: 2d, 50 mg/L).

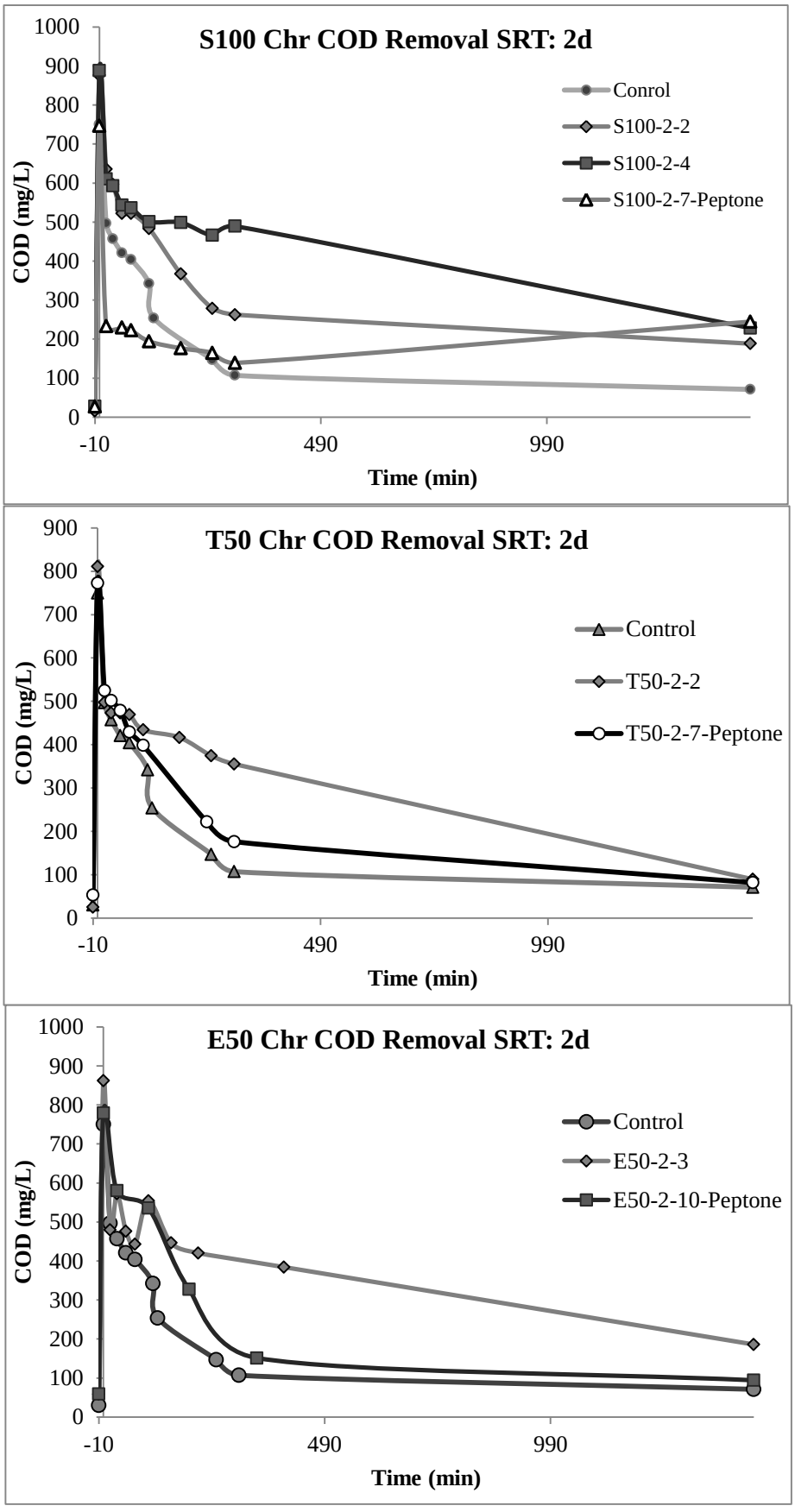

Figure 5.16: COD removal trends of chronic feeding reactors (SRT: 2d).

S50 SRT 10d chronic reactor was fed with a combination of 720 mgCOD/L of peptone-meat extract mixture and 50mg/L of SMX, which in total resulted in 790 mgCOD/L. SMX measurements and the obtained OUR curve on the day of only SMX-feeding showed that SMX was not degraded by the biomass. The change in the OUR curve profile during the course of 30 days suggest that chronic exposure to SMX alters the behavior of the biomass. The OUR profiles and COD removal trends of S50 SRT 10d chronic reactor can be seen in Figure 5.17 and Figure 5.20, respectively.

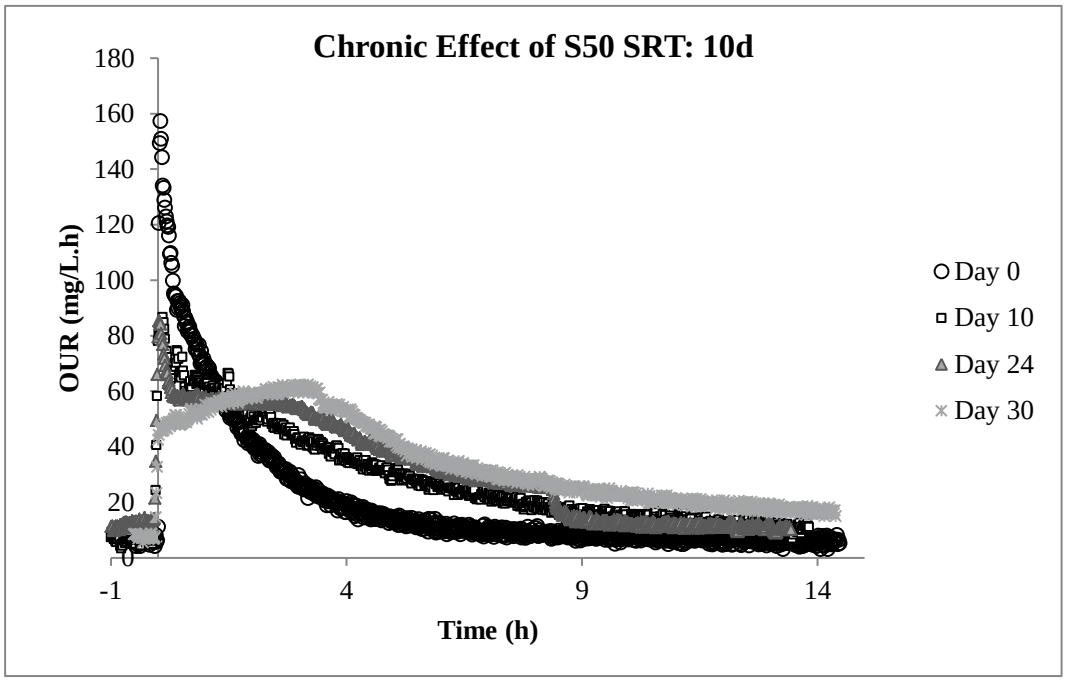

Figure 5.17: Chronic effect of SMX on activated sludge system (SRT: 10d, 50 mg/L).

T50 SRT 10d chronic reactor was fed with a combination of 720 mgCOD/L of peptone-meat extract mixture and 50mg/L of TET, which in total resulted in 786 mgCOD/L. The amount of oxygen consumed when only TET was fed, suggests that TET was not degraded by the biomass. On the 5th and the 10th days the amount of oxygen consumed for growth drops to 207 mg/L and 206mg/L, respectively, suggesting lower amount of COD consumption. However on the 31st day the oxygen consumption was 243 mg/L. Moreover, it can be seen that the OUR profile has altered in the course of 30 days of chronic exposure to TET. More insight in the change of degradation kinetics will be revealed in the activated sludge modeling section. The OUR profiles and COD removal trends of T50 SRT 10d chronic reactor can be seen in Figure 5.18 and Figure 5.20, respectively.

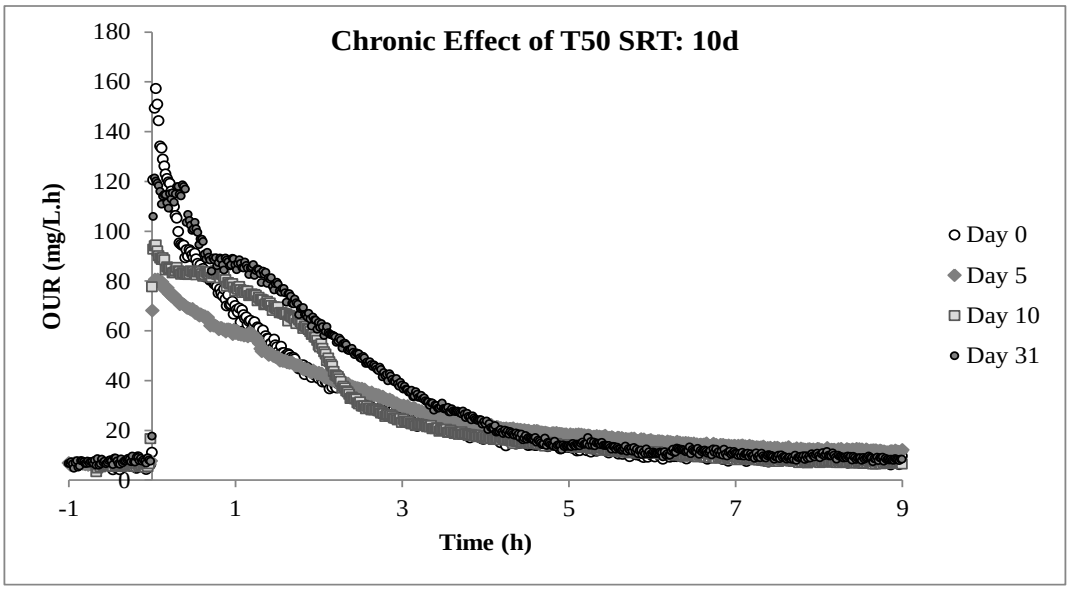

Figure 5.18: Chronic effect of TET on activated sludge system (SRT: 10d, 50 mg/L).

E50 SRT 10d chronic reactor was fed with a combination of 720 mgCOD/L of peptone-meat extract mixture and 50mg/L of ERY, which in total resulted in 804 mgCOD/L. The chronic test of ERY 50 mg/L of SRT 10d showed lower oxygen consumption of 110 mg/L on the 5th day of exposure. However after 30 days of exposure the system consumed almost twice as much oxygen (238 mgO_2/L), even though still lower than the control system. Chronic exposure of ERY has changed the OUR profile and the oxygen consumption decreased. The OUR profiles and COD removal trends of E50 SRT 10d chronic reactor can be seen in Figure 5.19 and Figure 5.20, respectively.

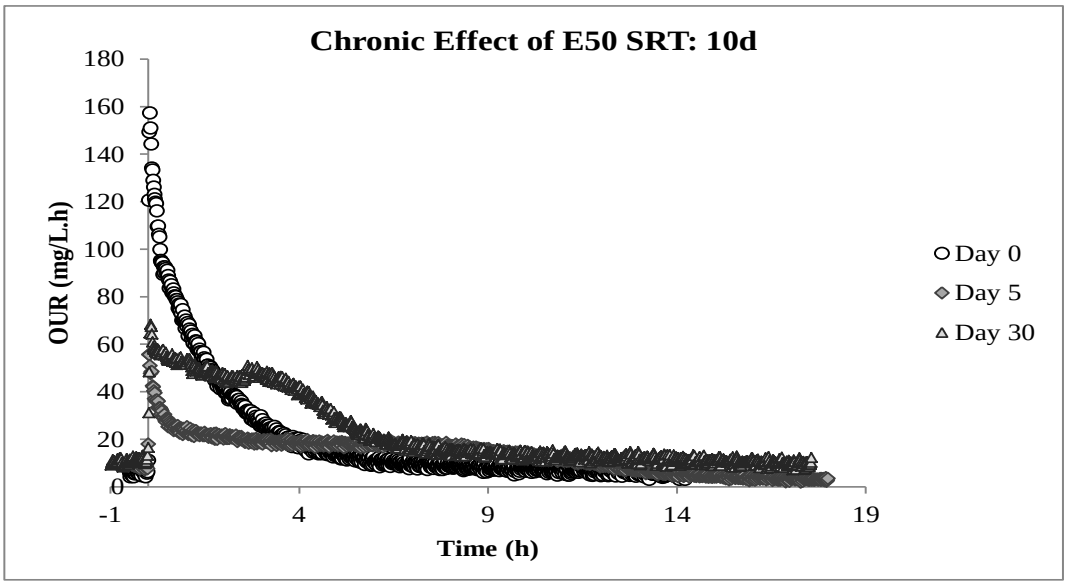

Figure 5.19: Chronic effect of ERY on activated sludge system (SRT: 10d, 50 mg/L).

The calculated peptone-COD removal efficiencies for acute and chronic tests for antibiotic substances may not be the correct approach for investigating the effect of antibiotics on the biomass activity. The reason for this is that the amount of oxygen consumed decreases with the addition of antibiotics in both acute and chronic experiments. However the system reaches the endogenous decay level almost at the same time as the control system, which suggests that the system consumes fewer amounts of COD, therefore that the antibiotic substances have the property to bind with the enzyme-substrate complex causing uncompetitive inhibition. This phenomenon will be explained in the following sections, however in this section the standard method is used to calculate the peptone-removal efficiencies, assuming that the concentration of antibiotic substances are stable throughout the experiment. Chronic exposure to SMX had different peptone-meat extract COD removal efficiencies on different days; 93% and 87% on 2^{nd} and 4^{th} days, respectively. SMX decreased the peptone removal efficiency of the system after 7 days from 91% (SRT 2d Control) to 68%. In the case of TET, due to its binding properties of TET with divalent ions standard COD removal efficiency calculations are not reliable. However, the calculated value is 97% on the 2^{nd} day of chronic feeding. Moreover, peptone removal efficiency of the system after 7 days of chronic exposure to TET was 89%. The chronic test of ERY 50 mg/L of SRT 2d showed 80% of peptone-meat extract mixture COD removal efficiency in the 3^{rd} day of exposure. The effect of ERY on peptone-meat extract mixture removal on the 10^{th} day was not very dramatic, however the OUR profile has changed and the oxygen consumption decreased slightly, whereas the peptone-meat extract removal efficiency dropped from 91% (SRT 2d Control) to 88% (day10). The SRT 10d chronic experiments had different results on peptone-meat extract COD removal efficiency. The efficiency of the SMX system changed from 94% (SRT 10d Control) to 95%, 87% and 93% on days 10, 24 and 30, respectively. Moreover when the system was fed with only peptone-meat extract mixture the COD removal efficiency was calculated as 92%. Chronic TET exposure had higher COD removal efficiencies, 97% and 95% efficiency on 5^{th} and 10^{th} days. Finally, the calculated efficiencies for chronic ERY exposure were 93%, 100% and 93% on 5^{th}, 10^{th} and 30^{th} days. As can be seen from the calculation results, the peptone-meat extract COD removal efficiency cannot be interpreted with the usual vision, and binding of antibiotics on the substrate-enzyme complex should be taken into consideration. (Figure 5.20)

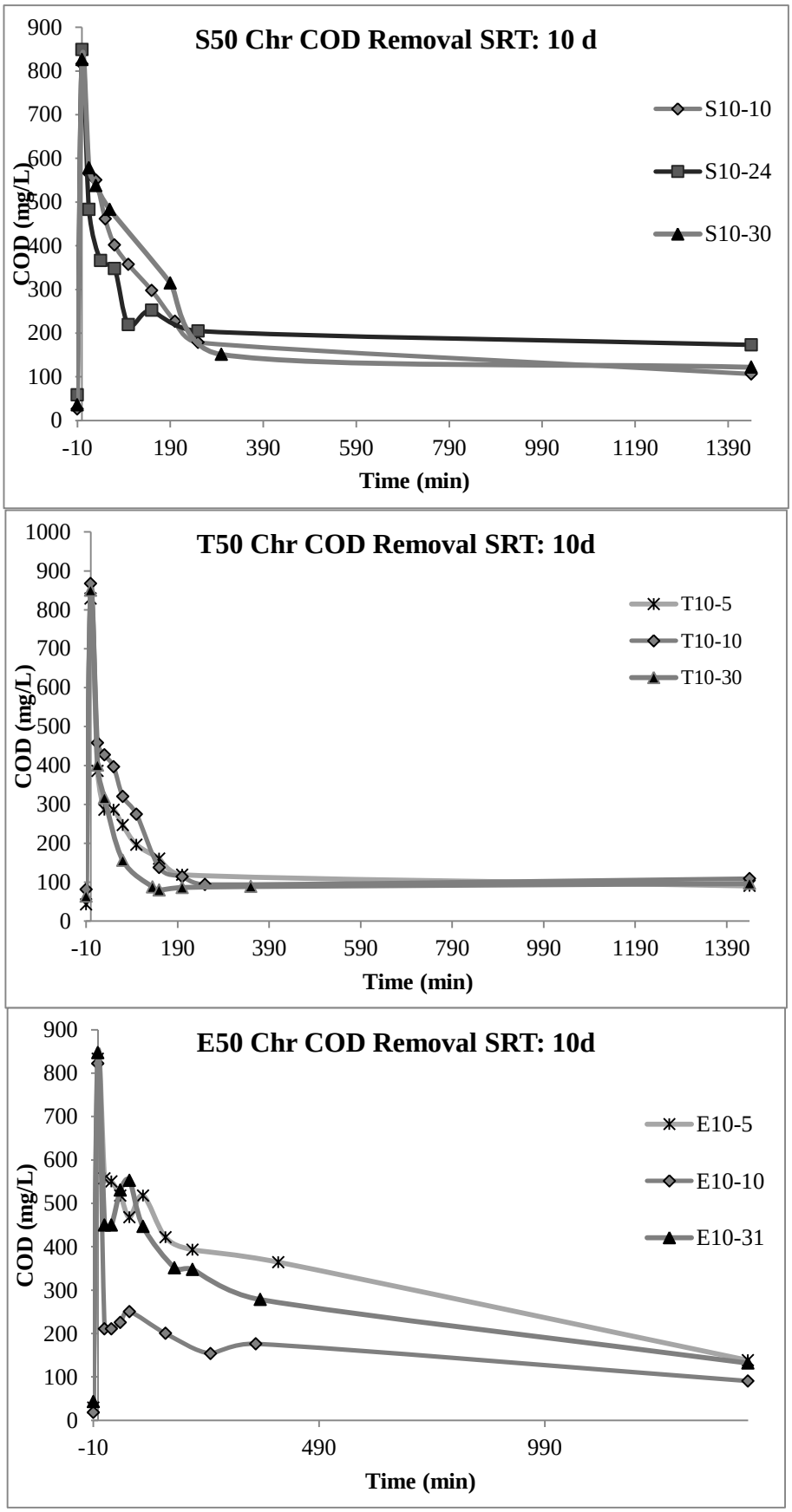

Figure 5.20: COD removal trends of chronic feeding reactors (SRT: 10d).

As can be seen from Figure 5.21, the biomass concentration in the chronic reactors decreased with increasing time of exposure to antibiotics. Additionally, the SRT 2d reactors show an imbalanced profile under the effect of antibiotics.

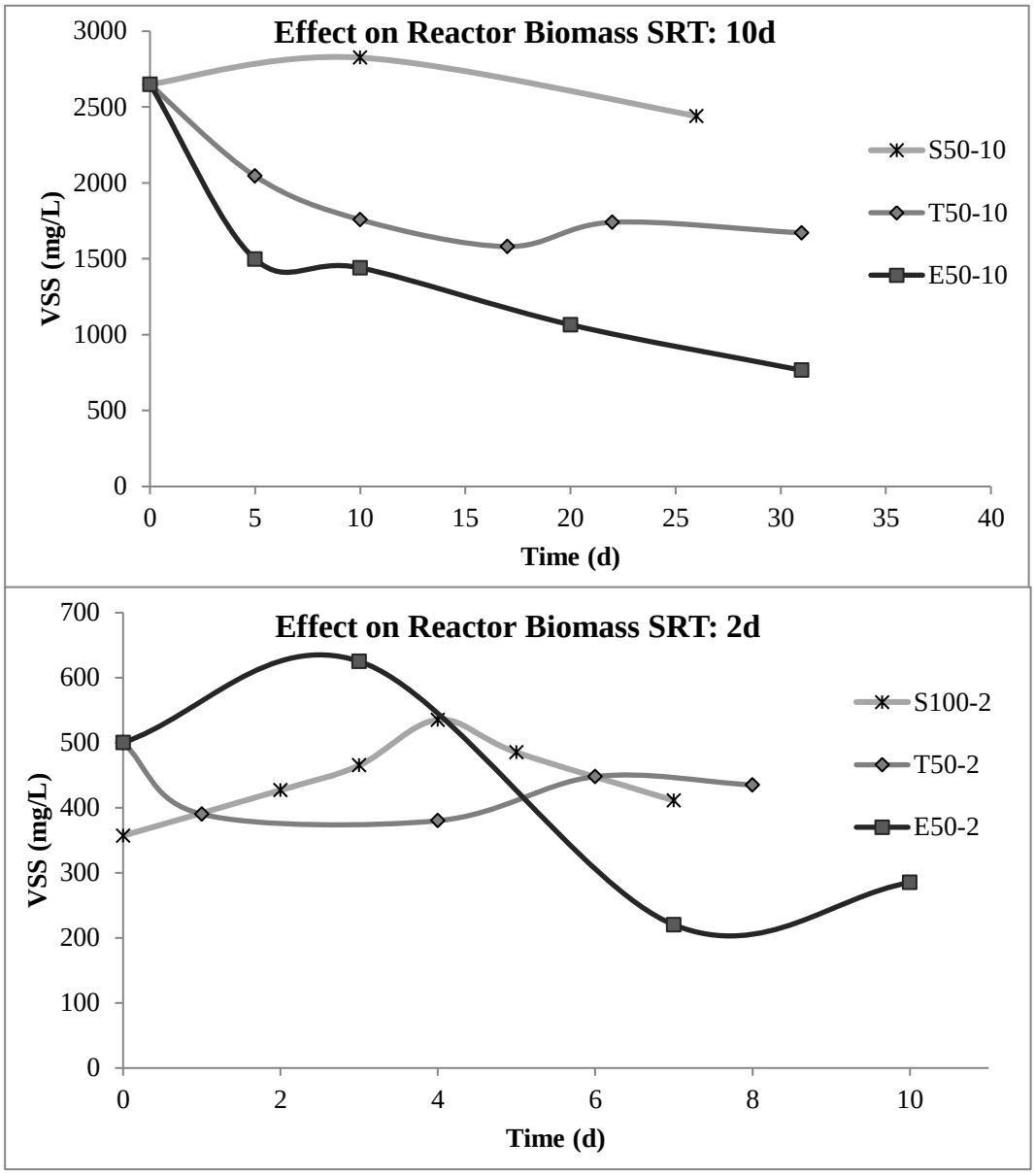

Figure 5.21: Chronic effect of antibiotics on reactor biomasses (Top: SRT 10d, Bottom: SRT 2d).

5.5 Antibiotic Measurements

The measurements of SMX showed that the substance is kept in the mixed liquor. In acute and also in chronic inhibition experiments all the given SMX has been measured in the 0.45 μm filtered samples.

Figure 5.22 Figure 5.22, Figure 5.23 and Figure 5.24 show the effluent SMX concentrations of the acute experiments and the chronic reactors (SRT 2 and 10 days), respectively. As can be seen in the figures all the fed antibiotic compound was measured in the effluent. These findings are supported with the knowledge in the literature that SMX does not have the property to adsorb onto the sludge, and moreover shows that the substance has not been degraded by the activated sludge biomass.

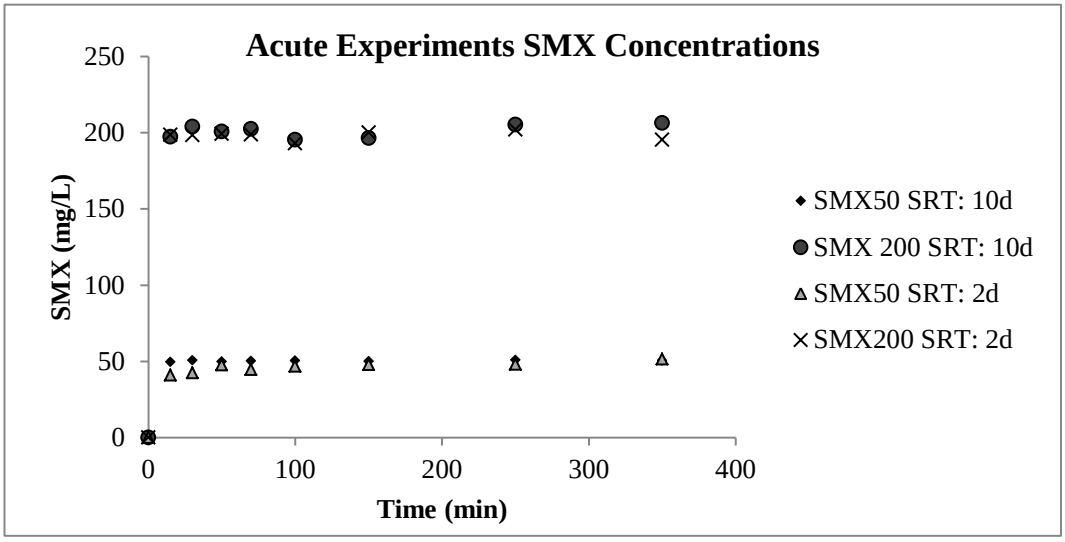

Figure 5.22: SMX concentrations in the acute inhibition experiments.

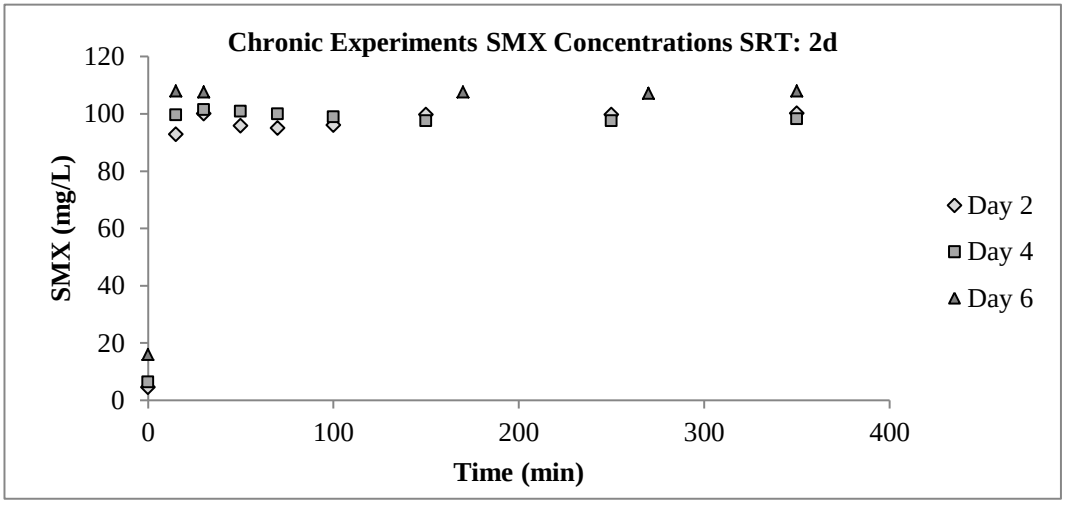

Figure 5.23: Effluent SMX concentrations in the chronic reactor (SRT: 2d).

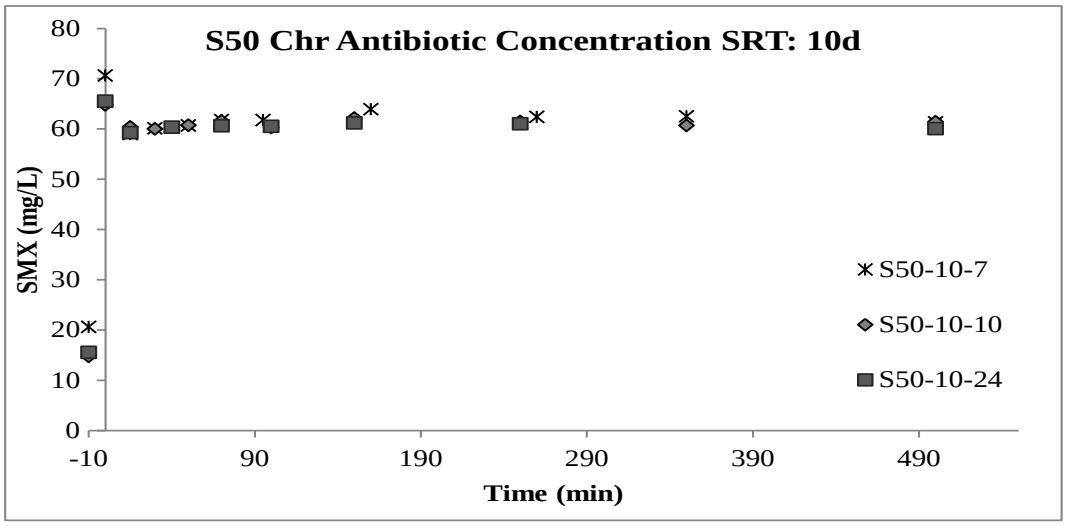

Figure 5.24: Effluent SMX concentrations in the chronic reactor (SRT: 10d).

Since the main of the study was to determine the effect of antibiotic substance on the substrate biodegradation properties of the activated sludge biomass, mainly the behavior of the three selected antibiotics were not of interest. However since there is information of SMX being removed as nitrogen source given in the literature SMX was successfully measured (Drillia et al., 2005). Additionally, in the literature there is no information of TET and ERY being biodegraded by activated sludge biomass, therefore measuring these substances was not of importance. However, TET and ERY were also tried to be measured, and different methods were applied, none of which gave positive results.

5.6 Conceptual Framework on Enzyme Inhibition

Inhibitory actions in substrate biodegradation are conveniently evaluated using the analogy of enzyme-catalyzed reactions. In fact, the same approach was adopted to provide conceptual support to the empirical Monod-type expression now commonly utilized in defining microbial growth in activated sludge systems. As described in detail in the literature (Mulchandani et al., 1989; Orhon and Artan, 1994), the enzyme analogy was mostly introduced to differentiate two major types of inhibitory effects with retardation effects on microbial growth: In competitive inhibition, the inhibitor (I) forms with the enzyme (E) an enzyme-inhibitor complex, [EI] and competes with substrate (S) for the same enzymatic site in biomass. This effect is kinetically expressed in terms of a higher half saturation coefficient, which can be reversed by increasing the substrate concentration.

In non-competitive inhibition, the enzyme-inhibitor complex [EI] cannot be reversed by the substrate concentration, which becomes unable to prevent the combination of the inhibitor with the enzyme. This time the effect is on the maximum specific growth rate.

Recent studies have also indicated that the inhibitory impacts of chemicals should be visualized, not only in the utilization of the readily biodegradable substrate for microbial growth, but also in the hydrolysis of the slowly biodegradable substrate (Insel et al., 2006). The common feature of both types of inhibition is that the inhibitory action only affects process kinetics so that the available biodegradable substrate is fully utilized.

In uncompetitive inhibition however, the inhibitor (I) attacks the enzyme substrate sites, [ES], and forms an [ESI] complex, which does not undergo further biochemical reactions and this way, it blocks a part of the available substrate for biodegradation.

The significant aspect that differentiates uncompetitive inhibition from the other types is that the induced effect is primarily stoichiometric, i.e. the fraction of substrate bound by the inhibitor becomes not available for microbial growth as indicated by the following mass balance equation:

$$\boldsymbol{S = [ES] + [ESI]} \qquad \textbf{(5.1)}$$

The basic stoichiometry and mass balance for available substrate is of capital importance for evaluating the impact of inhibitors, mainly because without any consideration of substrate blockage, a kinetic interpretation is bound to be distorted and misleading. Almost all similar studies reported in the literature overlooked substrate blockage as they only relied on measurements of substrate profiles which cannot differentiate the bound fraction not utilized by biochemical reactions. The introduction of the OUR profiles for inhibitory impact constitutes the basis of the original approach in this study in determining substrate binding potential of the selected antibiotics by means of uncompetitive inhibition.

Obtained OUR profiles mostly have the same properties, one of which is that they reach the endogenous decay level at the same time as the control experiment, indicating that all the external carbon source has been utilized for metabolic activities. Additionally after the addition of antibiotic substances the amount of consumed oxygen decreases, which means that the system is utilizing less amount of

substrate than the control experiment. This situation shows that antibiotic substances have substrate binding properties, which leads to uncompetitive inhibition of the system.

In this context, two characteristics of the OUR profile should be considered for the evaluation of the results:

(i) The OUR area above the endogenous respiration level directly gives the amount of oxygen consumed, O_2, at the expense of all available organic substrate (biodegradable COD) utilized by means of the following mass balance expression:

$$O_2 = C_S(1 - Y_H) \quad \textbf{(5.2)}$$

where C_S is the biodegradable COD concentration and Y_H is the heterotrophic yield coefficient (mg cell COD/mg COD). Consequently, with a known/predetermined amount of biodegradable substrate, the OUR curve may be used to determine Y_H and/or inert COD components (Orhon and Okutman, 2003).

(ii) The OUR experiment is started at the endogenous respiration level before the addition of substrate onto biomass in the reactor; the experiment ends when the OUR drops to the same level again, indicating that all available external substrate has been consumed.

The organic substrate (peptone-meat extract mixture) used in the experiments is by nature totally biodegradable; this is one of the main reasons for its selection and recommendation as the standard substrate for biodegradation experiments. Because the biodegradable COD in the control reactor was completely depleted after the OUR profile dropped to the initial endogenous respiration level, COD remaining in the control reactor represents the residual soluble microbial products, S_P, generated in the course of biochemical reactions; (Chudoba et al., 1985; Artan and Orhon, 1989) in the proposed decay associated models, S_P is conveniently expressed as a fraction of the influent biodegradable COD, C_{S1} in terms of a yield coefficient, Y_{SP}: (Orhon et al., 1999)

$$S_P = Y_{SP}C_{S1} \quad \textbf{(5.3)}$$

Using the data of the control reactor, a Y_{SP} value of 0.06 mg COD/mg COD was calculated, since an S_P value 36 mg/L was generated at the expense of 600 mg/L of peptone mixture COD initially supplied in the reactor. Furthermore, 211 mg/L of

oxygen consumed during the experiment corresponded to a yield coefficient, Y_H, of 0.60 mg cell COD/mg COD using the simulation results of the control data and the basic mass balance expression given above (5.2).

The significant feature of the impact of antibiotics on peptone mixture biodegradation is the reduction of oxygen consumption in the OUR experiments despite the fact that the OUR profiles drop down to the level of endogenous respiration within the observation period, indicating that all available biodegradable COD is utilized. This observation is against basic stoichiometry and cannot be explained by the conventional understanding of the inhibitory impact, which would retard biodegradation by either reducing the maximum specific growth rate, μ_H and/or increase the half saturation coefficient, K_S. Both types of effects are kinetic in nature, slowing down the rate of substrate utilization. The observed change in the OUR profile inflicted by this type of inhibition would be a longer period to reach the endogenous respiration level but the same area under the OUR curve or the same level of oxygen consumption.

Moreover, the decrease in oxygen utilization cannot be explained with the inactivation and/or decrease of the biomass in the system either. The result of reduced active biomass concentration in the system would cause the system to continue substrate degradation at a slower rate, which would prolong the period required for the substrate to be depleted. The corresponding OUR curve would eventually reach the endogenous decay level, thus keeping the area under the OUR curve same as the non-inhibited system, as the amount of substrate utilized remains the same.

Table 5.9 and Table 5.11, Table 5.10 and Table 5.12 show the mass balance between oxygen consumption and COD utilization in the SRT 10d and 2d acute and chronic inhibition experiments. In this context using the total area under the OUR curve the amount of COD corresponding to the amount of oxygen consumed has been calculated, and since the given amount of COD is known, the amount of COD bound by the antibiotic substance has been calculated. Moreover, using the utilized COD and Y_{SP}, the soluble metabolic products and amount of bound substrate and antibiotic-substrate complex amount has been calculated.

From Table 5.9 and Table 5.10 it can be seen that uncompetitive inhibition theory can be applied to all acute experimental runs, however the extent of the inhibitory impact greatly varied as a function of dosage and type of antibiotics. At 50 mg/L dosage, during SRT 10d acute experiments the amount of peptone mixture utilized dropped from 600 mg/L in the unaffected control reactor to 515 mg/L with SMX; to 428 mg/L with TET and to 280 mg/L with ERY, which exerted the strongest effect. For sludge age of 2 days the amount of peptone mixture utilized dropped from 760 mg/L in the control reactor to 665 mg/L with SMX (with 720 mg/L peptone addition); to 573 mg/L with TET (with 720 mg/L peptone addition) and to 310 mg/L with ERY (with 720 mg/L peptone addition), which again exerted the strongest effect. However, this shows that the substrate binding effect of antibiotic differs with the sludge history as well.

At 200 mg/L dosage of SRT 10d acute experiments, the amount of peptone mixture utilized dropped from 600 mg/L in the unaffected control reactor to 628 mg/L with SMX (with 650 mg/L peptone addition); to 435 mg/L with TET and to 140 mg/L with ERY, which again exerted the strongest effect. For sludge age of 2 days the amount of peptone mixture utilized dropped from 760 mg/L in the control reactor to 650 mg/L with SMX (with 720 mg/L peptone addition); to 468 mg/L with TET (with 720 mg/L peptone addition). However, this shows that the substrate binding effect of antibiotic differs with the sludge history as well.

A parallel decrease could be calculated for the generation of the residual soluble metabolic products, S_P as shown in Table 5.9 to Table 5.12. Interestingly, the remaining soluble COD in the reactor at the completion of the OUR test (endogenous respiration level) did not show the same trend for 50 mg/L antibiotic addition (acute SRT 10d): for SMX, the total COD associated with the [ESI] complex was calculated as 155 mg/L and the remaining COD contained around 97% of the antibiotic/substrate complex, the remaining 3% presumably being entrapped/attached to the biomass. The strongest biomass entrapment was attributed to TET, which yielded the lowest remaining COD level of 52 mg/L including S_P (Table 5.9). Also for the SRT 2 days acute experiments TET again showed the lowest remaining COD level of 75 mg/L inclusive S_P (Table 5.10).

When the antibiotic dosage was increased to 200 mg/L the remaining COD concentrations were substantially higher, indicating that not all available antibiotics

were bound with substrate and the remaining COD included aside the [ESI] complex, the unattached/free antibiotic fraction. Complex formation potential of the selected antibiotics maintained the same character so that TET yielded again the lowest level of remaining COD, which yielded the lowest remaining COD level of 143 mg/L including S_P (Table 5.9). Also for the SRT 2 days acute experiments TET again showed the lowest remaining COD level of 267 mg/L inclusive S_P (Table 5.10).

From Table 5.11 and Table 5.12 it can be seen that uncompetitive inhibition theory can also be applied to chronic exposure experiments. At 50 mg/L chronic dosage, the amount of peptone mixture utilized dropped from 600 mg/L in the unaffected control reactor to 695 mg/L with SMX after 30 days (with 720 mg/L peptone addition), 608 mg/L with TET after 31 days (with 720 mg/L peptone addition) and again 30 days of exposure to 595 mg/L with ERY (with 720 mg/L peptone addition). For sludge age of 2 days the amount of peptone mixture utilized dropped from 760 mg/L in the control reactor to 637 mg/L with SMX (with 720 mg/L peptone addition); to 695 mg/L with TET (with 720 mg/L peptone addition) and to 545 mg/L with ERY (with 720 mg/L peptone addition), which again exerted the strongest effect.

Remaining soluble COD in the reactor at the completion of the OUR test (endogenous respiration level) during the SRT 10d chronic exposure studies showed that for SMX, the total COD associated with the [ESI] complex was calculated as 95 mg/L and the remaining COD contained around 84% of the antibiotic/substrate complex, the remaining 16% presumably being entrapped/attached to the biomass. For SRT 2d system after 4 days of SMX exposure the total COD associated with the [ESI] complex was calculated as 223 mg/L and the remaining COD contained around 78% of the antibiotic/substrate complex, the remaining 22% presumably being entrapped/attached to the biomass. For the SRT 2 days chronic experiments the strongest biomass entrapment was attributed to TET, which yielded the lowest remaining COD level of 89 mg/L including S_P (Table 5.12).

Additionally, in SRT 10d chronic experiments, after 30 days of exposure to the antibiotic substance, the systems was stopped to be fed for 20 days, and on the 50^{th} day systems were fed with the antibiotic substance again. In these cases, the amount of peptone mixture utilized dropped from 600 mg/L in the unaffected control reactor to 688 mg/L with SMX on the 50^{th} day (with 720 mg/L peptone addition), and again to 540 mg/L with ERY (with 720 mg/L peptone addition). Remaining soluble COD

in the reactor at the completion of the OUR test (endogenous respiration level) during the SRT 10d chronic exposure studies (day 50) showed that for SMX, the total COD associated with the [ESI] complex was calculated as 103 mg/L and the remaining COD contained around 91% of the antibiotic/substrate complex, the remaining 9% presumably being entrapped/attached to the biomass. For ERY however, total COD associated with the [ESI] complex was calculated as 264 mg/L and the remaining COD contained around 23% of the antibiotic/substrate complex, the remaining 77% presumably being entrapped/attached to the biomass.

In the light of these information substrate binding properties of antibiotic substances were taken into consideration for simulation of the behavior of activated sludge biomass of different runs. The mass balances presented in this section were used as input data for activated sludge models.

Table 5.9: Mass balance between oxygen consumption and COD utilization based on OUR profiles in acute inhibition studies (SRT 10d).

Run	Antibiotic Concentration (mg/L)	Initial Peptone COD (mg/L)	Oxygen Consumed (mg/L)	COD Utilized (mg/L)	COD Bound (mg/L)	Remaining Soluble COD (mg/L)		
						Total	Soluble Metabolic Product, S_P	Peptone + Antibiotic
Control	-	600	211	600	-	36	36	-
SMX	50	600	206	515	85	182	31	151
TET	50	600	171	428	173	52	26	26
ERY	50	600	112	280	320	109	17	92
SMX	200	650	251	628	23	343	38	305
TET	200	600	174	435	165	143	26	117
ERY	200	600	56	140	460	329	8	321

Table 5.10: Mass balance between oxygen consumption and COD utilization based on OUR profiles in acute inhibition studies (SRT 2d).

Run	Antibiotic Concentration (mg/L)	Initial Peptone COD (mg/L)	Oxygen Consumed (mg/L)	COD Utilized (mg/L)	COD Bound (mg/L)	Remaining Soluble COD (mg/L)		
						Total	Soluble Metabolic Product, S_P	Peptone + Antibiotic
Control	-	760	284	760	-	71	71	-
SMX	50	720	266	665	55	189	62	127
TET	50	720	229	573	148	75	53	22
ERY	50	720	124	310	410	379	29	350
SMX	200	720	260	650	70	326	61	265
TET	200	720	187	468	253	267	44	223

Table 5.11: Mass balance between oxygen consumption and COD utilization based on OUR profiles in chronic inhibition studies (SRT 10d).

Run	Antibiotic Concentration (mg/L)	Initial Peptone COD (mg/L)	Oxygen Consumed (mg/L)	COD Utilized (mg/L)	COD Bound (mg/L)	Remaining Soluble COD (mg/L)		
						Total	Soluble Metabolic Product, S_P	Peptone + Antibiotic
Control	-	600	211	600	-	36	36	-
SMX – Day 30	50	720	278	695	25	122	42	80
SMX – Day 50	50	720	275	688	33	135	41	94
TET – Day 31	50	720	243	608	113	100	36	64
ERY – Day 31	50	720	238	595	125	132	36	96
ERY – Day 50	50	720	216	540	180	93	32	61

Table 5.12: Mass balance between oxygen consumption and COD utilization based on OUR profiles in chronic inhibition studies (SRT 2d).

Run	Antibiotic Concentration (mg/L)	Initial Peptone COD (mg/L)	Oxygen Consumed (mg/L)	COD Utilized (mg/L)	COD Bound (mg/L)	Remaining Soluble COD (mg/L)		
						Total	Soluble Metabolic Product, S_P	Peptone + Antibiotic
Control	-	760	284	760	-	71	71	-
SMX – Day 4	100	720	255	637	83	235	60	175
TET – Day 2	50	720	278	695	25	89	65	24
ERY – Day 3	50	720	218	545	175	233	51	182

5.7 Modeling of Activated Sludge Systems

In order to determine the effect of antibiotic compounds on the biodegradation of peptone-meat extract mixture various simulations were run using the AQUASIM program, which simulates oxygen utilization rate (OUR), chemical oxygen demand (COD) and polyhydroxy alkanoates (PHA) data at the same time. To be able to establish a baseline for comparison model calibration of control reactors of different sludge ages acclimated on peptone-meat extract mixture were completed. Table 5.13 gives the kinetic information describing the biodegradation of peptone-meat extract mixture at SRT 10d and SRT 2d.

Simulations of both SRT2d and SRT10d control systems showed that sludge history plays an important role on the kinetics of substrate removal. SRT 2d system having higher growth rate and faster hydrolysis of X_S, shows slower hydrolysis of S_H than that of SRT 10d system. Additionally, the simulations showed that since it is a fast growing system, the endogenous decay rate of the SRT 2d system is higher than the SRT 10d system. Model calibration of control systems showed that the readily biodegradable fraction of peptone mixture is 9.5%, readily hydrolysable COD is 56% and hydrolysable COD is 34.5% of the total biodegradable COD given to the system. PHA analysis showed that the SRT 10d system has a 10 mgCOD/L PHA pool and maximum PHA storage is 32 mgCOD/L. However, previous studies revealed that SRT 2d systems do not have significant storage properties (Orhon et al., 2009). Therefore SRT 2d systems were not monitored for their storage products.

COD and OUR profiles and model simulations of both SRT 10d and 2d control systems are given in Figure 5.25, Figure 5.26, Figure 5.28 and Figure 5.29. Moreover PHA profile of SRT 10d control system is given in Figure 5.27.

Table 5.13: Model calibration of peptone-meat extract acclimated control reactors.

Model Parameter		Unit	Control – SRT 10d	Control – SRT 2d
Maximum growth rate for X_H	μ_H	1/day	5.2	7.2
Half saturation constant for growth of X_H	K_S	mg COD/L	24	30
Endogenous decay rate for X_H and	b_H	1/day	0.1	0.2
Heterotrophic half saturation coefficient for oxygen	K_{OH}	mg O_2/L	0.01	0.01
Maximum hydrolysis rate for S_{H1}	k_h	1/day	5.2	4
Hydrolysis half saturation constant for S_{H1}	K_X	g COD/g COD	0.15	0.15
Maximum hydrolysis rate for X_{S1}	k_{hx}	1/day	0.56	1
Hydrolysis half saturation constant for X_{S1}	K_{XX}	g COD/g COD	0.05	0.05
Maximum storage rate of PHA by X_H	k_{STO}	1/day	1.2	0
Maximum growth rate on PHA for X_H	μ_{STO}	1/day	0.8	0
Half saturation constant for storage of PHA by X_H	K_{STO}	mg COD/L	0.5	0
Yield coefficient of X_H	Y_H	g COD/g COD	0.6	0.6
Yield coefficient of PHA	Y_{STO}	g COD/g COD	0.8	0
Fraction of biomass converted to S_P	f_{ES}	-	0.05	0.05
Fraction of biomass converted to X_P	f_{EX}	-	0.15	0.15
State variables		Unit		
Total biomass		mgCOD /L	2010	809
Initial active biomass	X_{H1}	mg COD/L	1450	630
Activity		%	72	78
Initial amount of PHA	X_{STO1}	mg COD/L	10	0
Initial amount of biodegradable COD	C_{S1}	mg COD/L	600	760
Initial amount of readily biodegradable COD	S_{S1}	mg COD/L	57	72
Initial amount of readily hydrolysable COD	S_{H1}	mg COD/L	335	424
Initial amount of hydrolysable COD	X_{S1}	mg COD/L	208	264
Bound COD		mgCOD /L	-	-

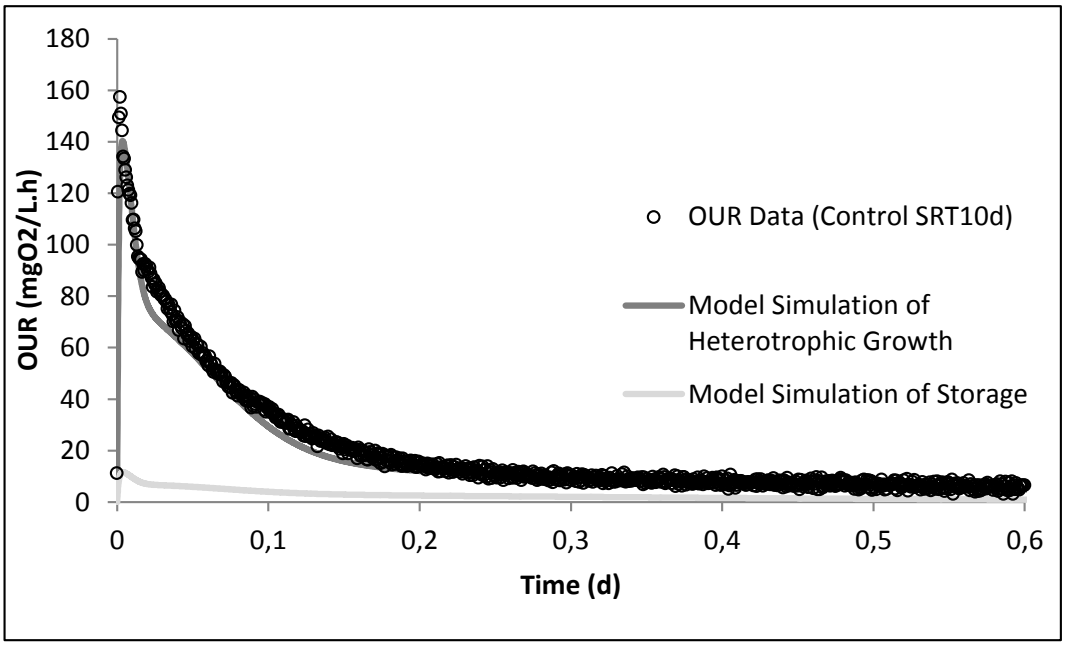

Figure 5.25: OUR profile of peptone-meat extract biodegradation and simulation (SRT 10d).

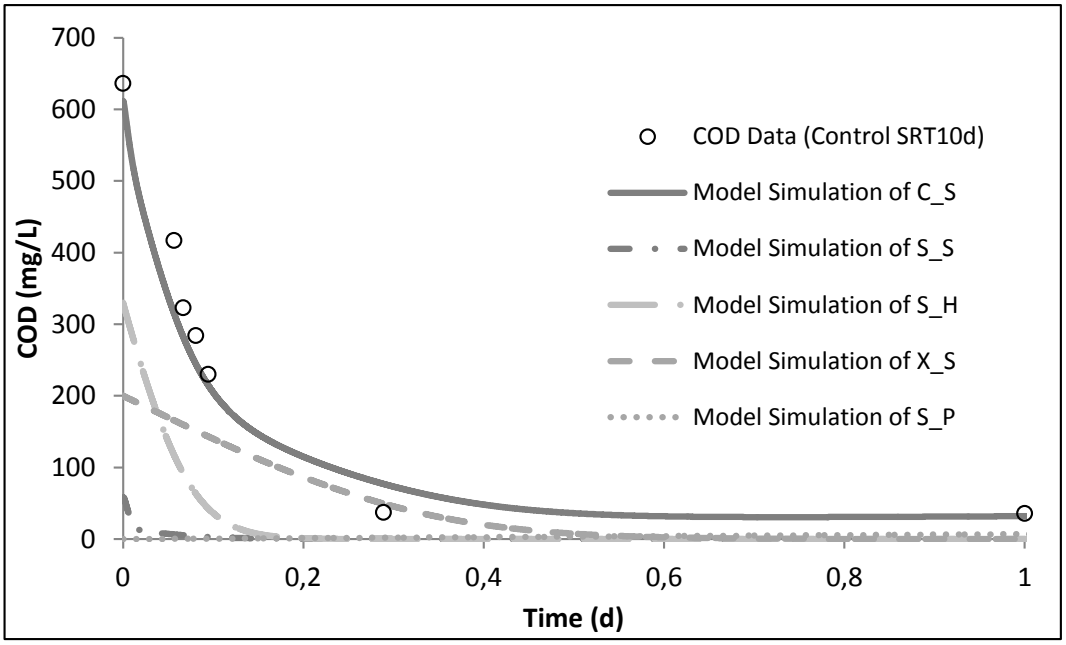

Figure 5.26: COD removal profile of peptone-meat extract biodegradation and simulation (SRT 10d).

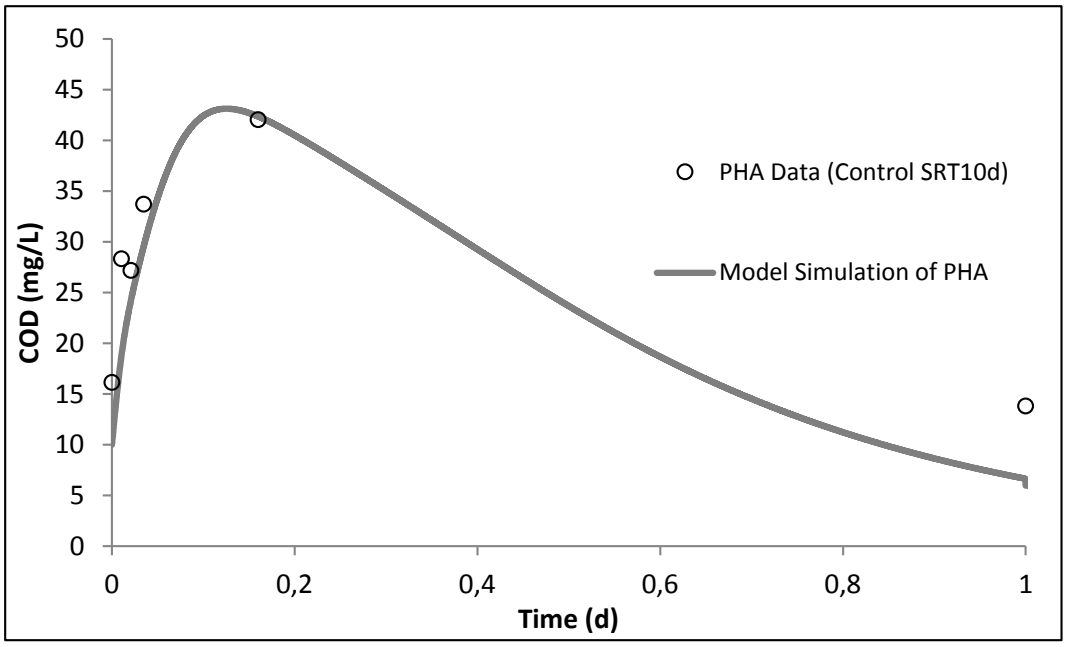

Figure 5.27: PHA storage profile of peptone-meat extract biodegradation and simulation (SRT 10d).

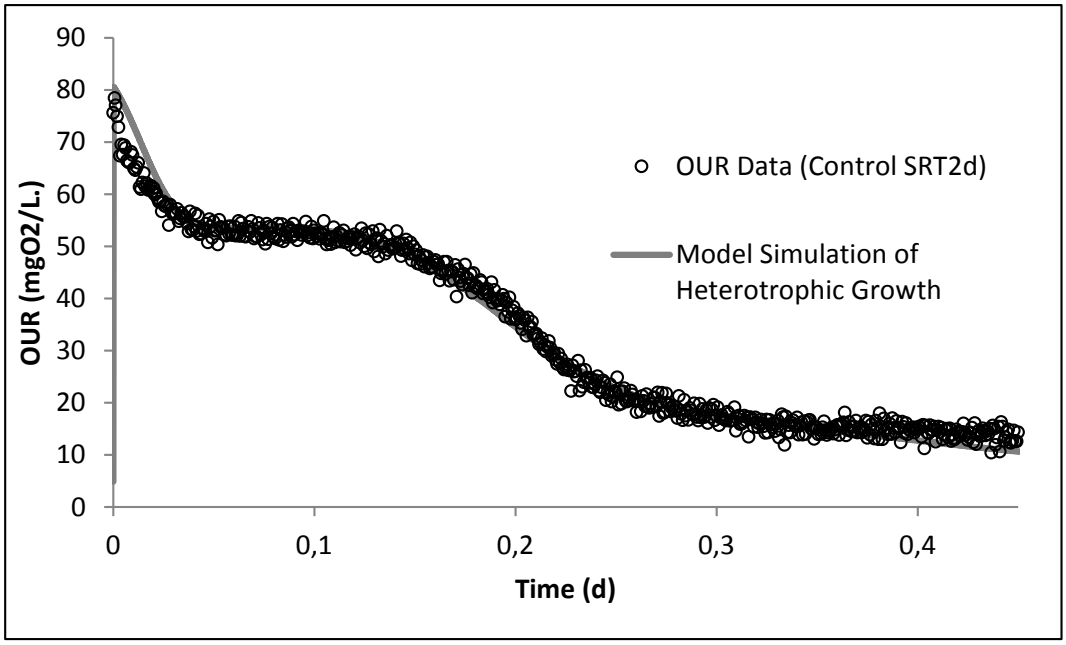

Figure 5.28: OUR profile of peptone-meat extract biodegradation and simulation (SRT 2d).

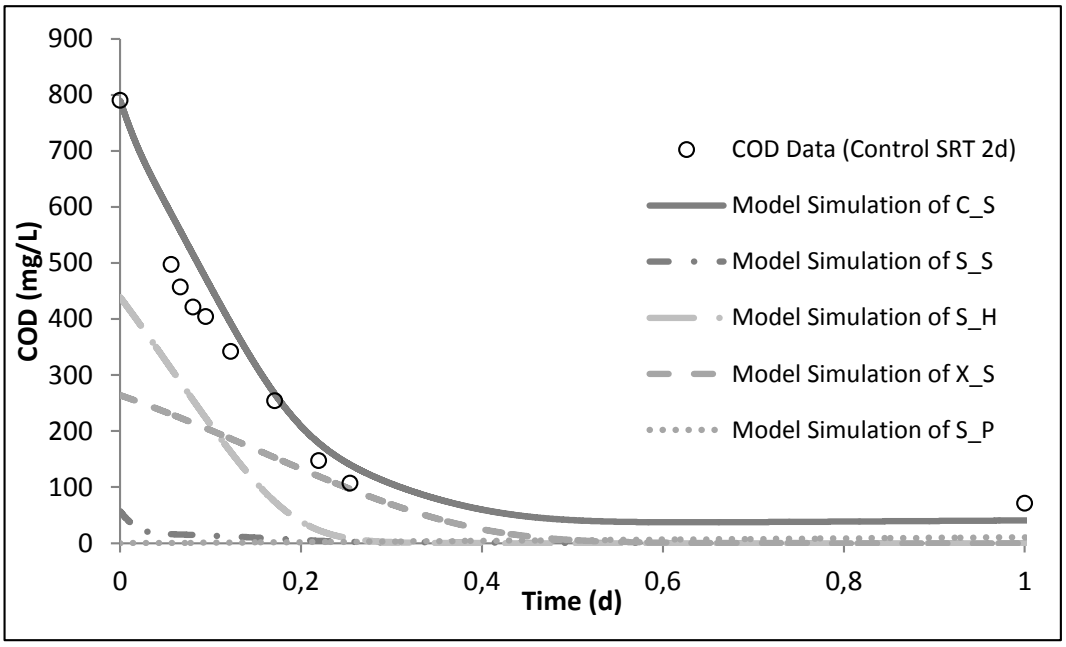

Figure 5.29: COD removal profile of peptone-meat extract biodegradation and simulation (SRT 2d).

During the course of the acute and chronic experimental runs polyhydroxyalkanoates (PHA) samples were collected from each set to characterize the bacterial storage mechanism in the reactors. Results of PHA measurements showed that primary effect of antibiotics on the metabolism of activated sludge biomass is that in the SRT 10d system storage mechanism is inhibited completely. Therefore it has been established that in acute inhibition experiments the system continued to utilize the PHA pool in the sludge, since the sludge was taken from the control reactor. However, in the chronic exposure experiments, since the storage mechanism was completely inhibited the PHA pools were also non-existent, leading to the inability to storage of and grow on PHA molecules.

Moreover preliminary evaluation of OUR profiles showed that with addition of antibiotic substance the system responded with lower oxygen consumption compared to the control sample, which coincided with uncompetitive inhibition, of which the effect on the OUR profile has been demonstrated before. Additionally, the amount of COD bound for each run of experiment was calculated and used in simulation studies, which was given in the previous section (Table 5.9 to Table 5.12).

5.7.1 Sulfamethoxazole simulations

5.7.1.1 SRT: 10 d

Results of simulation studies to determine the kinetic effect of SMX on the biodegradation of peptone-meat extract showed the antibiotic inhibits the PHA storage of the SRT 10d system (Figure 5.30 to Figure 5.32). Kinetics of acute inhibition studies showed that the system, however unable to store PHA was still able to grow on already stored PHA. Moreover it was shown that SMX increases the half saturation constant of the substrate, therefore making it less available for the biomass. The system also demonstrated that with increasing antibiotic concentration rate of hydrolysis of S_H decreases as well, which is presented by decreased rate and increased half saturation constant for S_H hydrolysis. Finally, it has been determined that the system utilizes not all the COD given, but 85 and 23 mgCOD/L less than given amount for SMX50 and SMX200 acute additions, respectively (Table 5.14). Additionally, it is very important to note that the endogenous decay level of the system increases with the addition of the antibiotic substance.

Table 5.14: Effect of SMX on kinetics of peptone-meat extract removal (SRT 10d).

Model Parameter		Unit	Control – SRT 10d	Acute – SMX200	Acute – SMX50	Chronic – SMX Day 30	Chronic – SMX Day 50
Maximum growth rate for X_H	μ'_H	1/day	5.2	5.2	5.2	3	5.2
Half saturation constant for growth of X_H	K_S	mg COD/L	24	40	40	80	50
Endogenous decay rate for X_H and	b_H	1/day	0.1	0.2	0.2	0.27	0.27
Heterotrophic half saturation coefficient for oxygen	K_{OH}	mg O_2/L	0.01	0.01	0.01	0.01	0.01
Maximum hydrolysis rate for S_{H1}	k_h	1/day	5.2	4.06	5.2	3.9	3.8
Hydrolysis half saturation constant for S_{H1}	K_X	g COD/g COD	0.15	0.21	0.15	0.21	0.15
Maximum hydrolysis rate for X_{S1}	k_{hx}	1/day	0.56	0.56	0.56	0.56	0.56
Hydrolysis half saturation constant for X_{S1}	K_{XX}	g COD/g COD	0.05	0.05	0.05	0.05	0.05
Maximum storage rate of PHA by X_H	k_{STO}	1/day	1.2	0	0	0	0
Maximum growth rate on PHA for X_H	μ'_{STO}	1/day	0.8	0.8	0.8	0	0
Half saturation constant for storage of PHA by X_H	K_{STO}	mg COD/L	0.5	0.5	0.5	0	0
Yield coefficient of X_H	Y_H	g COD/g COD	0.6	0.6	0.6	0.6	0.6
Yield coefficient of PHA	Y_{STO}	g COD/g COD	0.8	0.8	0.8	0.8	0.8
Fraction of biomass converted to S_P	f_{ES}	-	0.05	0.05	0.05	0.05	0.05
Fraction of biomass converted to X_P	f_{EX}	-	0.15	0.15	0.15	0.15	0.15

Table 5.14 (continued): Effect of SMX on kinetics of peptone-meat extract removal (SRT 10d).

State variables		Unit	Control – SRT 10d	Acute – SMX200	Acute – SMX50	Chronic – SMX Day 30	Chronic – SMX Day 50
Total biomass		mgCOD/L	2010	2009	1891	1640	1846
Initial active biomass	X_{H1}	mg COD/L	1450	1450	1200	932	1000
Activity		%	72	72	64	57	54
Initial amount of PHA	X_{STO1}	mg COD/L	10	20	16	0	0
Initial amount of biodegradable COD	C_{S1}	mg COD/L	600	650	600	720	720
Initial amount of readily biodegradable COD	S_{S1}	mg COD/L	57	62	57	68	68
Initial amount of readily hydrolysable COD	S_{H1}	mg COD/L	335	363	280	402	390
Initial amount of hydrolysable COD	X_{S1}	mg COD/L	208	202	178	225	229
Bound COD		mgCOD/L	-	23	85	25	33

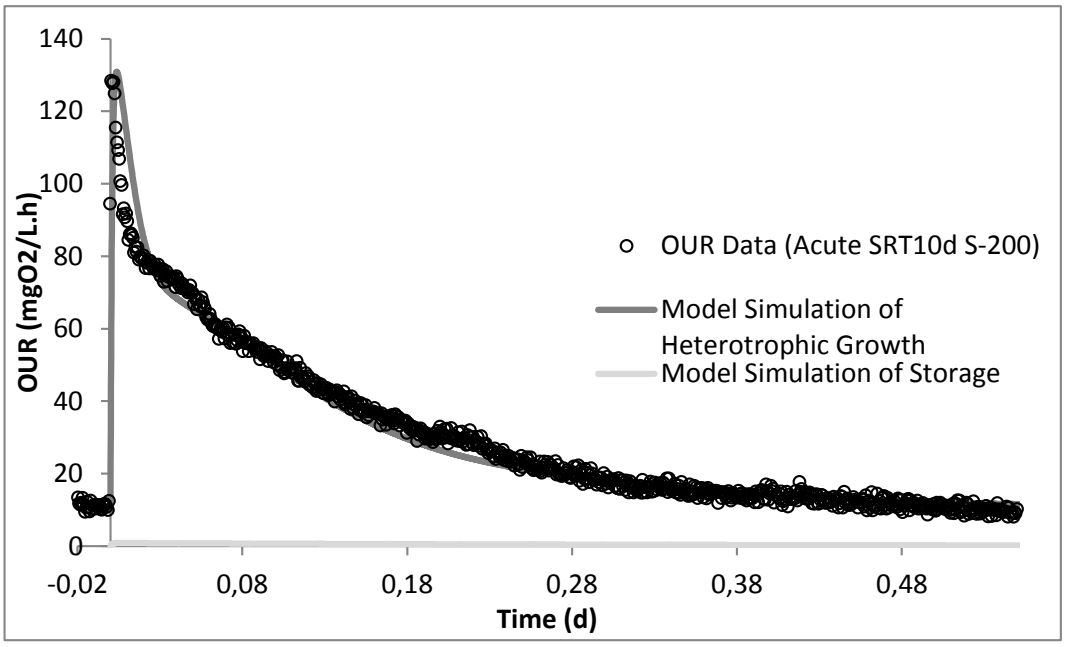

Figure 5.30: OUR simulation of peptone-meat extract biodegradation and simulation (Acute SMX200 SRT 10d).

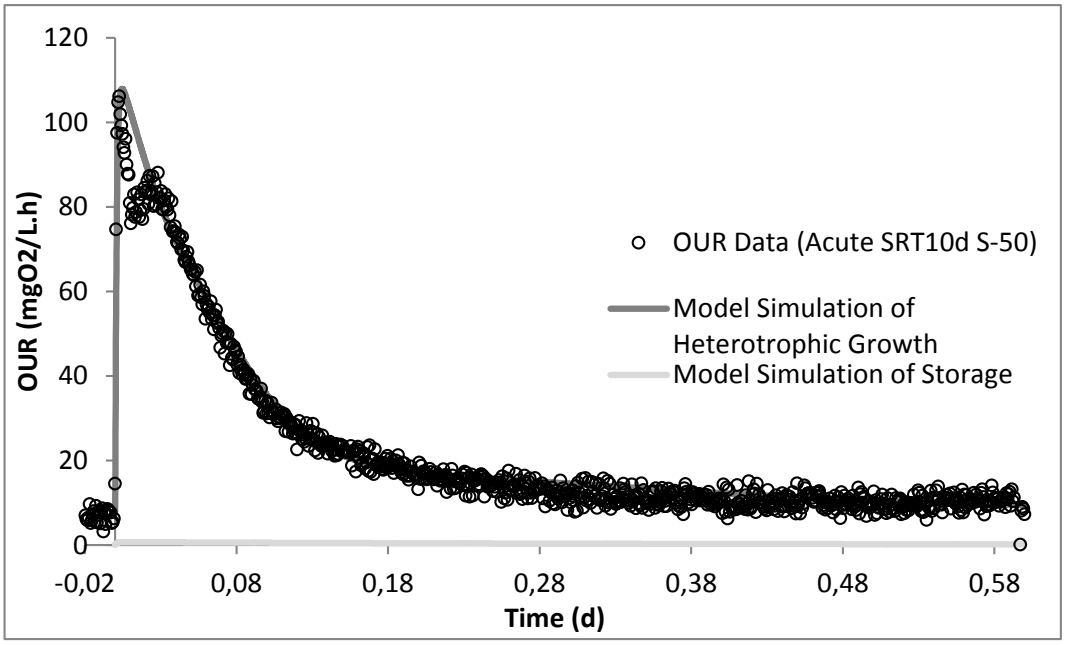

Figure 5.31: OUR simulation of peptone-meat extract biodegradation and simulation (Acute SMX50 SRT 10d).

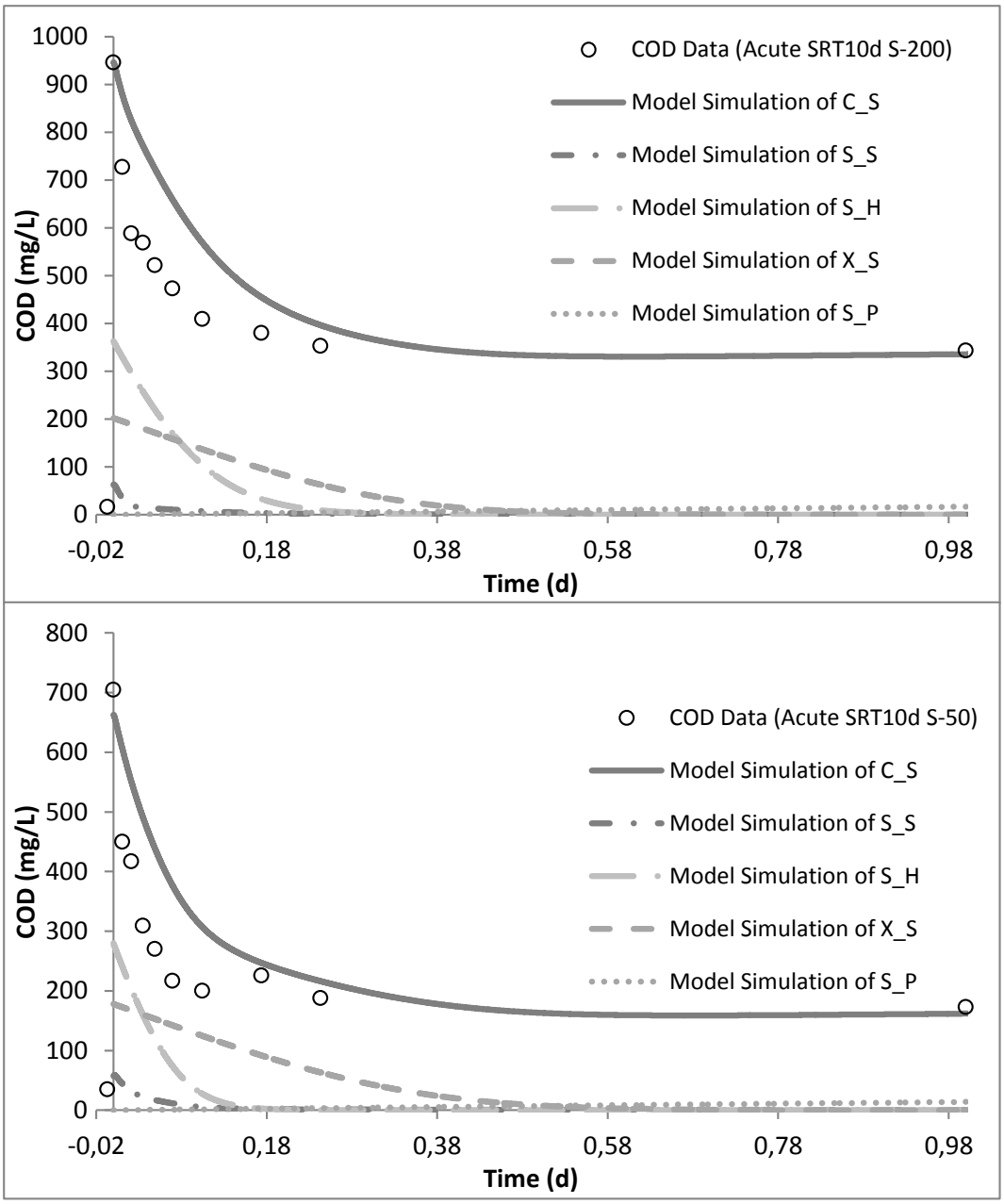

Figure 5.32: COD removal profile of peptone-meat extract biodegradation and simulation (Top: Acute SMX200 SRT 10d; Bottom: Acute SMX50 SRT 10d).

In addition to the acute inhibition studies, simulations of the chronic inhibition data revealed that exposed to 50 mg/L SMX for 30 days, the half saturation constant of the substrate increases and the maximum growth rate of the microorganisms decreases, affecting both substrate degradation and growth (Table 5.14). Moreover, the endogenous decay level increases under the effect of constant exposure. Finally, consistent with the stoichiometric calculations the model simulation showed that the system utilized 25 mgCOD/L less than given amount and it can also be seen that the rate of hydrolysis for S_H decreased further than the SMX50 acute inhibition and the

half saturation constant increased to the level of acute effect of 200 mg/L SMX addition. (Figure 5.33 and Figure 5.34)

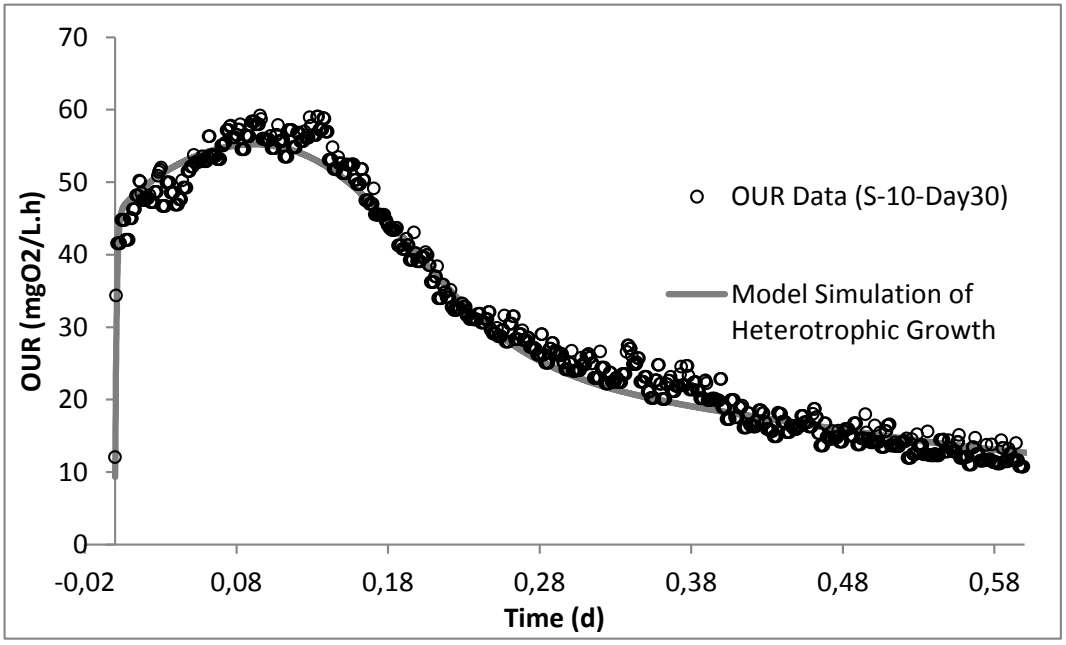

Figure 5.33: OUR simulation of peptone-meat extract biodegradation and simulation (Chronic SMX50 SRT 10d Day30).

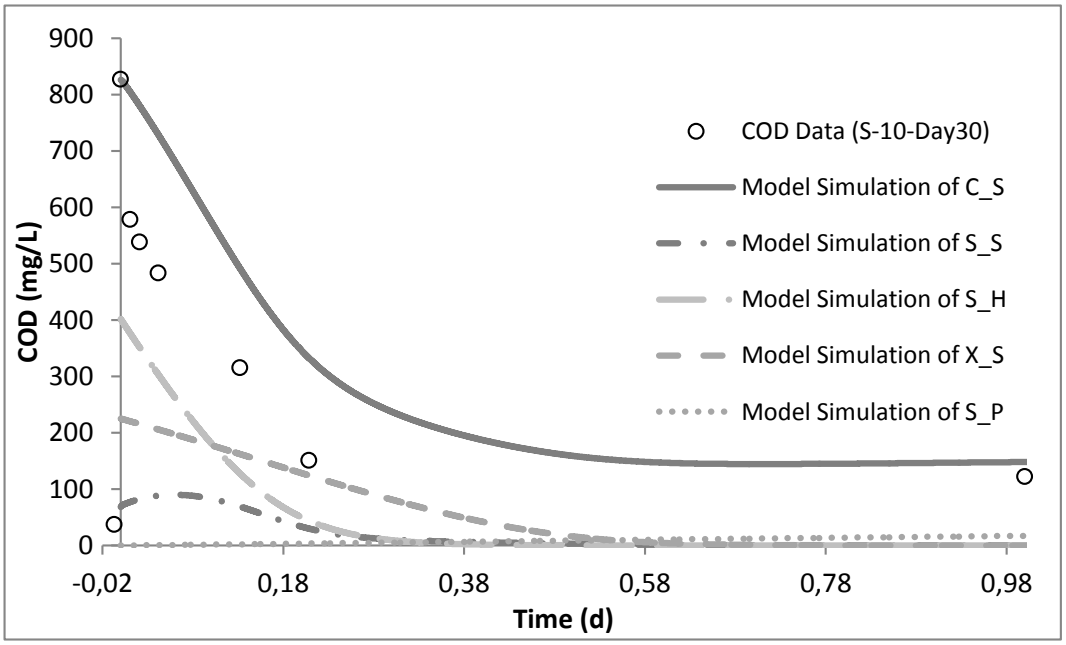

Figure 5.34: COD removal profile of peptone-meat extract biodegradation and simulation (Chronic SMX50 SRT 10d Day30).

After 30 days of exposure the 50 mg/L SMX, the systems was not fed with the antibiotic for 20 days, but only fed with peptone-meat extract mixture. On the 50th day 50 mg/L SMX was added to the system again and it has been observed that the system responded with decreased hydrolysis and growth rates and increased half

saturation constant (K_S). However the effect was not as severe as on the 30th day. Moreover the system again utilized 33 mgCOD/L less substrate than given to the system. Finally, the endogenous decay rate of the biomass increased to 0.27 d^{-1} for both 30th and 50th days, indicating that chronic exposure to SMX besides lowering the growth and the hydrolysis rate of S_H almost triples the endogenous decay of the organisms. However it can also be seen that for both acute and chronic exposures the hydrolysis rates of X_S remained unaffected (Table 5.14).

Additionally, the COD removal profiles indicate that the system seems to have a faster COD removal. However the simulation suggests otherwise, indicating that the COD was bound and removed, but not utilized for growth. (Figure 5.35 and Figure 5.36)

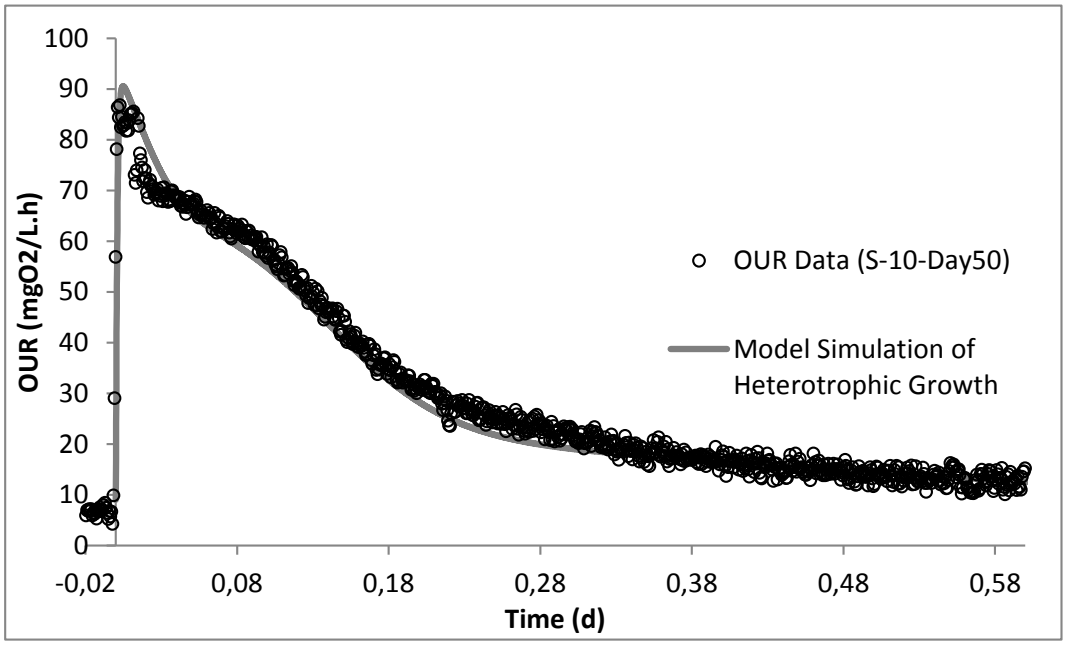

Figure 5.35: OUR simulation of peptone-meat extract biodegradation and simulation (Chronic SMX50 SRT 10d Day50).

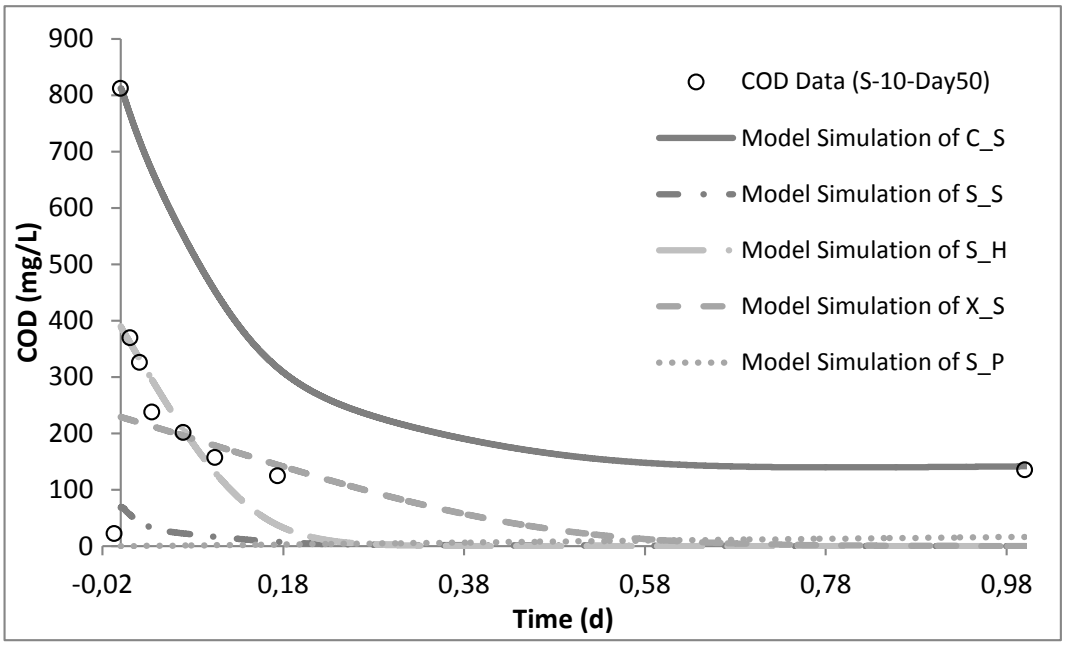

Figure 5.36: COD removal profile of peptone-meat extract biodegradation and simulation (Chronic SMX50 SRT 10d Day50).

5.7.1.2 SRT: 2 d

Results of SRT 2d system simulation studies to determine the kinetic effect of SMX on the biodegradation of peptone-meat extract showed acute exposure to the antibiotic does not affect the growth kinetic of the system, resulting unchanged maximum growth rate and half saturation constant of the biomass. Kinetics of both 50 mg/L and 200 mg/L SMX acute inhibition studies showed that substance does not adversely affect the hydrolysis kinetics of the system as well. Additionally, it has been determined that the SRT 2d system utilizes 59 and 70 mgCOD/L less than given amount for SMX50 and SMX200 acute additions, respectively. Finally, in contrast to SRT 10d system, it has been observed that the endogenous decay level of the SRT 2d control system, which due to its fast nature is already double as much as the SRT 10d control system, does not increase further under the effect of antibiotic substance (Table 5.15). (Figure 5.37, Figure 5.38 and Figure 5.39)

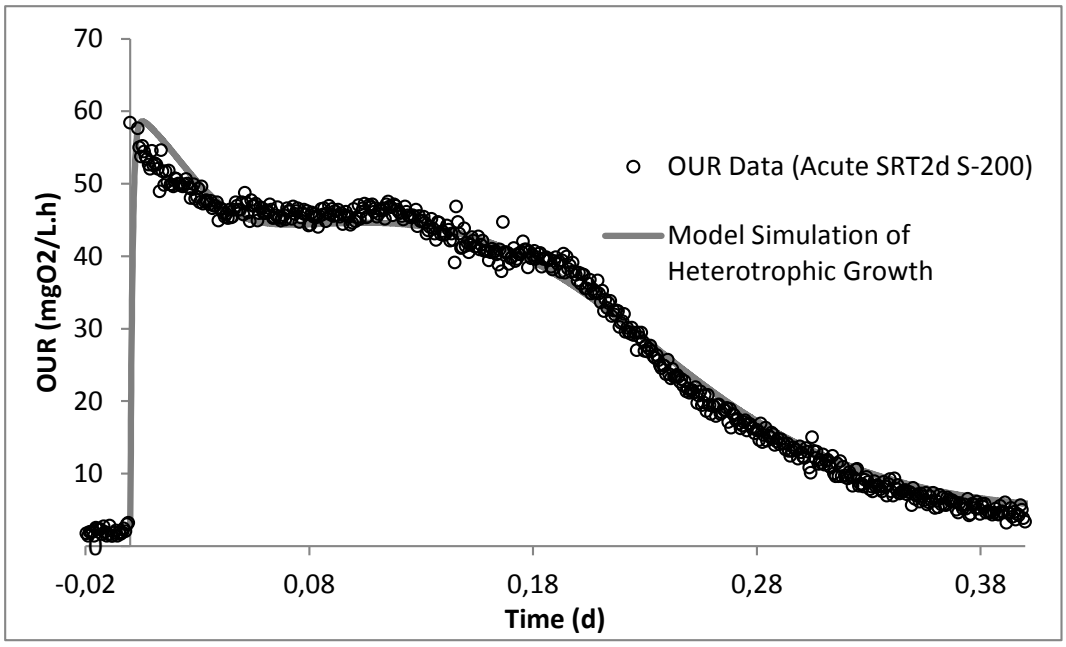

Figure 5.37: OUR simulation of peptone-meat extract biodegradation and simulation (Acute SMX200 SRT 2d).

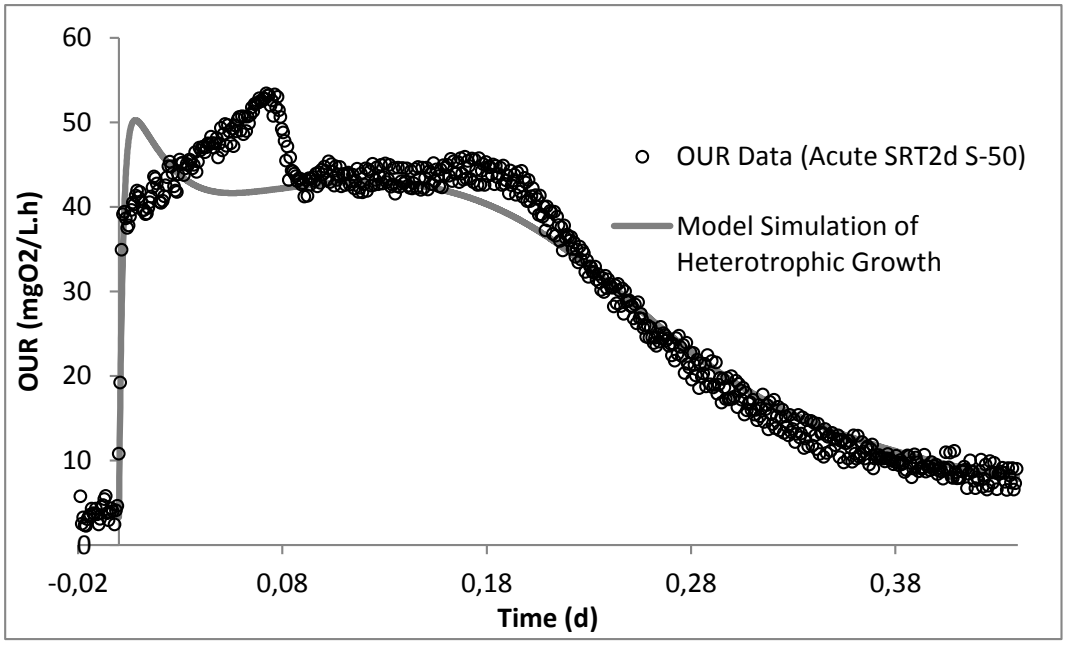

Figure 5.38: OUR simulation of peptone-meat extract biodegradation and simulation (Acute SMX50 SRT 2d).

Table 5.15: Effect of SMX on kinetics of peptone-meat extract removal (SRT 2d).

Model Parameter		Unit	Control – SRT 2d	Acute – SMX200	Acute – SMX50	Chronic – SMX100 Day 4
Maximum growth rate for X_H	μ'_H	1/day	7.2	7.2	7.2	1.5
Half saturation constant for growth of X_H	K_S	mg COD/L	30	30	30	25
Endogenous decay rate for X_H and	b_H	1/day	0.2	0.2	0.2	0.2
Heterotrophic half saturation coefficient for oxygen	K_{OH}	mg O_2/L	0.01	0.01	0.01	0.01
Maximum hydrolysis rate for S_{H1}	k_h	1/day	4	4	4	3.1
Hydrolysis half saturation constant for S_{H1}	K_X	g COD/g COD	0.15	0.15	0.15	0.15
Maximum hydrolysis rate for X_{S1}	k_{hx}	1/day	1	1.2	1	0.7
Hydrolysis half saturation constant for X_{S1}	K_{XX}	g COD/g COD	0.05	0.05	0.05	0.26
Maximum storage rate of PHA by X_H	k_{STO}	1/day	0	0	0	0
Maximum growth rate on PHA for X_H	μ'_{STO}	1/day	0	0	0	0
Half saturation constant for storage of PHA by X_H	K_{STO}	mg COD/L	0	0	0	0
Yield coefficient of X_H	Y_H	g COD/g COD	0.6	0.6	0.6	0.6
Yield coefficient of PHA	Y_{STO}	g COD/g COD	0	0	0	0
Fraction of biomass converted to S_P	f_{ES}	-	0.05	0.05	0.05	0.05
Fraction of biomass converted to X_P	f_{EX}	-	0.15	0.15	0.15	0.15

Table 5.15 (continued): Effect of SMX on kinetics of peptone-meat extract removal (SRT 2d).

State variables		Unit	Control – SRT 2d	Acute – SMX200	Acute – SMX50	Chronic – SMX100 Day 4
Total biomass		mgCOD/L	809	568	567	653
Initial active biomass	X_{H1}	mg COD/L	630	440	400	480
Activity		%	78	77	71	74
Initial amount of PHA	X_{STO1}	mg COD/L	0	0	0	0
Initial amount of biodegradable COD	C_{S1}	mg COD/L	760	720	720	720
Initial amount of readily biodegradable COD	S_{S1}	mg COD/L	72	54	54	40
Initial amount of readily hydrolysable COD	S_{H1}	mg COD/L	424	402	402	347
Initial amount of hydrolysable COD	X_{S1}	mg COD/L	264	186	205	250
Bound COD		mgCOD/L	-	70	59	83

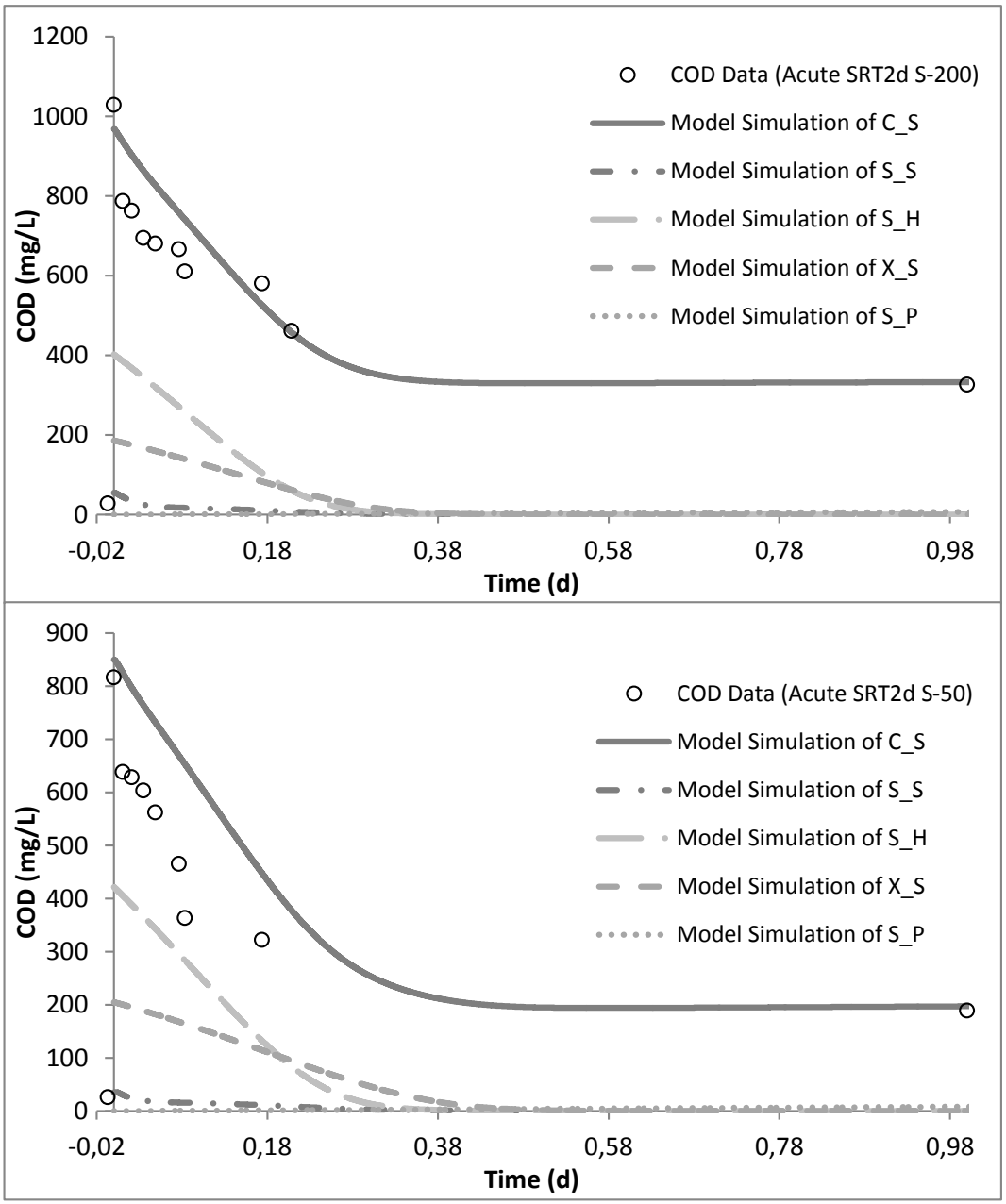

Figure 5.39: COD removal profile of peptone-meat extract biodegradation and simulation (Top: Acute SMX200 SRT 2d; Bottom: Acute SMX50 SRT 2d).

Simulations of the chronic inhibition data revealed that exposed to 100 mg/L SMX for 4 days, both the half saturation constant of the substrate and the maximum growth rate of the microorganisms decreased, affecting both substrate degradation and growth by showing the properties of uncompetitive inhibition (Table 5.15). Moreover, it has been seen that hydrolysis rate of S_H decreased together with a decrease of X_S hydrolysis rate, showing that constant exposure to 100 mg/L SMX retarded both hydrolysis mechanisms. Finally, consistent with the stoichiometric

calculations the model simulation showed that the system utilized 83 mgCOD/L less than given amount. (Figure 5.40 and Figure 5.41)

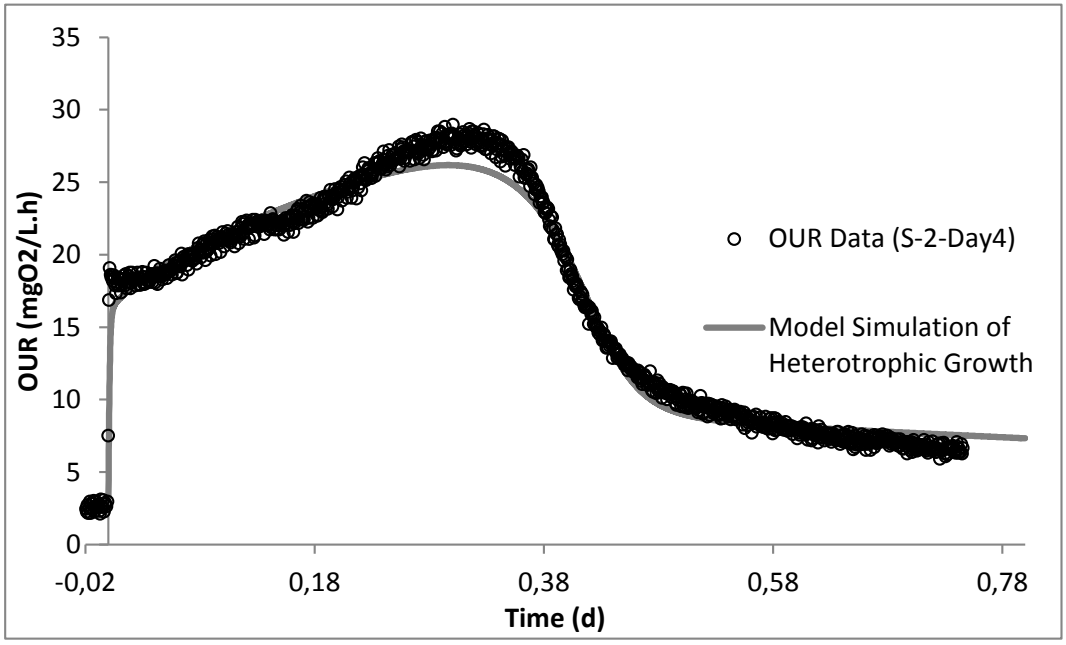

Figure 5.40: OUR simulation of peptone-meat extract biodegradation and simulation (Chronic SMX50 SRT 2d Day4).

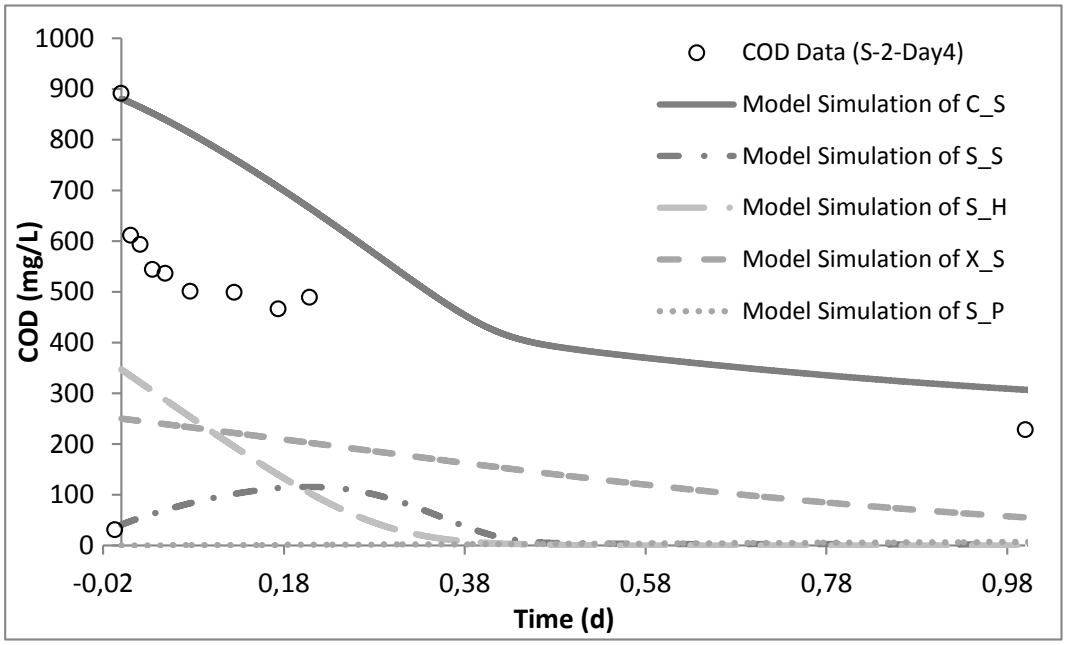

Figure 5.41: COD removal profile of peptone-meat extract biodegradation and simulation (Chronic SMX50 SRT 2d Day4).

5.7.2 Tetracycline simulations

5.7.2.1 SRT: 10 d

Results of simulation studies to determine the kinetic effect of TET on the biodegradation of peptone-meat extract showed the antibiotic inhibits the PHA storage of the SRT 10d system. Kinetics of acute inhibition studies showed that the system, however unable to store PHA was still able to grow on already stored PHA. Moreover it was shown that TET does not affect the half saturation constant of the substrate (K_S). The system also demonstrated that with increasing antibiotic concentration half saturation constant of S_H hydrolysis increases, which adversely affects degradation of S_H fraction of the substrate. Moreover, hydrolysis of X_S was shown not to be affected by acute inhibition of TET. Finally, it has been determined that the system utilizes not all the COD given, but 173 and 165 mgCOD/L less than given amount for TET50 and TET200 acute additions. Additionally, as shown in the SMX simulations the antibiotic substance causes the endogenous decay level of the system to increase (Table 5.16). (Figure 5.42, Figure 5.43 and Figure 5.44)

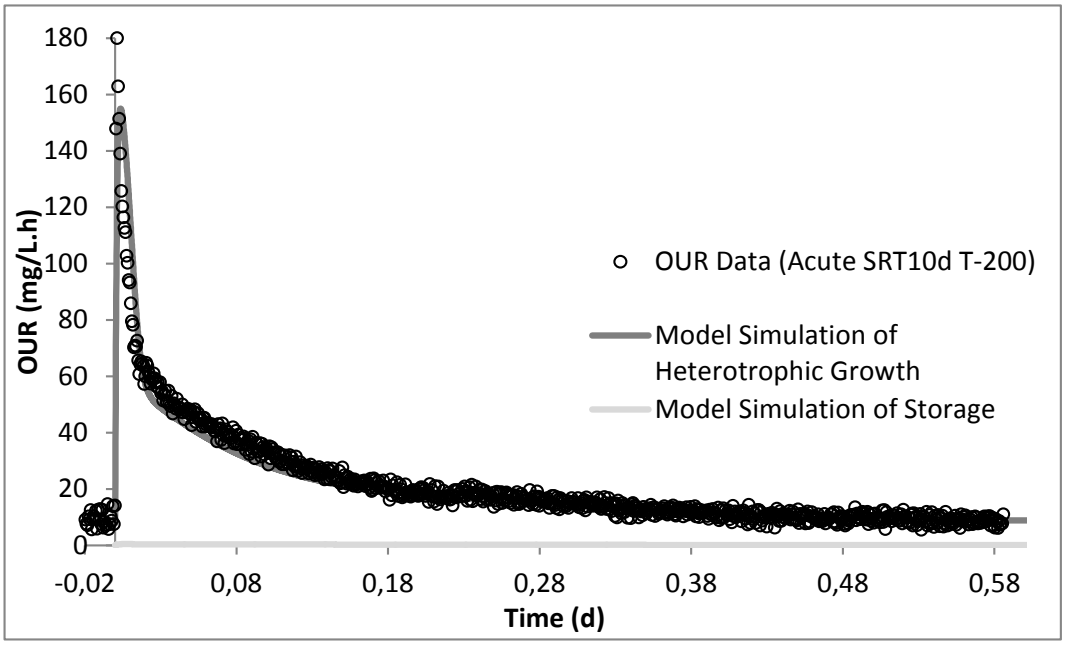

Figure 5.42: OUR simulation of peptone-meat extract biodegradation and simulation (Acute TET200 SRT 10d).

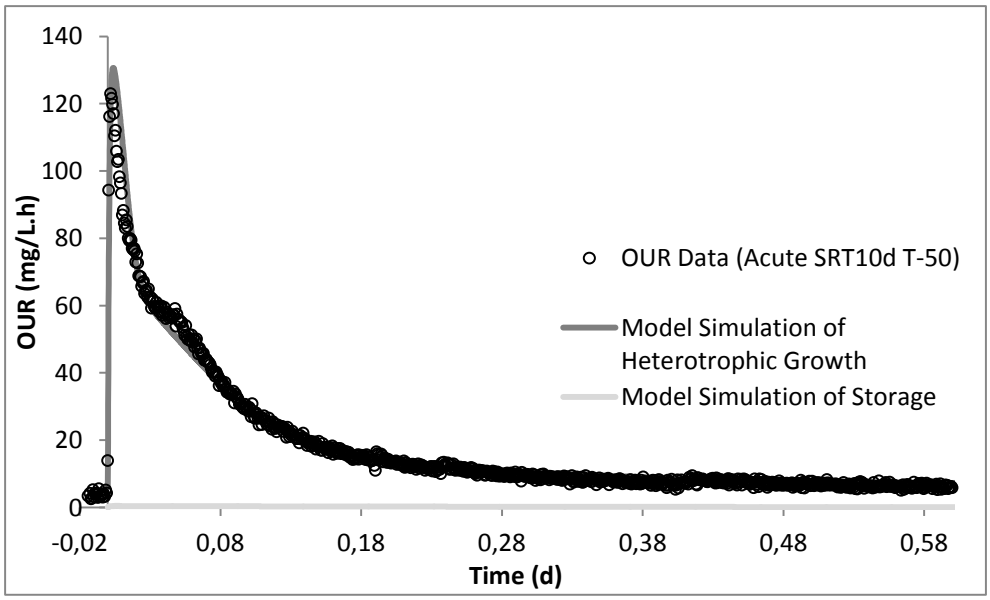

Figure 5.43: OUR simulation of peptone-meat extract biodegradation and simulation (Acute TET50 SRT 10d).

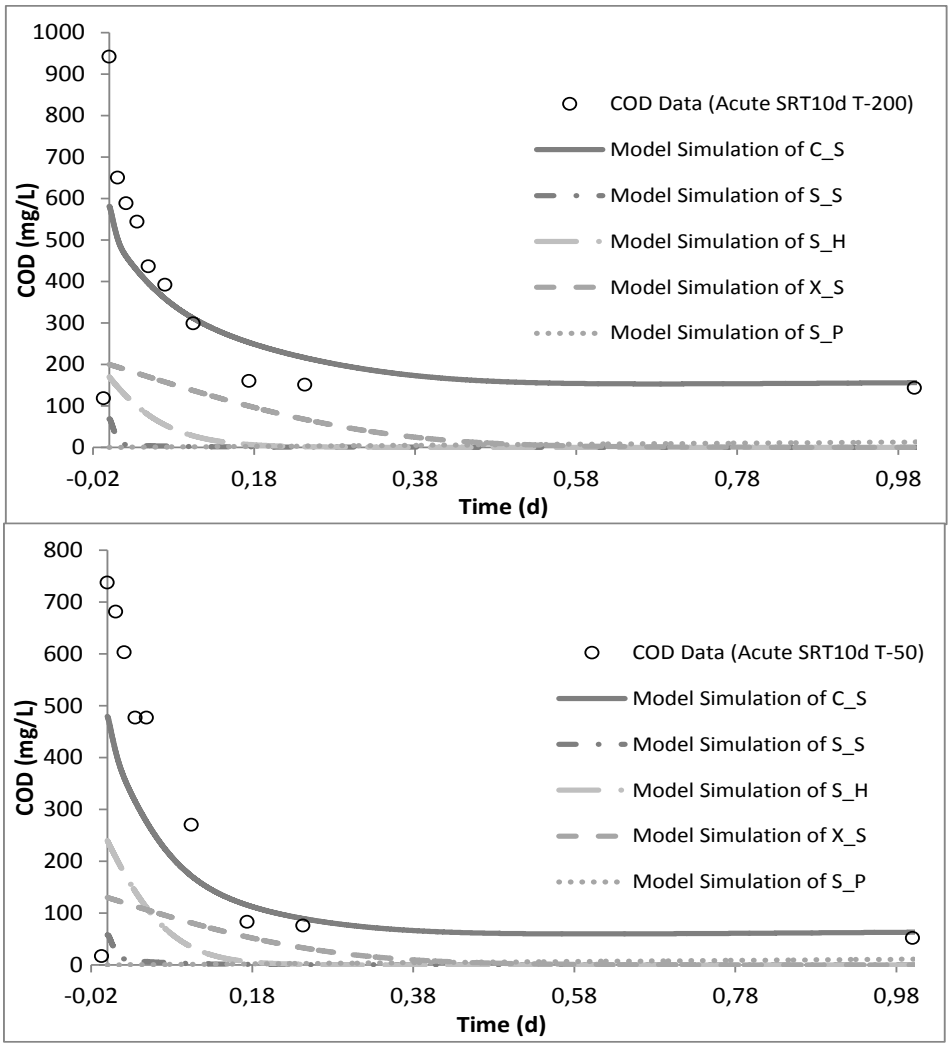

Figure 5.44: COD removal profile of peptone-meat extract biodegradation and simulation (Top: Acute TET200 SRT 10d; Bottom: Acute TET50 SRT 10d).

Table 5.16: Effect of TET on kinetics of peptone-meat extract removal (SRT 10d).

Model Parameter		Unit	Control – SRT 10d	Acute – TET200	Acute – TET50	Chronic – TET Day 30
Maximum growth rate for X_H	μ'_H	1/day	5.2	5.2	5.2	5
Half saturation constant for growth of X_H	K_S	mg COD/L	24	24	24	33
Endogenous decay rate for X_H and	b_H	1/day	0.1	0.15	0.15	0.15
Heterotrophic half saturation coefficient for oxygen	K_{OH}	mg O_2/L	0.01	0.01	0.01	0.01
Maximum hydrolysis rate for S_{H1}	k_h	1/day	5.2	5.2	5.2	5.2
Hydrolysis half saturation constant for S_{H1}	K_X	g COD/g COD	0.15	0.25	0.20	0.15
Maximum hydrolysis rate for X_{S1}	k_{hx}	1/day	0.56	0.56	0.56	0.56
Hydrolysis half saturation constant for X_{S1}	K_{XX}	g COD/g COD	0.05	0.05	0.05	0.05
Maximum storage rate of PHA by X_H	k_{STO}	1/day	1.2	0	0	0
Maximum growth rate on PHA for X_H	μ'_{STO}	1/day	0.8	0.8	0.8	0
Half saturation constant for storage of PHA by X_H	K_{STO}	mg COD/L	0.5	0.5	0.5	0
Yield coefficient of X_H	Y_H	g COD/g COD	0.6	0.6	0.6	0.6
Yield coefficient of PHA	Y_{STO}	g COD/g COD	0.8	0.8	0.8	0.8
Fraction of biomass converted to S_P	f_{ES}	-	0.05	0.05	0.05	0.05
Fraction of biomass converted to X_P	f_{EX}	-	0.15	0.15	0.15	0.15

Table 5.16 (continued): Effect of TET on kinetics of peptone-meat extract removal (SRT 10d).

State variables		Unit	Control – SRT 10d	Acute – TET200	Acute – TET50	Chronic – TET Day 30
Total biomass		mgCOD/L	2010	2010	1980	2370
Initial active biomass	X_{H1}	mg COD/L	1450	1500	1300	1150
Activity		%	72	75	66	48
Initial amount of PHA	X_{STO1}	mg COD/L	10	10	10	0
Initial amount of biodegradable COD	C_{S1}	mg COD/L	600	600	600	720
Initial amount of readily biodegradable COD	S_{S1}	mg COD/L	57	57	57	68
Initial amount of readily hydrolysable COD	S_{H1}	mg COD/L	335	200	240	402
Initial amount of hydrolysable COD	X_{S1}	mg COD/L	208	178	130	138
Bound COD		mgCOD/L	-	165	173	112

In addition to the acute inhibition studies, simulations of the chronic inhibition data revealed that exposed to 50 mg/L TET for 30 days, the half saturation constant of the substrate increases and the maximum growth rate of the microorganisms decreases. Moreover, the endogenous decay level increases under the effect of constant exposure. However, the endogenous decay rate, in contrast with chronic exposure to SMX does not increase further than in acute exposure simulations in the course of 30 days of exposure to TET. Finally, simulation showed that the system utilized 112 mgCOD/L less than given amount and it can also be seen that the hydrolysis mechanisms of both S_H and X_S remain unaffected under chronic exposure to TET (Table 5.16). (Figure 5.45 and Figure 5.46)

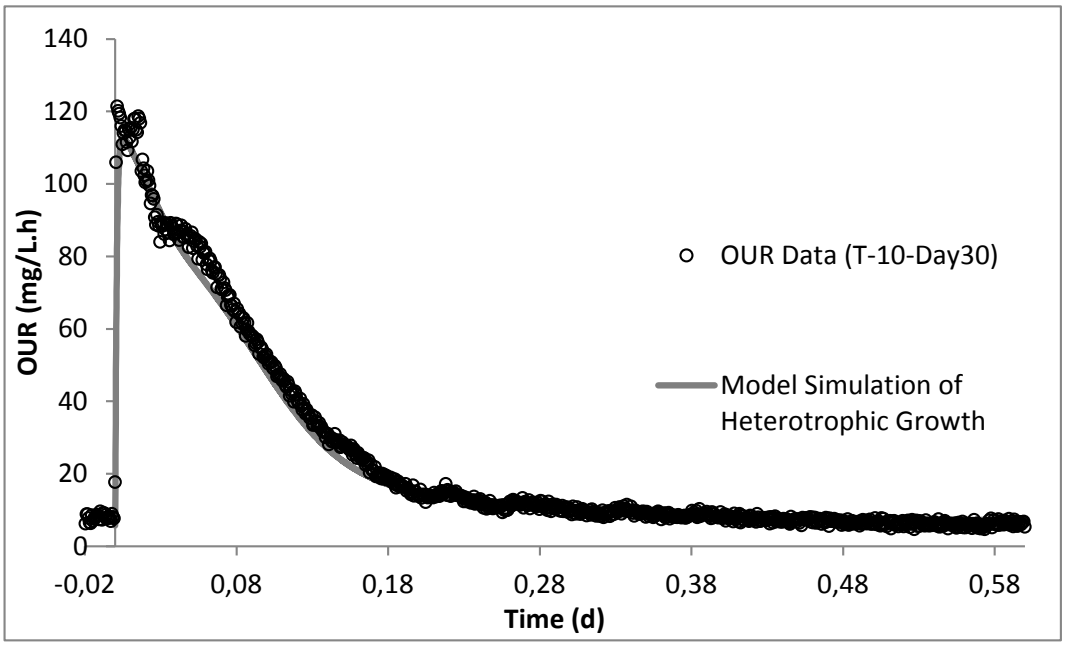

Figure 5.45: OUR simulation of peptone-meat extract biodegradation and simulation (Chronic TET50 SRT 10d Day30).

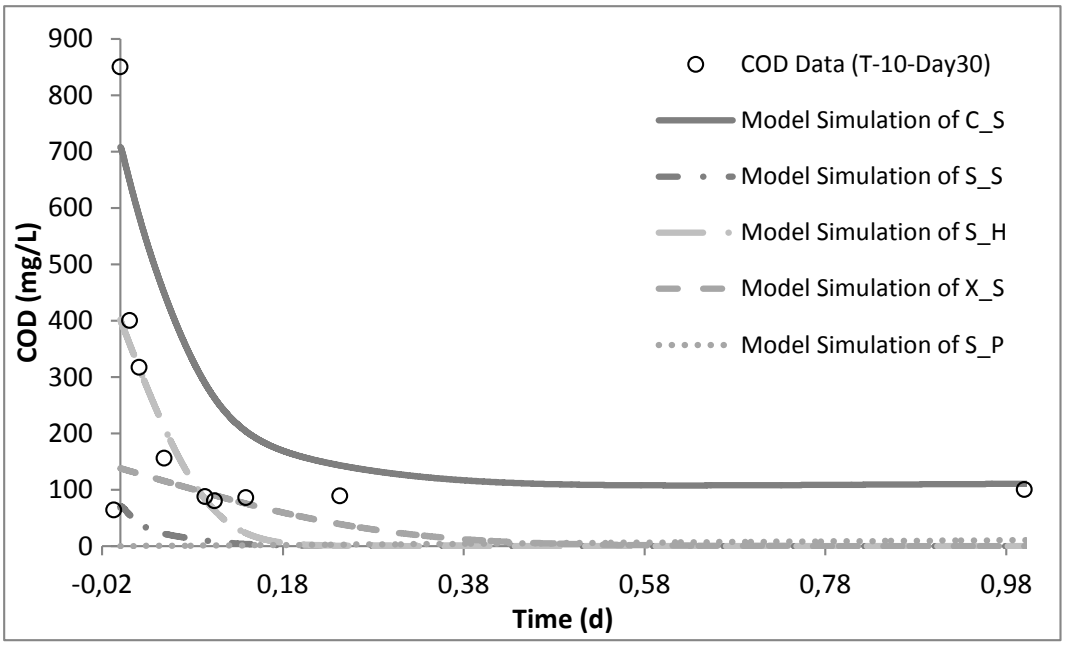

Figure 5.46: COD removal profile of peptone-meat extract biodegradation and simulation (Chronic TET50 SRT 10d Day30).

5.7.2.2 SRT: 2 d

Results of SRT 2d system simulation studies to determine the kinetic effect of TET on the biodegradation of peptone-meat extract showed that acute exposure to the 50 mg/L and 200 mg/L concentrations of antibiotic has significant effects on the growth kinetics of the system, resulting in decreased maximum growth rate and increased half saturation constant of the biomass. Kinetics of both acute inhibition studies showed that substance significantly increases the half saturation constant and decreases the rate of S_H hydrolysis, showing that TET additions adversely affected the S_H hydrolysis mechanism. Moreover it has been observed that the X_S hydrolysis rate was not significantly affected by acute inhibition of TET. Finally, it has been determined that the SRT 2d system utilizes 148 and 253 mgCOD/L less than given amount for TET50 and TET200 acute additions (Table 5.17). Additionally, in contrast to SRT 10d system, it has been observed that the endogenous decay level of the SRT 2d control system, which is due to its fast nature already double as much as the SRT 10d control system, does not increase under the effect of antibiotic substance. (Figure 5.47, Figure 5.48 and Figure 5.49)

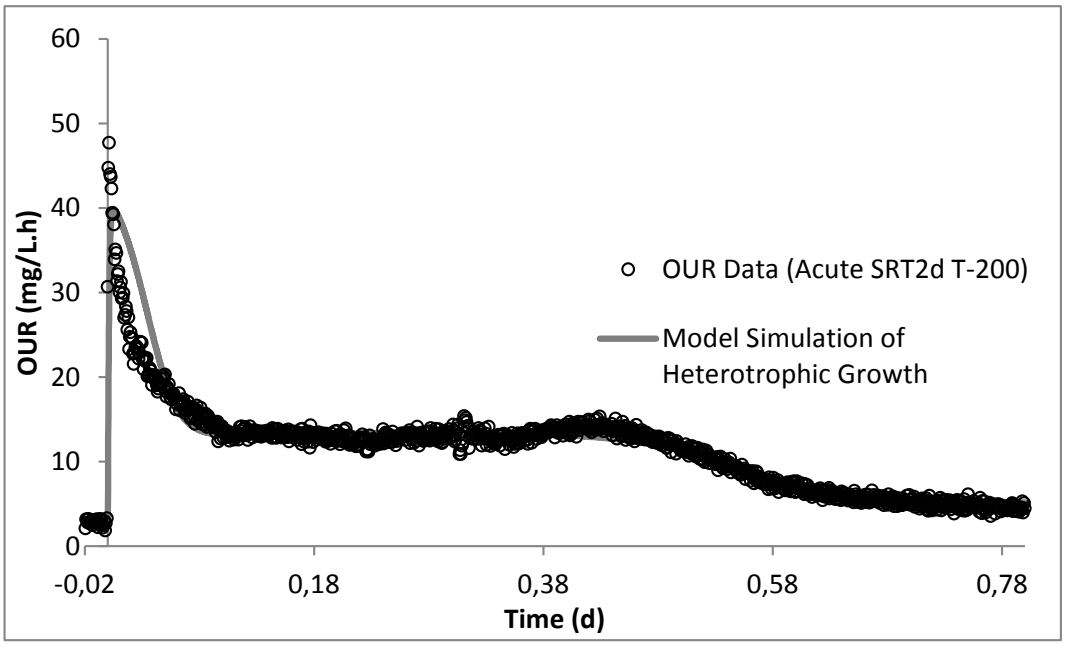

Figure 5.47: OUR simulation of peptone-meat extract biodegradation and simulation (Acute TET200 SRT 2d).

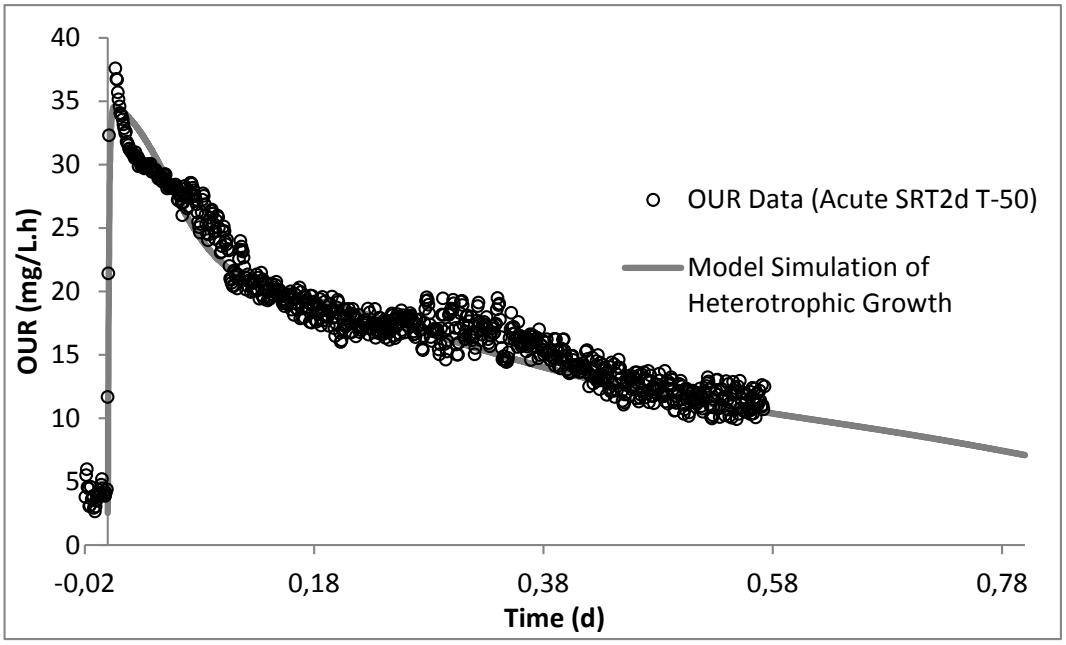

Figure 5.48: OUR simulation of peptone-meat extract biodegradation and simulation (Acute TET50 SRT 2d).

Table 5.17: Effect of TET on kinetics of peptone-meat extract removal (SRT 2d).

Model Parameter		Unit	Control – SRT 2d	Acute – TET200	Acute – TET50	Chronic – TET50 Day 2
Maximum growth rate for X_H	μ_H	1/day	7.2	4.6	4.6	6.5
Half saturation constant for growth of X_H	K_S	mg COD/L	30	33	33	30
Endogenous decay rate for X_H and	b_H	1/day	0.2	0.2	0.2	0.2
Heterotrophic half saturation coefficient for oxygen	K_{OH}	mg O_2/L	0.01	0.01	0.01	0.01
Maximum hydrolysis rate for S_{H1}	k_h	1/day	4	0.68	3.37	4.4
Hydrolysis half saturation constant for S_{H1}	K_X	g COD/g COD	0.15	0.5	0.45	0.15
Maximum hydrolysis rate for X_{S1}	k_{hx}	1/day	1	1	0.7	1.37
Hydrolysis half saturation constant for X_{S1}	K_{XX}	g COD/g COD	0.05	0.05	0.05	0.05
Maximum storage rate of PHA by X_H	k_{STO}	1/day	0	0	0	0
Maximum growth rate on PHA for X_H	μ_{STO}	1/day	0	0	0	0
Half saturation constant for storage of PHA by X_H	K_{STO}	mg COD/L	0	0	0	0
Yield coefficient of X_H	Y_H	g COD/g COD	0.60	0.60	0.60	0.60
Yield coefficient of PHA	Y_{STO}	g COD/g COD	0	0	0	0
Fraction of biomass converted to S_P	f_{ES}	-	0.05	0.05	0.05	0.05
Fraction of biomass converted to X_P	f_{EX}	-	0.15	0.15	0.15	0.15

Table 5.17 (continued): Effect of TET on kinetics of peptone-meat extract removal (SRT 2d).

State variables		Unit	Control – SRT 2d	Acute – TET200	Acute – TET50	Chronic – TET50 Day 2
Total biomass		mgCOD/L	809	809	710	405
Initial active biomass	X_{H1}	mg COD/L	630	433	380	315
Activity		%	78	53	54	78
Initial amount of PHA	X_{STO1}	mg COD/L	0	0	0	0
Initial amount of biodegradable COD	C_{S1}	mg COD/L	760	720	720	720
Initial amount of readily biodegradable COD	S_{S1}	mg COD/L	72	68	68	68
Initial amount of readily hydrolysable COD	S_{H1}	mg COD/L	424	149	254	384
Initial amount of hydrolysable COD	X_{S1}	mg COD/L	264	250	250	244
Bound COD		mgCOD/L	-	253	148	24

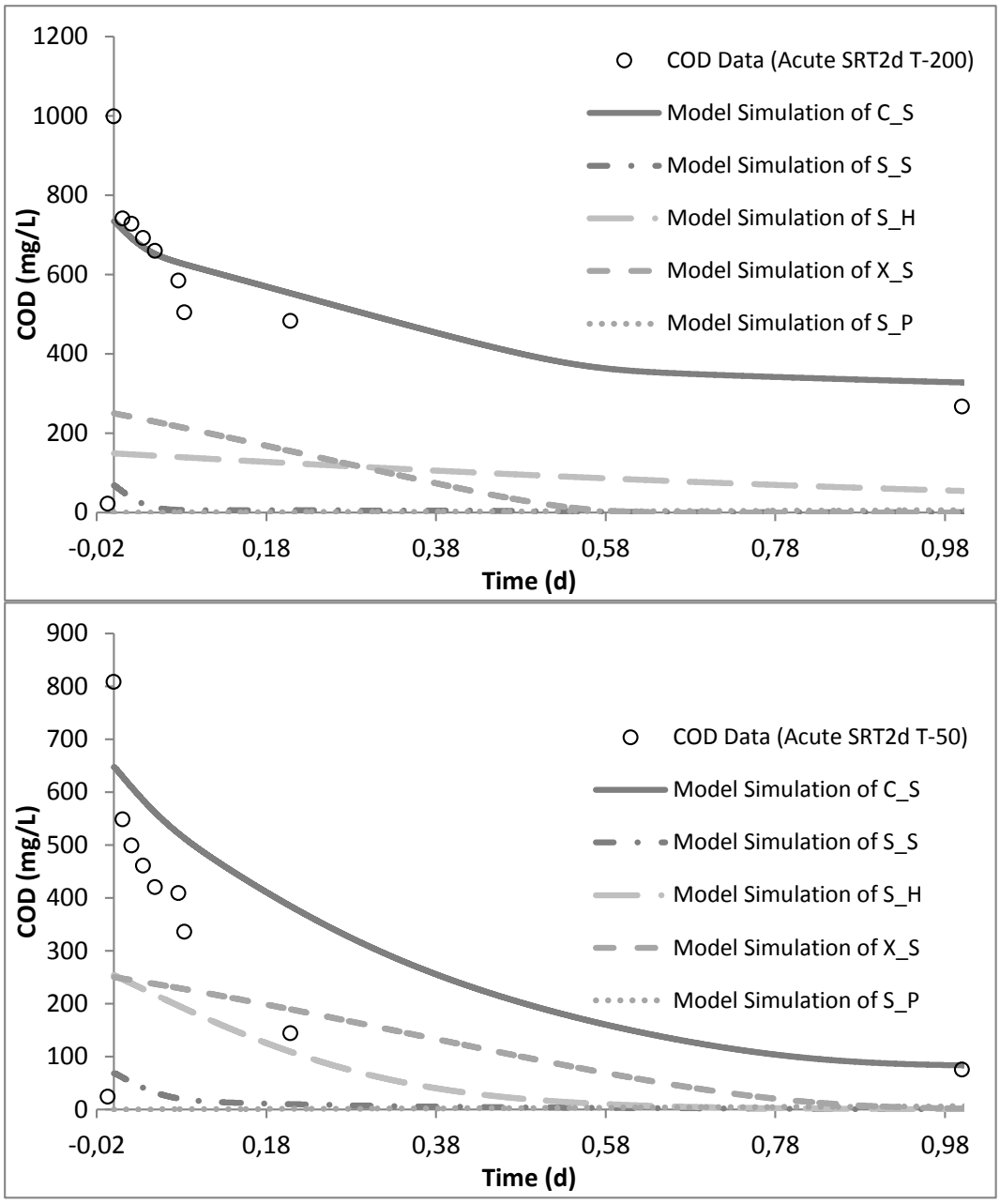

Figure 5.49: COD removal profile of peptone-meat extract biodegradation and simulation (Top: Acute TET200 SRT 2d; Bottom: Acute TET50 SRT 2d).

In addition to the acute inhibition studies, simulations of the chronic inhibition data revealed that chronic exposure to 50 mg/L TET for 2 days decreased the maximum growth rate of the biomass. However, under the effect of constant exposure the endogenous decay level does not increase further compared to control system. Simulations showed that the biomass consortia formed under the constant exposure to TET was able to degrade both hydrolysable COD fractions with higher rates than the control system. Finally, simulation showed that the system utilized 24 mgCOD/L less than given amount (Table 5.17). (Figure 5.50 and Figure 5.51)

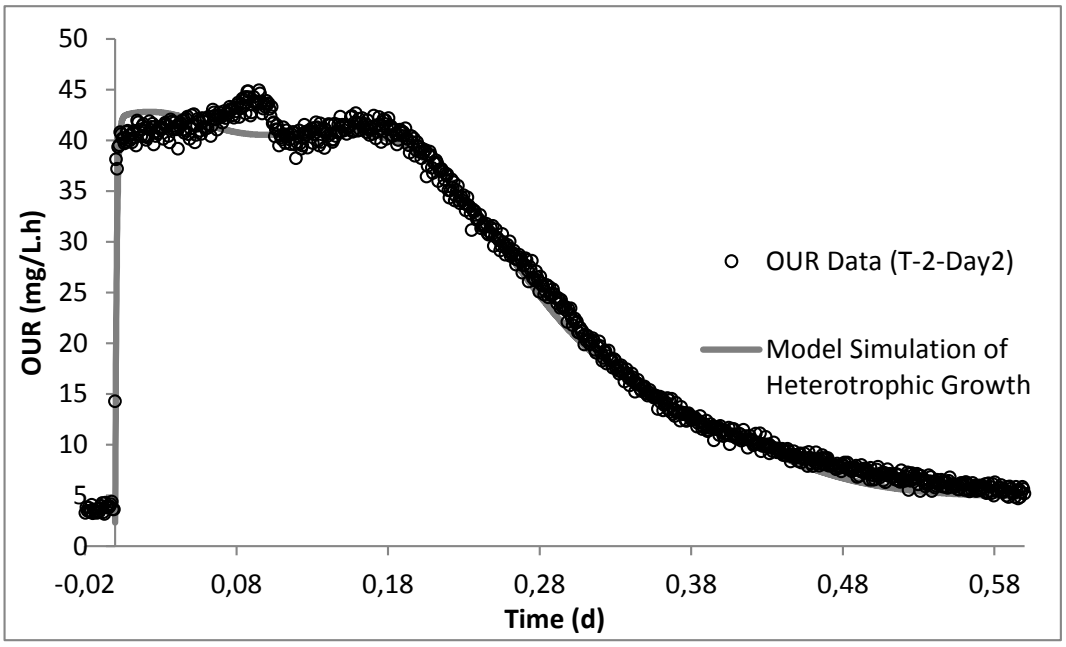

Figure 5.50: OUR simulation of peptone-meat extract biodegradation and simulation (Chronic TET50 SRT 2d Day2).

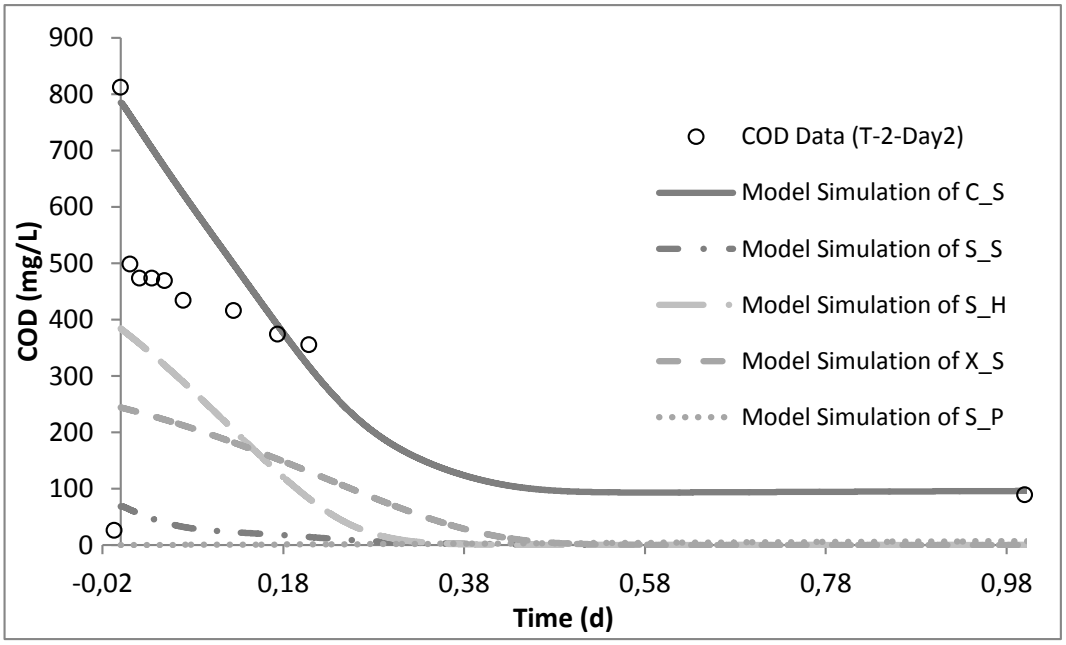

Figure 5.51: OUR simulation of peptone-meat extract biodegradation and simulation (Chronic TET50 SRT 2d Day2).

5.7.3 Erythromycin simulations

5.7.3.1 SRT: 10 d

Results of simulation studies to determine the kinetic effect of ERY on the biodegradation of peptone-meat extract showed the antibiotic inhibits the PHA storage of the SRT 10d system (Table 5.18). Kinetics of acute inhibition studies

showed that the system maintained to ability to grow on already stored PHA. Moreover it was shown that ERY did not affect the maximum growth rate of the system but increased the half saturation constant of the substrate, making it less available for the biomass. The system also demonstrated that with increasing antibiotic concentration half saturation constant of S_H hydrolysis increased. Additionally, acute addition of ERY did not affect kinetics of X_S hydrolysis. Finally, it has been determined that the system utilizes not all the COD given, but 313 and 443 mgCOD/L less than given amount for ERY50 and ERY200 acute additions. Additionally, it has been demonstrated that with the addition of the antibiotic substance the endogenous decay level of the system increased from $0.1d^{-1}$ in the SRT10d system to $0.20d^{-1}$ with 50 mg/L ERY addition and to $0.24d^{-1}$ with 200 mg/L ERY addition. (Figure 5.52, Figure 5.53 and Figure 5.54)

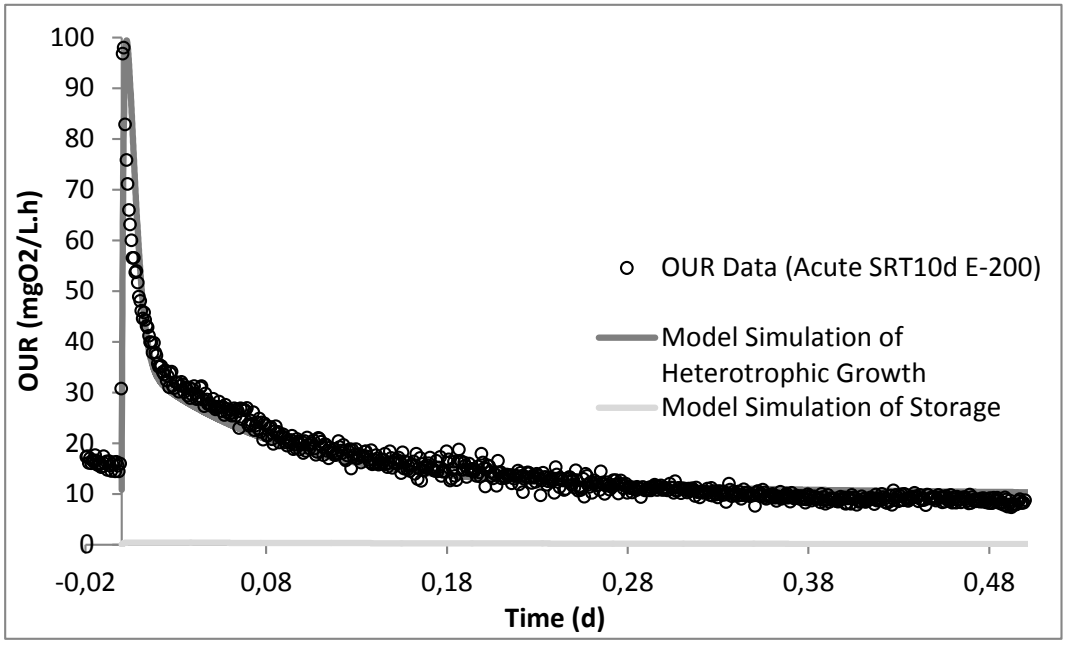

Figure 5.52: OUR simulation of peptone-meat extract biodegradation and simulation (Acute ERY200 SRT 10d).

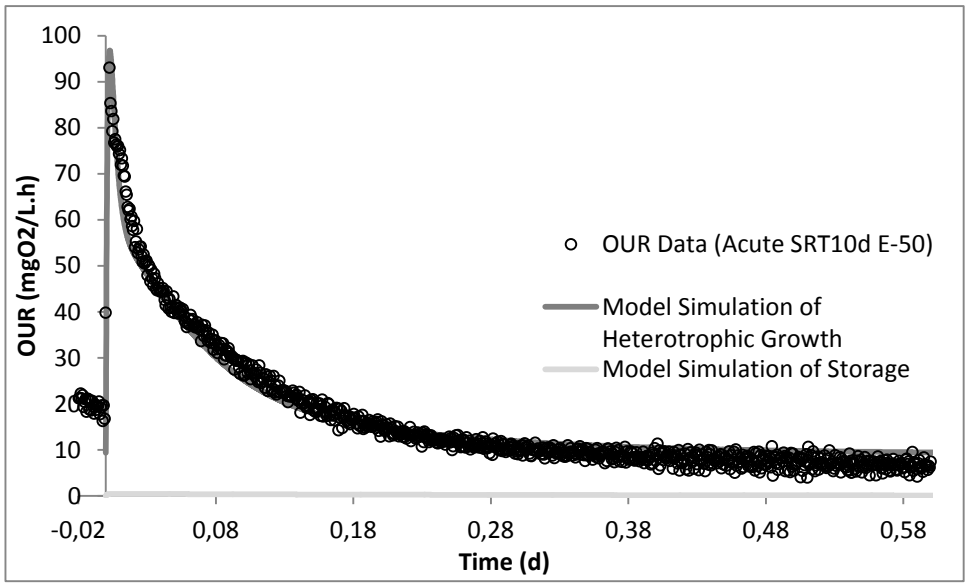

Figure 5.53: OUR simulation of peptone-meat extract biodegradation and simulation (Acute ERY50 SRT 10d).

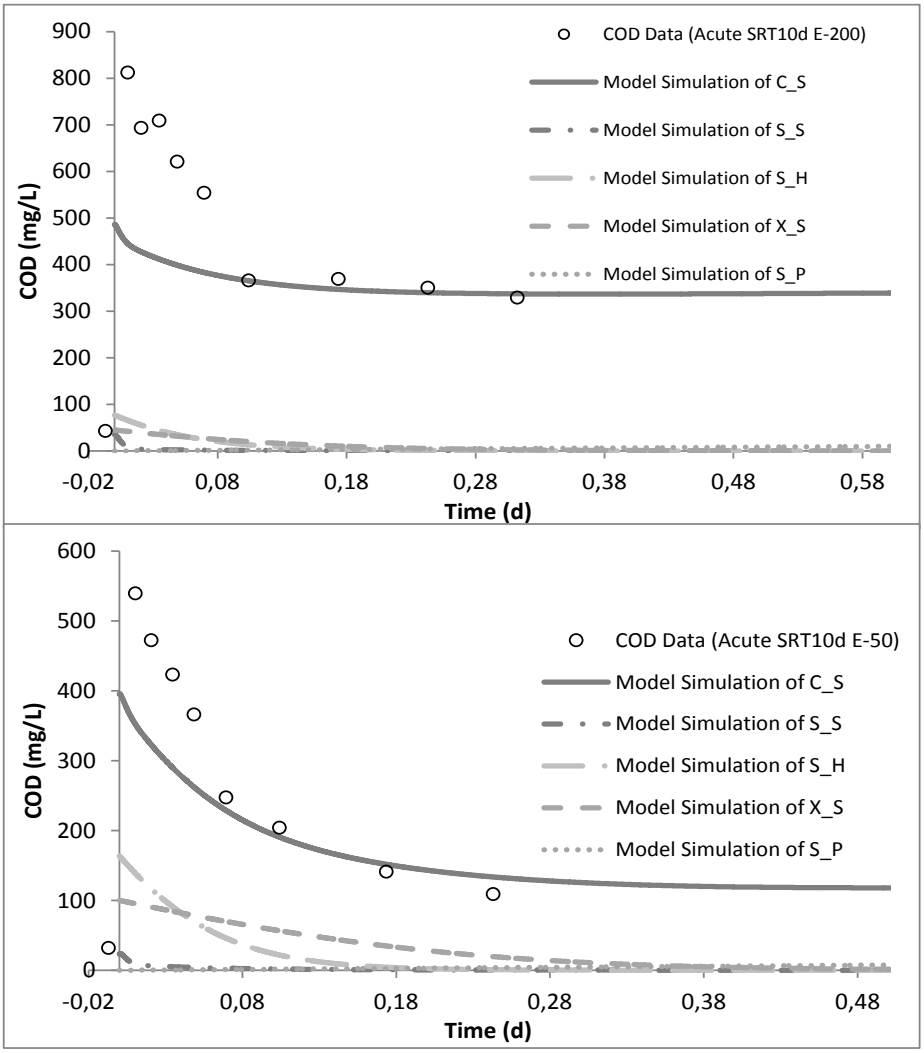

Figure 5.54: COD removal profile of peptone-meat extract biodegradation and simulation (Top: Acute ERY200 SRT 10d; Bottom: Acute ERY50 SRT 10d).

Table 5.18: Effect of ERY on kinetics of peptone-meat extract removal (SRT 10d).

Model Parameter		Unit	Control – SRT 10d	Acute – ERY200	Acute – ERY50	Chronic – ERY Day 31	Chronic – ERY Day 50
Maximum growth rate for X_H	μ'_H	1/day	5.2	5.2	5.2	4.2	5.2
Half saturation constant for growth of X_H	K_S	mg COD/L	24	30	30	30	32
Endogenous decay rate for X_H and	b_H	1/day	0.1	0.24	0.20	0.23	0.15
Heterotrophic half saturation coefficient for oxygen	K_{OH}	mg O_2/L	0.01	0.01	0.01	0.01	0.01
Maximum hydrolysis rate for S_{H1}	k_h	1/day	5.2	5.2	5.2	2.16	2.22
Hydrolysis half saturation constant for S_{H1}	K_X	g COD/g COD	0.15	0.28	0.22	0.05	0.15
Maximum hydrolysis rate for X_{S1}	k_{hx}	1/day	0.56	0.56	0.56	0.58	0.56
Hydrolysis half saturation constant for X_{S1}	K_{XX}	g COD/g COD	0.05	0.05	0.02	0.05	0.05
Maximum storage rate of PHA by X_H	k_{STO}	1/day	1.2	0	0	0	0
Maximum growth rate on PHA for X_H	μ'_{STO}	1/day	0.8	0.8	0.8	0	0
Half saturation constant for storage of PHA by X_H	K_{STO}	mg COD/L	0.5	0.5	0.5	0	0
Yield coefficient of X_H	Y_H	g COD/g COD	0.6	0.6	0.6	0.6	0.6
Yield coefficient of PHA	Y_{STO}	g COD/g COD	0.8	0.8	0.8	0.8	0.8
Fraction of biomass converted to S_P	f_{ES}	-	0.05	0.05	0.05	0.05	0.05
Fraction of biomass converted to X_P	f_{EX}	-	0.15	0.15	0.15	0.15	0.15

Table 5.18 (continued): Effect of ERY on kinetics of peptone-meat extract removal (SRT 10d).

State variables		Unit	Control – SRT 10d	Acute – ERY200	Acute – ERY50	Chronic – ERY Day 31	Chronic – ERY Day 50
Total biomass		mgCOD/L	2010	2037	2010	1666	1633
Initial active biomass	X_{H1}	mg COD/L	1450	1350	1400	1000	1016
Activity		%	72	66	70	60	62
Initial amount of PHA	X_{STO1}	mg COD/L	10	10	10	0	0
Initial amount of biodegradable COD	C_{S1}	mg COD/L	600	600	600	720	720
Initial amount of readily biodegradable COD	S_{S1}	mg COD/L	57	35	23	30	34
Initial amount of readily hydrolysable COD	S_{H1}	mg COD/L	335	77	164	353	300
Initial amount of hydrolysable COD	X_{S1}	mg COD/L	208	45	100	206	206
Bound COD		mgCOD/L	-	443	313	131	180

Simulations of chronic inhibition data revealed that exposed to 50 mg/L ERY for 31 days, the maximum growth rate of the microorganisms decreased (Table 5.18). However the half saturation constant of the substrate remained at 30 mg/L as in acute experiments. Moreover, the endogenous decay level increased to 0.23 d^{-1} under the effect of constant exposure. Finally, simulation showed that the system utilized 131mgCOD/L less than given amount and it can also be seen that both the rate and the half saturation constant of hydrolysis for S_H decreased, which coincides with the effect of uncompetitive inhibition. However, hydrolysis mechanism of X_S was not significantly affected under the effect of ERY50. (Figure 5.55 and Figure 5.56)

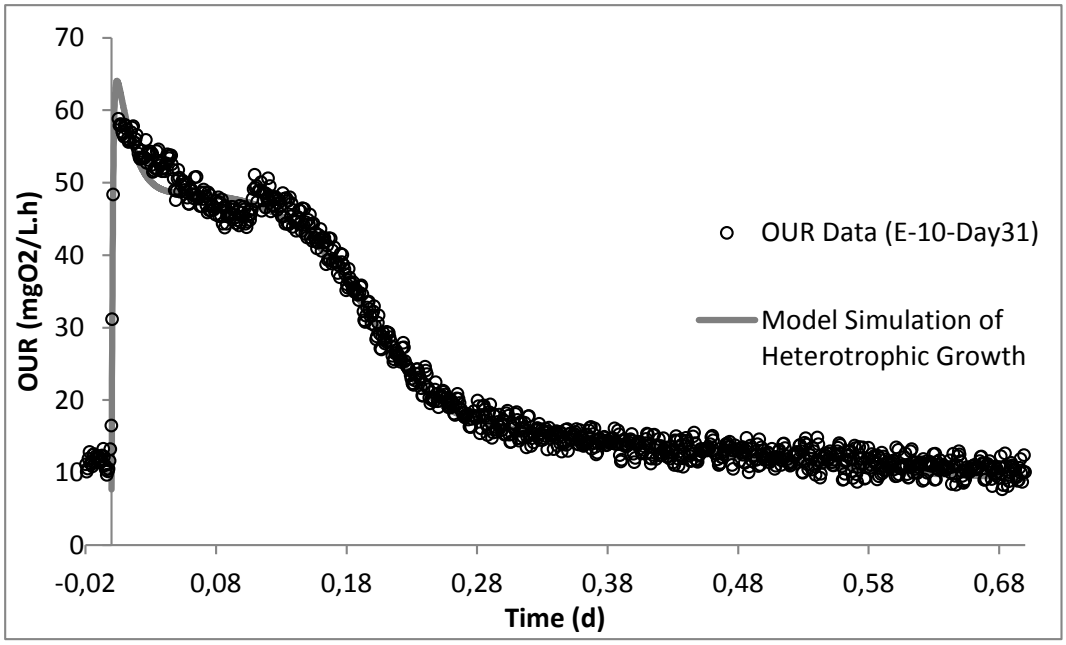

Figure 5.55: OUR simulation of peptone-meat extract biodegradation and simulation (Chronic ERY50 SRT 10d Day31).

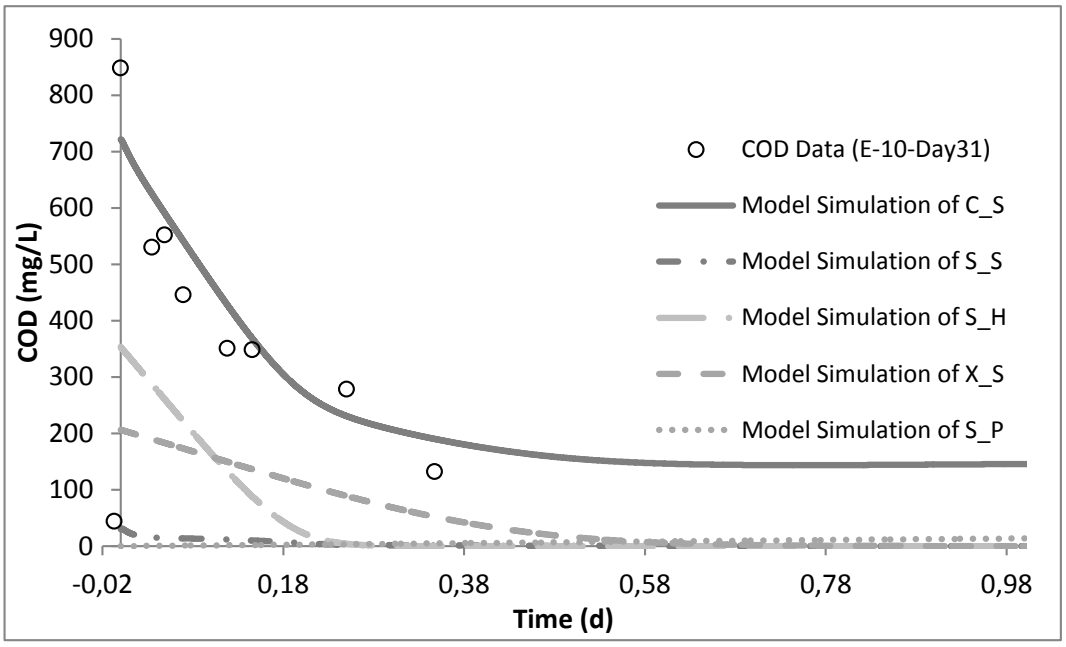

Figure 5.56: COD removal profile of peptone-meat extract biodegradation and simulation (Chronic ERY50 SRT 10d Day31).

After 30 days of exposure to 50 mg/L ERY, the system was not fed with the antibiotic for 20 days, but only fed with peptone-meat extract mixture. On the 50th day 50 mg/L ERY was added to the system again and it has been observed that the system responded with a decrease in hydrolysis rate of S_H. The maximum growth rate increased to the unaffected level, while the half saturation constant of the substrate remained increased (Table 5.18). Moreover, it has been observed that the X_S hydrolysis mechanism remain unaffected. Finally, the endogenous decay rate of the biomass increased to 0.15 d^{-1} for the 50th day, indicating that discontinuance of 20 days in ERY feeding resulted in recovery of the biomass. Moreover the system again utilized 180 mgCOD/L less substrate that given to the system. (Figure 5.57 and Figure 5.58)

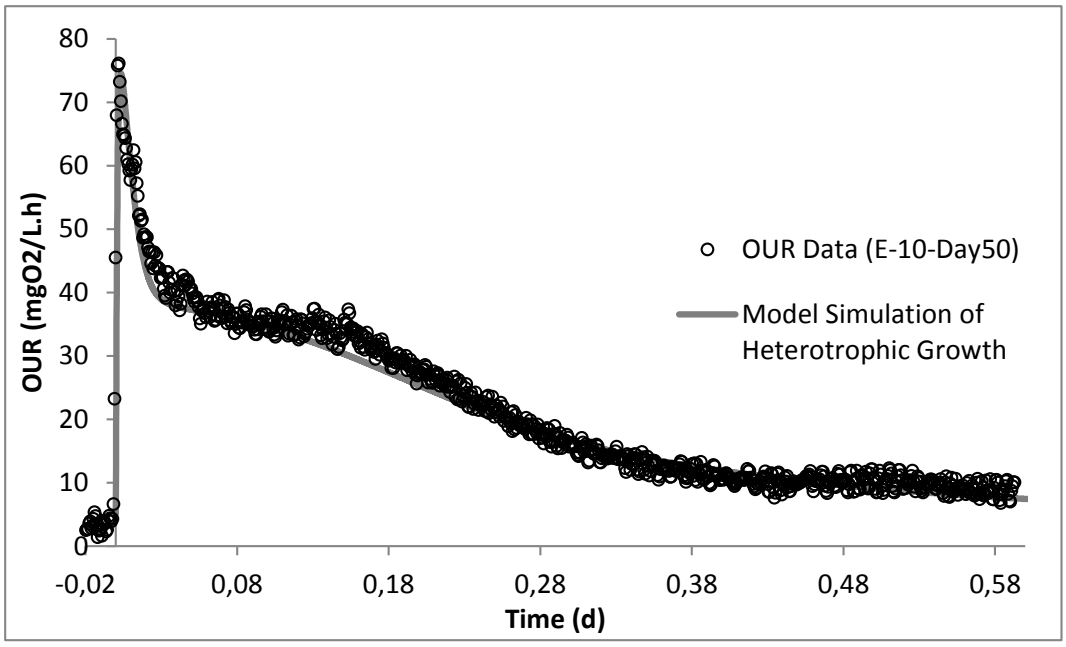

Figure 5.57: OUR simulation of peptone-meat extract biodegradation and simulation (Chronic ERY50 SRT 10d Day50).

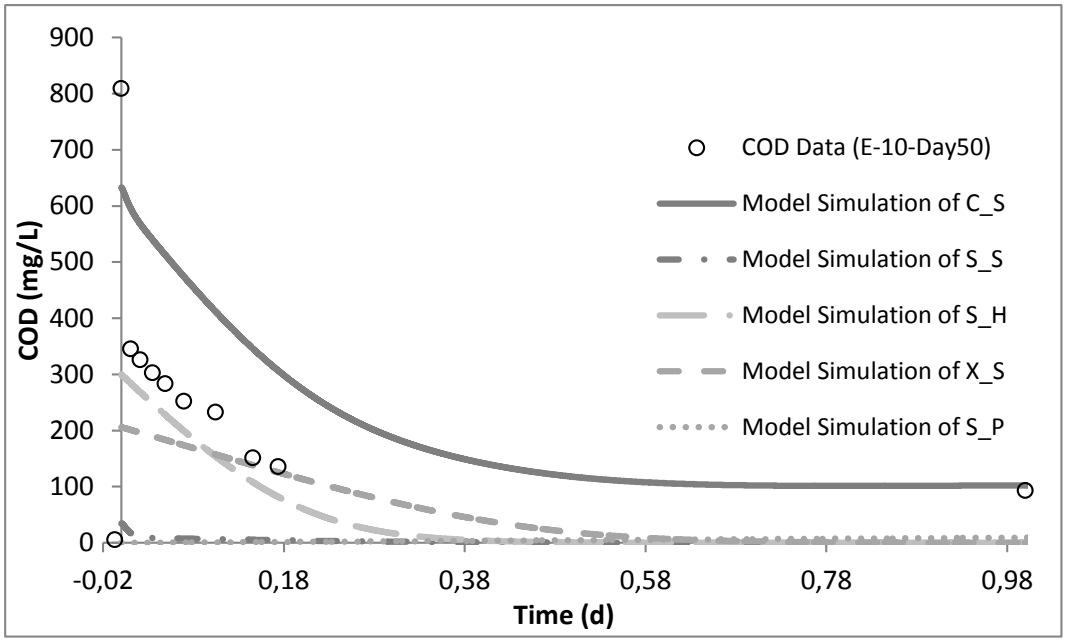

Figure 5.58: COD removal profile of peptone-meat extract biodegradation and simulation (Chronic ERY50 SRT 10d Day50).

5.7.3.2 SRT: 2 d

Results of SRT 2d system simulation studies to determine the kinetic effect of ERY on the biodegradation of peptone-meat extract showed acute exposure to the antibiotic does not affect the growth kinetics of the system, resulting unchanged maximum growth rate and half saturation constant of the biomass (Table 5.19). Kinetics of 50 mg/L ERY acute inhibition study showed that substance has a negative effect on the hydrolysis of S_H fraction of the peptone-meat extract mixture, where it decreases the rate of S_H hydrolysis substantially. Moreover kinetics of X_S hydrolysis is also affected by acute 50 mg/L ERY addition, which is seen as a small decrease of the hydrolysis rate of X_S fraction of the substrate. Finally, it has been determined that the SRT 2d system utilizes 420 mgCOD/L less than given amount for ERY50 acute additions. Moreover, the endogenous decay level increases significantly to 0.4 d^{-1} under the exposure of ERY. (Figure 5.59 and Figure 5.60)

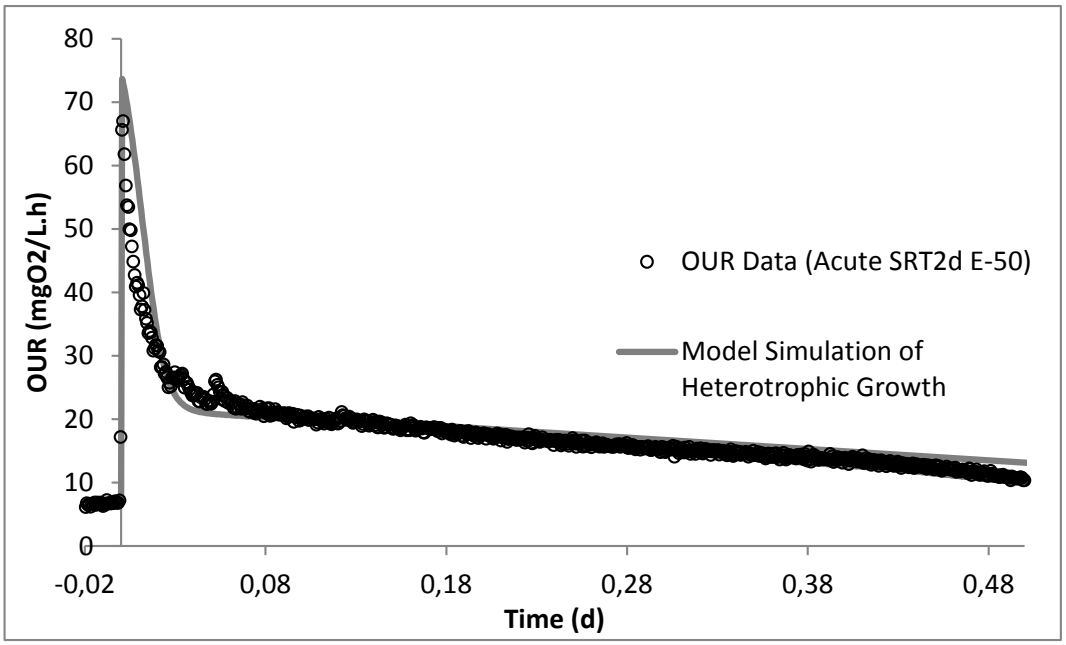

Figure 5.59: OUR simulation of peptone-meat extract biodegradation and simulation (Acute ERY50 SRT 2d).

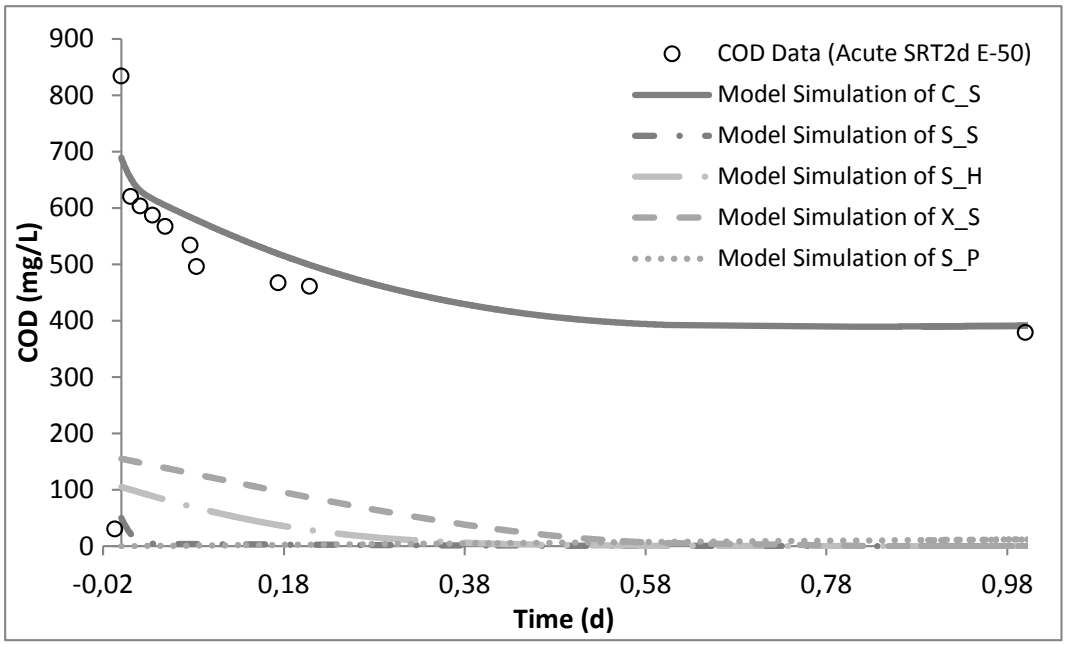

Figure 5.60: COD removal profile of peptone-meat extract biodegradation and simulation (Acute ERY50 SRT 2d).

Simulations of the chronic inhibition data revealed that exposed to 50 mg/L ERY for 3 days, the maximum growth rate of the microorganisms decreased significantly, affecting growth of microbial biomass. Moreover, it has been seen that hydrolysis of S_H was affected by the chronic exposure to ERY, where the half saturation constant increased substantially and the hydrolysis rate decreased. Moreover, the endogenous decay level increases significantly under chronic exposure to ERY. Moreover as in the ERY acute simulations, kinetics of X_S hydrolysis was affected by chronic exposure to 50 mg/L ERY, which is again seen as a small decrease of the hydrolysis rate of X_S fraction of the substrate. Finally, consistent with the stoichiometric calculations the model simulation showed that the system utilized 175 mgCOD/L less than given amount (Table 5.19). (Figure 5.61 and Figure 5.62)

Table 5.19: Effect of ERY on kinetics of peptone-meat extract removal (SRT 2d).

Model Parameter		Unit	Control – SRT 2d	Acute – ERY50	Chronic – ERY50 Day 3
Maximum growth rate for X_H	μ'_H	1/day	7.2	7.2	2.5
Half saturation constant for growth of X_H	K_S	mg COD/L	30	30	30
Endogenous decay rate for X_H and	b_H	1/day	0.2	0.4	0.35
Heterotrophic half saturation coefficient for oxygen	K_{OH}	mg O_2/L	0.01	0.01	0.01
Maximum hydrolysis rate for S_{H1}	k_h	1/day	4	1.56	3.6
Hydrolysis half saturation constant for S_{H1}	K_X	g COD/g COD	0.15	0.15	0.3
Maximum hydrolysis rate for X_{S1}	k_{hx}	1/day	1	0.70	0.84
Hydrolysis half saturation constant for X_{S1}	K_{XX}	g COD/g COD	0.05	0.05	0.05
Maximum storage rate of PHA by X_H	k_{STO}	1/day	0	0	0
Maximum growth rate on PHA for X_H	μ'_{STO}	1/day	0	0	0
Half saturation constant for storage of PHA by X_H	K_{STO}	mg COD/L	0	0	0
Yield coefficient of X_H	Y_H	g COD/g COD	0.6	0.6	0.6
Yield coefficient of PHA	Y_{STO}	g COD/g COD	0	0	0
Fraction of biomass converted to S_P	f_{ES}	-	0.05	0.05	0.05
Fraction of biomass converted to X_P	f_{EX}	-	0.15	0.15	0.15

Table 5.19 (continued): Effect of ERY on kinetics of peptone-meat extract removal (SRT 2d).

State variables		Unit	Control – SRT 2d	Acute – ERY50	Chronic – ERY50 Day 3
Total biomass		mgCOD/L	809	809	888
Initial active biomass	X_{H1}	mg COD/L	630	540	600
Activity		%	78	67	68
Initial amount of PHA	X_{STO1}	mg COD/L	0	0	0
Initial amount of biodegradable COD	C_{S1}	mg COD/L	760	720	720
Initial amount of readily biodegradable COD	S_{S1}	mg COD/L	72	50	50
Initial amount of readily hydrolysable COD	S_{H1}	mg COD/L	424	105	330
Initial amount of hydrolysable COD	X_{S1}	mg COD/L	264	155	165
Bound COD		mgCOD/L	-	420	175

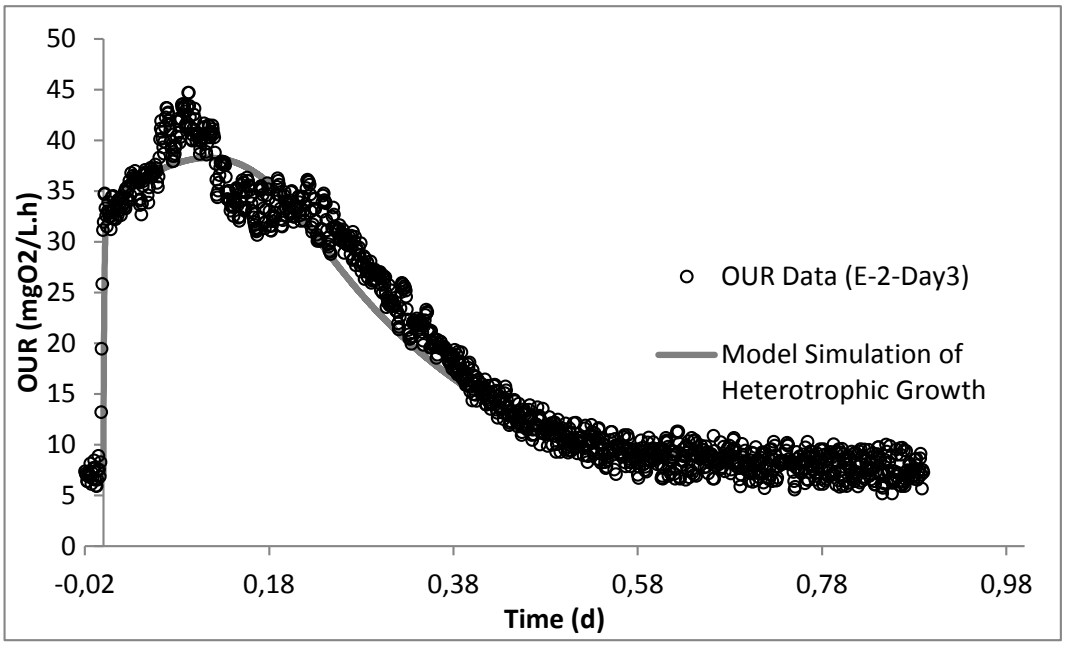

Figure 5.61: OUR simulation of peptone-meat extract biodegradation and simulation (Chronic ERY50 SRT 2d Day3).

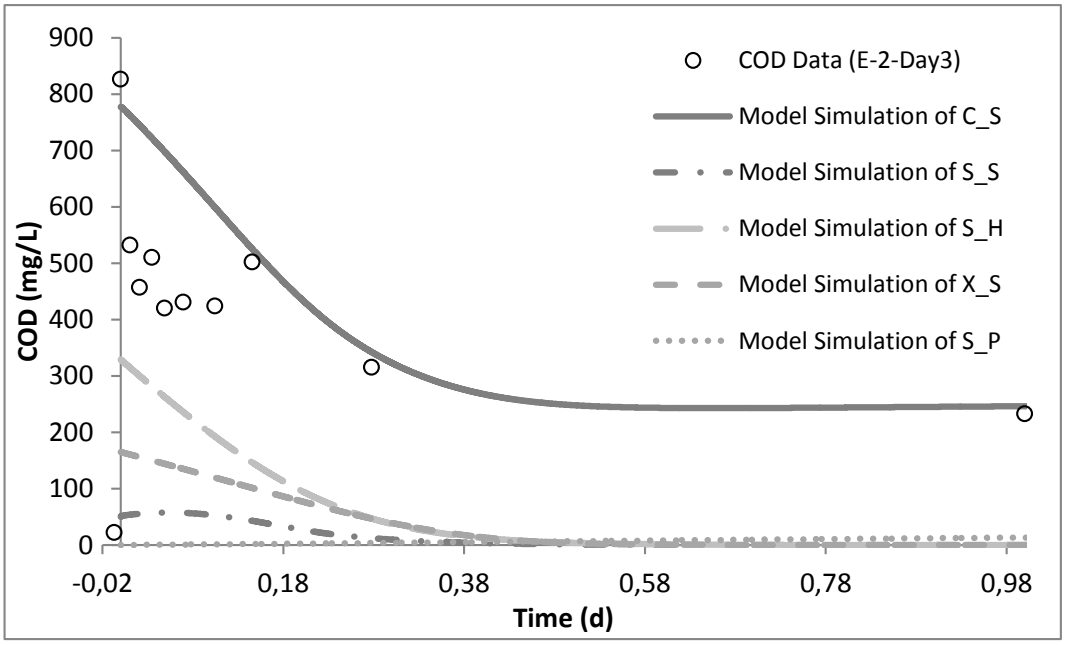

Figure 5.62: COD removal profile of peptone-meat extract biodegradation and simulation (Chronic ERY50 SRT 2d Day3).

5.8 Microbial Community Analysis

5.8.1 Antibiotic resistance analysis

5.8.1.1 Control of DNA extraction method

In order to determine the most effective DNA extraction method to be used for activated sludge samples 23Ins PCR has been applied to different DNA extraction methods applied on samples.

This reaction is reported to amplify the 270 and/or 380 bp fragment of Domain III of 23S rRNA. Therefore it was expected to locate 3 bands on the agarose gel. (Yu *et al.* 2002; Roller et al. 1992). As can be seen in Figure 5.63, each methods lane contains 3 bands. Top two bands correspond to 270 ad 380 bp sizes, whereas the lower band has the size 100 bp, the size of the fragment to be inserted in the 23S ribosomal RNA gene. The non-inserted potion is seen as a third band on the gel.

Comparing the three DNA extraction methods, it can be seen that Macherey-Nagel (MN) DNA extraction Kit gave the best results on activated sludge sample. Therefore it has been decided to continue the studies with the MN Kit.

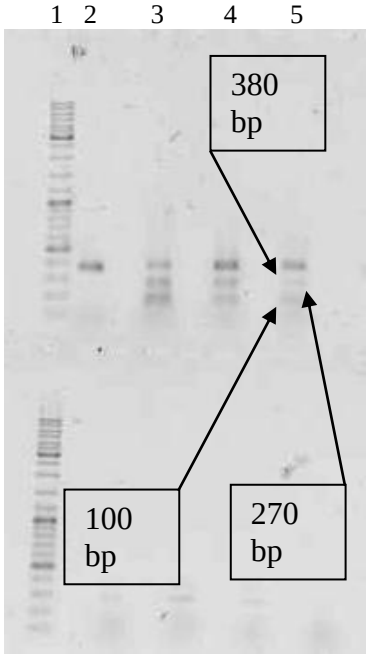

Top Lanes: 1) Marker, **2)** Positive Control, **3)** MN DNA, **4)** Method 2 DNA, **5)** Method 3 DNA
Lower Lanes: 1) Marker, **2)** MN (-) Control, **3)** Method 2 (-) Control, **4)** Method 3 (-) Control

Figure 5.63: Control of gram-positive bacteria.

DNA from all activated sludge samples collected from chronic exposure experiments have been extracted using the MN Kit. Obtained DNA was measured by NanoDrop spectrometer. Results are given in Table 5.20.

Table 5.20: Obtained DNA concentrations.

Sample	DNA Concentration [ng/µl]	Sludge Amount [mg]
Control-10	477.1	250
S10-24	100.9	25
S10-30	45.8	
T10-10	80.6	
T10-22	135.8	25
T10-30	69.8	
T10-50	21.8	
E10-10	192.1	25
E10-31	176	
Control-2	108.6	25
S2-2	185.4	
S2-4	77.5	25
S2-7	83.8	
T2-2	37.8	25
T2-4	18.2	13
T2-7	Inadequate amount of sludge	
E2-3	4.1	63 (watery)
E2-10	29.3	57 (watery)

5.8.1.2 Resistance to sulfonamides

PCR experiments have been run to determine the presence of *sul*I and *sul*II resistance genes in the genomic DNA extracted from activated sludge samples taken from SMX fed reactors. However the experiments also showed that the system did not contain *sul*III resistance gene. The results have shown that all the activated sludge samples including the control sample contains resistance genes against SMX antibiotic. Obtained results are summarized in Figure 5.64 and Table 5.21.

Table 5.21: Results of qualitative determination of SMX resistance genes.

Sample	*sul*I	*sul*II	*sul*III
Positive Control	+	+	-
Control-2	+	+	-
S2-2	+	+	-
S2-4	+	+	-
S2-7	+	+	-
Control-10	+	+	-
S10-24	+	+	-
S10-30	+	+	-
NTC	-	-	-

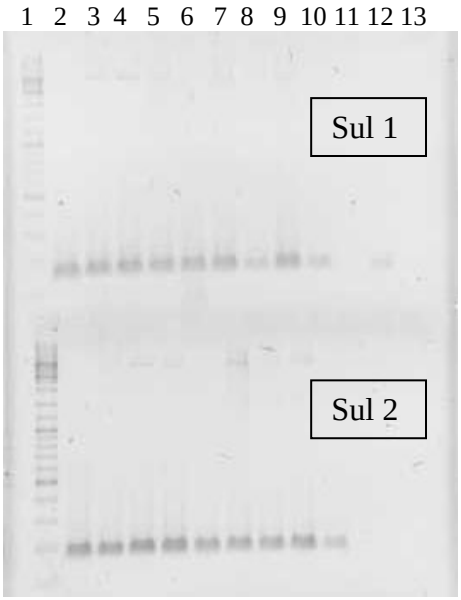

Top Lanes (*sul*I) ve Lower Lanes (*sul*II) 1) Marker, **2)** Positive Control, **3)** Θ10 Control, **4)** S10 – 24, **5)** S10 – 30, **6)** Θ2 Control, **7)** S2 – 2, **8)** S2 – 4, **9)** S2 – 8, **10)** Θ10 Control (-), **11)** Θ2 Control (-), **12)** S2+S10 Control (-), **13)** NTC

Figure 5.64: Qualitative determination of *sul*I and *sul*II genes.

5.8.1.3 Resistance to tetracyclines

PCR experiments have been run to determine the presence of *tet* A, B, C, D, E, G, K, L, M, O and *otr*B resistance genes in the genomic DNA extracted from activated sludge samples taken from TET fed reactors. The results showed that both systems did not contain any *tet* B, D, K, L and *otr*B resistance genes. Both control samples were positive for *tet*A and *tet*G. Moreover, *tet*A and *tet*G genes were present in all samples taken from chronic reactors. However, in the cases of *tet* C, M and O, they were only found in SRT 10d control reactor. Moreover SRT 2d control sample did not contain any *tet*C, *tet*E and *tet*M. Even though the system developed *tet*C and *tet*E resistances in time, the amount of genes present in the control system (SRT2d) was under detection limits. However SRT 2d chronic reactor did not contain any *tet*M resistance gene. The results are given in Table 5.22 and gel photos of qualitative determination of *tet* resistance genes are given in Figure 5.65 to Figure 5.70.

Additionally, after 30 days of chronic exposure to TET, feeding of antibiotic was stopped for 20 days and on the 50^{th} day system was fed with TET again, which was also analyzed for its resistance profile. The results revieled that the resistance profile did not change during intermittent feeding of TET to the reactor.

Table 5.22: Results of qualitative determination of TET resistance genes.

Sample	A	B	C	D	E	G	K	L	otrB	M	O
Positive Control	+	+	-	+	-	-	+	+	+	+	-
Control-2	+	-	-	-	-	+	-	-	-	-	-
T2-2	+	-	+	-	+	+	-	-	-	-	+
T2-4	+	-	+	-	+	+	-	-	-	-	+
Control-10	+	-	+	-	-	+	-	-	-	+	+
T10-10	+	-	+	-	+	+	-	-	-	+	+
T10-22	+	-	+	-	-	+	-	-	-	+	+
T10-30	+	-	+	-	-	+	-	-	-	+	+
T10-50	+	-	+	-	-	+	-	-	-	+	+
NTC	-	-	-	-	-	-	-	-	-	-	-

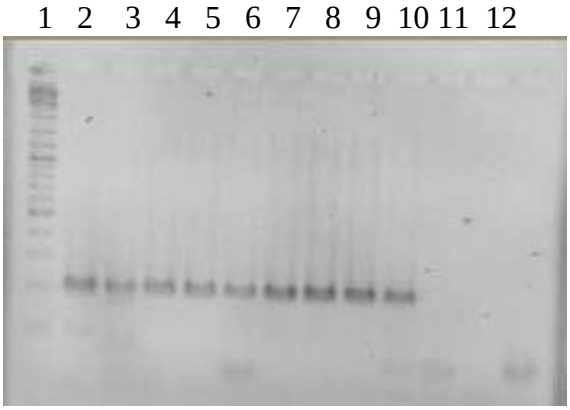

Lanes: 1: Marker, 2: Posivite Control, 3: Control (SRT 2d), 4: Chronic Feeding – Day 2 (SRT 2d), 5: Chronic Feeding – Day 4 (SRT 2d), 6: Control (SRT 10d), 7: Chronic Feeding – Day 10 (SRT 10d), 8: Chronic Feeding – Day 22 (SRT 10d), 9: Chronic Feeding – Day 30 (SRT 10d), 10: Chronic Feeding – Negative Control (SRT 2d), 11: Chronic Feeding – Negative Control (SRT 10d), 12: NTC

Figure 5.65: Qualitative determination of *tet*A gene.

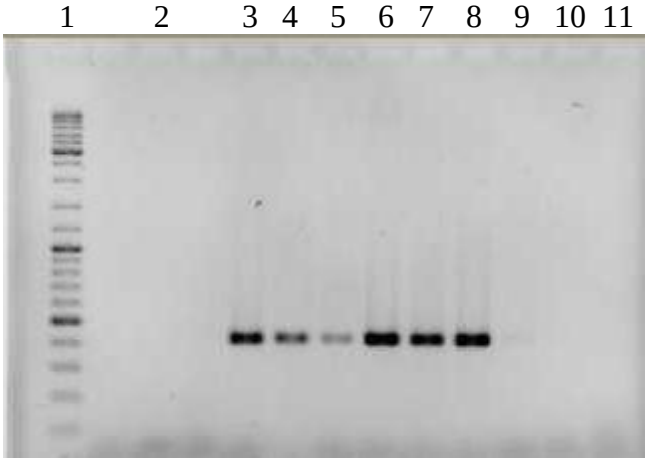

Lanes: 1: Marker, 2: Control (SRT 2d), 3: Chronic Feeding – Day 2 (SRT 2d), 4: Chronic Feeding – Day 4 (SRT 2d), 5: Control (SRT 10d), 6: Chronic Feeding – Day 10 (SRT 10d), 7: Chronic Feeding – Day 22 (SRT 10d), 8: Chronic Feeding – Day 30 (SRT 10d), 9: Chronic Feeding – Negative Control (SRT 2d), 10: Chronic Feeding – Negative Control (SRT 10d), 11: NTC

Figure 5.66: Qualitative determination of *tet*C gene.

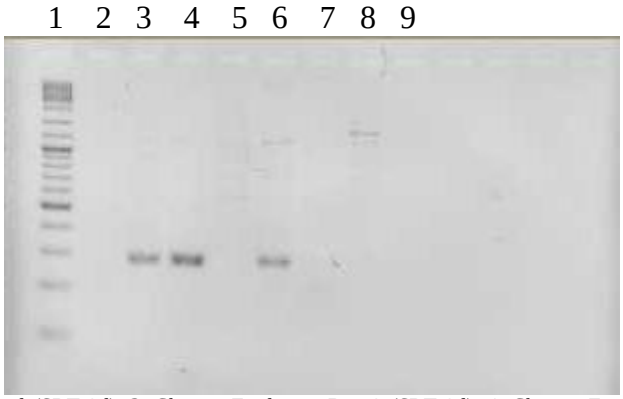

Lanes: 1: Marker, 2: Control (SRT 2d), 3: Chronic Feeding – Day 2 (SRT 2d), 4: Chronic Feeding – Day 4 (SRT 2d), 5: Control (SRT 10d), 6: Chronic Feeding – Day 10 (SRT 10d), 7: Chronic Feeding – Day 22 (SRT 10d), 8: Chronic Feeding – Day 30 (SRT 10d), 9: NTC

Figure 5.67: Qualitative determination of *tet*E gene.

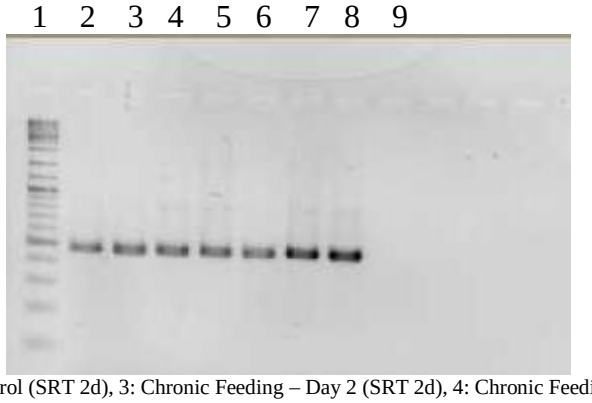

Lanes: 1: Marker, 2: Control (SRT 2d), 3: Chronic Feeding – Day 2 (SRT 2d), 4: Chronic Feeding – Day 4 (SRT 2d), 5: Control (SRT 10d), 6: Chronic Feeding – Day 10 (SRT 10d), 7: Chronic Feeding – Day 22 (SRT 10d), 8: Chronic Feeding – Day 30 (SRT 10d), 9: NTC

Figure 5.68: Qualitative determination of *tet*G gene.

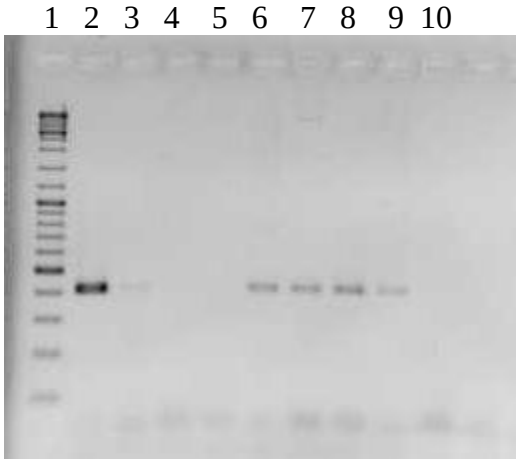

Lanes: 1: Marker, 2: Psitive Control , 3: Control (SRT 2d), 4: Chronic Feeding – Day 2 (SRT 2d), 5: Chronic Feeding – Day 4 (SRT 2d), 6: Control (SRT 10d), 7: Chronic Feeding – Day 10 (SRT 10d), 8: Chronic Feeding – Day 22 (SRT 10d), 9: Chronic Feeding – Day 30 (SRT 10d), 10: NTC

Figure 5.69: Qualitative determination of *tet*M gene.

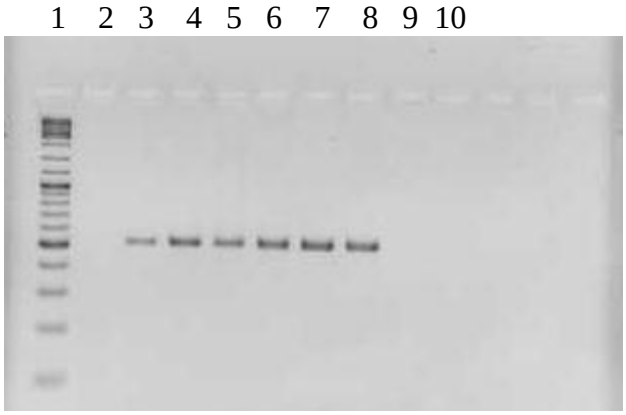

Lanes: 1: Marker, 2: Control (SRT 2d), 3: Chronic Feeding – Day 2 (SRT 2d), 4: Chronic Feeding – Day 4 (SRT 2d), 5: Control (SRT 10d), 6: Chronic Feeding – Day 10 (SRT 10d), 7: Chronic Feeding – Day 22 (SRT 10d), 8: Chronic Feeding – Day 30 (SRT 10d), 9: NTC

Figure 5.70: Qualitative determination of *tet*O gene.

5.8.1.4 Resistance to macrolides

PCR experiments have been run to determine the presence of *erm* A, B, C and *msr*A resistance genes in the genomic DNA extracted from activated sludge samples taken from ERY fed reactors. The results showed that none of the activated sludge samples including the control sample contained rRNA-methlylase type resistance genes against ERY antibiotic. During 3 sludge ages of time, in which the system has been exposed to the antibiotic substance resistance in the form of RNA methylase did not occur. Initial studies on *mph*A gene did not give positive results on the occurrence of mphA in the control samples. However, since its occurrence is found in the chronic samples, the experiment has been repeated for control samples, where C-2 was still negative for *mph*A, applying two different concentrations of C-10 sample DNA (1ng and 10ng) resulted in positive results. This result showed that the control sample (C-10) is also positive for *mph*A, and applying higher concentration of DNA showed that the amount of *mph*A in the control sample was under detection limits. Therefore, it can be said that the system harbours enzyme inactivating phosphorylase gene *mph*A. The results are given in Table 5.23 and gel photos of qualitative determination of *erm* A, B, C, *msr*A and *mph*A genes are given in Figure 5.71 to Figure 5.76.

Table 5.23: Results of qualitative determination of ERY resistance genes.

Sample	*erm*A	*erm*B	*erm*C	*msr*A	16S Internal Control	*mph*A
Positive Control	+	+	+	+	+	-
Control-2	-	-	-	-	+	-
E2-3	-	-	-	-	+	+
E2-10	-	-	-	-	+	+
Control-10	-	-	-	-	+	+
E10-10	-	-	-	-	+	+
E10-31	-	-	-	-	+	+
NTC	-	-	-	-	+	-

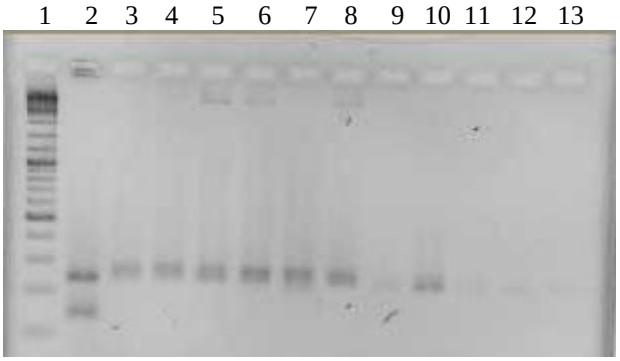

Lanes: 1: Marker, 2: Positive Control, 3: Chronic Feeding – Day 3 (SRT 2d), 4: Chronic Feeding – Day 10 (SRT 2d), 5: Chronic Feeding – Day 10 (SRT 10d), 6: Chronic Feeding – Day 31 (SRT 10d), 7: Control (SRT 2d), 8: Control (SRT 10d), 9: Chronic Feeding – Negative Control (SRT 2d), 10: Chronic Feeding – Negative Control (SRT 10d), 11: Control – Negative Control (SRT 2d), 12: Control – Negative Control (SRT 10d), 13: NTC

Figure 5.71: Qualitative determination of *erm*A gene.

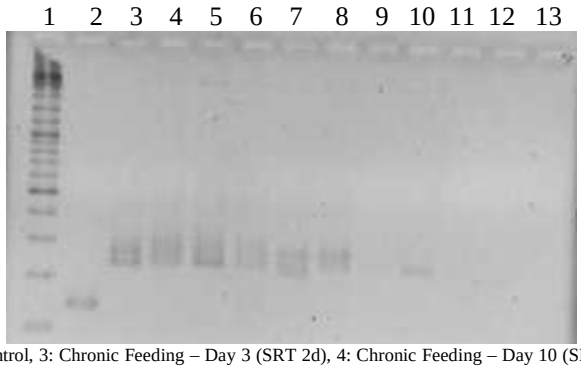

Lanes: 1: Marker, 2: Positive Control, 3: Chronic Feeding – Day 3 (SRT 2d), 4: Chronic Feeding – Day 10 (SRT 2d), 5: Chronic Feeding – Day 10 (SRT 10d), 6: Chronic Feeding – Day 31 (SRT 10d), 7: Control (SRT 2d), 8: Control (SRT 10d), 9: Chronic Feeding – Negative Control (SRT 2d), 10: Chronic Feeding – Negative Control (SRT 10d),), 11: Control – Negative Control (SRT 2d), 12: Control – Negative Control (SRT 10d), 13: NTC

Figure 5.72: Qualitative determination of *erm*B gene.

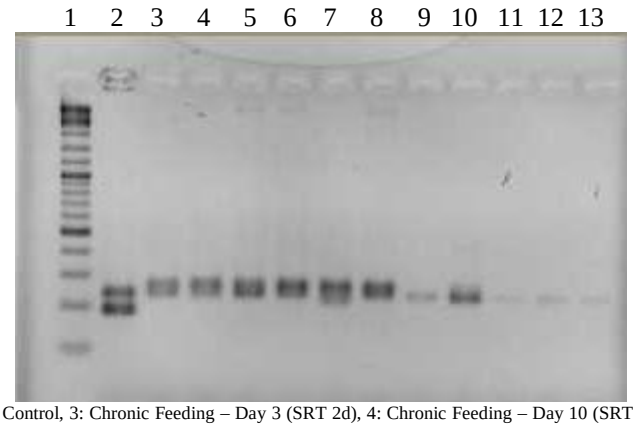

Lanes: 1: Marker, 2: Positive Control, 3: Chronic Feeding – Day 3 (SRT 2d), 4: Chronic Feeding – Day 10 (SRT 2d), 5: Chronic Feeding – Day 10 (SRT 10d), 6: Chronic Feeding – Day 31 (SRT 10d), 7: Control (SRT 2d), 8: Control (SRT 10d), 9: Chronic Feeding – Negative Control (SRT 2d), 10: Chronic Feeding – Negative Control (SRT 10d),), 11: Control – Negative Control (SRT 2d), 12: Control – Negative Control (SRT 10d), 13: NTC

Figure 5.73: Qualitative determination of *erm*C gene.

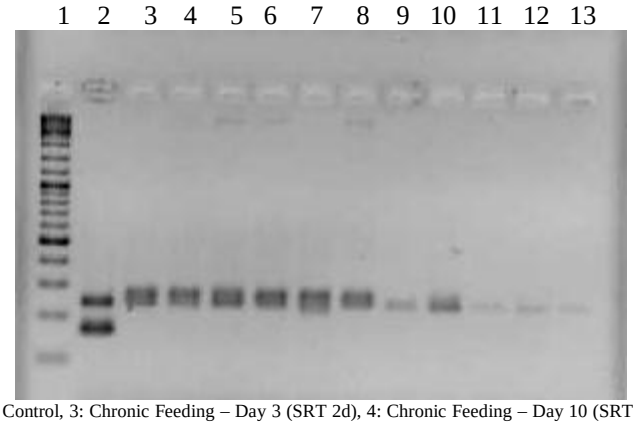

Lanes: 1: Marker, 2: Positive Control, 3: Chronic Feeding – Day 3 (SRT 2d), 4: Chronic Feeding – Day 10 (SRT 2d), 5: Chronic Feeding – Day 10 (SRT 10d), 6: Chronic Feeding – Day 31 (SRT 10d), 7: Control (SRT 2d), 8: Control (SRT 10d), 9: Chronic Feeding – Negative Control (SRT 2d), 10: Chronic Feeding – Negative Control (SRT 10d),), 11: Control – Negative Control (SRT 2d), 12: Control – Negative Control (SRT 10d), 13: NTC

Figure 5.74: Qualitative determination of *msr*A gene.

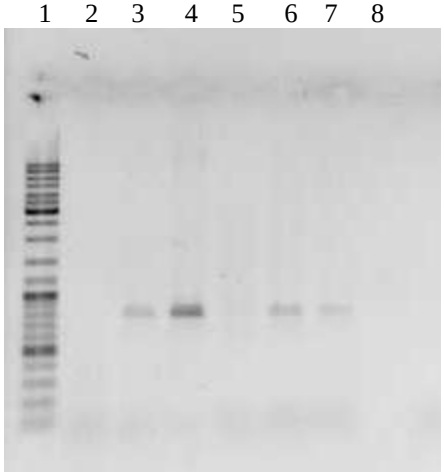

Lanes: 1: Marker, 2: Control (SRT 2d), 3: Chronic Feeding – Day 3 (SRT 2d), 4: Chronic Feeding – Day 10 (SRT 2d), 5: Control (SRT 10d), 6: Chronic Feeding – Day 10 (SRT 10d), 7: Chronic Feeding – Day 31 (SRT 10d), 8: NTC

Figure 5.75: Qualitative determination of *mph*A gene.

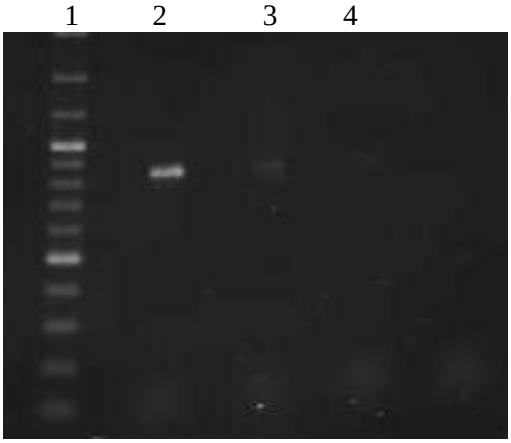

Lanes: 1: Marker, 2: Control (SRT 10d) 10ng , 3: Control (SRT 10d) 1ng (SRT 10d), 4: NTC

Figure 5.76: Determination of *mph*A gene in the control SRT 10d system (repeat).

5.8.2 454-pyrosequencing

Pyrosequencing was performed in order to determine the effect of antibiotic substances on the microbial biomass composition of activated sludge samples. Total number of 119955 sequences was obtained. Sequences were cleaned-up and grouped amongst each other. Each sample resulted with different amount of sequences, which are given in Table 5.24.

Table 5.24: Number of sequences in each sample after clean-up.

Sample Name	Sample Name Abbreviation	Number of Sequences
Control SRT10d	C-10	2977
SMX SRT10d Day 24	S-10-24	3118
SMX SRT10d Day 30	S-10-30	2752
TET SRT10d Day 10	T-10-10	1098
TET SRT10d Day 30	T-10-30	1695
ERY SRT10d Day 10	E-10-10	3865
ERY SRT10d Day 31	E-10-31	1239
Control SRT2d	C-2	1759
SMX SRT2d Day 2	S-2-2	728
SMX SRT2d Day 4	S-2-4	4882
SMX SRT2d Day 7	S-2-7	3616
TET SRT2d Day 2	T-2-2	6552
TET SRT2d Day 4	T-2-4	3555
ERY SRT2d Day 3	E-2-3	4257
ERY SRT2d Day 10	E-2-10	1744

5.8.2.1 Community structure of control samples

Sludge Age 10d System

Based on the classification of sequence reads by RDP classifier, the SRT 10day control system consists of five phyla namely *Actinobacteria (*59%), *Proteobacteria (*24%), *Bacteroidetes (15%), TM7(1%)* and an unclassified phylum (1%) (Figure 5.77). For the downstream analysis sequences were grouped in species (3%) and phyla (20%) level OTUs.

Most abundant species level OTU in SRT 10d control sample were related to family *Intrasporangiaceae* (*Actinobacteria)* and *Chitinophagaceae* (*Bacteriodetes)* with 45% and 10% abundances respectively.

Sludge Age 2d System

Bacterial community in SRT 2d system was distributed in five phyla; *Proteobacteria* (57%), *Actinobacteria* (22%), *Deinococcus-Thermus* (18%) and *Bacteroidetes* (3%) phyla. Most abundant OTUs in the SRT 2d control sample was bacteria belonging to *Paracoccus* genus of class *Alphaproteobacteria* (47%), *Deinococcus* genus of phylum *Deinococcus-Thermus* (18%), *Arthrobacter* genus of phylum *Actinobacteria* (10%) and an unclassified bacterium belonging to phylum *Actinobacteria* (9%) (Figure 5.77).

Differences observed between SRT 10d and SRT 2d control samples enlighten the effect of sludge age on the bacterial community structure. Both systems differ only in sludge age, while the feeding substrate and inoculum are same. Sludge age is considered to be a selection criterion for slow growing bacteria that can easily survive in a slow growing system like SRT 10d, where after every 10 days the bacterial community regenerates itself through sludge waste. However, the system with sludge age of 2d regenerates itself after every 2 days; in such system only rapidly growing bacteria can survive because of high regeneration pressure.

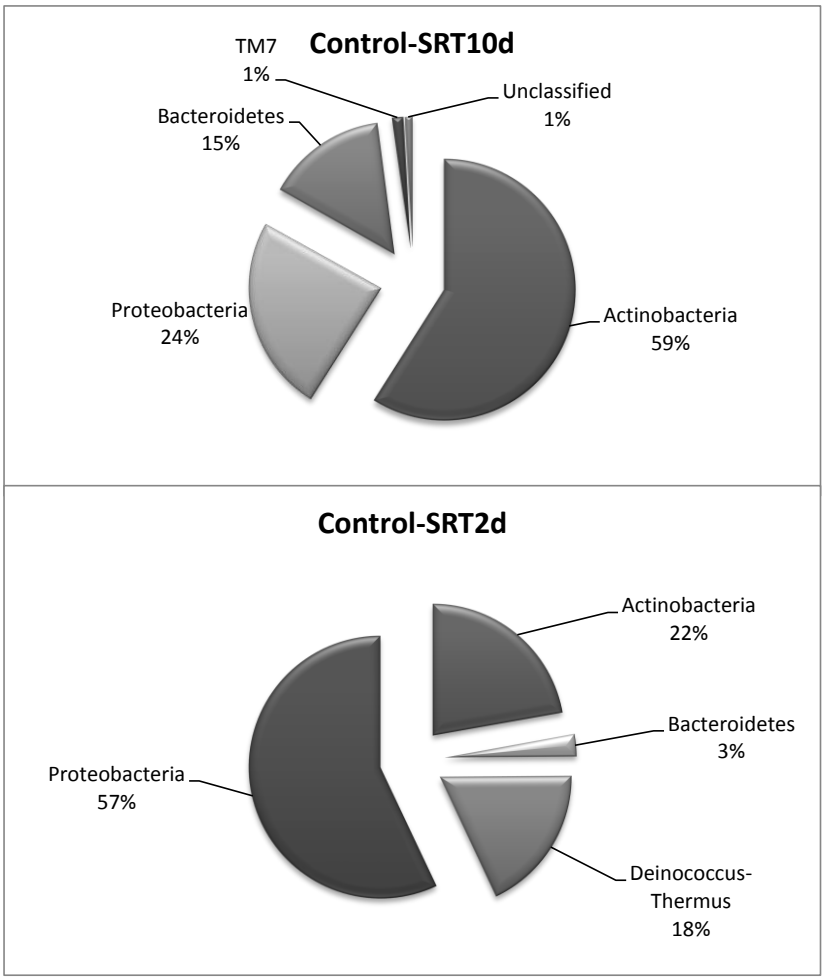

Figure 5.77: Distribution of phyla in control samples.

Analysis of microbial communities indicates that in the SRT 2d system, *Proteobacteria* are dominant; while in the SRT 10d system *Actinobacteria* is the dominant group. *Actinobacteria* are known to be slow growing bacteria (Rosetti et al, 2005, Seviour et al, 2008), and are fit to survive in a fast growing system but not to dominate the community. Additionally, it has been stated that filamentous members like *Haliscomenobacter hydrossis* of *Bacteroidetes* phylum were identified in activated sludge (Wagner et al., 1994, Kampfer, 1995, Eikelboom, 2002, Jenkins et al., 2004, Kragelund et al., 2008). Since it is known that filamentous bacteria grow slower than flock forming bacteria in non-substrate limiting conditions as it is in all the reactors (Seviour and Blackall, 1998, Jonsson, 2005), this may be a reason that members of phyla *Bacteroidetes* and *Actinobacteria* have a significantly lower abundance in the SRT 2d system.

5.8.2.2 Effect of sulfamethoxazole on the community structure

Sludge age 10 d system

At the phylum level constant exposure to SMX did not show a shift in community structure. However after 24 days of exposure the abundance of *Actinobacteria* phylum in C-10 sample changed from 59% to 64% and after 30 days of exposure their abundance was 59%. Phylum *Proteobacteria* had 19% abundance in C-10 sample, whereas after 24 days their abundance remained 19% and after 30 days increased to 26%. Moreover, abundance of *Bacteroidetes* phylum changed from 15% in C-10 to 8% and 9% after 24 and 30 days, respectively. Additionally, TM7 phylum having the abundance of 1% in C-10 sample increased to 4% after 24 days. On the 30th day *TM7* phylum had the abundance of 3%. Figure 5.79 shows the change in distribution of phyla with increasing time of exposure to SMX.

RDP library comparison showed that phylum *Bacteriodetes* significantly decreased throughout the treatment. Moreover, compared to C-10 sample on day 24 *Actinobacteria* increased and *Proteobacteria* decreased significantly. However day 30 did not show any significant changes in *Actinobacteria* and *Proteobacteria* phyla compared to C-10 sample (Figure 5.78).

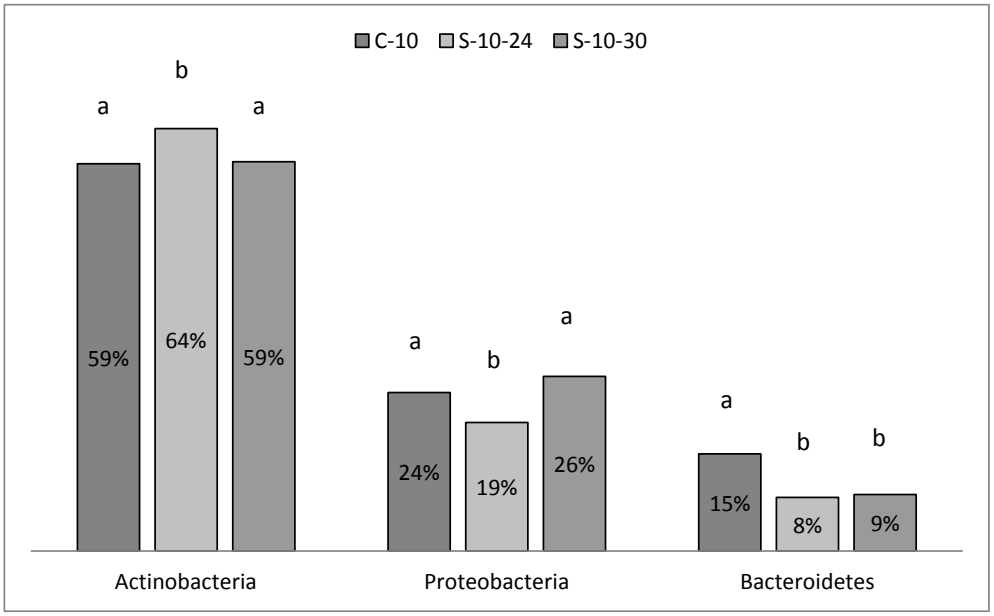

Figure 5.78: Significant changes in dominant phyla in the SMX reactor (*Bars with same letters are not significantly different).

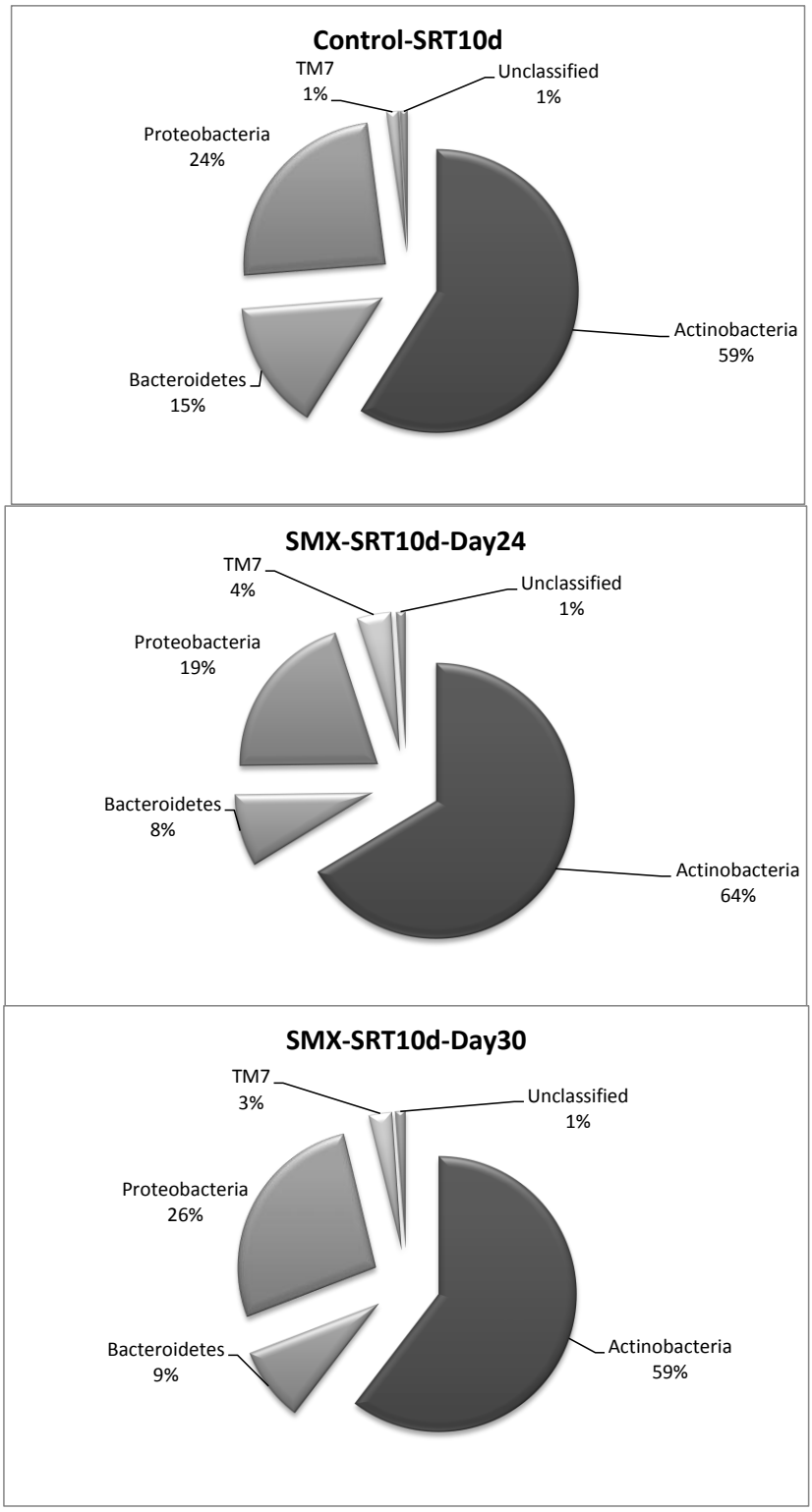

Figure 5.79: Bacterial community structures at phylum level for exposure to SMX.

Rarefaction curves generated to determine the change in richness during SMX treatment showed that compared to untreated samples (C-10), 24 days treatment of SMX resulted in lower richness at phyla (20%). Rarefaction curves at species (3%) level showed that the richness of the S-10-24 sample is higher than the C-10 sample.

However after 30th day treatment richness was almost similar to C-10 sample at species level (3%) and slightly higher at phyla level (20%) (Figure 5.80).

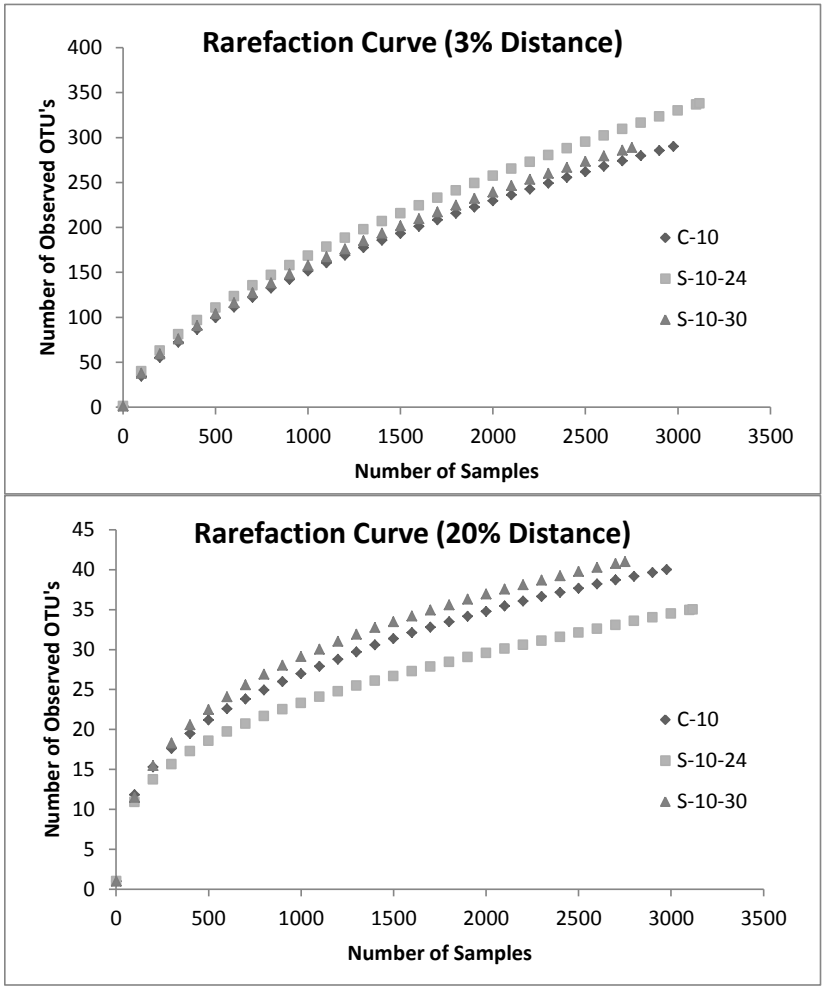

Figure 5.80: Rarefaction curves for SMX samples at 3% and 20% distances.

Both ACE and Chao1 estimators of richness suggest that the richness of the population changes with time. The information obtained from estimators suggests that richness increases by the 24th day of exposure; however decreases slightly by the 30th day compared to the control sample (Table 5.25). Evenness calculated from Shannon's index of diversity shows that all three samples exhibited dominant community structures at all levels. Further analysis also revealed that the dominance shifted with the effect of SMX (SRT10d) treatment.

Table 5.25: Statistical indicators for SMX feeding (SRT 10d).

	3%			20%		
	C-10	S-10-24	S-10-30	C-10	S-10-24	S-10-30
Number of OTUs	288	338	289	42	35	41
Singleton	168	206	169	14	14	13
Chao1 estimate of OTUs richness	647.7	807.2	619.1	55.0	65.3	52.1
ACE estimate of OTU richness	1019.5	1278.6	1058.1	66.9	78.2	56.4
Shannon index of diversity (H)	3.0	3.6	3.6	1.6	1.5	1.6
Evenness	0.53	0.62	0.63	0.41	0.41	0.43
Good's estimator of coverage (%)	41.67	39.05	41.52	66.67	60.00	68.29

According to the information given in the Venn diagrams, at species level C-10 contains 288 species, S-10-24 contains 338 species level OTUs and S-10-30 contains 289 species level OTUs. However groups C-10 and S-10-24 exclusively share 34 species level OTUs, but 154 and 159 species level OTUs belong to each of these groups alone, respectively. Moreover C-10 and S-10-24 exclusively share 20 and 63 species level OTUs with S-10-30, whereas S-10-30 has 124 unshared species level OTUs. Additionally, 82 species level OTUs are shared by all groups (total shared richness). Finally total richness of all groups together is calculated as 636 species level OTUs (Figure 5.81).

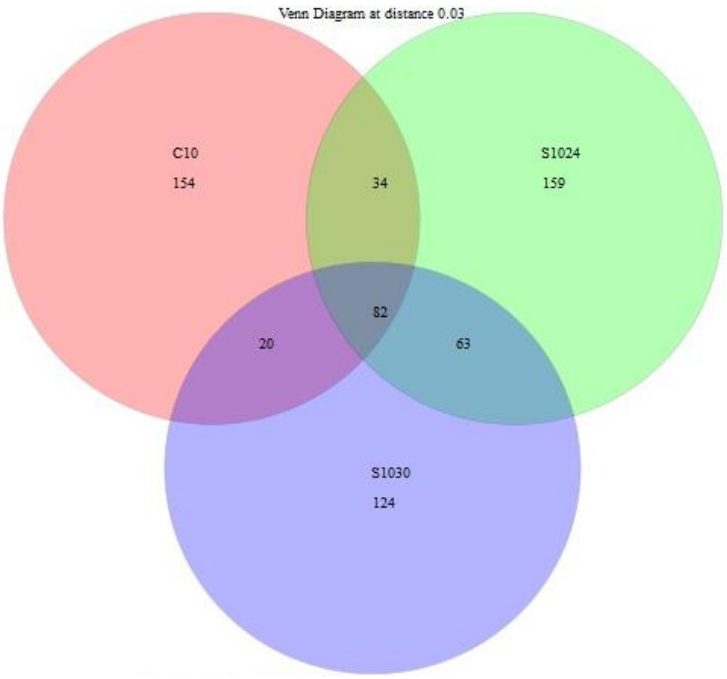

Figure 5.81: Venn diagram of SMX samples at 0.03 distance.

At phylum level however, C-10 contains 42 phylum level OTUs, S-10-24 contains 35 phylum level OTUs and S-10-30 contains 41 phylum level OTUs. However groups C-10 and S-10-24 exclusively share 3 phylum level OTUs, but 10 phylum level OTUs and 3 phylum level OTUs belong to each of these groups alone, respectively. Moreover C-10 and S-10-24 exclusively share 9 and 11 phylum level OTUs with S-10-30, whereas S-10-30 has 3 unshared phylum level OTUs. Additionally, 18 phylum level OTUs are shared by all three groups (total shared richness). Finally total richness of all groups together is calculated as 57 (Figure 5.82).

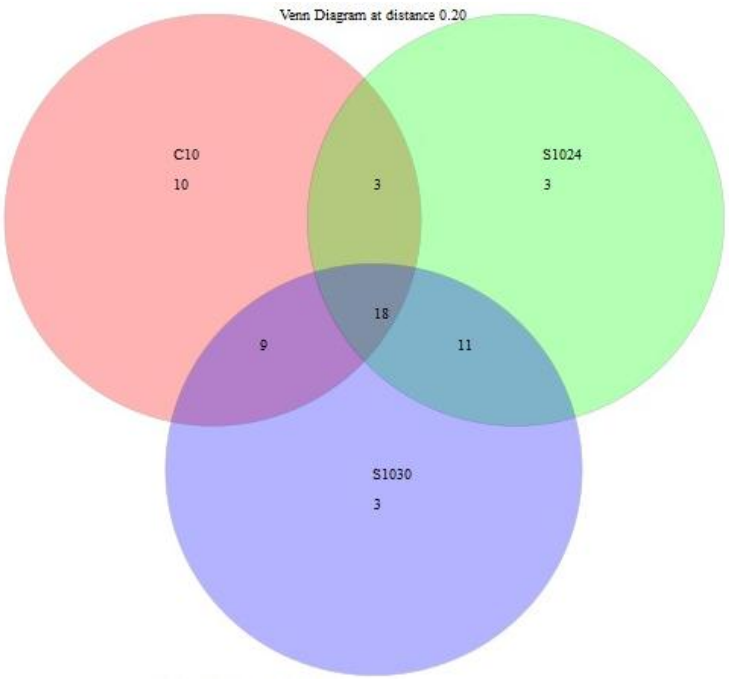

Figure 5.82: Venn diagram of SMX samples at 0.20 distance.

Results of statistical analysis revealed the significantly affected OTUs under chronic SMX inhibited conditions at SRT 10d. It can be seen that OTU#6 (member of unclassified genus of class *Actinobacteria*) and OTU#10 (member of unclassified *Chitinophagaceae*) were most abundant species in the control sample C-10 (45% and 10%). However, after 24 days of SMX treatment OTU#10 disappeared and did not reappear throughout the whole treatment ($p<0.05$, $q>0.05$), and OTU#6 decreased from 45% to 28%, after 30 days it decreased until 9%. Moreover, later in the treatment with SMX the microbial population shows further changes, that is bacteria that are very low abundant in the control sample increase significantly. Species of genus *Arthrobacter* OTU#2 becomes gradually abundant resulting in 24% at 30th day of treatment (Table 5.26).

Table 5.26: Significant changes in the activated sludge population under SMX effect (SRT10d) (species level OTUs are named by numbers).

Phylum	Nearest Classified Neighbour	OTU Number	C-10 (%)	S-10-24 (%)	S-10-30 (%)
Actinobacteria	*Arthrobacter*	2	0	2	24
Actinobacteria	*Unclassified Intrasporangiaceae*	6	45	28	9
Bacteroidetes	*Unclassified Chitinophagaceae*	10	10	0	0

Sludge age 2 d system

At the phylum level constant exposure to SMX (SRT 2d) shows a significant shift in community structure. After 2 days of exposure the percentages of present phyla change from 57%, 22%, 18% and 3% in the C-2 reactor to 17%, 65%, 14% and 4% for *Proteobacteria*, *Actinobacteria*, *Deinococcus-Thermus* and *Bacteroidetes* phyla, respectively, where dominance shifts from *Proteobacteria* to *Deinococcus-Thermus* phylum. Results obtained at the 4^{th} day show that the *Bacteroidetes* phylum disappears. Moreover, at the end of treatment the community structure on phylum level was *Proteobacteria* (7%), *Actinobacteria* (35%) and *Deinococcus-Thermus* (58%). These results showed that *Actinobacteria* although fit to survive under constant exposure of SMX, are not capable of sustaining dominance in a fast growing system, which is also confirmed by the structural differences between SRT 10d and SRT 2d control reactors. Figure 5.83 shows the change in distribution of phyla with increasing time of exposure to SMX (SRT 2d). Results revealed that members of phylum *Bacteroidetes* disappeared, *Proteobacteria* decreased significantly and *Deinococcus-Thermus* became dominant.

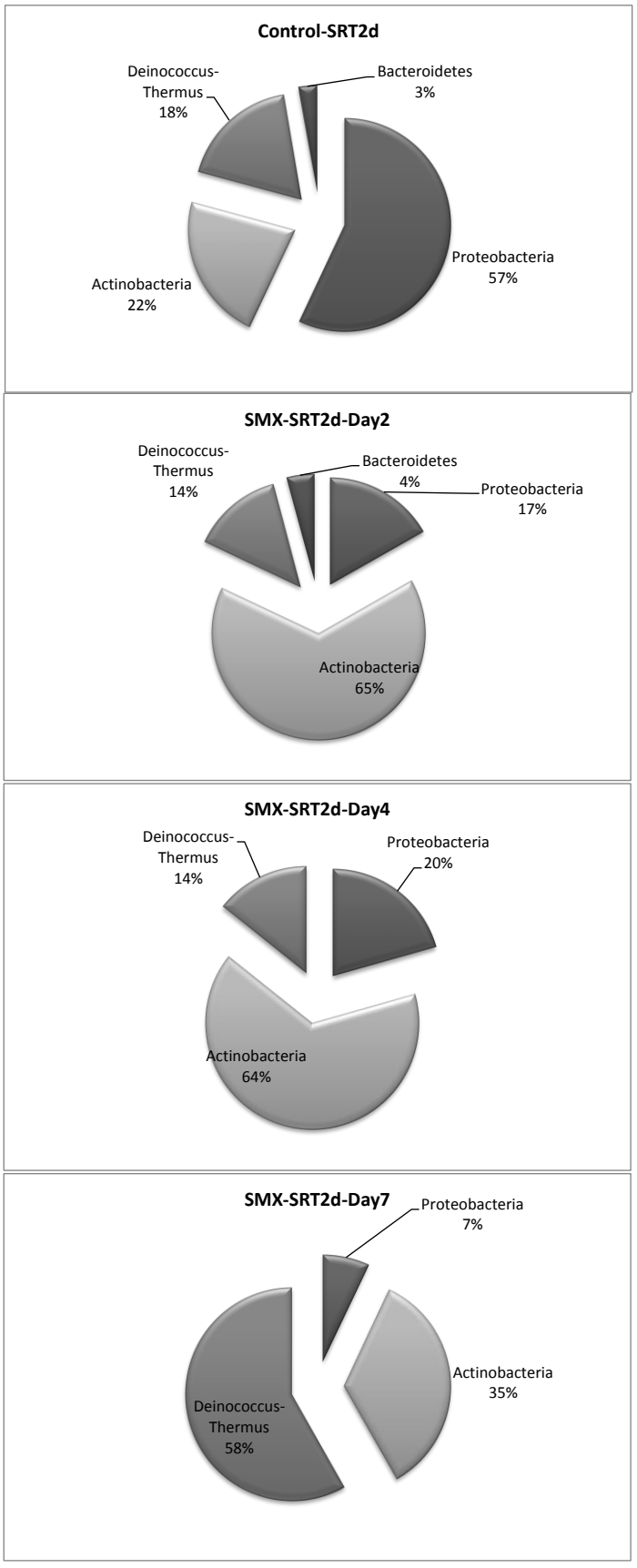

Figure 5.83: Bacterial community structures at phylum level for SMX (SRT2d) exposure.

RDP library comparison showed that phyla *Proteobacteria* and *Bacteriodetes* decreased significantly in time, whereas phylum *Deinococcus-Thermus* increased significantly. However, phylum *Actinobacteria,* showed first significant increase followed by significant decrease, resulting still significantly higher than that of C-2 sample on the 7th day of treatment (Figure 5.84).

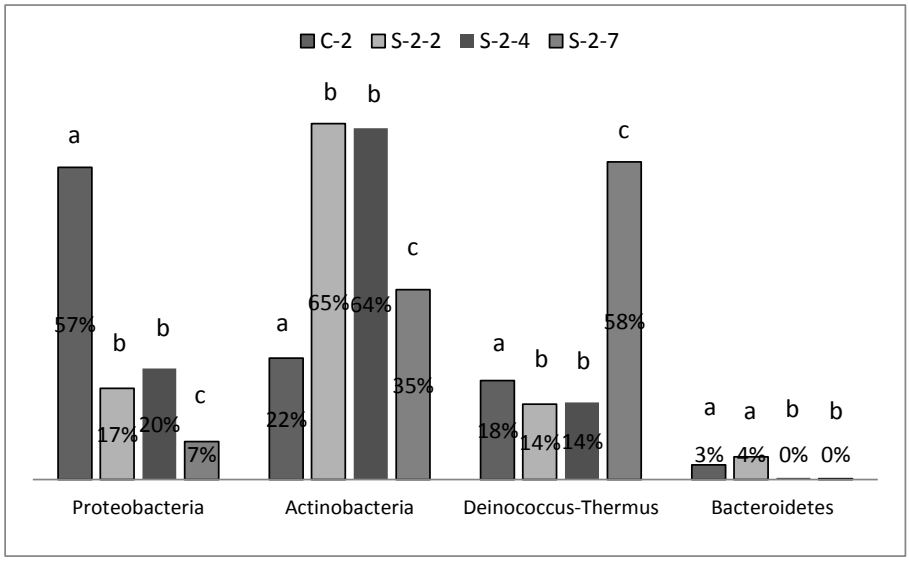

Figure 5.84: Significant changes in dominant phyla in the system (SMX SRT2d) (*Bars with same letters are not significantly different).

On the 2nd day of exposure information obtained from rarefaction curves showed that at both levels the richness of the systems is either equal or higher than that of C-2 sample, but always higher than S-2-4 and S-2-7 samples. Rarefaction curve at species (3%) level shows that the richness of S-2-4 and S-2-7 samples are lower than C-2 sample, also that S-2-4 has higher richness than S-2-7. However on the phyla (20%) level S-2-7 exerts increased richness (Figure 5.85).

Both non-parametric richness estimators, ACE and Chao1 suggest that the richness of the population changes with time. ACE estimator suggests that on species (3%) level the system shows first a decrease in richness followed by a constant increase. However, on the phyla level it slightly increases with time (Table 5.27). Information obtained from evenness calculated from Shannon's diversity index shows that all four samples exhibited dominant community structures at both levels. Further analysis also revealed that the dominance shifted with the effect of SMX (SRT2d) treatment.

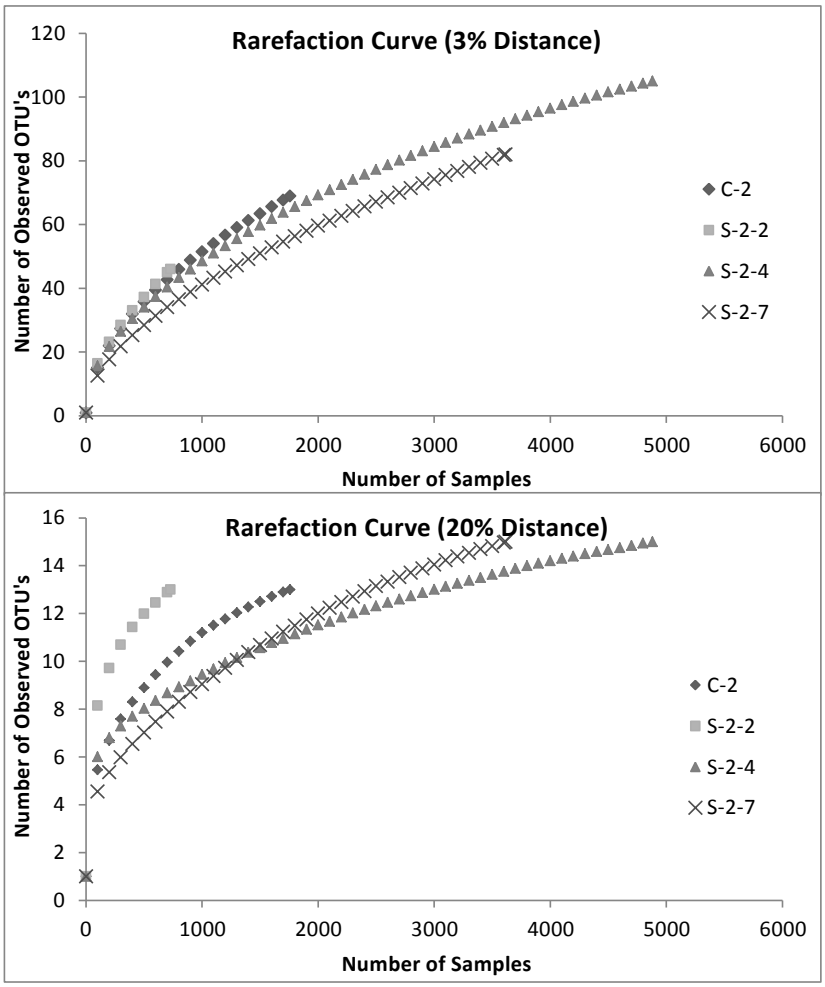

Figure 5.85: Rarefaction curves for SMX (SRT2d) samples at 3% and 20% distances.

Table 5.27: Statistical indicators for SMX feeding (SRT 2d).

	3%				20%			
	C-2	S-2-2	S-2-4	S-2-7	C-2	S-2-2	S-2-4	S-2-7
Number of OTUs	69	46	105	82	13	13	15	15
Singleton	36	27	43	44	3	3	4	5
Chao1 estimate of OTUs richness	139	222	143	168	14	16	17	18
ACE estimate of OTU richness	196	176	201	294	15	15	18	19
Shannon index of diversity (H)	1.9	2.1	2.2	2	1.2	1.3	1.2	0.96
Evenness	0.45	0.56	0.47	0.37	0.45	0.49	0.43	0.35
Good's estimator of coverage (%)	47.83	41.30	59.05	46.34	76.92	76.92	73.33	66.67

According to the information presented in Figure 5.86, at species level C-2 contains 70 species level OTUs, S-2-2 contains 46 species level OTUs, S-2-4 contains 105 species level OTUs, and S-2-7 contains 82 species level OTUs. However groups C-2

and S-2-2 exclusively share 2 species level OTUs, but 14 and 32 species level OTUs belong to each of these groups alone, respectively. Moreover C-2 and S-2-2 both exclusively share 4 species level OTUs with S-2-4, whereas S-2-4 has 48 unshared species level OTUs. S-2-7 has 33 unshared species level OTUs, but shares 3, 2 and 17 species level OTUs exclusively with C-2, S-2-2 and S-2-4, respectively. C-2, S-2-2 and S-2-7 don't have common species level OTUs. However C-2, S-2-2 and S-2-4 have 5 species level OTUs in common, whereas C-2, S-2-4 and S-2-7 have 8 species level OTUs in common. S-2-2, S-2-4 and S-2-7 share 4 species level OTUs. Additionally, 15 species level OTUs are shared by all four groups (total shared richness). Finally total richness of all groups together is calculated as 191 species level OTUs.

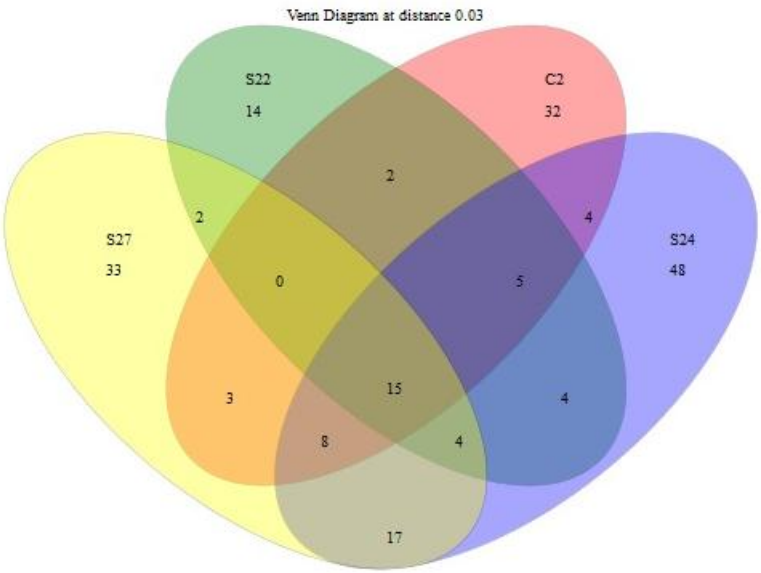

Figure 5.86: Venn diagram of SMX (SRT2d) samples at 0.03 distance.

At phylum level however, C-2 contains 12 phyla, S-2-2 contains 13 phylum level OTUs, S-2-4 contains 15 phylum level OTUs and S-2-7, 15 phylum level OTUs. However group C-2 does not share phylum level OTUs with S-2-2 and S-2-4. However three groups have 2 phyla in common and S-2-2 exclusively shares 1 phylum with S-2-4. C-2, S-2-2 and S-2-4 have 2, 1 and 3 unshared phylum level OTUs, respectively. S-2-7 has 3 unshared OTUs, but shares 1 phylum level OTU exclusively with each of the C-2, S-2-2 and S-2-4 groups. C-2, S-2-2 and S-2-7 don't have common phylum level OTUs. However C-2, S-2-2 and S-2-7 have 1 phylum level OTU in common, likewise S-2-2, S-2-4 and S-2-7 also have 1 phylum level OTU in common. Additionally, 6 phylum level OTUs are common in all four groups

(total shared richness). Finally total richness of all groups together is calculated as 24 phylum level OTUs (Figure 5.87).

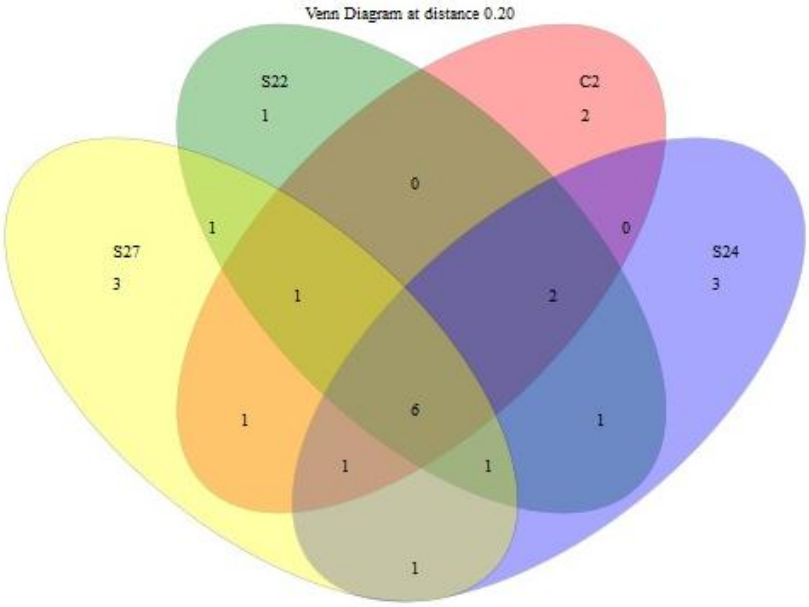

Figure 5.87: Venn diagram of SMX (SRT2d) samples at 0.20 distance.

Results of statistical analysis revealed the significantly affected OTUs under chronic inhibited conditions (Table 5.28). It can be seen that OTU#3 (*Paracoccus sp;* 47%), OTU#1 (*Deinococcus sp;* 18%) and OTU#4 (*Arthrobacter sp;* 10%) were most abundant in the control sample. However, after 2 days of SMX (SRT2d) treatment, OTU#3 decreased significantly, whereas OTU#4 increased up to 39%. Although the abundance of OTU#4 decreased after the 4th day of exposure, the statistical analysis suggests that this decrease was insignificant ($q>0.05$). After 7th day of exposure, OTU#1 (*Deinococcus sp*) increased significantly and became the most abundant specie in this system.

Table 5.28: Significant changes in the activated sludge population (SMX SRT2d) (species level OTUs are named by numbers).

Phylum	Nearest Classified Neighbour	OTU Number	C-2 (%)	S-2-2 (%)	S-2-4 (%)	S-2-7 (%)
Deinococcus-Thermus	*Deinococcus*	1	18	14	14	58
Proteobacteria	*Paracoccus*	3	47	2	6	4
Actinobacteria	*Arthrobacter*	4	10	39	36	14

Literature indicates that the dominant bacteria in both SMX systems were resistant to the antibiotic. It has been demonstrated that the genes coding for sulfonamide resistance, especially the *sul*1 gene, are located on mobile genetic elements, like

plasmids, transposons and integrons, which are responsible for dissemination of the resistance markers. One of the three known resistance genes to SMX, *sul1*, is known to be coded on the class1 integron (Liebert et al., 1999, Carattoli, 2001, Byrne-Bailey et al., 2009, Baran et al, 2011). Moreover, *Arthrobacter* sp., previously detected in activated sludge systems (Li et al., 2010), found abundantly in both SMX inhibited reactors, was shown to be positive for all three *sul* genes (Hoa et al., 2008). Additionally, *Deinococcus* sp, also previously isolated from activated sludge by Im et al. (2008), has become one of the most abundant species in SRT 2d system. It has also been determined that aerobic bacterium *Deinococcus maricopensis* DSM21211 (Accession Nr: CP002454) possesses a gene coding for multidrug resistance protein of the major facilitator superfamily (MFS), which either accumulate nutrients by a cation-substrate symport mechanism or efflux substances like antibiotics (Ward et al., 2001). OTUs closely related to these members were also detected in studied SMX system.

In the SRT 2d system, most of the OTUs from phyla *Proteobacteria* decreased, such as most abundant OTU#3 (*Paracoccus* sp) in control sample, which was not detected after 2 days, leading to the overgrowth of *Actinobacteria*. However *Deinococcus* sp became dominant after 7 days and outcompeted *Actinobacteria.*

The information gathered in the literature on the resistance of dominant species in the SMX reactors is also coinciding with the data obtained from the resistance gene studies conducted on the reactors. Resistance gene studies revealed that the SMX systems possess both sulfonamide resistance genes *sul*1 and *sul*2, however does not contain *sul*3.

5.8.2.3 Effect of tetracycline on the community structure

Sludge age 10 d system

At the phylum level constant exposure to TET (SRT10d) shows a shift in community structure with time. After 10 days of exposure the percentages of present phyla change from 59%, 24% and 15% in the C-10 reactor to 19%, 76%, 4% for *Actinobacteria, Proteobacteria,* and *Bacteroidetes* phyla, respectively, whereas phylum *TM7* disappeared completely. At the end of the treatment (30^{th} day) the distribution in phyla became *Actinobacteria* (55%), *Proteobacteria* (39%) and

Bacteroidetes (6%). Figure 5.88 shows the change in distribution of phyla with increasing time of exposure to TET (SRT10d).

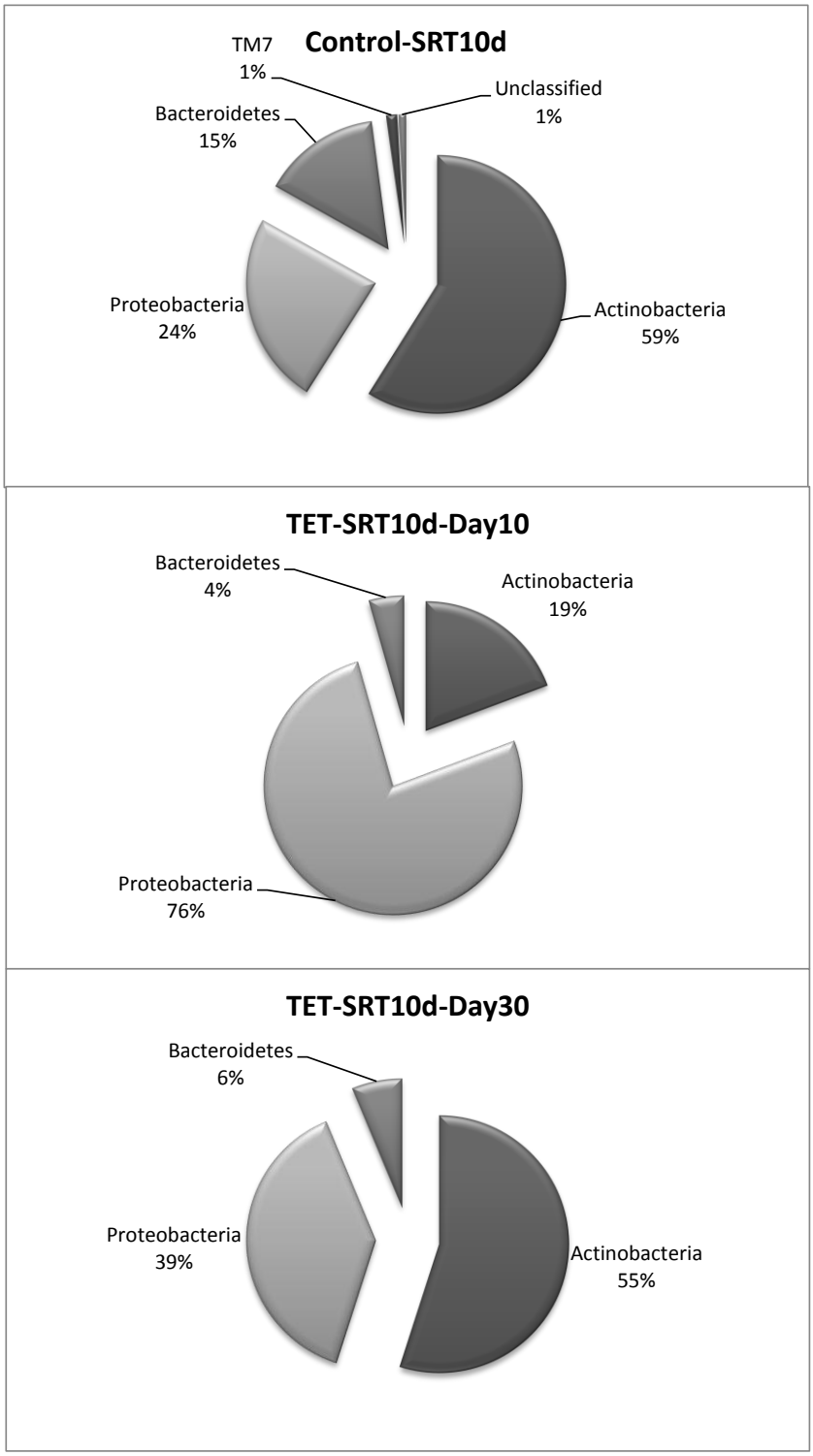

Figure 5.88: Distribution of phyla in TET (SRT10d) system.

RDP library comparison showed the significant changes in the phylum level among the group. The comparison revealed that *Actinobacteria*, significantly decreased by 10th day, later increasing gradually and reaching 55% abundance at end of treatment

by the 30th day. *Proteobacteria* showed significant increase at the end of treatment, whereas phylum *Bacteroidetes* significantly decreased throughout the treatment (Figure 5.89).

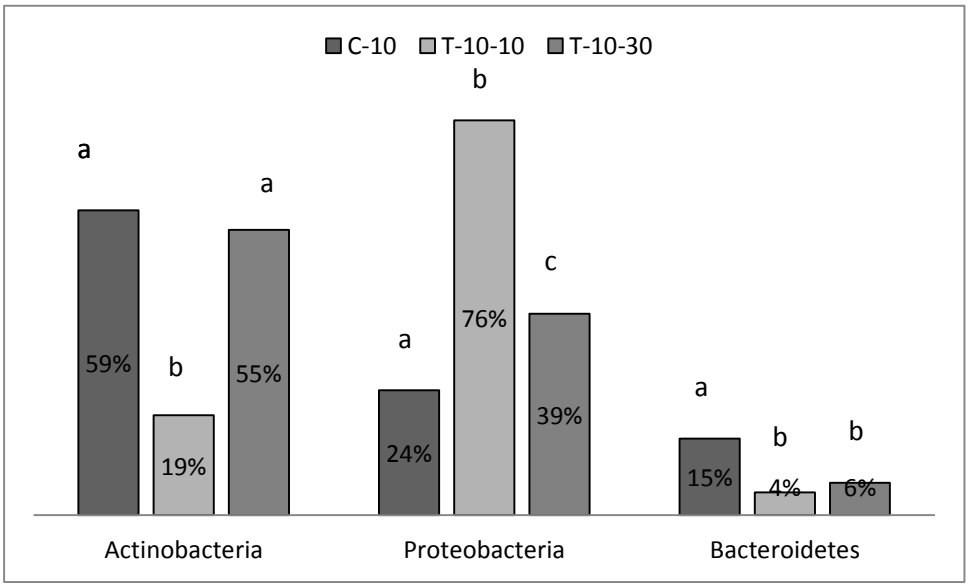

Figure 5.89: Significant changes in dominant phyla in the system (TET SRT10d) (*Bars with same letters are not significantly different).

Rarefaction curves showed that on the 10th and 30th days of exposure the richness was lower than the C-10 sample on all levels. At species (3%) level lowest richness is observed in the T-10-30 sample. Additionally, on phyla (20%) level T-10-10 sample showed higher richness than that of T-10-30, however lower than C-10 sample. This information suggests that the richness in the activated sludge community decreases under the influence of TET antibiotic (Figure 5.90).

Both ACE and Chao1 estimators of richness suggest that the richness of the population decreases with time (Table 5.29). Information obtained from evenness shows that all four samples exhibited dominant community structures at all levels. Further analysis also revealed that the dominance shifted with the effect of TET (SRT10d) treatment.

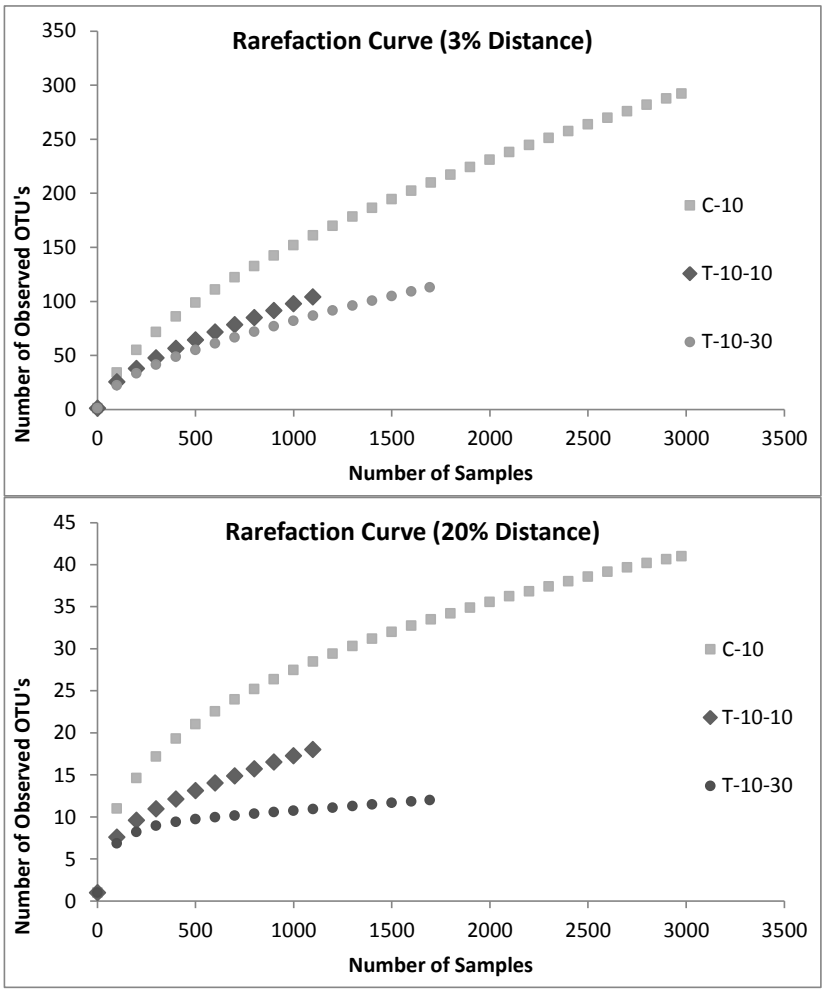

Figure 5.90: Rarefaction curves for TET (SRT10d) samples at 3% and 20% distances.

Table 5.29: Statistical indicators for TET feeding (SRT 10d).

	3%			20%		
	C-10	T-10-10	T-10-30	C-10	T-10-10	T-10-30
Number of OTUs	288	104	113	42	18	12
Singleton	168	67	69	14	8	3
Chao1 estimate of OTUs richness	647.7	350	260	55.0	32	15
ACE estimate of OTU richness	1019.5	657	642	66.9	60	21
Shannon index of diversity (H)	3.0	2.9	2.3	1.6	1.6	1.25
Evenness	0.53	0.61	0.49	0.41	0.54	0.50
Good's estimator of coverage (%)	41.67	35.58	38.94	66.67	55.56	75.00

According to the information presented in Figure 5.91, at species level C-10 contains 288 species level OTUs, T-10-10 contains 104 species level OTUs and T-10-30 contains 113 species level OTUs. However groups C-10 and T-10-10 exclusively

share 20 species level OTUs, but 238 and 44 species level OTUs belong to each of these groups alone, respectively. Moreover C-10 exclusively shares 14 species level OTUs with T-10-30. T-10-30 has 59 species level OTUs unique for itself. Additionally, 20 species level OTUs are shared by all groups (total shared richness). Finally total richness of all four groups together is calculated as 415 species level OTUs.

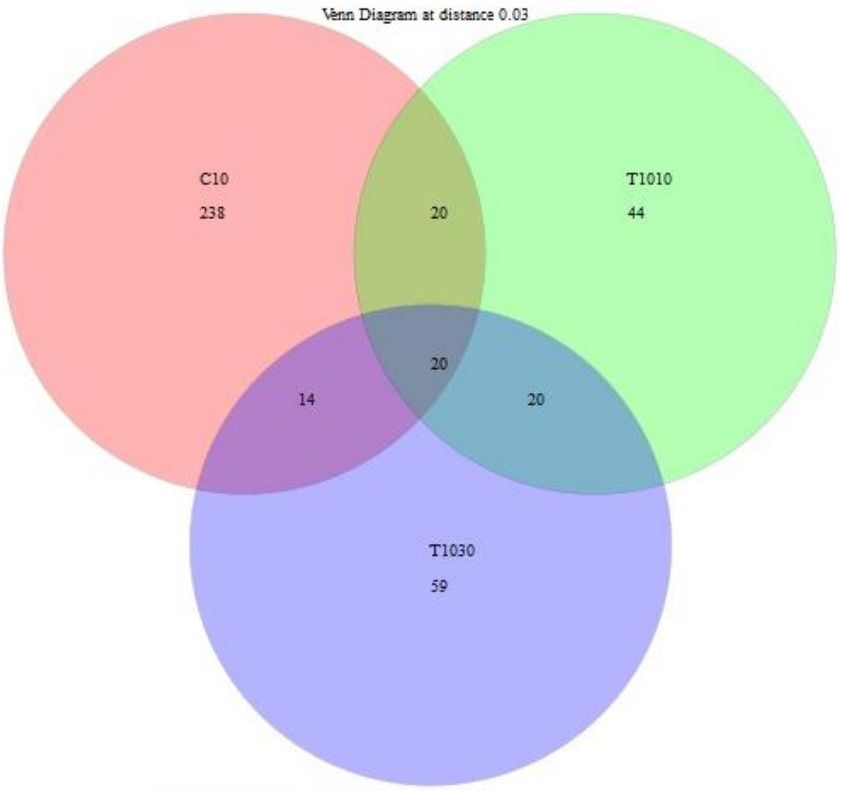

Figure 5.91: Venn diagram of TET (SRT10d) samples at 0.03 distance.

At phylum level however, C-10 contains 42 phylum level OTUs, T-10-10 contains 18 phylum level OTUs and T-10-30 contains 12 phylum level OTUs. However groups C-10 and T-10-10 share 4 phylum level OTUs, but 28 and 4 phylum level OTUs belong to each of these groups alone, respectively. Moreover C-10 shares 2 phylum level OTU exclusively with T-10-30. T-10-30 has no phylum level OTUs unique for itself. Moreover T-10-10 and T-10-30 exclusively share 3 phylum level OTUs. Additionally, 7 phylum level OTUs are shared by all four groups (total shared richness). Finally total richness of all four groups together is calculated as 48 (Figure 5.92).

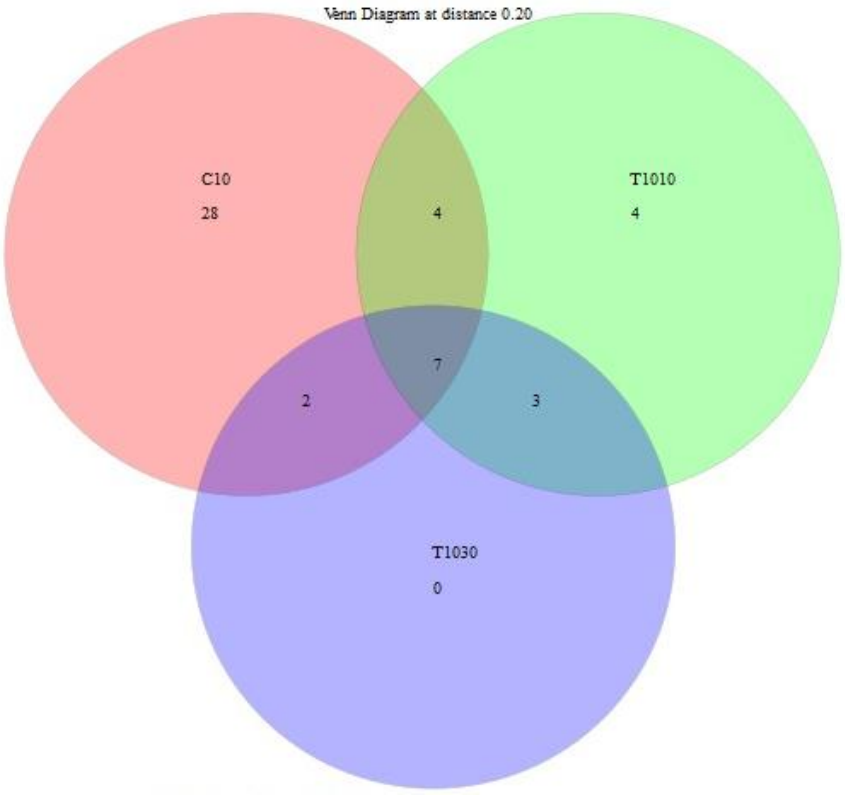

Figure 5.92: Venn diagram of TET (SRT10d) samples at 0.20 distance.

Results of statistical analysis revealed the significantly affected OTUs under chronic inhibited conditions (Table 5.30). It can be seen that OTU#6 (unclassified *Actinobacteria sp;* 45%) and OTU#45 (unclassified *Sphingobacteria* sp of *Bacteriodetes;* 10%) were most abundant species in the control sample (C-10). However, after 10 days of TET (SRT10d) treatment OTU#6 decreased significantly to 4%, whereas OTU#10 disappeared completely ($p<0.05$, $q>0.05$). However OTU#160 (*Acidovorax* sp), and OTU#336 (*Stenotrophomas* sp) increase significantly and become most abundant species in the system by the 10^{th} day of exposure. By the 30^{th} day it can be seen that OTU#55 of *Arthrobacter* sp increased gradually in time and became one of the most abundant species in the system together with OTU#24 of *Diaphorobacter* sp of *Betaproteobacteria* class.

Table 5.30: Significant changes in the activated sludge population (TET SRT10d) (species level OTUs are named by numbers).

Phylum	Nearest Classified Neighbour	OTU Number	C-10 (%)	T-10-10 (%)	T-10-30 (%)
Actinobacteria	*Unclassified Intrasporangiaceae*	6	45	4	1
Bacteroidetes	*Unclassified Chitinophagaceae*	10	10	0	0
Proteobacteria	*Diaphorobacter*	24	0	2	21
Actinobacteria	*Arthrobacter*	55	1	6	44
Proteobacteria	*Acidovorax*	160	0	18	2
Proteobacteria	*Stenotrophomonas*	336	0	24	1

Sludge age 2 d system

At the phylum level constant exposure to TET (SRT 2d) shows a significant shift in community structure. After 2 days of exposure the percentages of present phyla change from 57%, 22%, 18% and 3% in the C-2 reactor to 40%, 53%, 3% and 4% for *Proteobacteria*, *Actinobacteria*, *Deinococcus-Thermus* and *Bacteroidetes* phyla, respectively, where dominance shifts from *Proteobacteria* to *Actinobacteria* phylum. Results obtained at the 4^{th} day show that the *Deinococcus-Thermus* phylum disappears. Moreover, at the end of treatment the community structure on phyla level becomes *Proteobacteria* (60%), *Actinobacteria* (34%) and *Bacteroidetes* (5%). These results show that *Actinobacteria* although fit to survive under constant exposure of TET, are not capable of sustaining dominance in a fast growing system. Figure 5.93 shows the change in distribution of phyla with increasing time of exposure to TET (SRT 2d). Results revealed that the members of phylum *Deinococcus-Thermus* disappeared, *Proteobacteria* and *Actinobacteria* increased significantly.

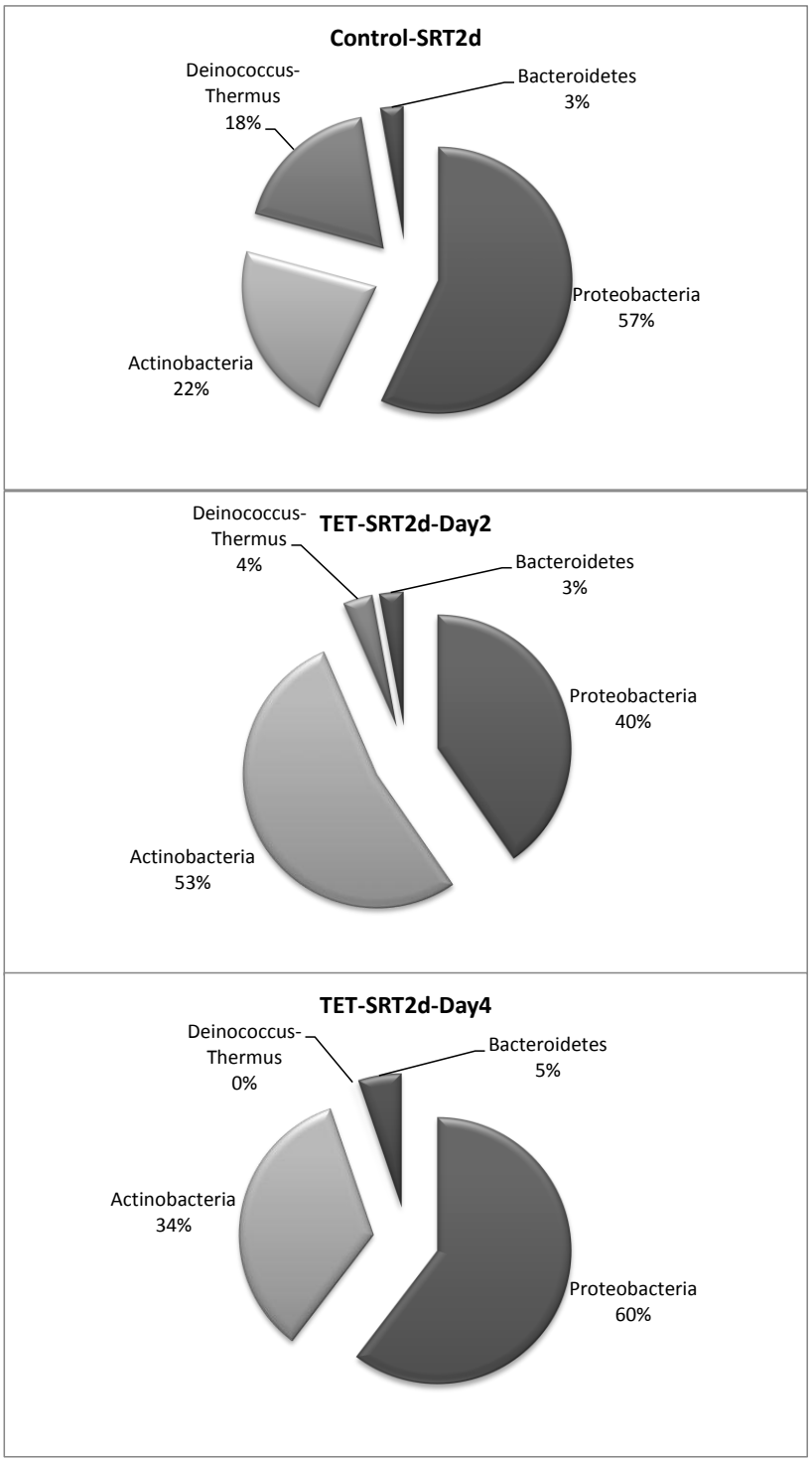

Figure 5.93: Bacterial community structures at phylum level for TET (SRT2d) exposure.

RDP library comparison showed that phylum *Deinococcus-Thermus* decreased significantly in time, whereas phylum *Actinobacteria* showed fluctuating dominance, which resulted in increased abundance compared to the C-2 sample on the 4th day of treatment. However, due to competence with *Actinobacteria* phylum, *Proetobacteria,* showed first significant decrease followed by significant increase,

resulting in insignificant increase in abundance compared to the C-2 sample on the 4th day of treatment with TET (SRT2d) (Figure 5.94).

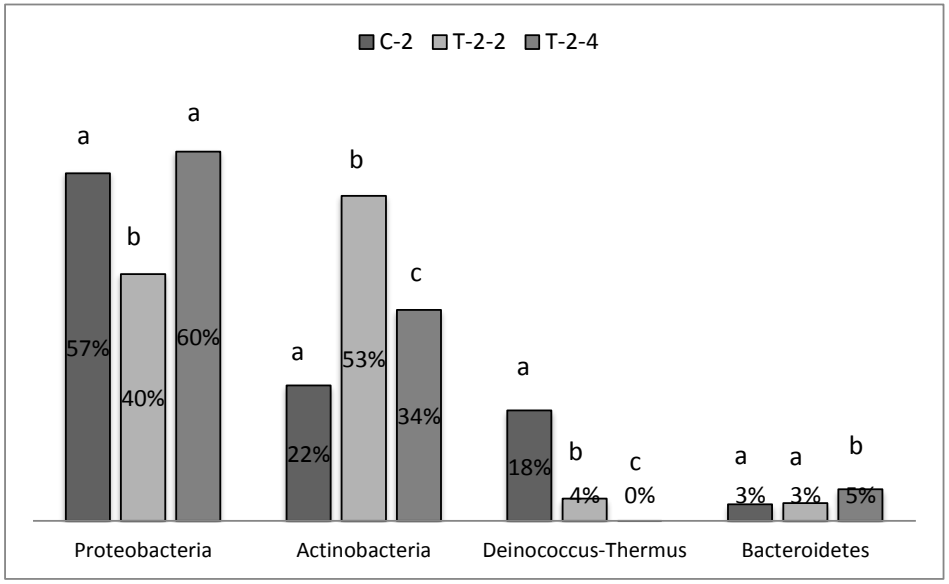

Figure 5.94: Significant changes in dominant phyla in the system (TET SRT2d) (*Bars with same letters are not significantly different).

Rarefaction curves showed that on the 2nd and 4th days of exposure the richness is lower than the C-2 sample on both species (3%) and phylum (20%) levels. Additionally, the figures always show a decreasing trend in richness of the systems at both levels under the influence of TET antibiotic (Figure 5.95). Both non-parametric richness estimators ACE and Chao1 estimators of richness suggest that the richness of the population changes with time. The information suggests that on both levels richness fluctuates. It increases on the 2nd day and decreases again on the 4th day. However on both levels the system reaches higher richness after 4th day of exposure compared to the C-2 sample. The fluctuation in richness might be attributed to the increase and decrease in the abundance of *Actinobacteria* species in the system (Table 5.31). Information obtained from evenness calculated from Shannon's index of diversity shows that all four samples exhibited dominant community structures at all levels. Further analysis also revealed that the dominance shifted with the effect of TET (SRT2d) treatment.

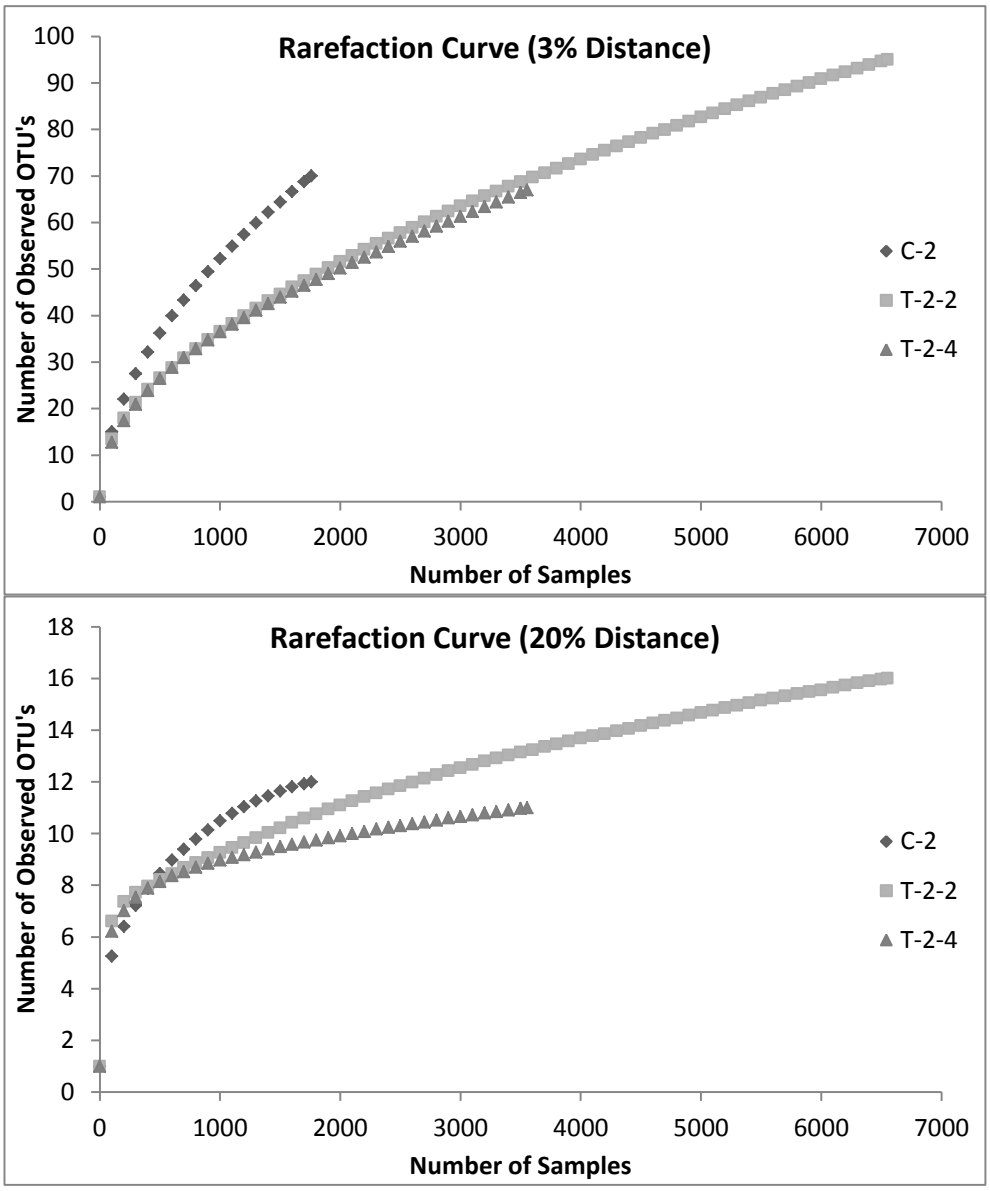

Figure 5.95: Rarefaction curves for TET(SRT2d) samples at 3% and 20% distances.

Table 5.31: Statistical indicators for TET feeding (SRT 2d).

	3%			20%		
	C-2	T-2-2	T-2-4	C-2	T-2-2	T-2-4
Number of OTUs	70	95	67	12	16	11
Singleton	36	49	35	2	5	2
Chao1 estimate of OTUs richness	133.0	185.5	166.2	12.3	19.3	11.5
ACE estimate of OTU richness	187.9	291.3	228.7	13.2	22.6	16.5
Shannon index of diversity (H)	1.9	1.9	2.0	1.1	1.2	1.5
Evenness	0.45	0.41	0.48	0.46	0.42	0.63
Good's estimator of coverage (%)	48.57	48.42	47.76	83.33	68.75	81.82

Venn diagrams in show that at species level C-2 contains 70 species level OTUs, T-2-2 contains 95 species level OTUs and T-2-4 contains 67 species level OTUs. However groups C-2 and T-2-2 exclusively share 9 species level OTUs, but 45 and

48 species level OTUs belong to each of these groups alone, respectively. Moreover C-2 and T-2-2 share 3 and 25 species level OTUs exclusively with T-2-4, respectively, whereas T-2-4 has 26 unshared species level OTUs. Additionally, 13 species level OTUs are common in all three groups (total shared richness). Finally total richness of all groups together is calculated as 169 species level OTUs. (Figure 5.96)

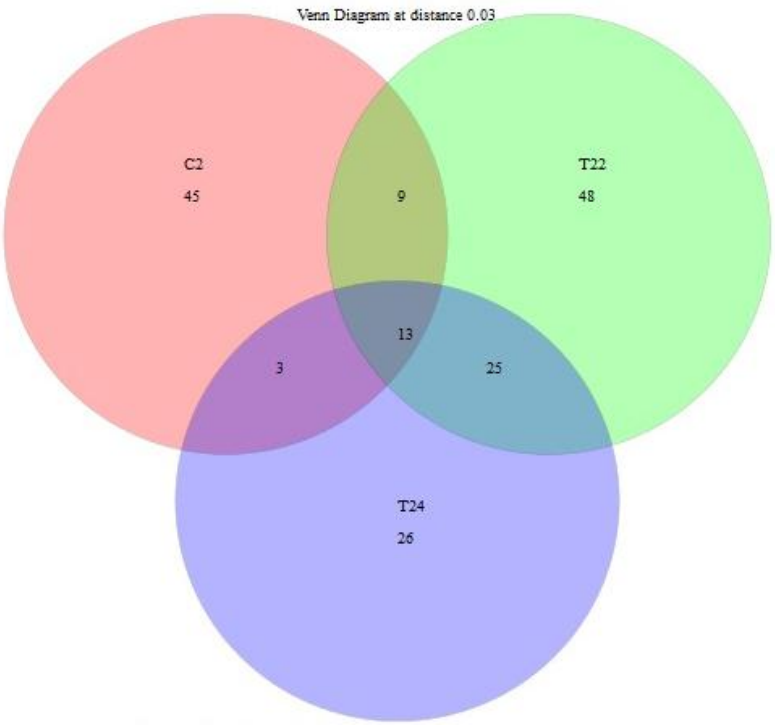

Figure 5.96: Venn diagram of TET (SRT2d) samples at 0.03 distance.

At phylum level however, C-2 contains 12 phylum level OTUs, T-2-2 contains 16 phylum level OTUs and T-2-4 contains 11 phylum level OTUs. However group C-2 exclusively shares 1 phylum level OTU with T-2-2 and 2 phylum level OTUs with T-2-4. T-2-2 and T-2-4 exclusively have 4 phylum level OTUs in common. C-2 and T-2-2 have 4 and 6 unshared phylum level OTUs, respectively, whereas T-2-4 does not have unshared phylum level OTUs. Additionally, 5 phylum level OTUs are common in all three groups (total shared richness). Finally total richness of all groups together is calculated as 22 phylum level OTUs (Figure 5.97).

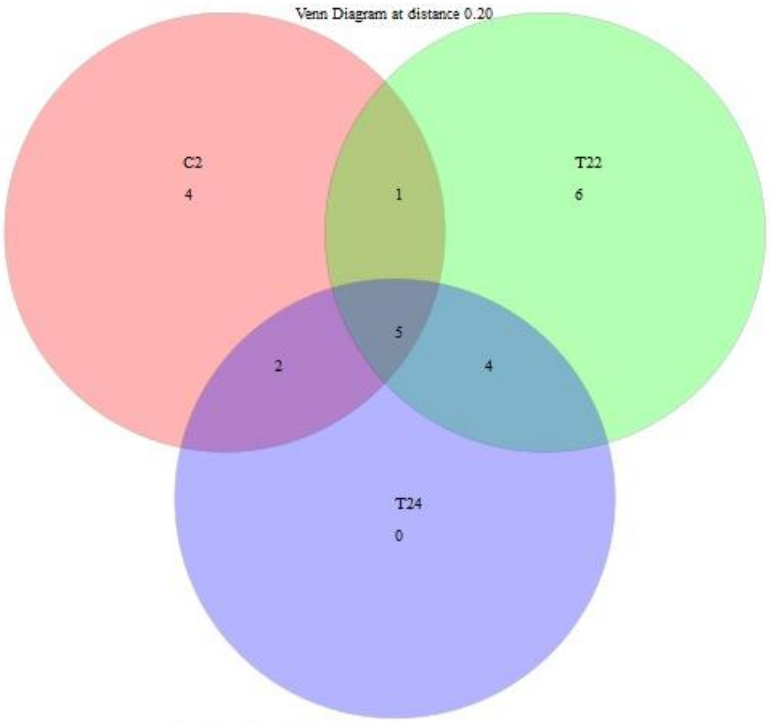

Figure 5.97: Venn diagram of TET (SRT2d) samples at 0.20 distance.

Results of statistical analysis revealed the significantly affected OTUs under chronic inhibited conditions (Table 5.32). It can be seen that OTU#3 (*Paracoccus* sp; 47%), OTU#1 (*Deinococcus* sp; 18%) and OTU#4 (*Arthrobacter* sp; 10%) were most abundant species in the control sample (C-2). However, after 4 days of TET (SRT2d) treatment OTU#3 disappeared, whereas OTU#4 increased up to 30%. Abundances of OTUs 88 (*Comamonas* sp) and 135 (*Stenotrophomonas* sp), non-abundant species in C-2 sample increased drastically and reached abundances of 21%, 12% and 20% by the 4th day of exposure, respectively.

Table 5.32: Significant changes in the activated sludge population (TET SRT2d).

Phylum	Nearest Classified Neighbour	OTU Number	C-2 (%)	T-2-2 (%)	T-2-4 (%)
Deinococcus-Thermus	*Deinococcus*	1	18	4	0
Proteobacteria	*Paracoccus*	3	47	0	0
Actinobacteria	*Arthrobacter*	4	10	37	30
Proteobacteria	*Comamonas*	88	0	32	21
Proteobacteria	*Stenotrophomonas*	135	0	2	20

Constant exposure to TET significantly affected the bacterial community structures of both activated sludge biomasses. However in general it can be seen that in the SRT 10d system *Proteobacteria* are outcompeted by the members of *Actinobacteria*

phylum, even though possessing resistance properties to TET. However, as is in the control systems *Actinobacteria* are outcompeted by *Proteobacteria* in the SRT2d system even under the influence of TET. It can be seen that in both systems *Arthrobacter* sp and *Stenotrophomonas* sp are present in significant percentages. Information in the literature suggests that species of both genera are resistant to tetracycline. *Arthrobacter* sp and *Stenotrophomonas* sp are shown to possess *tet*K, *tet*L and *tet*W and *tet*A, *tet*B, *tet*C, *tet*D, *tet*H, *tet*K, *tet*L, *tet*J, *tet*M, *tet*O, *tet*S, *tet*T, *tet*W, *tet*33 and *tet*(AP) resistance genes, respectively (Li et al., 2010). This information indicates that both *Arthrobacter* sp and *Stenotrophomonas* sp are possessing genes encoding both efflux and ribosomal protection protein genes.

Other genus found in TET inhibited SRT 2d system was *Comamonas* sp that was also shown to possess tetracycline resistance genes. Previously isolated from activated sludge systems (Boon et al., 2000) *Comamonas testosteroni* was shown to habour genes encoding both efflux (*tet*L) and ribosomal protection proteins (*tet*O) (Li et al., 2010).

Acidovorax sp, known to harbor transpoases and previously detected in activated sludge systems (Parsley et al., 2010), is being outcompeted by *Actinobacteria* species in the TET SRT10d reactor. However it is also known to possess resistance genes. *Acidovorax* sp strain MUL2G8 was shown to possess a gene encoding a TetR family transcriptional repressor (Ramos et al., 2005). Additionally, *Diaphorobacter* sp were observed in the TET SRT10d system, which was formerly isolated from activated sludge systems (Khan and Hiraishi, 2002). *Diaphorobacter* sp strain TPSY (Accession Nr: B9MG39), also known as *Acidovorax ebreus* (strain TPSY), was also shown to have a transcriptional regulator of TetR family. Tet repressor (TetR) protein controls the expression of the tetracycline resistance genes (Levy, 1984; 1988; Hinrichs et al., 1994; Kisker et al., 1995; Yamaguchi et al., 1990a; 1990b; Saenger et al., 2000; Ramos et al., 2005). This regulation takes place in the transcription level and is induced by $[Mg\text{-}TET]^+$ complex. Due to higher affinity of $[Mg\text{-}TET]^+$ complex to TetR, the complex binds with TetR, which was bound to the operators preventing the expression of resistance proteins, thereby initiating resistance expression in the cell, and TET is removed before the inhibition of protein synthesis begins (Hillen et al., 1983; Takhashi et al, 1986; Hinrichs et al., 1994).

These findings also coincide with the information gained from qualitative evaluation of antibiotic resistance genes in the TET reactor. The microbial population in both TET reactors was shown to possess *tet*A, *tet*C, *tet*G and *tet*O genes. However, *tet*E gene was only detected in the SRT2d reactor, whereas *tet*M only in SRT10d reactor.

5.8.2.4 Effect of erythromycin on the community structure

Sludge age 10 d system

10 days of exposure to ERY showed significant effect on the community structure. The abundances of present phyla change from 59%, 24%, 15% and 1% in the C-10 reactor to 13%, 61%, 24% and 2% for *Actinobacteria, Proteobacteria, Bacteroidetes* and *TM7* phyla, respectively. Figure 5.99 shows the change in distribution of different phyla with increasing time of exposure to ERY. Results revealed that the amount of members of phylum *Actinobacteria* decrease drastically. However, on the other hand amount of bacteria in phylum *Proteobacteria* increases substantially.

RDP library showed that *Actinobacteria, Proteobacteria* and *Bacteroidetes* phyla are significant (Figure 5.98). Drastic changes in the phylum level provided the information that the effect of ERY on the activated sludge biomass can even be seen on the 20% distance. Therefore changes in the genus and species levels were taken into consideration.

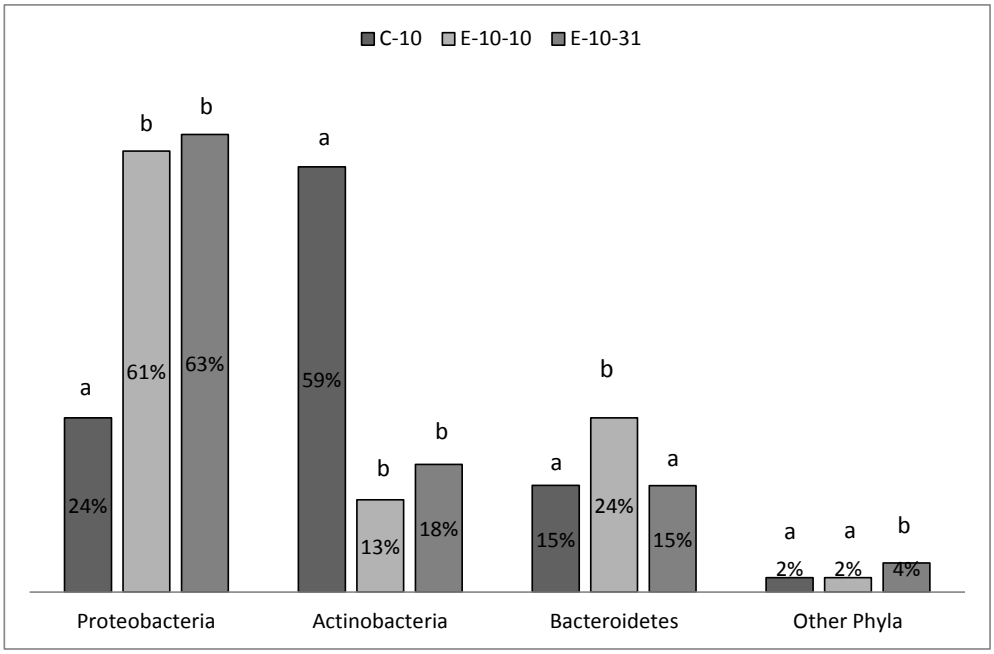

Figure 5.98: Significant changes in dominant phyla in the system (*Bars with same letters are not significantly different).

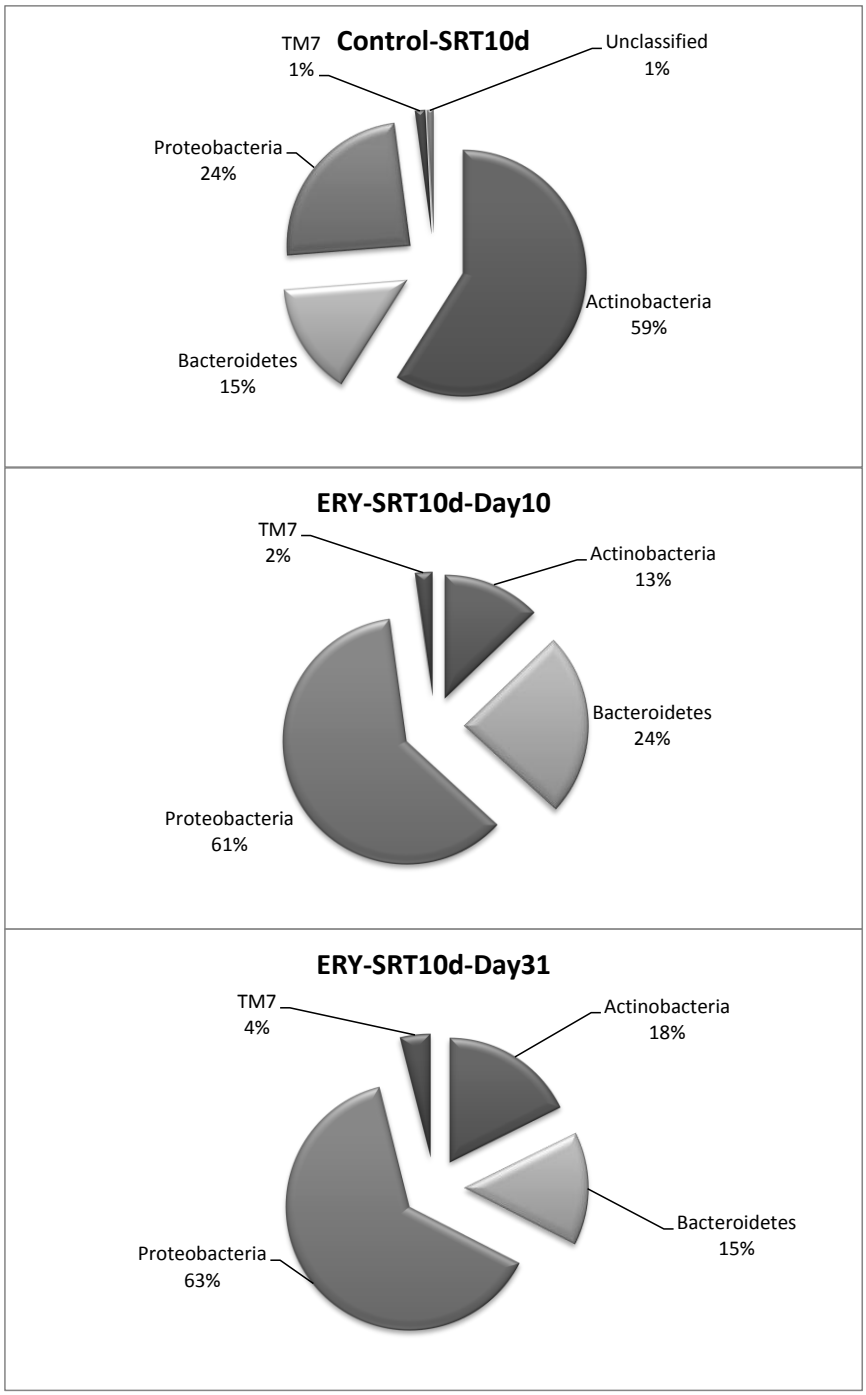

Figure 5.99: Bacterial community structures at phylum level (ERY SRT10d).

The information obtained from rarefaction curves on phylum (20%) level show that both inhibited samples have substantially lower richness compared to control sample (Figure 5.100). Rarefaction curves at species level show that the richness of the C-10 sample is higher than the ERY inhibited samples (E-10-10 and E-10-31). However it shows that E-10-31 has higher richness than that of E-10-10 at these distances.

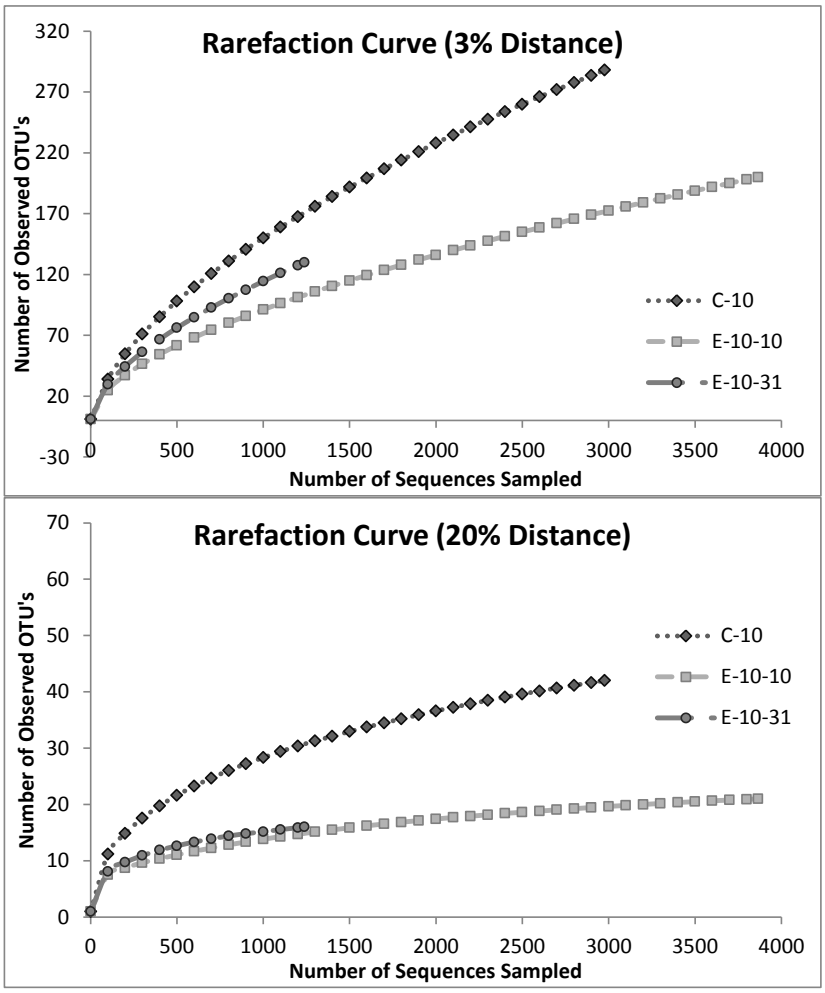

Figure 5.100: Rarefaction curves for ERY(SRT 10d) at 3% and 20% distances.

Both ACE and Chao1 estimators of richness suggest that the richness of the population decreases with time, therefore E-10-10 is estimated to have higher richness than E-10-31 at all distances (Table 5.33). Information obtained from evenness calculated from Shannon's index of diversity shows that all three samples exhibited dominant community structures at all levels. Further analysis also revealed that the dominance shifted with the effect of ERY treatment.

Table 5.33: Statistical indicators for ERY feeding (SRT 10d).

	3%			20%		
	C-10	E-10-10	E-10-31	C-10	E-10-10	E-10-31
Number of OTUs	288	200	130	42	21	16
Singleton	168	117	79	14	5	4
Chao1 estimate of OTUs richness	647.7	451.3	410.1	55.0	23.0	19.0
ACE estimate of OTU richness	1019.5	806.5	509.1	66.9	24.9	18.9
Shannon index of diversity (H)	3.0	2.8	3.1	1.6	1.4	1.6
Evenness	0.53	0.53	0.65	0.41	0.46	0.58
Good's estimator of coverage (%)	41.67	41.50	39.23	66.67	76.19	75.00

Venn diagrams shown in Figure 5.101 reveal that at species level C-10 contains 288 species level OTUs, E-10-10 contains 200 species level OTUs and E-10-31 contains 130 species level OTUs. However groups C-10 and E-10-10 exclusively share 29 species level OTUs, but 222 and 105 species level OTUs belong to each of these groups alone, respectively. Moreover C-10 and E-10-10 share 6 and 35 species level OTUs exclusively with E-10-31, whereas E-10-31 has 58 unshared species level OTUs. Additionally, 31 species level OTUs are shared by all three groups (total shared richness). Finally total richness of all groups together is calculated as 486 species level OTUs.

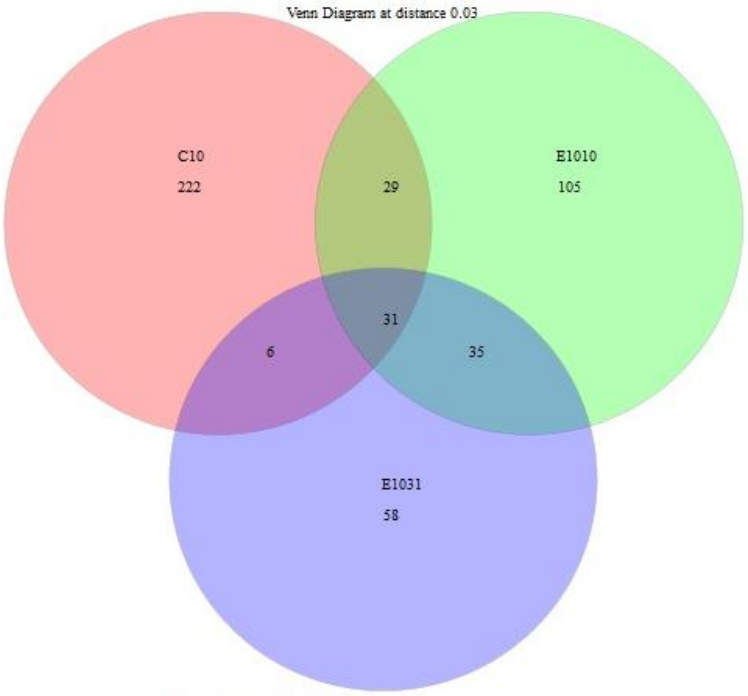

Figure 5.101: Venn diagram of ERY (SRT 10d) treatment samples at 0.03 distance.

At phylum level however, C-10 contains 42 species, E-10-10 contains 21 phyla level OTUs and E-10-31 contains 16 phyla level OTUs. However groups C-10 and E-10-10 exclusively share 8 phyla level OTUs, but 23 and 1 phyla level OTUs belong to each of these groups alone, respectively. Moreover C-10 and E-10-10 share 2 and 3 phyla level OTUs exclusively with E-10-31, whereas E-10-31 has 2 unshared phyla level OTUs. Additionally, 9 phyla level OTUs are shared by all groups (total shared richness). Finally total richness of all groups together is calculated as 48 OTUs (Figure 5.102).

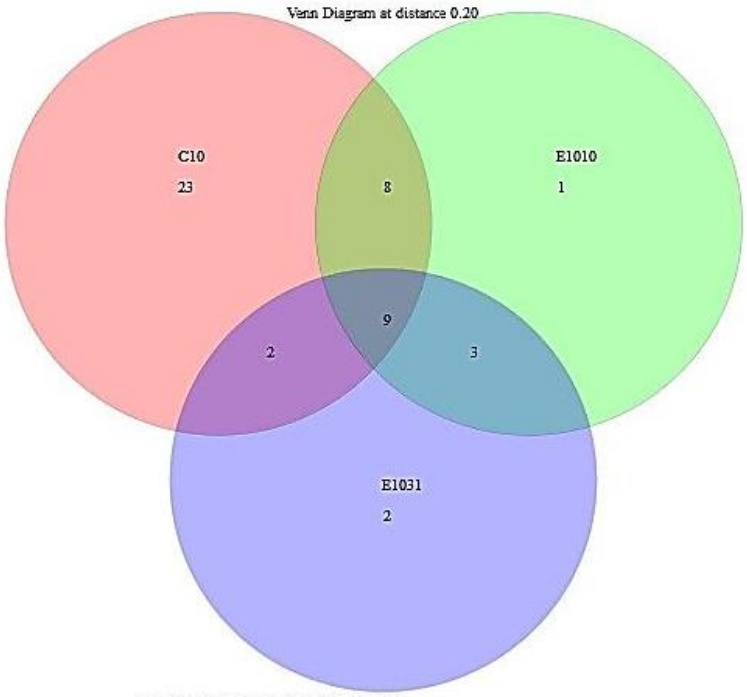

Figure 5.102: Venn diagram of ERY (SRT10d) treatment samples at 0.20 distance.

Results of statistical analysis revealed the significantly affected OTUs under chronic inhibited conditions. It can be seen that OTU#6 (unclassified *Intrasporangiaceae;* 45%) and OTU#10 (unclassified *Chitinophagaceae;* 10%) were most abundant species in the control sample (C-10). However, after 10 days of ERY treatment these species disappeared and did not reappear throughout the whole treatment. Moreover, later in the treatment with ERY the microbial population shows further changes, that is bacteria that are very low abundant in the control sample increase significantly. OTUs of genera *Comamonas* (30%) and *Acidovorax* (16%) become significantly abundant in the system after 10 days. Additionally, these species continue to be present in the system dominantly until the end of the treatment after 31 days (Table 5.34).

Table 5.34: Significant changes in the activated sludge population (ERY SRT10d).

Phylum	Nearest Classified Neighbour	OTU Number	C-10 (%)	E-10-10 (%)	E-10-31 (%)
Actinobacteria	*Unclassified Intrasporangiaceae*	6	45	1	0
Bacteroidetes	*Unclassified Chitinophagaceae*	10	10	0	0
Proteobacteria	*Acidovorax*	157	0	16	17
Proteobacteria	*Comamonas*	293	0	30	19

Sludge age 2 d system

At the phylum level constant exposure to ERY (SRT 2d) shows a significant shift in community structure. Figure 5.103 shows the change in distribution of phyla with increasing time of exposure to ERY (SRT 2d).

After 3 days of exposure the percentages of present phyla change from 57%, 22%, 18% and 3% in the C-2 reactor to 33%, 48%, 0% and 17% for *Proteobacteria, Actinobacteria, Deinococcus-Thermus* and *Bacteroidetes* phyla, respectively, where dominance shifts from *Proteobacteria* to *Actinobacteria* phylum. Results obtained at the 3rd day show that the *Deinococcus-Thermus* phylum disappears. Moreover, at the end of treatment the community structure on phyla level becomes *Proteobacteria* (49%), *Actinobacteria* (18%), *TM7* (23%) and *Bacteroidetes* (9%), where abundance of *TM7* increased drastically. These results show that *Actinobacteria* and *Bacteroidetes* although fit to survive under constant exposure of ERY, are not capable of sustaining dominance in a fast growing system, which is also confirmed by the structural differences between SRT 10d and SRT 2d control reactors. Results revealed that the members of phylum *Deinococcus-Thermus* disappeared and members of phylum *TM7* increased significantly.

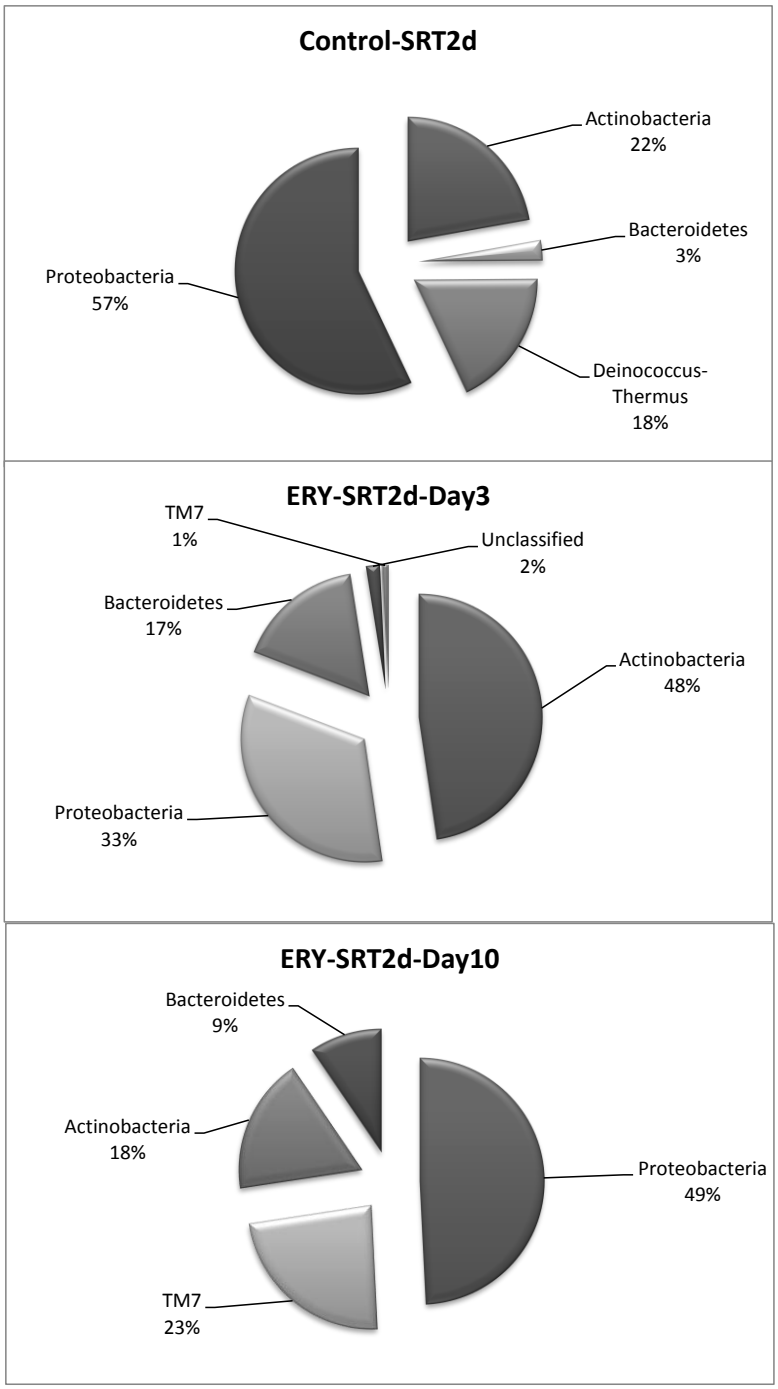

Figure 5.103: Bacterial community structures at phylum level (ERY SRT2d).

RDP library comparison on the phylum level showed that phylum *Deinococcus-Thermus* disappeared, whereas phylum *Actinobacteria* showed fluctuating dominance, which resulted in decreased abundance compared to the C-2 sample on the 10th day of treatment. However, due to competence with *Actinobacteria* phylum, *Proetobacteria,* showed first significant decrease followed by significant increase, resulting in increase in abundance compared to the C-2 sample on the 10th day of treatment with ERY. Additionally, phylum *Bacteroidetes* also showed a fluctuating

abundance profile ending with significant increase in abundance and phylum *TM7* increased in abundance and became one of the most abundant phyla in the system after 10 days of ERY treatment (SRT2d) (Figure 5.104).

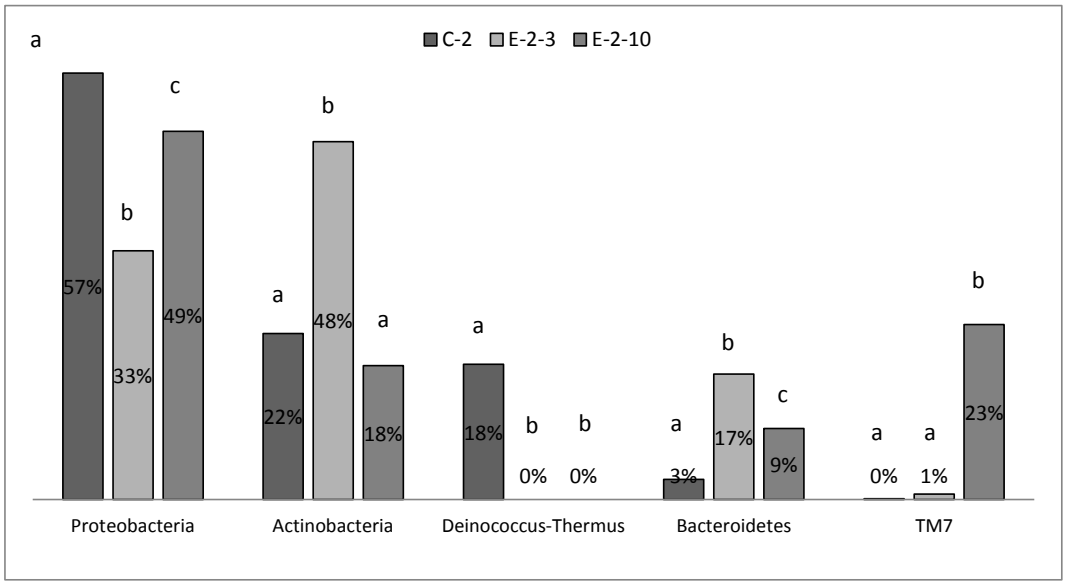

Figure 5.104: Significant changes in dominant phyla in the system (*Bars with same letters are not significantly different).

Rarefaction curves at species (3%) level show that on the 3rd and 10th days of exposures richness was higher than C-2 sample. However on the phyla (20%) level C-2 sample shows higher richness than both ERY inhibited samples (Figure 5.105). Moreover, both ACE and Chao1 estimators of richness suggest that the richness of the population changes with time. The information suggests that on all levels richness fluctuates. It increases on the 3rd day and decreases again on the 10th day. The fluctuation in richness might be attributed to the increase followed by a decrease in the abundance of *Actinobacteria* and *Bacteriodetes* species in the system (Table 5.35). Information obtained from evenness calculated from Shannon's index of diversity shows that all four samples exhibited dominant community structures at all levels. Further analysis also revealed that the dominance shifted with the effect of ERY (SRT2d) treatment.

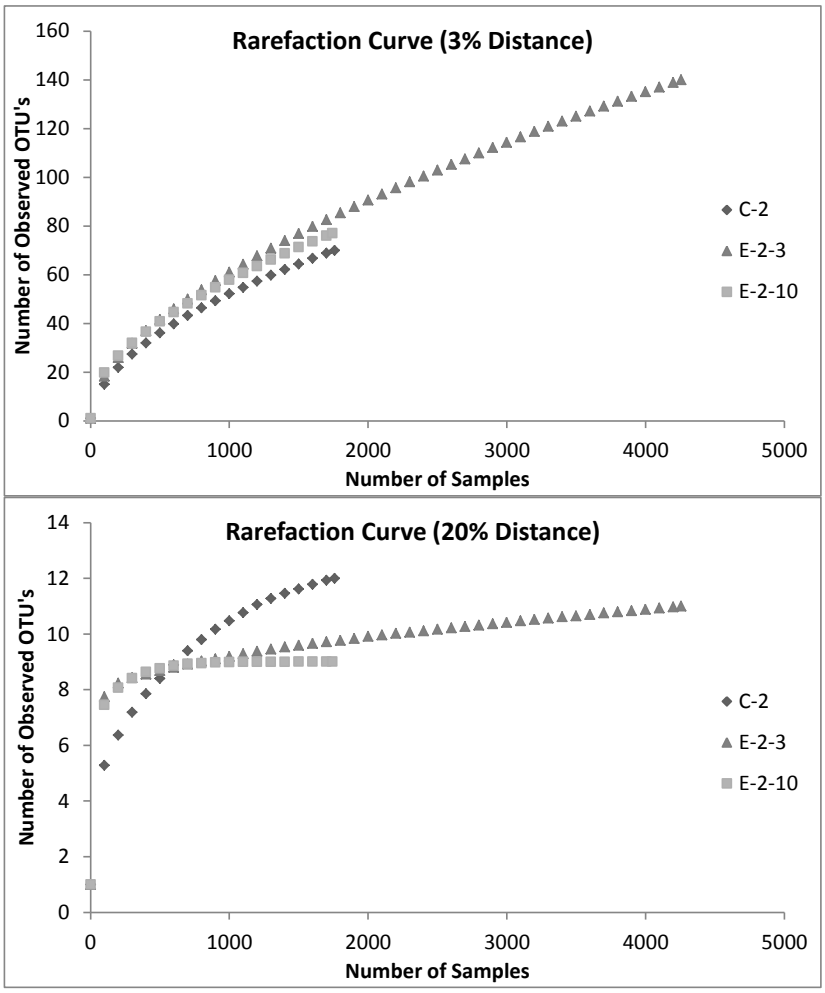

Figure 5.105: Rarefaction curves at 3% and 20% distances (ERY SRT2d).

Table 5.35: Statistical indicators for ERY feeding (SRT 2d).

	3%			20%		
	C-2	E-2-3	E-2-10	C-2	E-2-3	E-2-10
Number of OTUs	70	140	77	12	11	9
Singleton	36	80	40	2	2	0
Chao1 estimate of OTUs richness	133.0	298.0	163.7	12.3	12.0	9.0
ACE estimate of OTU richness	187.9	538.5	152.7	13.2	18.7	9.0
Shannon index of diversity (H)	1.9	2.4	2.6	1.1	1.5	1.7
Evenness	0.45	0.48	0.59	0.46	0.64	0.77
Good's estimator of coverage (%)	48.57	42.86	48.05	83.33	81.82	100.00

According to the information on shared species level OTUs (Figure 5.106), at species level C-2 contains 70 species level OTUs, E-2-3 contains 140 species level OTUs and E-2-10 contains 77 species level OTUs. However groups C-2 and E-2-3 exclusively share 7 species level OTUs, but 52 and 91 species level OTUs belong to each of these groups alone, respectively. Moreover C-2 and E-2-3 share 1 and 32 species level OTUs exclusively with E-2-10, respectively, whereas E-2-10 has 34 unshared species level OTUs. Additionally, 10 species level OTUs are shared by all

three groups (total shared richness). Finally total richness of all groups together is calculated as 227.

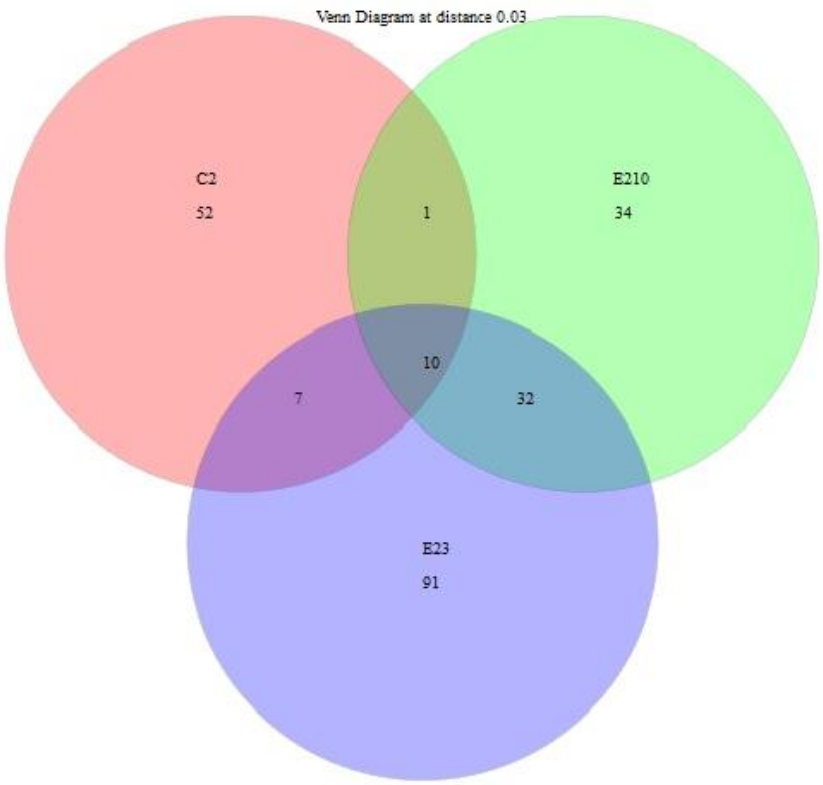

Figure 5.106: Venn diagram of ERY treatment samples at 0.03 distance (SRT2d).

At phylum level however, C-2 contains 12 phylum level OTUs, E-2-3 contains 11 phylum level OTUs and E-2-10 contains 9 phylum level OTUs. However group C-2 does not have any common phylum level OTUs with E-2-3 and E-2-10. E-2-3 and E-2-10 exclusively share 2 phylum level OTUs. C-2 and E-2-3 have 5 and 2 unshared phylum level OTUs, respectively, whereas E-2-10 has no unshared phylum level OTUs. Additionally, 7 phylum level OTUs are common in all three groups (total shared richness). Finally total richness of all groups together is calculated as 16 phylum level OTUs (Figure 5.107).

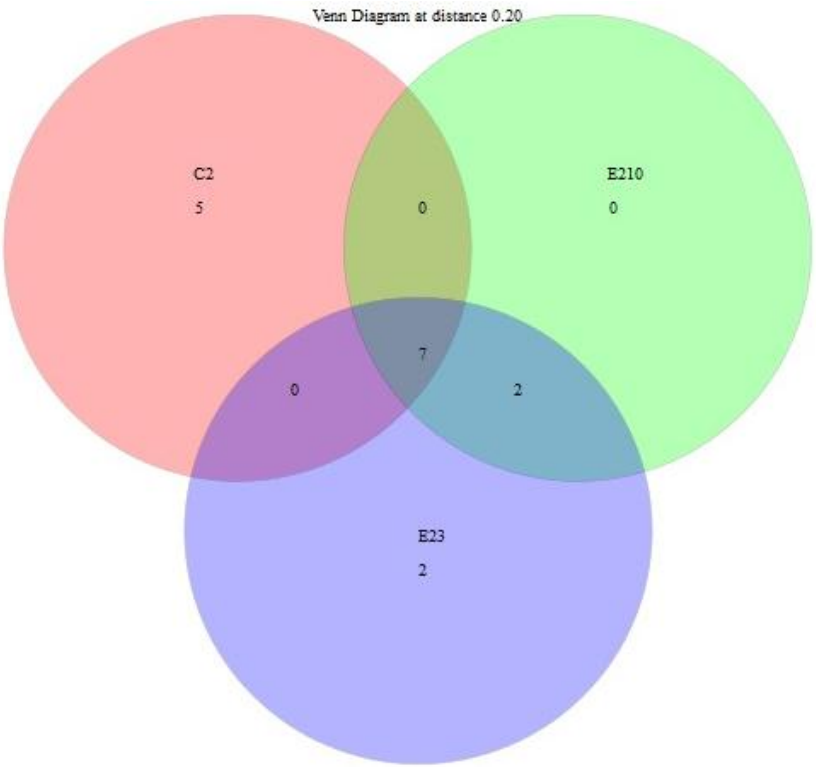

Figure 5.107: Venn diagram of ERY treatment samples at 0.20 distance (SRT2d).

Results of statistical analysis revealed the significantly affected OTUs under chronic inhibited conditions. It can be seen that OTU#3 (*Paracoccus* sp; 47%), OTU#1 (*Deinococcus* sp; 18%) and OTU#4 (*Arthrobacter* sp; 10%) were most abundant species in the control sample (C-2). However, after 3 days of ERY (SRT2d) treatment OTUs #1 and #3 disappeared, whereas OTU#4 increased up to 34%. However OTU#4 could not sustain its abundance due to the fast nature of the SRT 2d system and its abundance decreased to 5% by the 10th day of exposure. Additionally, on the 3rd day OTU#76 (*Comamonas* sp; 20%) showed increased abundance. Moreover OTU#83 (unclassified member of *TM7* phylum) reached 23% abundance on the 10th day of exposure, relatively (Table 5.36).

Table 5.36: Significant changes in the activated sludge population (ERY SRT2d).

Phylum	Nearest Classified Neighbour	OTU Number	C-2 (%)	E-2-3 (%)	E-2-10 (%)
Deinococcus-Thermus	*Deinococcus*	1	18	0	0
Proteobacteria	*Paracoccus*	3	47	0	0
Actinobacteria	*Arthrobacter*	4	10	34	5
Proteobacteria	*Comamonas*	76	0	20	20
TM7	*Unclassified TM7*	83	0	0	23

At the phylum level it can be seen that on the first days of exposure to ERY *Proteobacteria* sp were dominated by the phylum *Actinobacteria*, which then due to their low growth rates became less abundant in the system.

Literature indicated that the bacteria surviving under constant exposure to erythromycin are resistant to the antibiotic substance. *Comamonas sp.*, one of the most abundant *Proteobacterial* genera in the system after 10 and 31 days of exposure in the SRT10d and also after 3 and 10 days of exposure in the SRT2d system, have been studied and Xiong et al. (2011) showed that *Comamonas testosteroni S44* has a macrolide specific efflux-protein (*mac*(A) – Accession Nr: D8D8L7) and an erythromycin resistance ATP-binding protein (*msr*(A) – Accession Nr: D8D8F4).

Second most abundant bacterial genera in the SRT 10d system after treatment were shown to be *Acidovorax sp.* Among this bacterial genus *Acidovorax avenae*, also known to harbor transposase (Parsley et al., 2010), has been shown to be resistant to erythromycin by Oliveira et al. (2007).

Moreover, as was explained by Roberts (2008), most of the macrolide resistance genes are linked with other genes on portable elements found in bacteria. Among these linkage of *tet*O and *mef*(A) and linkage of *ere*(A) and *mph*(A) with class 1 integron has been shown (Roberts, 2008). *Arthrobacter* spp, detected in the SRT 2d system, was also shown to harbor integrons, showing that members of this genus may be resistant to erythromycin through *ere*(A) or *mph*(A) gene linked to the class 1 integron they possess. *Arthrobacter* sp however became less abundant due to their slower nature in the SRT2d system. Additionally, no information was available on the resistance of bacteria belonging to *TM7* phylum to erythromycin, which was 23% abundant at the end of the treatment in the SRT2d system.

Finally, sudden disappearance of *Deinococcus-Thermus* phylum under the pressure of ERY can be explained by the sensitivity of *Deinococcus* sp to antibiotics with protein synthesis inhibition properties, like erythromycin (Hawiger and Jeljaszewicz, 1967; Slade and Radman, 2011).

Resistance gene analysis has been done on both systems. *erm*(A), *erm*(B), *erm*(C), *msr*(A) and *mph*(A) genes were amplified in ERY samples. However only positive results were obtained from *mph*(A) gene. Sequence similarity search has been done using the *msr*(A) primer used for PCR amplifications and no hits were obtained,

indicating primers used were not specific enough to detect erythromycin resistant *Comamonas* sp, detected in both ERY inhibited systems, habouring *msr*(A) gene.

6. CONCLUSIONS AND FUTURE RECOMMENDATIONS

Main aim of this study was to determine the effects of antibiotics on the biodegradation characteristics of activated sludge systems. For this purpose three model antibiotic substances; sulfamethoxazole, tetracycline and erythromycin, were selected and acute and chronic effects on an activated sludge system acclimated on synthetic domestic wastewater were investigated. Model simulations were completed and microbial population dynamics were investigated. Detailed response profile of activated sludge biomass to antibiotic substances has been established.

Most important result obtained from this study was that the antibiotic substances have the property to bind the substrate. These substances have the capability to inhibit the substrate biodegradation pathway at any point of the pathway and cause the system to survive on less amount of substrate. Kinetic evaluation of the data obtained provided unique information on the effects of antibiotics on the substrate degradation properties of activated sludge biomass under acute and chronic pressure of antibiotics. The study revealed that antibiotic substances mainly increase the half saturation constant of the substrate (K_S), making it less available to biomass, and inhibit hydrolysis of either S_H or X_S. Moreover, it has been demonstrated that acute and chronic additions of antibiotics increase endogenous decay (b_H) levels of the microbial biomass significantly.

Moreover, information obtained from resistance and pyrosequencing studies showed that the community structure changes under chronic exposure to antibiotics, where only resistant bacteria can survive. Pyrosequencing studies showed serious population shifts in all three microbial communities. Additionally, the study enlightened the effect of sludge age on the bacterial community structure both with and without the effect of antibiotics. Results obtained showed that *Actinobacteria* as slow growing organisms do not have the capacity to dominate a fast growing system with the sludge age of 2days, instead *Proteobacteria* dominate the system. However in sludge age 10 day system, where *Actinobacteria* are not washed out, they were

shown to be dominant. However under the effect of erythromycin at sludge age 10 day system the dominance shifts from *Actinobacteria* to *Proteobacteria*, due to resistant strains present in the system, where *Comamonas* sp OTU#293 becomes the most abundant organism. At sludge age 2 day system an unclassified organism of candidate phylum *TM7* (OTU#83) becomes dominant, where without the pressure of erythromycin phylum *Proteobacteria* was dominant. However in both tetracycline systems the dominant phylum does not shift, since in 10day system *Actinobacteria* and in 2 day system *Proteobacteria* continue to dominate. On the other hand in the 2 day tetracycline system phylum *Deinococcus-Thermus* disappeares, whereas OTU#1, a member of *Deinococcus-Thermus* phylum becomes one of the most abundant species in the sulfamethoxazole 2 day system. In sulfamethoxazole 2 day system *Proteobacteria* decreases drastically, where *Deinococcus-Thermus* phylum increases substantially. However, in the 10 day sulfamethoxazole system *Bacteroidetes* decrease drastically. In both systems together with both tetracycline systems *Arthrobacter* spp were dominant that are OTU#2, OTU#55 and OTU#4 in sulfamethoxazole 10 day, tetracycline 10 day and 2 day systems, respectively.

Finally, it is recommended that future studies on antibiotics should include determination of ways to remove antibiotics via biological treatment systems. For instance, bacteria able to degrade antibiotic substances can be detected by stable isotope probing and characterized. Moreover model simulation studies on the removal antibiotics might enlighten very important questions in this field.

REFERENCES

Agersø, Y. and Petersen, A. (2007). The tetracycline resistance determinant Tet 39 and the sulphonamide resistance gene sulII are common among resistant Acinetobacter spp. isolated from integrated fish farms in Thailand, *J. Antimicrob. Chemother.*, ***59***, 23–27.

Agersø, Y. and Sandvang, D. (2005). Class 1 Integrons and Tetracycline Resistance Genes in *Alcaligenes*, *Arthrobacter*, and *Pseudomonas* spp. Isolated from Pigsties and Manured Soil, *Appl. Environ. Microb.*, ***71***(12), 7941–7947

Akinbowale, O.L., Peng, H. and Barton, M.D. (2007). Class 1 integron mediates antibiotic resistance in Aeromonas spp. from rainbow trout farms in Australia, *Int. J. Antimicrob. Agents.*, ***29***, S113.

Alberts, B., Johnson, A., Raff, M., Roberts, K. and Walter, P. (2002). *Molecular Biology of the Cell*, 4th Edition, Garland Science, New York (ISBN: 0-8153-4072-9).

Alexy, R., Kümpel, T. and Kümmerer, K. (2004). Assessment of degradation of 18 antibiotics in the Closed Bottle Test, *Chemosphere*, ***57***, 505–512.

Alexy, R., Sommer, A., Lange, F.T. and Kümmerer, K. (2006). Local use of antibiotics and their input and fate in a small sewage treatment plant – significance of balancing and analysis on a local scale vs. nationwide scale, *Acta. Hydroch. Hydrob.*, ***34***, 587–592.

Alonso, A., Sanchez, P. and Martinez, J.L. (2001). Environmental selection of antibiotic resistance genes, *Environ. Microbiol.*, ***3***(1), 1 – 9.

Antibiotic Resistance, http://www.antibioresistance.be/, last retrieved at 27.06.2011

Antunes, P., Machado, J. and Peixe, L. (2007). Dissemination of sul3-containing elements linked to class 1 integrons with an unusual 3' conserved sequence region among Salmonella isolates. *Antimicrob. Agents. Ch.*, ***51***(4), 1545-1548.

Artan, N. and Orhon, D. (1989). The effect of reactor hydraulics on the performance of activated sludge systems – II. The formation of microbial products, *Water Res.*, ***23***(12), 1519–1525.

Auerbach, E.A., Seyfried, E.E. and McMahon, K.D. (2007). Tetracycline resistance genes in activated sludge wastewater treatment plants, *Water Res.*, **41**, 1143-1151.

Avcıoğlu, E., Orhon, D. and Sözen, S. (1998). A new method for the assessment of heterotrophic endogenous respiration rate under aerobic and anoxic conditions, *Water Sci. Technol.*, ***38***(8–9), 95–103.

Baker, G.C., Smith, J.J. and Cowan, D.A. (2003). Review and re-analysis of domain-specific 16S primers, *J. Microbiol. Meth.*, ***55***, 541– 555.

Baran, W., Adamek, E.,Ziemianska, J. and Sobczak, A. (2011). Effects of the presence of sulfonamides in the environment and their influence on human health, *J. Hazard. Mater*., ***196***, 1– 15.

Beltran, F.J., Aguinaco, A., Garcia-Araya, J.F. and Oropesa, A. (2008). Ozone and photocatalytic processes to remove the antibiotic sulfamethoxazole from water, *Water Res.*, ***42***, 3799 – 3808.

Bernard, S. and Gray, N.F. (2000). Aerobic digestion of pharmaceutical and domestic wastewater sludges at ambient temperature, *Water Res.*, ***34***(3), 725-734.

Beun, J.J., Paletta, F., van Loosdrecht, M.C.M. and Heijnen, J.J. (2000). Stoichiometry and kinetics of poly-beta-hydroxybutyrate metabolism in aerobic, slowgrowing, activated sludge cultures, *Biotechnol. Bioeng*., ***67***(4), 379–389.

Blackwood, R. K. (1985). Structure determination and total synthesis of the tetracyclines. *In* J. J. Hlavka and J. H. Boothe (Ed.), *Handbook of Experimental Pharmacology:* Vol. 78. (p. 59–136). Germany: Springer-Verlag KG, Berlin.

Boon, N., Goris, J., De Vos, P., Verstraete, W. and Top, E.M. (2000). Bioaugmentation of Activated Sludge by an Indigenous 3-Chloroaniline-Degrading *Comamonas testosteroni* Strain, I2*gfp, Appl. Environ. Microb.*, ***66***(7), 2906–2913.

Boxall, A.B.A., Fogg, L.A., Blackwell, P.A., Kay, P. and Pemberton, E.J. (2004). Veterinary medicines in the environment, *Rev. Environ. Contam. Toxicol.*, ***180***, 1–91.

Boyer, R.F. (2006). *Concepts in Biochemistry* (3rd Ed.), Wiley&Sons Inc, New Jersey.

Byrne-Bailey, K.G., Gaze, W.H., Kay, P., Boxall, A.B.A., Hawkey, P.M. and Wellington, E.M.H. (2009). Prevalence of sulfonamide resistance genes in bacterial isolates from manured agricultural soils and pig slurry in the United Kingdom, Antimicrob, *Agents. Chemother.*, ***53***, 696–702.

Carattoli, A. (2001). Importance of integrons in the diffusion of resistance, *Vet. Res.*, ***32***, 243–259.

Chen, J., Yu, Z., Michel Jr., F.C., Wittum, T. and Morrison, M. (2007). Development and application of real-time PCR assays for quantification of erm genes conferring resistance to macrolides-lincosamides-streptogramin B in livestock manure and manure management systems, *Appl. Environ. Microb.*, ***73***(14), 4407-4416.

Chopra, I. and Roberts, M. (2001). Tetracycline Antibiotics: Mode of Action, Applications, Molecular Biology, and Epidemiology of Bacterial Resistance, *Microbiol. Mol. Biol. R.*, ***65***(2), 232–260

Chopra, I., P. M. Hawkey, and M. Hinton. (1992). Tetracyclines, molecular and clinical aspects, *J. Antimicrob. Chemother.*, ***29***, 245–277.

Chrencik, J.E., Orans, J., Moore, L. B., Xue, Y., Peng, L., Collins, J.L., Wisely, G.B., Lambert, M.H., Kliewer, S.A. and Redinbo, M.R. (2005). Structural Disorder in the Complex of Human PXR and the Macrolide Antibiotic Rifampicin, *Mol. Endoc.*, ***19***(5), 1125-1134.

Chudoba, J. (1985). Quantitative estimation in COD units of refractory organic compounds produced by activated sludge microorganisms, *Water Res.*, ***19***(1), 37–43.

Cokgor, E.U., Sozen, S., Orhon, D. and Henze, M. (1998). Respirometric analysis of activated sludge behavior - I. assessment of the readily biodegradable substrate. *Water Res.*, ***32***(2), 461–475.

Conn, E.E., Stumpf, P.K., Breuning, G. and Doi, R. H. (Ed.) (1987). *Outlines of Biochemistry* (p.151-155). USA: Wiley&Sons Inc.

Dawes, E.A. (1990). Novel Microbial Polymers: An Introductory Overview. In Dawes, E.A. (Ed.), *Novel Biodegradable Microbial Polymers* (p.3-16). The Netherlands: Kluwer Academic Publishers.

Delseny, M., Han, B. and Hsing, Y.L. (2010). High throughput DNA sequencing: The new sequencing revolution, *Plant Sci.*, ***179***, 407–422.

Desai, C., Pathak, H. and Madamwar, D. (2010). Advances in molecular and "-omics" technologies to gauge microbial communities and bioremediation at xenobiotic/anthropogen contaminated sites, *Bioresource Technol.*, ***101***, 1558 – 1569.

DeSantis, T. Z., Brodie, E. L., Moberg, J. P., Zubieta, I. X., Piceno,Y. M. and Andersen, G. L. (2007). High-density universal 16S rRNA microarray analysis reveals broader diversity than typical clone library when sampling the environment, *Microbial Ecol.*, ***53***, 371–383.

Dircks, K., Beun, J.J., van Loosdrecht, M., Heijnen, J.J. and Henze, M. (2001). Glycogen metabolism in aerobic mixed cultures, *Biotechnol. Bioeng.*, ***73***(2), 85-94.

Dogruel, S., Genceli, E.A., Babuna, F.G. and Orhon, D. (2004). Ozonation of Nonbiodegradable Organics in Tannery Wastewater. *J. Environ. Sci. Heal. A,* ***39***(7), 1705 – 1715.

Doi, Y. (1990). *Microbial Polyesters*. USA: VCH Publichers, Inc. New York.

Dou, J., Liu, X. and Hu, Z. (2008). Substrate interactions during anaerobic biodegradation of BTEX by the mixed cultures under nitrate reducing conditions, *J. Hazard. Mater.*, ***158***(2-3), 264-72.

Drillia, P., Dokianakis, S.N., Fountoulakis, M.S., Kornaros, M., Stamatelatou, K. and Lyberatos, G. (2005). On the occasional biodegradation of pharmaceuticals in the activated sludge process: The example of the antibiotic Sulfamethoxazole, *J. Hazard. Mater.*, ***122***, 259–265.

Dunbar, J., Ticknor, L. O. and Kuske, C. R. (2000). Assessment of microbial diversity in four southwestern United States soils by 16S rRNA gene terminal restriction fragment analysis, *Appl. Environ. Microbiol.*, ***66***, 2943–2950.

Edwards, R.A., Rodriguez-Brito, B., Wegley, L., Haynes, M., Breitbart, M., Peterson, D.M., Saar,M.O., Alexander, S., Alexander Jr., E.C. and Rohwer, F. (2006). Using pyrosequencing to shed light on deep mine microbial ecology, *BMC Genomics*, ***7***, 57.

Eikelboom, D.H. (2002). *Process Control of Activated Sludge Plants by Microscopic Investigation.* London, UK: IWA Publishing.

Ekama, G.A., Dold, P.L. and Marais, G.V.R. (1986). Procedures for determining influent COD fractions and the maximum specific growth rate of heterotrophs in activated sludge systems, *Water Sci. Tech.*, ***18***, 91–114.

Ellis, T.G., Barbeau, D.S., Smets, B.F. and Grady, C.P.L. (1996). Respirometric technique for determination of extant kinetic parameters describing biodegradation, *Water Env. Res.*, ***68*** (5), 917–926.

Feuerpfeil, I., López-Pila, J., Schmidt, R., Schneider, E. and Szewzyk, R. (1999) Antibiotic resistant bacteria and antibiotics in the environment (Antibiotikaresistente Bakterien und Antibiotika in der Umwelt). *Bundesgesundheitsblatt*, ***42***, 37–50.

Fiebelkorn, K.R., Crawford, S.A., McElmeel, M.L. and Jorgensen J.H. (2003). Practical disk diffusion method for detection of inducible clindamycin resistance in Staphylococcus aureus and Coagu- lase-negative Staphylococci, *J. Clin. Microbiol.*, ***41***, 4740-4744.

Fuhrman, J. A. (2009). Microbial community structure and its functional implications, *Nature*, ***459***, 193–199.

Garcia-Galan, M.J., Diaz-Cruz, M.S. and Barcelo, D. (2008). Identification and determination of metabolites and degradation products of sulfonamide antibiotics, *Trends Anal. Chem.*, ***27***(11), 1008 – 1022.

Gartiser, S., Urich, E., Alexy, R. and Kümmerer K. (2007). Ultimate biodegradation and elimination of antibiotics in inherent tests, *Chemosphere*, ***67***, 604–613.

Giger, W., Alder, A.C., Golet, E.M., Kohler, H.P.E., McArdell, C.S., Molnar, E., Siegrist, H. and Suter, M.J.F. (2003). Occurrence and fate of antibiotics as trace contaminants in wastewaters, sewage sludges, and surface waters, *Chimia*, ***57***, 485–491.

Giongo, A., Crabb, D.B., Davis-Richardson, A.G., Chauliac, D., Mobberley, J.M., Gano, K.A., Mukherjee, N., Casella, G., Roesch, L.F.W., Walts, B., Riva, A., King, G. and Triplett, E.W. (2010). PANGEA: pipeline for analysis of next generation amplicons, *ISME J.*, ***4***, 852–861.

Göbel, A., McArdell, C.S., Joss, A., Siegrist, H. and Giger, W. (2007). Fate of sulfonamides, macrolides, and trimethoprim in different wastewater treatment technologies, *Sci. Total Environ.*, ***372***, 361–371.

Göbel, A., Thomsen, A., McArdell, C. S., Joss, A. and Giger, W. (2005). Occurrence and sorption behavior of sulfonamides, macrolides, and trimethoprim in activated sludge treatment, *Environ. Sci. Technol.*, ***39*** (11), 3981–3989.

Golet, E. M., Alder, A. C. and Giger, W. (2002). Environmental exposure and risk assessment of fluoroquinolone antibacterial agents in wastewater and

river water of the Glatt Valley Watershed, Switzerland, *Environ. Sci. Technol.*, ***36*** (17), 3645–3651.

Golet, E. M., Xifra, I., Siegrist, H., Alder, A. C. and Giger, W. (2003). Environmental exposure assessment of fluoroquinolone antibacterial agents from sewage to soil, *Environ. Sci. Technol.*, ***37*** (15), 3243–3249.

Guissesola, A., Baeza, J.A., Carree, J., Casas, C. and Lafuente, J. (2003). An offline respirometric procedure to determine inhibition and toxicity of biodegradable compounds in biomass from industrial WWTP, *Water Sci. Tech.*, ***48*** (11–12), 267–275.

Gujer, W., Henze, M., Mino, T. and Loosdrecht M.v. (1999). Activated Sludge Model No. 3, *Water Sci. Tech.*, ***39***(1), 183-193.

Hamady, M., Walker, J. J., Harris, J. K., Gold, N. J. and Knight, R. (2008). Error-correcting barcoded primers for pyrosequencing hundreds of samples in multiplex, *Nat. Methods*, ***5***, 235–237.

Hamscher, G., Sczesny, S., Hoper, H. and Nau, H. (2002). Determination of persistent tetracycline residues in soil fertilized with liquid manure by high-performance liquid chromatography with electrospray ionization tandem mass spectrometry, *Anal. Chem.*, ***74*** (7), 1509–1518.

Hartig, C., Storm, T. and Jekel, M. (1999). Detection and identification of sulphonamide drugs in municipal wastewater by liquid chromatography coupled with electrospray ionization tandem mass spectrometry, *J. Chromatogr. A*, ***854***, 163-173.

Harwood, V.J., Whitlock, J. and Withington, V. (2000). Classification of antibiotic resistance patterns of indicator bacteria by discriminant analysis: use in predicting the source of fecal contamination in subtropical waters, *Appl. Environ. Microbiol.*, ***66*** (9), 3698–3704.

Hawiger, J. and Jeljaszewicz, J. (1967). Antibiotic sensitivity of Micrococcus radiodurans, *Appl. Microbiol.*, ***15***, 304–306.

Hayes, J.R., Wagner, D.D., English, L.L., Carr, L.E. and Joseph, S.W. (2005). Distribution of streptogramin resistance determinants among Enterococcus faecium from a poultry production environment of the USA, *J Antimicrob Chemother*, ***55***, 123–126.

Henze, M. (2005). Modeling of Aerobic Wastewater Treatment Processes. In H.-J. Jördening and J. Winter (Ed.), *Environmental Botechnology: Concepts and Applications*, (p.121- 134). Weinheim: Wiley- VCH Verlag (ISBN: 3-527-30585-8).

Hillen, W., Gatz, C., Altschmied, L., Schollmeier, K. and Meier, I. (1983). Control of expression of the Tn10-encoded tetracycline resistance genes. Equilibrium and kinetic investigation of the regulatory reactions, *J Mol Biol.*, ***169***(3), 707–721.

Hinrichs, W., Kisker, C., Düvel, M., Müller, A., Tovar, K., Hillen, W. and Saenger, W. (1994). Structure of the Tet Repressor-Tetracycline Comples and Regulation of Antibiotic Resistance, *Science*, ***264***, 418-420.

Hirsch, R., Ternes, T., Haberer, K. and Kratz, K-L. (1999). Occurrence of antibiotics in the aquatic environment, *Sci. Total Environ.*, ***225***, 109–118.

Hoa, P.T.P, Nonaka, L., Viet, P.H. and Suzuki, S. (2008). Detection of the *sul*1, *sul*2 and *sul*3 genes in sulfonamide resistant bacteria from wastewater and shrimp ponds of North Vietnam, *Sci. Total Environ.*, ***405***, 377-384.

Hu, J.Y., Shi, J.C., Chang, H., Li, D., Yang, M. and Kamagata, Y.C. (2008). Phenotyping and genotyping of antihiotic-resistant Escherichia coli isolated from a natural river basin, *Environ. Sci. Technol.*, ***42***, 3415–3420.

Huovinen, P. (2001). Resistance to Trimethoprim-Sulfamethoxazole, *Clinical Infectious Deseases*, ***32***, 1608-1614.

Im, W.T., Jung, H.M., Ten, L.N., Kim, M.K., Bora, N., Goodfellow, M., Lim, S., Jung, J. and Lee, S.T. (2008). *Deinococcus aquaticus* sp. nov., isolated from fresh water, and *Deinococcus caeni* sp. nov., isolated from activated sludge, *Int. J. Syst. Evol. Microbiol.*, ***58***, 2348-2353.

Insel, G., Karahan Gül, Ö., Orhon, D., Vanrolleghem, P.A. and Henze, M. (2002). Important limitations in the modeling of activated sludge: biased calibration of the hydrolysis process, *Water Sci. Technol.*,***45***(12), 23–36.

Insel, G., Karahan, O., Ozdemir, S., Pala I., Katipoglu T., Ubay Cokgor E. and Orhon D. (2006). Unified Basis for the Respirometric Evaluation of Inhibition for Activated Sludge, *J. Environ. Sci. Heal. A*, ***41***, 1763–1780.

Insel, G., Orhon, D. and van Rolleghem, P.A. (2003). Identification and modelling of aerobic hydrolysis mechanism-application of optimal experimental design, *J. Chem. Tech. Biotech.*, ***78***(4), 437–445.

ISO 6060 (1986). *Water quality-determination of the chemical oxygen demand*. International Standards Organization, Switzerland.

ISO 8192 (2007). *Water Quality-Test for Inhibition of Oxygen Consumption by Activated Sludge.* International Standards Organization, Switzerland.

Jenkins, D., Richard, M.G. and Daigger, G.T. (2004). *Manual on the Causes and Control of Activated Sludge Bulking, Foaming, and Other Solids Separation Problems*, London: Lewis Publishers.

Jonsson, L. (2005). *Control of sludge bulking in an SBR-plant treating slaughterhouse wastewater* (M.Sc. Thesis), Swedish University of Agricultural Sciences.

Kampfer, P. (1995). Physiological and chemotaxonomic characterization of filamentous bacteria belonging to the genus f Haliscomenobacter, *Syst. Appl. Microbiol.*, ***18***, 363–367.

Kappeler, J. and Gujer, W. (1992). Estimation of kinetic parameters of heterotrophic biomass under aerobic conditions and characterization of wastewater for activated sludge modeling, *Water Sci. Technol.*, ***25***(6), 125–139.

Karahan-Gul, O., Artan, N., Orhon, D., Henze, M. and van Loosdrecht, M.C.M. (2002). Experimental assessment of bacterial storage yield, *J. Env. Eng.-ASCE*, ***128***(11), 1030–1035.

Kemper, N. (2008). Veterinary antibiotics in the aquatic and terrestrial environment. *Ecol. Indic.*, ***8***, 1-13.

Khan, S.T. and Hiraishi, A. (2002). *Diaphorobacter nitroreducens* gen. nov., sp. nov., a poly(3-hydroxybutyrate)-degrading denitrifying bacterium isolated from activated sludge, *J. Gen. Appl. Microbiol.*, ***48***, 299–308

Kim, S., Eichhorn, P., Jensen, J.N., Weber, A.S. and Aga, A. (2005). Removal of Antibiotics in Wastewater: Effect of Hydraulic and Solid Retention Times on the Fate of Tetracycline in the Activated Sludge Process, *Environ. Sci. Technol.*, ***39***, 5816-5823.

Kisker, C., Hinrichs, W., Tovar, K., Hillen, W. and Saenger, W. (1995). The complex formed between Tet repressor and tetracycline-Mg2_ reveals mechanism of antibiotic resistance, *J. Mol. Biol.*, ***247***, 260–280.

Kragelund, C., Levantesi, C., Borger, A., Thelen, K., Eikelboom, D., Tandoi, V., Kong, Y., Krooneman, J., Larsen, P., Thomsen, T.R. and Nielsen, P.H. (2008). Identity, abundance and ecophysiology of filamentous bacteria belonging to the Bacteroidetes present in activated sludge plants, *Microbiology*, ***154***, 886–894.

Krause, L., Diaz, N.N., Bartels, D., Edwards, R.A., Pühler, A., Rohwer, F., Meyer, F. and Stoye, J. (2006). Finding novel genes in bacterial communities isolated from the environment, *Bioinformatics*, ***22***, e281–e289.

Kümmerer, K. (2009). Antibiotics in the aquatic environment – A review – Part I, *Chemosphere*, ***75***, 417–434.

Kümmerer, K. and Henninger, A. (2003). Promoting resistance by the emission of antibiotics from hospitals and households into effluents, *Clin. Microbiol. Infec.*, ***9***, 1203–1214.

Kwon, S., Kim, T., Yu, G., Jung, J. and Park, H. (2010). Bacterial community composition and diversity of a full-scale integrated fixed-film activated sludge system as investigated by pyrosequencing, *J. Microbiol. Biotechnol.*, ***20***, 1717-1723.

Leclercq, R. (2002). Mechanisms of resistance to macrolides and lin- cosamides: Nature of the resistance elements and their clinical implications, *Clin. Infect. Dis.*, ***34***, 482-492.

Leclercq, R. and Courvalin, P. (1991). Bacterial resistance to macrolide, lincosamide and streptogramin antibiotics by target modification,. *Antimicrob. Agents Chemother.*, ***35***, 1267 – 1272.

Le-Minh, N., Khan, S.J., Drewes, J.E. and Stuetz, R.M. (2010). Fate of antibiotics during municipal water recycling treatment processes, *Water Res.*, ***44***, 4295 – 4323.

Levy, S. B. (1984). Resistance to tetracyclines. In L. E. Bryan (Ed.), *Antimicrobial drug resistance* (p. 191–204). Academic Press, New York.

Levy, S. B. (1988). Tetracycline resistance determinants are widespread, *ASM News*, ***54***,418–421.

Li, B. and Zhang, T. (2010). Biodegradation and Adsorption of Antibiotics in the Activated Sludge Process, *Environ. Sci. Technol.*, ***44***, 3468–3473.

Li, D., Yu, T., Zhang, Y., Yang, M., Li, Z., Liu, M., and Qi, R. (2010). Antibiotic Resistance Characteristics of Environmental Bacteria from an Oxytetracycline Production Wastewater Treatment Plant and the Receiving River, *Appl. Environ. Microb*, ***76***(11), 3444–3451.

Liebert, C.A., Hall, R.M. and Summers, A.O. (1999). Transposon Tn21, flagship of the floating genome, *Microbiol. Mol. Biol. Rev.*, ***63***, 507–522.

Liu, Y.F., Wang, C.H., Janapatla, R.P., Fu, H.M., Wu, H.M. and Wu, J.J. (2007). Presence of plasmid pA15 correlates with prevalence of constitutive MLSB resistance in group A streptococcal isolates at a university hospital in southern Taiwan, *J. Antimicrob. Chemother.*, ***59***, 1167–1170.

Louvet, J.N., Giammarino, C., Potier, O. and Pons, M.N. (2010). Adverse effects of erythromycin on the structure and chemistry of activated sludge, *Environ. Pollut.*, ***158***, 688–693.

Lunestad, B.T. and Goksøyr, J. (1990). Reduction in the antibacterial effect of oxytetracycline in sea water by complex formation with magnesium and calcium, *Dis. Aquat. Organ.*, ***9***, 67–72.

Ma, L., Zhang, X.X., Cheng, S., Zhang, Z., Shi, P., Liu, B., Wu, B. and Zhang, Y. (2011). Occurrence, abundance and elimination of class 1 integrons in one municipal sewage treatment plant, *Ecotoxicology*, ***20***(5), 968-73.

Macherey-Nagel (2010). *Genomic DNA from Soil, User Manual, NucleoSpin Soil*, (July/Rev02).

Margulies, M., Egholm, M., Altman, W., Attiya, S., Bader, J., Bemben, L., Berka, J., Braverman, M., Chen, Y. and Chen, Z. (2005). Genome sequencing in microfabricated high-density picolitre reactors, *Nature*, ***437***, 376-380.

Martineau, F., Picard, F.J., Lansac, N., Ménard, C., Roy, P.H., Ouellette, C., and Bergeroni, M.G. (2000). Correlation between the Resistance Genotype Determined by Multiplex PCR Assays and the Antibiotic Susceptibility Patterns of Staphylococcus aureus and Staphylococcus epidermidis, *J. Antimicrob. Chemother.*, ***44***(2), 231-238.

Martinez, J. L. (2008). Antibiotics and antibiotic resistance genes in natural environments, *Science*, ***321*** (5887), 365–367.

Maskell, J.P., Sefton, A.M. and Hall, L.M.C. (1997). Mechanism of Sulfonamide Resistance in Clinical Isolates of Streptococcus pneumonia, *J. Antimicrob. Chemother.*, ***41***(10), 2121-2126.

McKeon, D., Calabrese, J. and Bissonnette, G. (1995). Antibiotic resistant gram-negative bacteria in rural groundwater supplies, *Water Res.*, ***29***(8), 1902–1908.

McLellan, S., Huse, S., Mueller Spitz, S., Andreishcheva, E. and Sogin, M. (2010). Diversity and population structure of sewage derived microorganisms in wastewater treatment plant influent, *Environ. Microbiol.*, ***12***, 378-392.

Mohapatra, H., Mohapatra, S.S., Mantri, C.K., Colwell, R.R. and Singh, D.V. (2008). Vibrio cholerae non-O1, non-O139 strains isolated before 1992 from Varanasi, India are multiple drug resistant, contain intSXT, dfr18 and aadA5 genes, *Environ. Microbiol.*, ***10***, 866–873.

Mukherjee, S. and Chakraborty, R. (2006). Incidence of class 1 integrons in multiple antibiotic-resistant Gram-negative copiotrophic bacteria from the River Torsa in India, *Res. Microbiol.*, ***157***, 220-226.

Mulchandani, A. (1989). Luong, J.H.T. Microbial inhibition kinetics revisited, *Enzyme Microb. Tech.*, ***11***(2), 66–73.

Muyzer, G., Brinkhoff, T., Nubel, U., Santegoeds, C., Schafer, H. and Wawer, C. (1998). Denaturing gradient gel electrophoresis (DGGE) in microbial ecology. In: Akkermans, A.D.L., van Elsas, J.D., de Bruijn, F.J. (Ed.), *Molecular Microbial Ecology Manual* (p. 1–27). Kluwer Academic Publishers, Dordrecht.

Nikolakopoulou, T.L., Egan, S., van Overbeek, L.S., Guillaume, G., Heuer, H., Wellington, E.M.H., van Elsas, J.D., Collard, J.-M., Smalla, K. and Karagoun, A.D. (2005). PCR detection of oxytetracycline resistance genes otr(a) and otr(b) in tetracycline-resistant streptomycete ısolates from diverse habitats, *Curr. Microbiol.*, ***51***, 211–216.

Oka, H., Ikai, Y., Kawamura, N., Yamada, M., Harada, K., Ito, S. and Suzuki, M. (1989). Photodecomposition products of tetracycline in aqueous solution, *J. Agric. Food Chem.*, ***37***, 226–231

Okitsu, N., Kaieda, S., Yano, H., Nakano, R., Hosaka, Y., Okamoto, R., Kobayashi, T. and Inoue, M. (2005). Characterization of ermB gene transposition by Tn1545 and Tn917 in macrolide-resistant Streptococcus pneumoniae isolates, *J. Clin. Microbiol.*, ***43***, 168–173.

Oktem, Y.A., Ince, O., Donnelly, T., Sallis, P. and Ince, B.K. (2006). Determination of optimum operating conditions of an acidification reactor treating a chemical synthesis-based pharmaceutical wastewater, *Process. Biochem.*, ***41***, 2258-2263.

Oliveira, J.C., Silveira, E.B., Mariano, R.L.R., Cardoso, E. and Viana, I.O. (2007). Characterization of strains of *Acidovorax avenae subsp. citrulli*, *Fitopatol. Bras.*, ***32***(6), 480 – 487.

O'Neill, C., Lopez, A., Esteves, S., Hawkes, F.R., Hawkes, D.L. and Wilcox, S. (2000). Azo-dye degradation in an anaerobic-aerobic treatment system operating on simulated textile effluent, *Appl. Microbiol. Biotechnol.*, ***53***, 249-254.

Orhon, D. and Okutman, D. (2003). Respirometric assessment of residual organic matter for domestic sewage, *Enzyme Microb. Tech.*, ***32***(5), 560–566.

Orhon, D., Artan, N. (1994). *Modelling of Activated Sludge Systems,* Switzerland: Technomic Publishing AG, Basel.

Orhon, D., Karahan, O. and Sozen, S. (1999). The effect of residual microbial products on the experimental assessment of the particulate COD in wastewaters, *Water Res.*, ***33***(14), 3191–3203.

Orhon, D., Okutman, D. and Insel, G. (2002). Characterization and biodegradation of settleable organic matter for domestic wastewater, *Water SA*, 299–305.

Orhon, D., Ubay Cokgor , E., Insel, G., Karahan, O. and Katipoglu, T. (2009). Validity of Monod kinetics at different sludge ages – Peptone biodegradation under aerobic conditions, *Bioresource Technol.*,***100***, 5678–5686.

Ozkok, I.P., Yazan, T.K., Cokgor, E.U., Insel, G., Talinli, I. and Orhon, D. (2011). Respirometric assessment of substrate binding by antibiotics in peptone biodegradation, *J. Environ. Sci. Heal. A*, ***46***, 1588–1597.

Park, S., Yu, J., Byun, I., Cho,S., Park, T. and Lee, T. (2011). Microbial community structure and dynamics in a mixotrophic nitrogen removal process using recycled spent caustic under different loading conditions, *Bioresource Technol.*,***102***, 7265–7271.

Parsley, L.C., Consuegra, E.J., Kakirde,K.S., Land, A.M., Harper Jr., W.F. and Liles, M.R. (2010). Identification of diverse antimicrobial resistance determinants carried on bacterial, plasmid, or viral metagenomes from an activated sludge microbial assemblage, *Appl. Environ. Micro.*, ***76***(11), 3753-3757.

Patterson, A.J., Colangeli, R., Spigaglia, P. and Scott, K.P. (2007). Distribution of specific tetracycline and erythromycin resistance genes in environmental samples assessed by macroarray detection, *Environ. Microbiol.*, ***9***, 703–715.

Pei, R., Kim, S.-C., Carlson, K.H. and Pruden, A. (2006). Effect of River Landscape on the sediment concentrations of antibiotics and corresponding antibiotic resistance genes (ARG). *Water Res.*, ***40***, 2427 - 2435.

Perez, S., Eichhorn, P. and Aga, D.S. (2005). Evaluating the biodegradability of sulfamethazine, sulfamethoxazole, sulfathiazole, and trimethoprim at different stages of sewage treatment, *Environ. Toxicol. Chem.*, ***24***(6), 1361–1367.

Prescott, L.M., Harlez, J.P. and Klein, D.A. (1990). *Microbiology*. Dubuque: W.C. Browm Publisher.

Press-Kristensen, K. (2007). *Biodegradation of Xenobiotic Organic Compounds in Wastewater Treatment Plants* (Ph.D. Thesis). Technical University of Denmark, Institute of Environment & Resources.

QIAGEN (2006). *MinElute Handbook for MinElute Gel Extraction Kit* (p. 23-26).

Qian, P., Wang, Y., Lee, O., Lau, S., Yang, J., Lafi, F., Al-Suwailem, A. and Wong, T. (2011). Vertical stratification of microbial communities in the Red Sea revealed by 16S rDNA pyrosequencing, *ISME J.*, ***5***, 507-518.

Radjenovic, J., Petrovic, M. and Barcelo, D. (2007). Analysis of pharmaceuticals in wastewater and removal using a membrane bioreactor, *Anal. Bioanal. Chem.*, ***387***, 1365–1377.

Raj, S., and Anjaneyulu, Y. (2005). Evaluation of biokinetic parameters for pharmaceutical wastewaters using aerobic oxidation integrated with chemical treatment, *Process Biochem.*, ***40***(1):165-175.

Ramos, J.L., Bueno, M.M., Molina-Henares, A.J., Teran, W., Watanebe, K., Zhang, X., Gallegos, M.T., Brennan, R. and Tobes, R. (2005). The TetR Family of Transcriptional Repressors, *Microbiol. Mol. Biol. R.*, ***69***(2), 326–356.

Reinthaler, F.F., Posch, J., Feierl, G., Wust, G., Haas, D., Ruckenbauer, G., Mascher, F. and Marth, E. (2003). Antibiotic resistance of E. coli in sewage and sludge, *Water Res.*, ***37***(8), 1685–1690.

Reis, M.A.M, Serafim, L.S., Lemoa, P.C., Ramos, A.M., Aquiar, F.R., Van Loosdrecht, M.C.M. (2003). Production of polyhdroxyalkanoates by mixed microbial cultures, *Bioprocess Biosyst. Eng.*, ***25***, 377-385.

Richardson, M.L. and Bowron, J.M.. (1985). The fate of pharmaceutical chemicals in the aquatic environment, *J. Pharm. Pharmacol.*, ***37***, 1–12.

Roberts, M.C. (2003). Acquired tetracycline and/or macrolide–lincosamides–streptogramin resistance in anaerobes, *Anaerobe*, ***9***, 63–69.

Roberts, M.C. (2008). Update on macrolide-lincosamide-streptogramin, ketolide, and oxazolidinone resistance genes, *FEMS Microbiol. Letters*, ***282***, 147-159.

Roesch, L., Fulthorpe, R., Riva, A., Casella, G., Hadwin, A., Kent, A., Daroub, S., Camargo, F., Farmerie, W. and Triplett, E. (2007). Pyrosequencing enumerates and contrasts soil microbial diversity, *ISME J.*, ***1***, 283-290.

Roh, S.W., Abell, G.C.J., Kim, K.-H., Nam, Y.-D. and Bae, J.W. (2010). Comparing microarrays and nextgeneration sequencing technologies for microbial ecology research, *Trends Biotechnol*, ***28***, 291–299.

Roller, C., Ludwig, W. and Schleifer, K.H. (1992). Gram-positive bacteria with a high DNA G + C content are characterized by a common insertion within their 23s rRNA genes, *J. Gen. Microbiol.*, ***138***, 1167-1175.

Rosetti, S., Tomei, M.C., Nielsen, P.H. and Tandoi, V. (2005). "*Microthrix parvicella*", a filamentous bacterium causing bulking and foaming in activated sludge systems: a review of durrent knowledge, *FEMS Microbiol. Rev.*, ***29***, 49-64.

Saenger, W., P. Orth, C. Kisker, W. Hillen, and W. Hinrichs. (2000). The tetracycline repressor-A paradigm for a biological switch, *Angew. Chem. Int. ed. Engl.* ***39***, 2042–2052.

Sakano, Y. and Kerkhof, L. (1998). Assessment of changes in microbial community structure during operation of an ammonia biofilter with molecular tools, *Appl. Environ. Microbiol.*, ***64***, 4877–4882.

Sanapareddy, N., Hamp, T.J., Gonzalez, L.C., Hilger, H.A., Fodor, A.A. and Clinton, S.M., (2009). Molecular Diversity of a North Carolina Wastewater Treatment Plant as Revealed by Pyrosequencing, *Appl. Environ. Microbiol.*, ***75***(6), 1688–1696.

Schloss, P.D., Westcott, S.L., Ryabin, T., Hall, J.R., Hartmann, M., Hollister, E.B., Lesniewski, R.A., Oakley, B.B., Parks, D.H., Robinson, C.J., Sahl, J.W., Stres, B., Thallinger, G.G., Van Horn, D.J. and Weber, C.F. (2009). Introducing mothur: Open-source, platform-independent,

community-supported software for describing and comparing microbial communities, *Appl. Environ. Microbiol.*, ***75***(23):7537-41.

Schlüter, A., Krause, L., Szczepanowski, R., Goesmann, A. and Pühler, A. (2008). Genetic diversity and composition of a plasmid metagenome from a wastewater treatment plant, *J. Biotechnol.*, ***136***(1-2):65-76. 2008.

Schnappinger, D., and W. Hillen. (1996). Tetracyclines: antibiotic action, uptake, and resistance mechanisms, *Arch. Microbiol.*, ***165,*** 359–369.

Seviour, R.J. and Blackall, L.L. (1998). *The Microbiology of Activated Sludge.* London: Chapman and Hall (ISBN 0 412 79380 6).

Seviour, R.J., Kragelund, C., Kong, Y., Eales, K., Nielsen, J.L. and Nielsen, P.H. (2008). Ecophysiology of the *Actinobacteria* in activated sludge systems, *Antoine van Leeuvenhoek*, ***94***, 21-33.

Shi, Y.J, Wang, X.H, Qi, Z., Diao, M.H., Gao, M.M., Xing, S.F., Wang, S.G., Zhao, X.C. (2011). Sorption and biodegradation of tetracycline by nitrifying granules and the toxicity of tetracycline on granules, *J. Hazard. Mater.*, *191*, 103–109.

Sköld, O. (2000). Sulfonamide resistance: mechanisms and trends, *Drug Resist. Updat.*, ***3***, 155-160.

Sköld, O. (2001). Resistance to trimethoprim and sulfonamides, *Vet. Res.*, ***32***(3 – 4), 261 – 273 .

Slade, D. and Radman, M. (2011). Oxidative Stress Resistance in *Deinococcus radiodurans*, *Microbiol. Mol. Biol. R.*, ***75***(1), 133–191.

Smith, B. and Wilson, B.J. (1996). A consumer's guide to evenness indices, *Oikos*, 76, 70-82.

Smith, C. A. (2002). Managing pharmaceutical waste, *J. Pharm. Soc. Wisconsin*, (Nov/Dec), 17-22.

Sollfrank, U. and Gujer, W. (1991). Characterization of domestic wastewater for mathematical modelling of the activated sludge process, *Water Sci. Technol.*, ***23***(4), 1057–1066.

Sozen, S., Ubay Cokgor, E., Orhon, D. and Henze, M. (1998). Respirometric analysis of activated sludge behaviour-II. Heterotrophic growth under aerobic and anoxic conditions, *Water Res.*, ***32***(2), 476–488.

Spanjers, H. and Vanrolleghem, P.A. (1995). Respirometry as a tool for rapid characterization wastewater and activated sludge, *Water Sci. Technol.*, ***31***(2), 105–114.

Srinivasan, V., Nam, H.M., Nguyen, L.T., Tamilselvam, B., Murinda, S.E. and Oliver, S.P. (2005). Prevalence of antimicrobial resistance genes in Listeria monocytogenes isolated from dairy farms, *Foodborne Patho. Dis.*, ***2***, 201–211.

Standard Methods for the Examination of Water and Wastewater, 21st ed. American Public Health Association/American Water Works Association/Water Environment Federation, Washington DC, U.S.A., 2005.

Sutcliffe, J., Grebe, T.,Tait-Kamradt, A. and Wondrack, L. (1996) Detection of Erythromycin-Resistant Determinants by PCR. *Antimicrob. Agents. Chemother.,* **40**(11), 2562–2566.

Szczepanowski, R., Bekel, T., Goesmann, A., Krause, L., Krömeke, H., Kaiser, O., Eichler, W., Pühler, A. and Schlüter, A. (2008). Insight into the plasmid metagenome of wastewater treatment plant bacteria showing reduced susceptibility to antimicrobial drugs analysed by the 454-pyrosequencing technology, *J. Biotechnol., **136***, 54–64.

Szczepanowski, R., Eikmeyer, F., Harfmann, J., Blom, J., Rogers, L.M., Top, E.M. and Schlüter, A. (2011). Sequencing and comparative analysis of IncP-1_ antibiotic resistance plasmids reveal a highly conserved backbone and differences within accessory regions, *J. Biotechnol., **155***, 95– 103.

Szczepanowski, R., Krahn, I., Linke, B., Goesmann, A., Pühler, A. and Schlüter, A. (2004). Antibiotic multiresistance plasmid pRSB101 isolated from a wastewater treatment plant is related to plasmids residing in phytopathogenic bacteria and carries eight different resistance determinants including a multidrug transport system, *Microbiology, **150***, 3613-3630.

Takahashi, M., Altschmied, L. and Hillen, W. (1986). Kinetic and Equilibrium Characterization of the Tet Repressor-Tetracycline Complex by Fluorescence Measurements, *J. Mol. Biol., **187***,341-348.

Taviani, E., Ceccarelli, D., Lazaro, N., Bani, S., Cappuccinelli, P., Colwell, R.R. and Colombo, M.M. (2008). Environmental Vibrio spp., isolated in Mozambique, contain a polymorphic group of integrative conjugative elements and class 1 integrons, *FEMS Microbiol Ecol, **64***, 45–54.

Tennstedt, T., Szczepanowski, R., Braun, S., Pühler, A. and Schlüter, A. (2003). Occurrence of integron-associated resistance gene cassettes located on antibiotic resistance plasmids isolated from a wastewater treatment plant, *FEMS Microbiol. Ecol., **45***, 239–252.

Tennstedt, T., Szczepanowski, R., Krahn, I., Pühler, A. and Schlüter, A. (2005). Sequence of the 68,869 bp IncP-1a plasmid pTB11 from a wastewater treatment plant reveals a highly conserved backbone, a Tn402-like integron and other transposable elements, *Plasmid, **53***, 218–238.

Tenson, T., Lovmar, M. and Ehrenberg, M. (2003). The mechanism of action of macrolides, lincosamides and streptogramin B reveals the nascent peptide exit path in the ribosome, *J. Mol. Biol., **330*** (5), 1005 – 1014.

Tetracycline and MLS Nomenclature, http://faculty.washington.edu/marilynr/, last retrieved at 27.06.2011

van der Meer, J.R., De Vos, W., Harayama, S. and Zehnder, A.J.B. (1992). Molecular mechanisms of genetic adaptation to xenobiotic compounds, *Microbiol. Rev., **56***(4), 677 – 694.

van Loosdrecht, M.C.M., Pot, M.A. and Heijnen, J.J. (1997). Importance of bacterial storage polymers in bioprocesses, *Water Sci. Technol.,**35***(1), 41-47.

Vanrolleghem, P.A. (2002). Principles of Respirometry in Activated Sludge Wastewater Treatment. In *Proceedings International Workshop on Recent Development in Respirometry for Wastewater Treatment Plant Monitoring and Control*, Taipei, Taiwan, October 22-23, (p. 2/1-20).

Voet, D. and Voet, J.G. (1990). *Inhibition. Biochemistry* (p.340 – 344), USA: Wiley&Sons Inc.

Wagner, M., Amann, R., Kampfer, P., Assmus, B., Hartmann, A., Hutzler, P., Springer, N. and Schleifer, K.H. (1994). Identification and in situ detection of Gram-negative filamentous bacteria in activated sludge, *Syst. Appl. Microbiol.*, ***17***, 405–417.

Ward, A., Hoyle, C., Palmer, S., O'Reilly, J., Griffith, J., Pos, M., Morrison, S., Poolman, Gwyne, M. and Henderson, P. (2001). Prokaryote multidrug efflux proteins of the major facilitator superfamily: Amplified expression, purification and characterization, J. *Mol. Microbiol. Biotechnol.*, ***3***(2), 193-200.

Watkinson, A. J., Murby, E. J. and Costanzo, S. D. (2007). Removal of antibiotics in conventional and advanced wastewater treatment: Implications for environmental discharge and wastewater recycling, *Water Res.*, ***41*** (18), 4164–4176.

Weisblum, B. (1995). Erythromycin resistance by ribosome modification, *Antimicrob. Agents Chemother*, ***39***, 577–585.

White, J.R., Nagarajan, N. and Pop, M. (2009). Statistical Methods for Detecting Differentially Abundant Features in Clinical Metagenomic Samples, *PLoS Comput. Biol.*, ***5***(4): e1000352.

Woo, P.C.Y., Lau, S.K.P., Teng, J.L.L., Tse, H. and Yuen, K.-Y. (2008). Then and now: use of 16S rDNA gene sequencing for bacterial identification and discovery of novel bacteria in clinical microbiology laboratories, *Clin Microbiol Infect*, ***14***, 908–934.

Wright, G.D. (2011). Molecular mechanisms of antibiotic resistance, *Chem. Commun.*, ***14***, 4055 – 4061.

Xia, S., Duan, L., Song, Y., Li, J., Piceno, Y.M., Andersen, G.L., Alvarez-Cohen, L., Moreno-Andrade, L., Huang, C-L. and Hermanowicz, S. (2010). Bacterial community structure in geographically distributed biological wastewater treatment reactors, *Environ. Sci. Technol.*, ***44***, 7391–7396.

Xiong, J., Li, D., Li, H., He, M., Miller, S.J., Yu, L., Rensing, C. and Wang, G. (2011). Genome analysis and characterization of zinc efflux systems of a highly zinc-resistant bacterium, *Comamonas testosteroni* S44, *Res. Microbiol.*, ***162***, 671-679.

Xu, B., Mao, D., Luo, Y. and Xu, L. (2011). Sulfamethoxazole biodegradation and biotransformation in the water–sediment system of a natural river, *Bioresource Technol., 102*, 7069–7076.

Xu, W. H., Zhang, G., Li, X. D., Zou, S. C., Li, P., Hu, Z. H. and Li, J. (2007). Occurrence and elimination of antibiotics at four sewage treatment plants in the Pearl River Delta (PRD), South China, *Water Res.*, ***41***(19), 4526–4534.

Yamaguchi, A., Ono, N., Akasaka, T., Noumi, T., and Sawai, T. (1990b). Metal-tetracycline/H+ antiporter of Escherichia coli encoded by a transposon, Tn10. The role of the conserved dipeptide, Ser65-Asp66, in tetracycline transport, *J. Biol. Chem.*, ***265***(26), 15525-15530.

Yamaguchi, A., Udagawa T. and Sawai, T. (1990a). Transport of divalent cations with tetracycline as mediated by the transposon Tn*10*-encoded tetracycline resistance protein, *J. Biol. Chem.*, ***265*** (9), 4809–4813.

Ye, L., Shao, M-F., Zhang, T., Tong, AHY. and Lok, S. (2011). Analysis of the bacterial community in a laboratory-scale nitrification reactor and a wastewater treatment plant by 454-pyrosequencing, *Water Res.*, ***45***, 4390 – 4398.

Yu, L., Takahashi, Y, Matsumoto, A., Seino, A., Iwai, Y. and Omura, S. (2002). Application of PCR for Selection of Gram-Positive Bacteria with High DNA G + C Content among New Isolates, *Actinomycetol.*, ***16***(1), 1-5.

Zhang, T.T., Ye, L., Tong, A.H.Y., Shao, M.F. and Lok, S. (2011). Ammonia-oxidizing archaea and ammonia-oxidizing bacteria in six full-scale wastewater treatment bioreactors, *Appl. Microbiol. Biotechnol.*, ***91***, 1215–1225.

Zhang, X.-X., Zhang, T. and Fang, H.H.P. (2009). Antibiotic resistance genes in water environment, *Appl. Microbiol. Biot.*, ***82***, 397-414.

CURRICULUM VITAE

Name Surname	**:** Ilke Pala Özkök
Place and Date of Birth	**:** Istanbul, 06.01.1982
Adress	**:** Istanbul Technical University Civil Engineering Faculty Department of Environmental Engineering 34469 Maslak, İstanbul
E-mail	**:** palai@itu.edu.tr
B.Sc	**:** Istanbul Technical University Faculty of Civil Engineering Environmental Engineering Department Istanbul Technical University Faculty of Science and Letters Molecular Biology and Genetics Department

Professional Experience and Rewards:

- Research and Teaching Assistant Istanbul Technical University
  Faculty of Civil Engineering Environmental Engineering Department
  (2005 –)
- Visiting Researcher
  Albert Ludwig's Universitaet Freiburg Universitaets Klinikum
  Institut für Umweltmedizin und Krankenhaushygiene
  (31.01.2010 – 31.01.2011)
- The Scientific and Technological Research Council of Turkey
  National Scholarship Programme for PhD Students
  (2006 - 2010)
- Turkish Academy of Sciences Joint Doctoral Degree Program
  (23.10.2008 – 23.10.2011)

List of Publications and Patents:

Research Papers

- **Pala Ozkok, I.,** Katipoglu Yazan, T., Ubay Cokgor, E., Insel, G., Talinli, I., Orhon, D. (2011). Respirometric Assessment of Substrate Binding by Antibiotics in Peptone Biodegradation, *Journal of Environmantal Science and Health Part A, 46, 1588–1597.*

- Ciggin, A.S., **Pala, I.,** Katipoglu, T., Dulekgurgen, E.S., Meric, S., Orhon, D., 2011: Research Potential of Doctoral Studies on Environmental Sciences and Engineering, *Desalination and Water Treatment, 26(1 – 3), 3 – 13.*

- **Pala, I.,** Kolukirik, M., Insel, G., Ince, O., Cakar, Z.P., Orhon, D., 2008. Fluorescence in situ hybridization (FISH) for the assessment of nitrifying bacteria in a pilot-scale membrane bioreactor, *Fresenius Environmental Bulletin, 17(11), 2255 – 2261.*

- Insel, G., Karahan, Ö., Özdemir, S., **Pala, I.,** Katipoğlu, T., Çokgör, E.U., Orhon, D., 2006. Unified basis for the respirometric evaluation of inhibition for activated sludge, *Journal Of Environmental Science and Health Part A-Toxic/Hazardous Substances & Environmental Engineering, 41(9), 1763 – 1780.*

Actual Articles

- Orhon, D., **Pala, I,** Katipoğlu, T., 2010. Scientific publications with hih impact factors on environmental sciences an engineering, *Cumhuriyet Gazetesi Bilim Teknik Dergisi, 1208/18. (in Turkish)*

- Orhon, D., **Pala, I.,** Çığgın, A., 2007. A new Approach for Evaluating the Scientific Production: G Factor and G/H, *Cumhuriyet Gazetesi Bilim Teknik Dergisi, 1076. (in Turkish)*

National Books

Editorial

- Alp, K., Altınbaş, M., Genceli, E., Yağcı, N., Hanedar, A., Pala, I., Avşar, E., Erşahin, M.E., Allar, A.D., Topuz, E., Çetecioğlu, Z., XII. Symposium on Industrial Pollution Control Proceedings Book, 2010, İstanbul, Turkey

Scientific Technical Reports

- Sözen S., Orhon D., Çokgör E.U., Görgün E., İnsel G., Karahan Ö., Yağcı Ö.N., Taş O.D., Dülekgürgen E., Doğruel S., Ölmez T., Zengin G., Çığgın A., **Pala İ.,** Katipoğlu T., Eldem N., Ünal A., 2007. Evaluation of Design Criteria of İSKİ Tuzla and Paşaköy Advanced Biological Wastewater Treatment Plants: Tuzla Wastewater Treatment Plant Case – II. Report", Project supported by ISKI. (in Turkish)

- Sözen S., Orhon D., Çokgör E.U., Görgün E., İnsel G., Karahan Ö., Yağcı Ö.N., Taş O.D., Dülekgürgen E., Doğruel S., Ölmez T., Zengin G., Çığgın A., **Pala I.,** Katipoğlu T., Eldem N., Ünal A., 2007. Evaluation of Design Criteria of İSKİ Tuzla and Paşaköy Advanced Biological Wastewater Treatment Plants: Pasakoy Advanced Wastewater Treatment Plant Case – III. Report", Project supported by ISKI. (in Turkish)

- Sözen S., Orhon D., Çokgör E.U., Görgün E., İnsel G., Karahan Ö., Yağcı Ö.N., Taş O.D., Dülekgürgen E., Doğruel S., Ölmez T., Zengin G., Çığgın A., **Pala I.,** Katipoğlu T., Eldem N., Ünal A., 2008. Evaluation of Design Criteria of İSKİ Tuzla and Paşaköy Advanced Biological Wastewater Treatment Plants: Tuzla Wastewater Treatment Plant Case – Final Report, Project supported by ISKI. (in Turkish)

PUBLICATIONS/PRESENTATIONS ON THE THESIS

Pala Ozkok, I., Katipoglu Yazan, T., Ubay Cokgor, E., Insel, G., Talinli, I., Orhon, D. (2011). Respirometric Assessment of Substrate Binding by Antibiotics in Peptone Biodegradation, *Journal of Environmantal Science and Health Part A*, 46, 1588–1597.

İstanbul, 02.07.2012